USC UNIVERSIDADE DE SANTIAGO DE COMPOSTELA

CENTRO INTERNACIONAL DE ESTUDOS DE DOUTORAMENTO E AVANZADOS DA USC (CIEDUS)

DOCTORAL THESIS

NANOTECHNOLOGY FOR THE MODULATION OF THE IMMUNE RESPONSE IN HIV AND CANCER

Tamara Gómez Dacoba

INTERNATIONAL DOCTORAL SCHOOL

DOCTORAL PROGRAM IN DRUG RESEARCH AND DEVELOPMENT

SANTIAGO DE COMPOSTELA

2020

CENTRO INTERNACIONAL DE ESTUDOS
DE DOUTORAMENTO E AVANZADOS
DA USC (CIEDUS)

TESE DE DOUTORAMENTO

NANOTECNOLOXÍA PARA A MODULACIÓN DA RESPOSTA INMUNE EN VIH E CANCRO

Tamara Gómez Dacoba

ESCOLA DE DOUTORAMENTO INTERNACIONAL

PROGRAMA DE DOUTORAMENTO EN I + D DE MEDICAMENTOS

SANTIAGO DE COMPOSTELA

2020

AUTHORIZATION OF THE THESIS SUPERVISORS

Nanotechnology for the modulation of the immune response in HIV and cancer

Prof. **María José Alonso Fernández**, Full Professor in the Department of Pharmacology, Pharmacy and Pharmaceutical Technology at the University of Santiago de Compostela.

Dr. **José Crecente Campo**, researcher in the Department of Pharmacology, Pharmacy and Pharmaceutical Technology at the University of Santiago de Compostela.

REPORT:

That the present thesis, corresponds to the work carried out by Ms. ***Tamara Gómez Dacoba****, under our supervision, and that we authorize its presentation considering it gathers the necessary requirements of article 34 of USC Doctoral Studies regulation, and that as supervisors of this thesis, it does not incur in the abstention causes stablished by the law 40/2015.*

Santiago de Compostela, January 31st, 2020

Sgd.: **María José Alonso Fernández**

Sgd.: **José Crecente Campo**

AUTORIZACIÓN DO DIRECTOR / TITOR DA TESE

Nanotecnoloxía para a modulación da resposta inmune en VIH e cancro

Dna. **María José Alonso Fernández**, Catedrática do Departamento de Farmacoloxía, Farmacia e Tecnoloxía Farmacéutica da Universidade de Santiago de Compostela.

D. **José Crecente Campo**, investigador no Departamento de Farmacoloxía, Farmacia e Tecnoloxía Farmacéutica da Universidade de Santiago de Compostela.

INFORMAN:

Que a presente tese, correspóndese co traballo realizado por Dna. ***Tamara Gómez Dacoba****, baixo a nosa dirección, e autorizamos a súa presentación, considerando que reúne os requisitos esixidos no Regulamento de Estudos de Doutoramento da USC, e que como directores desta non incorre nas causas de abstención establecidas na Lei 40/2015.*

En Santiago de Compostela, 31 de Xaneiro de 2020

Asdo.: **María José Alonso Fernández**

Asdo.: **José Crecente Campo**

PhD CANDIDATE STATEMENT

Nanotechnology for the modulation of the immune response in HIV and cancer

Ms. **Tamara Gómez Dacoba**

I submit my Doctoral thesis, following the procedure according to the Regulation, stating that:

1) This thesis gathers the results corresponding to my work.
2) When applicable, explicit mention is given to the collaborations this work may have had.
3) The present document is the final version submitted for its defense, and coincides with the document sent in electronic format.
4) I confirm that this thesis does not incur in any plagiarism of any other authors or documents submitted by me for obtaining other degrees.

Santiago de Compostela, January 31st, 2020

Sgd.: **Tamara Gómez Dacoba**

DECLARACIÓN DO AUTOR/A DA TESE

Nanotecnoloxía para a modulación da resposta inmune en VIH e cancro

Dna. **Tamara Gómez Dacoba**

Presento a miña tese, seguindo o procedemento axeitado ao Regulamento, e declaro que:

1) A tese abarca os resultados da elaboración do meu traballo.
2) De selo caso, na tese faise referencia ás colaboracións que tivo este traballo.
3) A tese é a versión definitiva presentada para a súa defensa e coincide coa versión enviada en formato electrónico.
4) Confirmo que a tese non incorre en ningún tipo de plaxio doutros autores nin de traballos presentados por min para a obtención doutros títulos.

En Santiago de Compostela, 31 de Xaneiro de 2020

Asdo.: **Tamara Gómez Dacoba**

Conflict of interest

I hereby declare that there is no conflict of interest with the topics or materials discussed in this doctoral thesis.

Sgd.: **Tamara Gómez Dacoba**

Á miña familia

Á miña xente

"Sorte… e xustiza"

Sabiduría paterna

"Paciencia, que es la madre de la ciencia"

Sabiduría popular

"We knew the world would not be the same"

Oppenheimer

Acknowledgments

Y después de tanto tiempo, por fin me encuentro aquí, al final del camino. Pero sin duda no habría podido llegar hasta este punto sin la ayuda inestimable de tanta gente, que intentaré plasmar en las próximas líneas, pero sabiendo que las palabras no podrán expresar todo el agradecimiento que siento. Así pues, GRACIAS a todos los que me habéis acompañado en este trayecto.

En primer lugar, gracias a María José y a Jose, mis directores de tesis. Gracias, María José, por haberme aceptado en este maravilloso grupo hace ya más de 6 años, por darme la oportunidad de descubrir el mundo de la investigación, y por enseñarme lo que es la pasión por el trabajo. Gracias Jose, pola túa continua dispoñibilidade, os sabios consellos e por axudarme ao longo de todo este camiño.

Gracias á Universidade de Santiago, e ao CIMUS, por poñer á miña disposición todos os medios para desenvolver á miña tese. Gracias al Ministerio de Educación (en todos sus nombres), por haberme concedido una beca FPU para la realización de la tesis, y por la beca que me permitió cruzar el charco y descubrir el mundo de la investigación americano. Gracias a todas las entidades que han financiado los proyectos en los que he trabajado.

Gracias a todo el profesorado del Departamento de Farmacología, Farmacia y Tecnología Farmacéutica. Gracias Noemi, Marcos y Loli, por los buenos consejos y por vuestro apoyo durante estos años. Agradecer también, a los servicios generales de apoyo a la investigación de la USC (RIAIDT), por el uso de sus infraestructuras y la colaboración de sus técnicos. En especial gracias a Raquel, del servicio de microscopía, por tantas horas en busca de una buena foto de mis nanopartículas. Thank you, as well, to our collaborators from the University of Manitoba (Canada). Thanks to Ma, Were and Hongzhao, for teaching me so much about HIV immunology, and for all the help provided throughout these years. Also, thank you to our collaborators from Humanitas Research Hospital (Italy). Thanks to Paola, Fernando, Clément and Francesco, for performing all the cell an animal studies, and for always being available for discussing the results.

Special thanks to Paula, for receiving me in your group with such kindness and enthusiasm. Thank you for your availability, your wise advices, and for being an example of hard work. Thank you for allowing me to be a part of that amazing group that you have.

Gracias a Puri, Sagrario y a Jesús Esmorís por toda la ayuda a la hora de intentar comprender la complicada burocracia de la universidad, el ministerio, o de cualquier entidad. Sin vuestro conocimiento aún estaría enterrada en papeles. Gracias a María y a Vanesa por esos acertados consejos. Gracias Rafa, por sempre estar disposto a axudarme cos meus problemas informáticos, que non foron poucos. Gracias Balbi, por tu ayuda constante, por tomar prestado el material sin preguntar, y por siempre querer asustarme con que el liofilizador se ha estropeado. Gracias Fernando, por ser un exemplo de optimismo e de creatividade. Gracias Desi, por haberme enseñado tanto sobre cómo ser metódica en mi trabajo, sobre la insulina oral, y por siempre estar dispuesta a ayudar. Gracias también por haberme animado a seguir en este camino, a hacerme ver que detrás de tanto sacrificio hay una recompensa. Gracias Belén, por tus sabios consejos, por aguantar mis lloros y por siempre estar ahí para escucharme. Gracias por ser la mami del laboratorio, por cuidar siempre de nosotros, y por ser la pureta más cañera.

Un gracias muy grande y especial a toda mi familia de *Nanochachos*, por el apoyo, la ayuda y comprensión a lo largo de esta maratón. No sois pocos los que habéis contribuido al desarrollo de esta tesis, desde mis primeros pasos en este el mundo de la investigación. Gracias a los veteranos JeiVi, Ana

Paredes y Adam, por vuestras sabias palabras a mi llegada. Gracias Pinto, por esos grandes consejos, esos f*, y por enseñarnos que “no hay huevos para una pandemia”. Gracias Raquel, por esos divertidos bailes de zumbadas. Obrigada minha Sarinha, por tu gran acogida a mi llegada al labo, llena de cariño, y por tu ayuda al adentrarme en el mundo de las vacunas. Obrigada por tu constante apoyo, tu disponibilidad para hacer planes sociales, y por no dejarme olvidar que estoy en algún top.

Gracias a toda la gente que he conocido a lo largo de estos años. Gracias Belén Álvarez, Blanca, Cecilia, Cris, Edi, Francesco, Federico, Ivana, Lali, María, Mireia, Nacho, Nataliya, Noelia, Ovidio, Paulina, Ricardo, Sakti, Silvia, Surasa, por todos los momentos compartidos. Gracias Rosana, Esther, por vuestra breve pero intensa compañía. Gracias Ana Abadessa, Catarina, Khair, Mariajo, Raneem, Shubaash, Tania y Vanessa, por tantas conversaciones y buenos momentos en cualquier esquina del laboratorio. Gracias Germán, Carmen, Ana López y Mireya, las nuevas generaciones, por vuestra alegría y buen rollismo constante.

Gracias a los de la 2, Sheila, Sandra, Chema, Saeede, Héctor, Paul, Howl, que aunque en la distancia, siempre presentes. Thanks Maruthi, for your kindness and for being an example of hard work and patience. Gracias Diego, por las continuas charlas en la ultra compartiendo alegrías y penas (sobre todo penas). Gracias Carla, por esas charlas de 5 min que se vuelven horas intentando entender la vida, pero que todavía no nos han llevado a ninguna conclusión.

Gracias al antiguo Transint team, por enseñarme tanto y hacer más llevaderas esas largas tardes-noche de trabajo. Gracias, señor Niu, por todos esos buenos momentos aprendiendo sobre China, y demostrando tu capacidad para hablar gallego como cualquier local. Thanks my Lucecita, for your sweetness, for being such a nice friend, I will never forget that amazing cake. Gracias Miguel, Enrique y Sonia, por ese trabajo constante codo con codo. Gracias Mati, por ser un ejemplo de pelazo con cerebro debajo, y por descubrirme lo maravilloso que es el espumoso.

Thanks Bhanu, for being such a kind person and for your contagious smile. Gracias Sergio por tantos juegos nuevos que me has enseñado. Gracias Iago, por ser un digno continuador de la organización y limpieza del laboratorio, y por tu continua disposición para ayudar. Obrigada Sofia, por tu sonrisa y abrazos, que alegran el día a cualquiera, y por estar siempre disponible para cualquier plan. Gracias Ana, que empezamos esta aventura¿? juntas, por estar codo con codo a lo largo de este no corto camino, y por ese chocolate que ha endulzado duros momentos.

Gracias mi Belenciña, por haberme recibido con los brazos abiertos nada más llegar, por todas esas comidas, cafés… por estar siempre ahí. Gracias por ser un ejemplo de organización y trabajo ejemplar, de superación constante. Gracias por tu sinceridad sin límites, también llamada falta de filtro.

Gracias Inma por tanto. Gracias por esos cafés mañaneros, esas charlas de poyata, los planes fuera del laboratorio. Gracias por tu infinito cariño, tu disponibilidad, gracias por ese enorme corazón que tienes. Gracias por siempre escucharme, por darme los mejores consejos. Gracias por todos esos abrazos que tanto me han ayudado, y que tanto echo de menos. Sin ti la quinta no es lo mismo.

A mi Cadetinha, por haber sido mi hermana mayor en Boston. Por enseñarme que el trabajo duro también tiene derecho a vida social. Gracias por todos los planes (super awesome!) que siempre organizas con la mejor de las sonrisas. Gracias por tu optimismo, y por siempre preocuparte por los demás. Que lo que ha unido el pHmetro no lo separe un charco.

Gracias a mis Astuvievis, por siempre estar ahí. Gracias por esos viajes y planes inolvidables, por todas esas cañas y tapeos intentando arreglar el mundo, buscando soluciones a las injusticias que nos rodean. Gracias por tantas horas inolvidables en el tarasca.

Gracias Adri, mi pequeño saltamontes. Gracias por esa fuerza que desprendes, por ser el claro ejemplo de "pequeña, pero matona". Gracias por tus siempre sabios consejos, por tu templanza salpicada de cabreos repentinos. Gracias por todos esos vídeos de perros, gatos y demás seres adorables, que siempre me arrancan una sonrisa. Gracias por haberme hecho una fiel amante de las IPAs.

Gracias mi Carmiña, por tu dulzura infinita. Gracias por estar siempre dispuesta a escuchar mis penas, por tu cariño y todos tus abrazos. Gracias por tantas horas de baile en el gimnasio, y por enseñarme el valor de la comida gourmet. Gracias por tu constante apoyo, por tantos cafés desestresantes. Gracias por ser la única que sabe apreciar mis "¡hola!" y mis visitas tan infrecuentes al despacho.

Gracias Eleniña, por hacerme reír constantemente. Gracias por intentar buscarle siempre el lado divertido a la vida, por tus GIFs locos, por tus gritos en público que nos avergüenzan a todos (y a la vez nos dan envidia). Gracias por haber tu cercanía, a pesar de estar siempre a muchos km de distancia. Gracias por ser la "llama" el grupo.

Gracias Ire, por ser mi madre y mi hermana, por estar siempre ahí. Gracias por tus abrazos y gritos, por poner orden en el caos. Gracias por tantas cañas desestresantes, por esas partidas de hotel, por las noches de nachos, por descubrirme el mundo de las manualidades. Gracias por llevarme de paseo por las tiendas, por siempre buscar planes y por ser la primera dispuesta a organizar todo. Gracias por esas noches increíbles en tarasca, y por todavía no haberme sacado un ojo con la coleta.

Grazas Joseito, por compartir toda a túa sabiduría comigo. Grazas por toda a túa axuda, por escoitar as miñas penas, e por sempre estar dispoñible. Grazas por axudarme a manter a cordura, por facerme ver que o malo ten un final, e que hai que buscarlle o lado bo as cousas. Grazas por ser o único que entende o meu sentido do humor, e por facer chistes máis malos cos meus. E grazas por aguantarme todo este tempo sen mandarme á paseo, sei que non foi fácil.

Gracias Sonita, por todas esas risas. Gracias por intentar ser puntual y nunca cumplirlo (salvo una vez!). Gracias por los cariñitos que das (y por los que pides), gracias por todas esas cañas para despejar después de interminables horas de trabajo, acompañadas siempre de sabias palabras. Gracias por siempre intentar dar lo máximo, aunque se te cierren los ojos del cansancio. Gracias por tu continua sonrisa.

My dearest Lena, thanks for everything. Thanks for always listening to my problems, for your kindness, for trying to make everyone feeling at home. Thanks for trusting my opinion from the very beginning. Thanks for all your crazy stories that always make my day. Thanks for being part of the family, for all the laughs, trips to the beach, beers and meals (especially that amazing chocolate pizza!). Thank you for being the best host, and for showing me how awesome Vancouver is!

Gracie mi querido spagettini Andreini. Gracias por ser único, por tu constante rebeldía hacia la autoridad, pero siendo un ejemplo de trabajo duro. Gracias por tantas cervezas y cafés (de los de verdad). Gracias por tu enorme corazón, y por hacernos sentir parte de tu familia gallega. Gracias por tu constante disposición a hacer planes, ya sean unas cervezas, cenas multitudinarias o una escapada a los carnavales ourensanos.

Also, my deepest gratitude to the Hammond lab. Thank you so much to the whole group for making me feel like I was at home, even with the pond in between. A very special mention to Betty, Elad, Joelle and Natalie for your continuous support, for all the shared lunches learning about the American culture. Thank you for showing me the amazing and addictive world of the bubble tea. Thanks for being my American family, for always being willing to help, hear or talk at any time. Thank you for sharing all your wisdom with me, for teaching me new techniques, and also for teaching me English. Thanks for always being willing to do any plan, for all those beers, for being such good friends. Thanks for that contagious optimism that I was lacking and that has made me a better person and scientist.

Obrigada também à minha querida família portuguesa em Boston, pelas festas, jantares, cervejas… obrigada por me adotarem como uma portuguesinha mais do Norte.

Y como no, infinitas gracias a mis españoles en Boston, por siempre estar dispuestos a hacer un viaje, tomar algo o a ir de fiesta a cualquier lado, cualquier día en cualquier momento.

Pero fuera del mundo de la investigación también tengo a mucha gente que agradecer. Muchas gracias a Mis Sabias: Andrea, Bea, Lucía y Uxía. Gracias por estar siempre ahí, por los cotilleos que me mantienen al día de la vida, por vuestro apoyo intentando comprender a qué me dedico, por ser fans incondicionales. Gracias Diana, por haberme apoyado desde el primer momento. Gracias también a mi querida Ana, por esos planes no planificados en cualquier lugar, hora y con cualquier excusa, que siempre son geniales, aunque sean en un sofá viendo *Friends*.

Grazas tamén a Ermitas, Sindo, Adrián, Gre e Rude, por facerme sentir da familia. E unha mención especial às croquetas da “abuela” Gre, que me deron forzas durante ao longo deste camiño.

Un gracias infinito a Rodrigo, por haber permanecido a mi lado todo este tiempo. Gracias por tu apoyo constante, por acompañarme (¡y sobretodo aguantarme!) a lo largo de todo este camino, que ha parecido eterno. Gracias por tu paciencia, por tus cuidados y tu amor, por escuchar mis enfados, por sobrellevar mis (no pocos) lloros. Gracias por tus bromas tontas para sacarme una sonrisa, por buscar planes para hacerme desconectar, por casi obligarme a ir al gimnasio. Tengo la certeza que sin ti no hubiese llegado a donde estoy. Esta tesis es casi tan tuya como mía.

Y por último, gracias a mi familia. Gracias a mis abuelos Tono y Corona, a mis tíos Toñito, Pepa, Rosi y Cesáreo, y a mis primos Miguel, Bea, Diego y Deborah (y a las peques también), por apoyarme siempre aa seguir adelante y a luchar por lo mío. Gracias a Marité y Juan, por haber vislumbrado, antes de yo siquiera imaginarlo, que acabaría dedicándome a la investigación.

Y en especial, gracias a mis padres, por siempre confiar y apoyarme en todas las decisiones que he tomado. Gracias por nunca dudar de mí, por darme la fuerza para seguir luchando por lo que quiero, aunque sea a contracorriente. Gracias por ser mi ejemplo a seguir. Gracias por enseñarme a tener “cabeciña”, y a que “sorte e xustiza” van de la mano.

GRACIAS

Table of Contents

Table of Contents

Abstract / Resumen

Abstract

The immune system plays an important role in the progression and eradication of several illnesses, notably in cancer and infectious diseases. Although in the last decades we have witnessed an unprecedented progress in the development of therapies in these two areas, significant challenges remained to be tackled.

A number of infectious diseases, such as HIV, still remain elusive to vaccination. A key limitation of the most recent antigens is their poor immunogenic character, a fact that has encouraged the search for new adjuvants and antigen delivery carriers. Based on this premise, the objective of the first chapter of this thesis has been to develop polysaccharide-based nanoparticles as adjuvant carriers for an SIV peptide antigen (the simian equivalent of HIV). To this end, different types of nanoparticles, containing poly(I:C) as adjuvant, were developed. The influence of the type of attachment of the peptide to these nanoparticles in the final immune response was then studied. All nanoparticles elicited robust humoral responses in mice, while T cell activation patterns varied depending on antigen/nanoparticles association. Further efficacy studies performed in non-human primates confirmed the potential of one prototype, consisting of chitosan/dextran sulfate nanoparticles associating SIV peptide antigens by ionic interactions. The second chapter of this thesis was focused on adapting the manufacturing process of these polysaccharide-based nanoparticles for their fabrication in a pilot plant under GMP-like conditions. By implementing risk analysis tools, and combining orthogonal techniques, a deeper and more robust characterization of the formulation was achieved. In addition, both continuous and discontinuous scale-up methods were developed for the fabrication of these nanoparticles.

On the other hand, the development of immunotherapies has been recognized as a major milestone in the treatment of cancer. However, there is plenty of room for the optimization of these therapies in terms of improving efficacy and reducing side effects. Within this frame, the objective of the last chapter of this thesis was to develop a new nanoformulation of poly(I:C), intended to target and reactivate tumor-associated macrophages. The results showed that, *in vitro*, macrophages treated with the poly(I:C) nanocomplexes were able to secrete T cell-attracting chemokines and also mediate direct tumor cell killing.

Overall, the results of this thesis have led to the conclusion that a deeper understanding of the role of the immune system in diseases can be leveraged to improve the design of nanosystems to modulate specific immune cell subsets, generating new promising therapies for vaccination and cancer treatment.

Resumen

El sistema inmune juega un papel importante en el desarrollo y la erradicación de enfermedades infecciosas y del cáncer. A pesar de que en el último siglo hemos sido testigos de un progreso sin precedentes en el desarrollo de terapias para estas enfermedades, todavía existen importantes limitaciones.

En el caso de las enfermedades infecciosas, algunas, como la infección por VIH, todavía no son prevenibles a través de la vacunación. Una importante limitación de los antígenos más modernos se debe a su carácter poco inmunogénico, lo que ha llevado a la búsqueda de nuevos adyuvantes y transportadores de antígenos. En base a esto, el primer capítulo de esta tesis se ha centrado en el desarrollo de nanopartículas a base de polisacáridos, con un antígeno peptídico contra el VIS (el equivalente simio al VIH). Con este fin, se desarrollaron varios tipos de nanopartículas, incluyendo el poly(I:C) como adyuvante, y se estudió el efecto en la respuesta inmune del tipo de unión entre las nanopartículas y el antígeno peptídico. En estudios en ratones todos los nanosistemas generaron importantes niveles de anticuerpos contra el antígeno, mientras que la cinética de activación de las células T se vio afectada por el tipo de unión antígeno/nanopartículas. Estudios de eficacia en primates confirmaron el potencial de uno de estos prototipos: nanopartículas a base de quitosano y sulfato de dextrano con antígenos peptídicos contra el VIS asociados mediante enlaces iónicos. El segundo capítulo de esta tesis se centró en adaptar el proceso de fabricación de estas nanopartículas para ser producidas en una planta piloto. Empleando herramientas de análisis de riesgos, y combinando técnicas analíticas complementarias, se consiguió una caracterización más completa y robusta de la formulación. Además, estas nanopartículas pudieron ser producidas a través de procesos continuos y discontinuos, trasladables a la industria.

Por otra parte, a pesar de que el desarrollo de inmunoterapias ha supuesto un gran cambio en la lucha contra el cáncer, estos tratamientos todavía presentan importantes efectos secundarios y resistencias. Por lo tanto, el último objetivo de esta tesis fue el desarrollo de una nanoformulación de poly(I:C), capaz de dirigirlos hacia macrófagos asociados a tumores y así, reactivarlos. *In vitro*, los macrófagos tratados con los nanocomplejos de poly(I:C) secretaron quimoquinas implicadas en el reclutamiento de células T citotóxicas, además de destruir directamente las células tumorales.

En resumen, los resultados de esta tesis demuestran que, a través del conocimiento del papel del sistema inmune en el desarrollo de diferentes patologías, se pueden desarrollar de manera racional nanotransportadores capaces de interaccionar y modular específicamente células del sistema inmune, obteniendo así prometedoras terapias tanto para vacunas como para el tratamiento del cáncer.

Resumen *in extenso*

El sistema inmune está formado por una red compleja de órganos, tejidos y células linfoides innatas y adaptativas que se comunican entren ellas, orquestando diferentes respuestas. Además, el sistema inmune está involucrado tanto en el desarrollo como en la eliminación de muchas enfermedades, tales como infecciones, procesos inflamatorios, enfermedades autoinmunes y cáncer. Por ello, desde un punto de vista terapéutico, la modulación del sistema inmune es extraordinariamente importante para prevenir o tratar un gran número de enfermedades.

Las nanopartículas (NPs) son sistemas versátiles que pueden ser empleados para modular una respuesta inmune, ya sea disminuyendo la inflamación, generando respuestas humorales y celulares más potentes, o a través de la reactivación de las células del sistema inmune para luchar contra el cáncer [1,2]. Las NPs pueden tener tamaños que van desde unos pocos a varios cientos de nanómetros, diferentes propiedades superficiales, y una rigidez y forma variables, propiedades que determinan su interacción con estas células. Al mismo tiempo, las NPs son capaces de transportar uno o más fármacos, y pueden ser modificadas con ligandos capaces de dirigirlas a un órgano, tejido o a una población celular específica [1,2]. Por todo ello, hoy en día se considera que la combinación del conocimiento sobre el papel del sistema inmune en la fisiopatología de diferentes enfermedades, con el de la capacidad diseñar de forma racional nanosistemas con propiedades modulables, puede tener un gran impacto en el tratamiento de enfermedades y, notablemente, de aquéllas en las que el sistema inmune juega un papel relevante.

Nuestro grupo de investigación acumula tres décadas de experiencia en la aplicación de la nanotecnología a la modulación del sistema inmune. Concretamente, en el campo de la vacunación, la actividad del grupo se ha centrado en el diseño de diferentes nanotransportadores adaptados a las necesidades de distintos tipos de antígeno. A principios de los 90, nuestro laboratorio desarrolló NPs de ácido poliláctico y derivados, en el contexto de una vacuna de "dosis única" para el toxoide tetánico [3,4]. Posteriormente, desarrolló NPs y nanocápsulas (NCs) a base de polisacáridos y de polipéptidos para el transporte del toxoide tetánico, antígenos de superficie del virus de la Hepatitis B, o antígenos de *E. coli* uropatogénica [5–14]. Asimismo, en el marco de la inmunoterapia del cáncer, el grupo ha desarrollado diferentes tipos de NCs para transportar citoquinas y polinucleótidos con la finalidad de disminuir la presencia de células supresoras de estirpe mieloide en el microambiente tumoral [15].

Teniendo en cuenta toda nuestra experiencia en la formulación de antígenos, hemos trabajado, en colaboración con la Universidad de Manitoba (Canadá), en el desarrollo de una vacuna formada por péptidos antigénicos asociados a NPs, cuya finalidad es la prevención de la infección por el virus de inmunodeficiencia humana (VIH). La necesidad de una vacuna contra este virus es evidente, teniendo

en cuenta que el VIH sigue siendo una de las enfermedades infecciosas más mortales, y que carece de una vacuna preventiva [16]. Por lo tanto, el primer objetivo de esta tesis ha sido el diseño y desarrollo de NPs a base de polisacáridos capaces de asociar un antígeno peptídico contra el VIS (equivalente simio al VIH), con la idea de generar una respuesta inmune potente frente al virus.

1. Desarrollo de NPs polisacarídicas para la modulación de la respuesta inmune contra un antígeno peptídico del VIS

El desarrollo de una vacuna efectiva contra el virus del VIH ha demostrado ser un gran desafío, especialmente debido a las características especiales de este virus. De hecho, el VIH infecta a las células T CD4, que juegan un papel importante en el desarrollo de la respuesta inmune adquirida. Por otro lado, este virus muta rápidamente, lo que lleva a una activación ineficiente del sistema inmune. Además, las diferentes cepas del virus son altamente variables, hecho que complica aún más la generación de una respuesta inmune amplia y protectora [17].

En este trabajo, nuestra estrategia para el diseño de una vacuna contra el VIH ha sido emplear como antígenos las secuencias peptídicas que flanquean los doce puntos de corte de la proteasa del virus (PCSs, por sus siglas en inglés) (**Fig. 1**). Estos doce puntos son aquéllos en los que la proteasa corta las proteínas del virus Gag, Pol y Nef, obteniendo así las estructuras necesarias para la que los viriones sean infectivos [18–20]. La proteólisis de estas proteínas debe tener lugar en los doce puntos de manera controlada y secuencial, de forma que si el proceso se ve interrumpido, aunque solo sea en un punto, se podría evitar la infección [18,19,21]. Otra ventaja de usar dichos antígenos es que estas secuencias están muy conservadas entre las distintas cepas del virus, por lo que su mutación no disminuiría la efectividad de la vacuna [18–21]. Previamente, los doce antígenos peptídicos del VIS fueron encapsulados en NPs de quitosano (CS) y sulfato de dextrano (DS) por complejación iónica. Estas NPs fueron administradas a primates no-humanos que habían sido también vacunados con vectores virales codificando las secuencias de los doce péptidos. En este estudio se observó que los niveles de inmunoglobulinas G (IgGs) contra los péptidos aumentaron de manera significativa tras la administración nasal de las NPs [22,23].

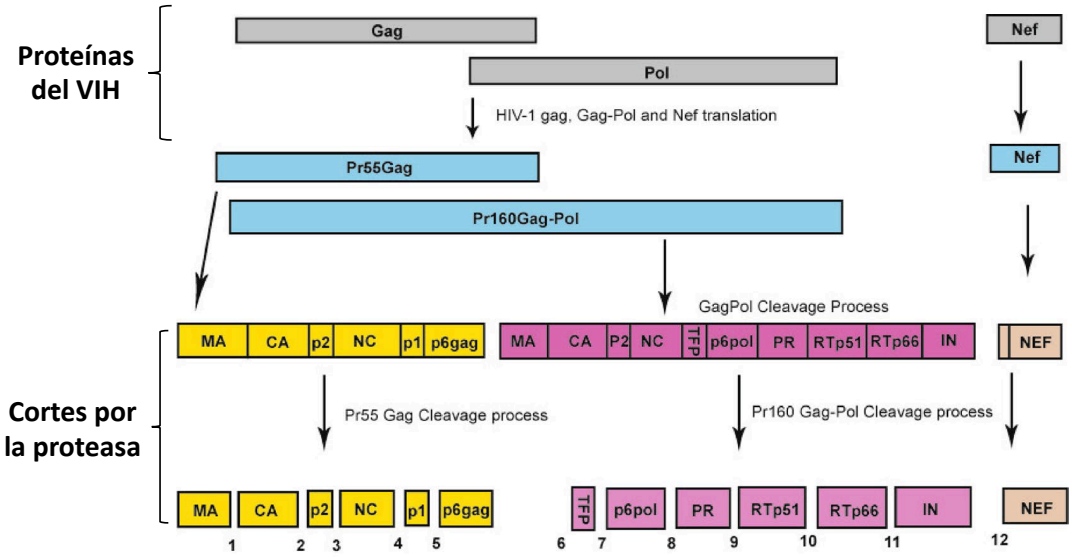

Figura 1. Fragmentos de las proteínas Gag, Pol y Nef del VIH producidos como consecuencia de su corte por la proteasa del virus. Los doce antígenos peptídicos (1–12) son secuencias de 20 aminoácidos que flanquean estos doce puntos, (diez aminoácidos anteriores y diez posteriores a cada punto). Imagen adaptada y modificada de [19], reproducido bajo una licencia *Creative Commons Attribution 4.0 International License* http://creativecommons.org/licenses/by/4.0/.

En base a esta información, el objetivo principal de este trabajo fue evaluar si el tipo de unión química de uno de los doce péptidos (PCS5, usado como modelo) a las NPs, y la presencia del adyuvante poly(I:C) en la formulación, podrían aumentar la inmunogenicidad del péptido en comparación con su asociación a las NPs por fuerzas iónicas. Nuestra hipótesis fue que la conjugación química del antígeno a los polisacáridos podría prevenir su liberación prematura hasta que las partículas fuesen capturadas por las células presentadoras de antígenos (APCs, por sus siglas en inglés), mejorando y prolongando así la respuesta inmune generada. El CS y el ácido hialurónico (HA) fueron los polisacáridos seleccionados para unir a ellos el antígeno peptídico PCS5. Además, el agonista del receptor 3 de tipo *toll* (TLR3), poly(I:C), fue incorporado a dos de los nanosistemas desarrollados para mejorar la respuesta celular contra el antígeno [7,24–26]. Como formulación comparativa se emplearon las NPs a base de CS y DS en las que el péptido PCS5 está asociado por interacciones iónicas. La selección se basó en resultados previos sobre el potencial de dichas nanopartículas como transportadores de estos antígenos a través de la mucosa [22,23]. Las propiedades fisicoquímicas de los conjugados polímero–PCS5 y las NPs preparadas fueron analizadas a través de diferentes técnicas. Finalmente, la capacidad de estas NPs para generar una respuesta inmune contra en antígeno fue evaluada en ratones, midiendo los niveles de anticuerpos, la activación de APCs y de células T.

1.1. Desarrollo de NPs a base de polisacáridos cargadas con un antígeno peptídico del VIS

Los polisacáridos, y en especial el CS, han sido ampliamente utilizados como biomaterial para el diseño de transportadores de antígenos [27–29]. De hecho, nuestro grupo ha desarrollado nanosistemas a base de CS para el transporte de una gran variedad de antígenos tanto por vía parenteral como por vía nasal [6,7,30–32]. Otros autores también han empleado nanosistemas a base de DS [27,33–35] o de HA [36–41], ambos polisacáridos de carga negativa, con el fin de mejorar la respuesta inmune. En la mayoría de estos estudios, la asociación del antígeno a las NPs estaba basada en un simple proceso de asociación por interacciones iónicas entre polímeros y antígenos. Sin embargo, nuestro objetivo en este trabajo se centró en conjugar covalentemente el péptido PCS5 a las NPs, para conseguir una presentación más sostenida y mejorada del antígeno a las células del sistema inmune.

Usando el método de preparación de las NPs de CS/DS descrito previamente [22], el péptido PCS5 fue asociado a las NPs ajustando las interacciones entre el péptido y el polímero catiónicos (PCS5 y CS), con el polímero de carga negativa (DS) (**Fig. 2A**).

Para el desarrollo de los nuevos prototipos donde la unión del péptido PCS5 a los polímeros es mediante enlace covalente, se procedió, en primer lugar, a la conjugación del péptido antigénico al CS a través de un enlace oxima. Seguidamente, el conjugado CS–PCS5 obtenido fue empleado para formar NPs mediante interacciones iónicas con el DS, en las que el adyuvante poly(I:C) fue también incorporado (**Fig. 2B**). Finalmente, para el tercer prototipo, la conjugación de PCS5 al HA fue realizada mediante un enlace tioéter, degradable en medios ricos en tioles libres, como el citoplasma (con grandes cantidades de glutatión) [42]. En este caso, las NPs se formaron a partir de las interacciones iónicas entre el conjugado HA–PCS5 y el CS, incorporando también el adyuvante poly(I:C) (**Fig. 2C**). En ambos nanosistemas, se esperaba también que la unión covalente ayudase a exponer al antígeno en la superficie de las NPs. Esta exposición en superficie, supuestamente, debería facilitar la presentación del antígeno a las células B, mejorando la respuesta humoral frente al mismo [43,44]. El análisis por espectrometría de fotoelectrones inducidos por rayos X confirmó la presencia de PCS5 en la superficie de las NPs de CS/HA–PCS5/pIC.

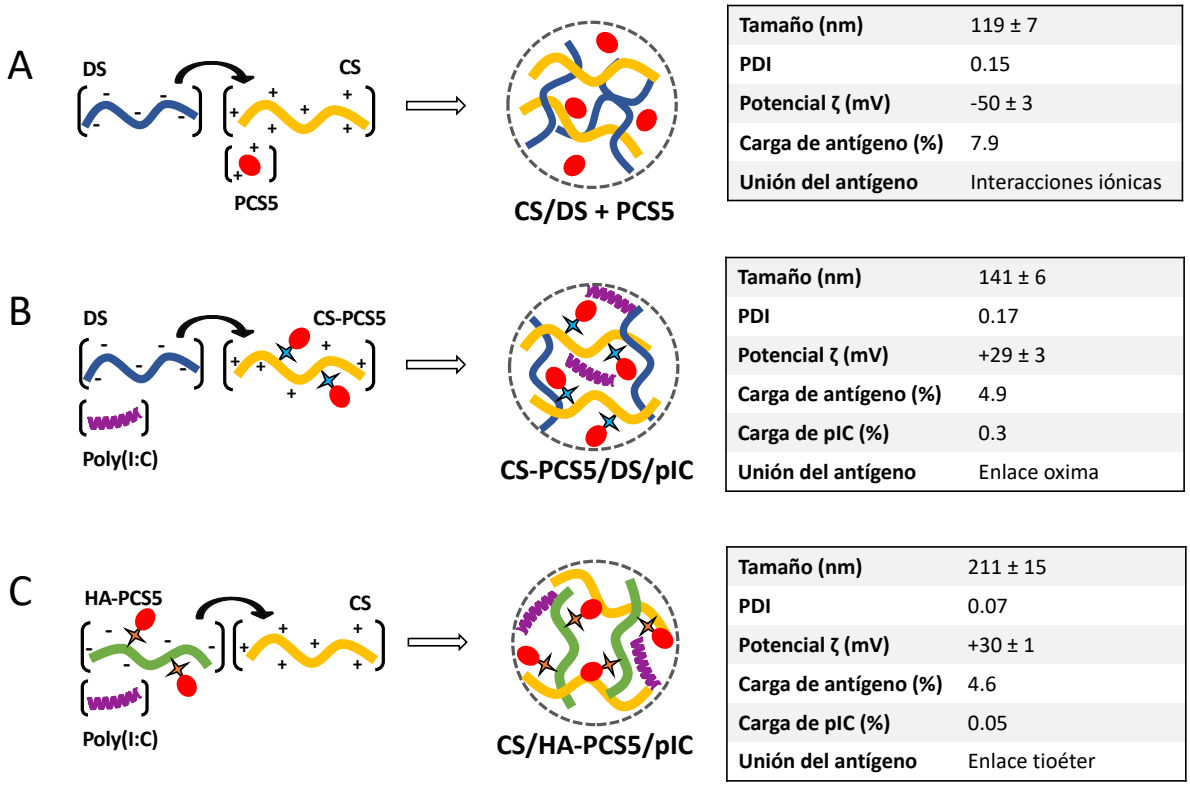

Tamaño (nm)	119 ± 7
PDI	0.15
Potencial ζ (mV)	-50 ± 3
Carga de antígeno (%)	7.9
Unión del antígeno	Interacciones iónicas

Tamaño (nm)	141 ± 6
PDI	0.17
Potencial ζ (mV)	+29 ± 3
Carga de antígeno (%)	4.9
Carga de pIC (%)	0.3
Unión del antígeno	Enlace oxima

Tamaño (nm)	211 ± 15
PDI	0.07
Potencial ζ (mV)	+30 ± 1
Carga de antígeno (%)	4.6
Carga de pIC (%)	0.05
Unión del antígeno	Enlace tioéter

Figura 1. **Composición de los diferentes nanosistemas desarrollados en este trabajo.** Representación esquemática del proceso de preparación de los tres sistemas: (A) NPs de CS/DS + PCS5, (B) NPs de CS–PCS5/DS/pIC, y (C) NPs de CS/HA–PCS5/pIC, junto con sus propiedades fisicoquímicas. CS, quitosano; DS, sulfato de dextrano; HA, ácido hialurónico; NPs, nanopartículas; PCS5, punto 5 de corte de la proteasa; PDI, índice de polidispersión; pIC, poly(I:C).

Con el objetivo de mejorar la estabilidad a largo plazo de las NPs con antígeno, cada una de las formulaciones fue liofilizada empleando trehalosa como crioprotector. Finalmente, se seleccionó un 7% de trehalosa como concentración óptima para las NPs de CS/DS + PCS5 y de CS/HA–PCS5/pIC; mientras que para las NPs de CS–PCS5/DS/pIC, un 4% de trehalosa fue suficiente para una correcta liofilización.

1.2. Liberación de PCS5 a partir del enlace covalente

Teniendo en cuenta que nuestro objetivo era comparar dos tipos de enlaces covalentes, también se estudió el modo de liberación del PCS5 a partir de las NPs conteniendo dichas uniones. En el caso del conjugado CS–PCS5, la unión del péptido fue realizada a través de un enlace oxima, estable a pH fisiológico [45–47]. Por lo tanto, se esperaría que el antígeno fuese liberado durante el procesamiento por las APCs. Por otro lado, en el caso del conjugado HA–PCS5, el enlace tioéter sufriría, previsiblemente, reacciones retro-Michael en presencia de tioles libres [42,48,49], los cuales están presentes en grandes cantidades en el citoplasma de las células en forma de glutatión (GSH). En

consonancia con esto, los resultados *in vitro* mostraron que el péptido PCS5 solo se liberaba de las NPs de CS/HA–PCS5/pIC en presencia de GSH, y no en medio sin tioles libres (como en tampón fosfato salino). Por lo tanto, en este caso se espera que el péptido no se libere en el medio extracelular, y sólo una vez dentro de la célula donde hay grandes cantidades de GSH [50,51].

1.3. Evaluación de la respuesta inmune generada *in vivo* en diferentes modelos animales

1.3.1. Respuesta inmune en ratones

Con respecto a la respuesta humoral, en general, los niveles de inmunogobulinas G (IgGs) generados tras la vacunación con las distintas NPs aumentaron de manera significativa con el tiempo, alcanzando valores máximos en la última semana de estudio (semana 16) (**Fig. 3A**). En este punto, los niveles de anticuerpos anti-PCS5 detectados tras la vacunación con los distintos nanosistemas fueron hasta tres veces superiores que los valores detectados en ratones control (sin vacunar). Esta elevada y sostenida respuesta humoral tiene un gran interés en el caso del diseño de vacunas contra el VIH, ya que se considera que niveles constantes de anticuerpos son importantes para una vacunación efectiva [52]. La respuesta obtenida concuerda con otros estudios de NPs cargadas con antígenos, en los que se vio que los niveles de IgGs contra los antígenos permanecían en valores elevados hasta 28 y 37 semanas tras la inmunización [12,13]. Teniendo esto en cuenta, es posible que a semanas posteriores nuestras NPs también generasen niveles elevados de anticuerpos anti-PCS5.

Sin embargo, estos resultados indican que, en este caso, el enlace covalente entre péptido y NPs no tuvo un efecto en la respuesta humoral, lo cual contrasta con otros estudios donde la conjugación sí mejoró la respuesta humoral en comparación con las interacciones iónicas [43,53].

La activación de las APCs se midió a través de los niveles de expresión de las señales co-estimuladoras de células T: CD40 y CD86 [54–56]. En el caso de los niveles de CD40 en macrófagos, el nanosistema con HA generó una mayor expresión de esta señal, en comparación con los ratones no vacunados y con los otros tratamientos (**Fig. 3B**). En el caso de CD86, las dos formulaciones con enlace covalente y poly(I:C) incrementaron su expresión en macrófagos (**Fig. 3C**). Estos resultados podrían indicar que la conjugación mejora la respuesta inmune, en comparación con las interacciones iónicas. De todas formas, no podemos descartar que el poly(I:C) también haya podido jugar un papel en esta activación [57].

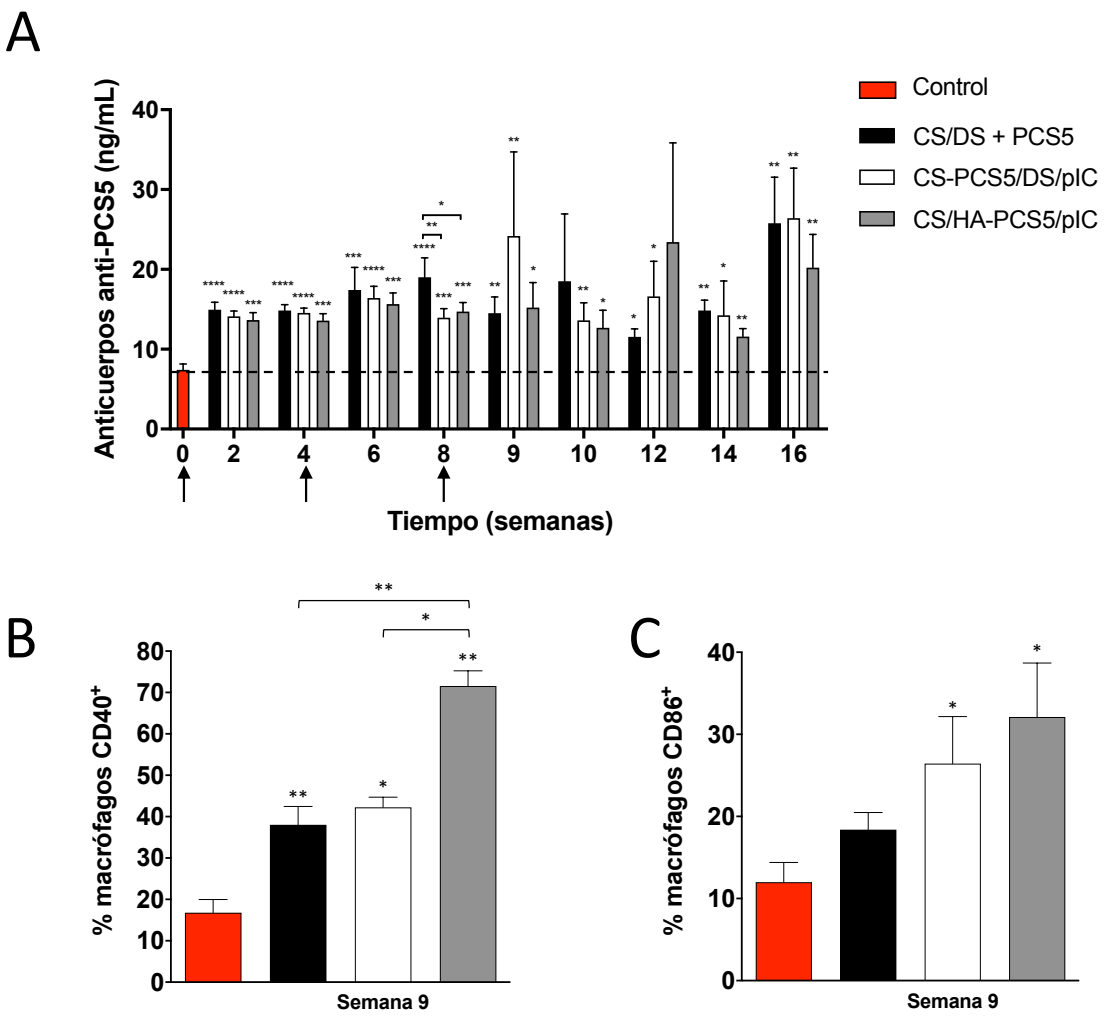

Figura 3. Evaluación *in vivo* de las NPs. (A) Niveles de anticuerpos anti-PCS5 tras la administración intramuscular de las tres nanoformulaciones. (B, C) Expresión de los factores co-estimuladores CD40 y CD86 en macrófagos a las 9 semanas post-administración. Las barras representan los valores en los ratones no tratados (barras rojas), y en los vacunados con: CS/DS + PCS5 (barras negras), CS–PCS5/DS/pIC (barras blancas), y CS/HA–PCS5/pIC (barras grises). Los valores representan la media ± SEM (n ≥ 5). El análisis estadístico fue hecho con una prueba Mann-Whitney. Las diferencias significativas entre los grupos están representadas como * ($p < 0.05$), ** ($p < 0.01$), *** ($p < 0.001$) y **** ($p < 0.0001$). CS, quitosano; DS, sulfato de dextrano; HA, ácido hialurónico; NPs, nanopartículas; PCS5, punto 5 de corte de la proteasa; pIC, poly(I:C).

Por último, la capacidad de activar las células T fue determinada a través de los niveles de secreción de IL-2 y TNFα. En este sentido, todas las formulaciones activaron las células T CD4 y CD8, pero con arreglo a diferentes patrones de secreción. Así, las NPs de CS/DS + PCS5, basadas en interacciones iónicas, activaron las células T a tiempos cortos (a las 10 semanas). La formulación de CS/HA–PCS5/pIC, con el enlace degradable en presencia de GSH, generó niveles más sostenido de activación de células T (de las semanas 12 a la 16). Finalmente, las NPs con el enlace más estable (CS—PCS5/DS/pIC) indujeron mayores secreciones de estas citoquinas en la semana 9, y especialmente en la 16 (**Fig. 4**). Este patrón de secreción podría ser causado por las diferentes cinéticas de liberación del antígeno

PCS5 a partir de cada nanosistema. En este punto es importante destacar que esta activación más lenta de células T, en comparación con otras vacunas, ha sido también descrita en el caso de una vacuna de VIH con ARNm [58], resultados que plantean la pregunta sobre cuál es el perfil ideal de activación de células T en una vacuna contra el VIH. La posible correlación entre los perfiles de activación de células T y la eficacia de protección es un aspecto que deberá ser estudiado en mayor profundidad, y preferiblemente en modelos animales de mayor tamaño.

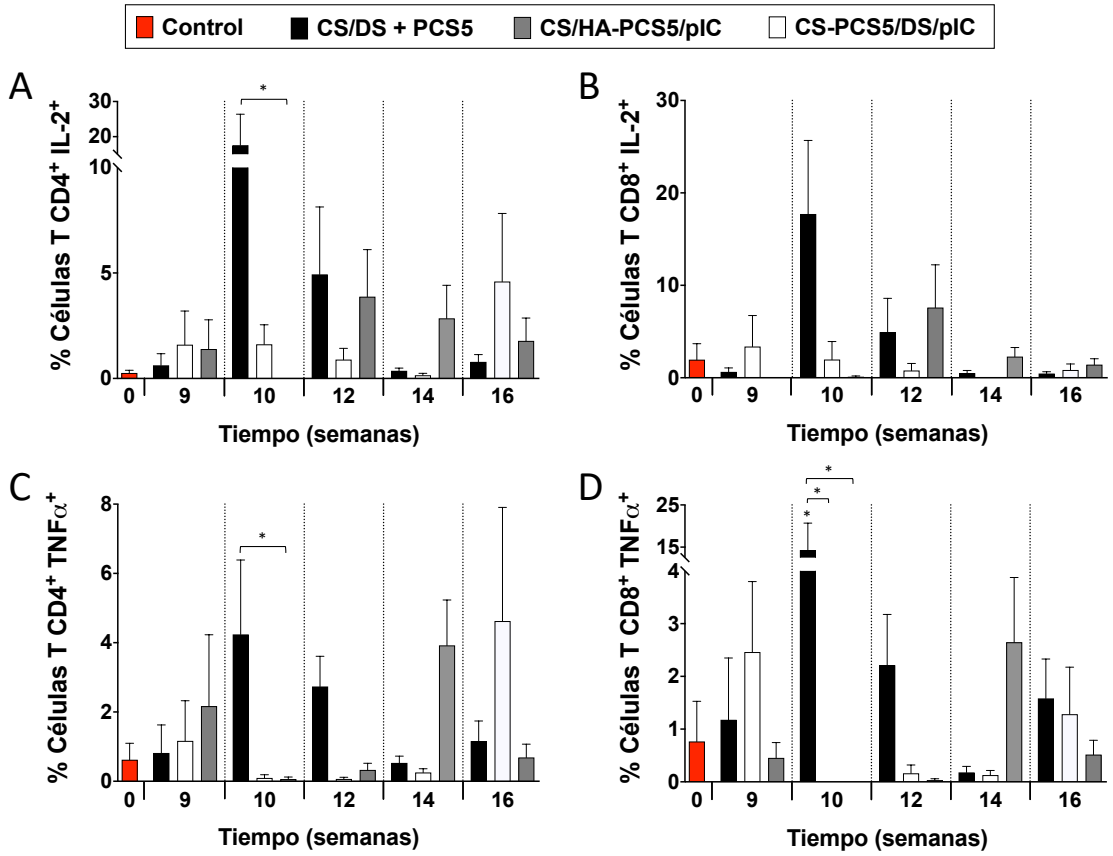

Figura 4. Activación de células T CD4 y CD8. Secreción de IL-2 y TNFα en células T (A, C) CD4 y (B, D) CD8, cuantificado por FACS. Las barras representan los valores en los ratones no tratados (barras rojas), y en los vacunados con: CS/DS + PCS5 (barras negras), CS–PCS5/DS/pIC (barras blancas), y CS/HA–PCS5/pIC (barras grises). Los valores representan la media ± SEM (n ≥ 5). El análisis estadístico fue hecho con una prueba Mann-Whitney. Las diferencias significativas entre los grupos están representadas como * ($p < 0.05$), ** ($p < 0.01$), *** ($p < 0.001$) y **** ($p < 0.0001$). CS, quitosano; DS, sulfato de dextrano; HA, ácido hialurónico; NPs, nanopartículas; PCS5, punto 5 de corte de la proteasa; pIC, poly(I:C).

En resumen, en esta parte del trabajo se desarrollaron diferentes composiciones de NPs a base de polisacáridos, cargadas con un antígeno peptídico frente al VIS, PCS5. Los resultados demuestran que factores como el tipo de interacción antígeno–NPs (iónica, por enlace covalente estable o degradable), la presencia de adyuvantes como el poly(I:C), o incluso la naturaleza de los polímeros que las conforman (CS, DS o HA), pueden influir de manera destacada en el tipo de respuesta inmune

generada. En este caso, todos los nanosistemas fueron capaces de generar niveles de anticuerpos anti-PCS5 importantes, mientras que la cinética de activación de las células T fue diferente para cada vacuna. Estudios en modelos animales superiores podrán determinar si estas respuestas humorales y celulares se traducirían en una protección eficaz.

1.3.2. Respuesta inmune en primates no humanos

Finalmente, se seleccionaron dos de las NPs previamente desarrolladas para su administración combinada en un estudio en primates no humanos, dado que este es un mejor modelo para estudios de vacunación [59]. Por una parte, se eligieron las NPs de CS/DS teniendo en cuenta su capacidad para generar una pronta respuesta celular en ratones [60]. Además, la composición de esta NPs es la misma que la de las NPs usadas en la formulación de referencia que contiene los doce PCSs, y que ha generado una buena respuesta inmune en primates [22,23]. Dado que estas NPs ya habían sido administradas por vía intranasal (i.n.) con el objetivo de aumentar la protección en mucosas, la misma ruta se mantuvo en este nuevo estudio. Por otra parte, también se seleccionó el prototipo compuesto por las NPs de CS/HA/pIC, en base a su capacidad para generar una moderada pero sostenida activación de células T en ratones [60]. Estas NPs se administraron por vía intramuscular (i.m.), con el objetivo de generar una respuesta inmune sistémica. Con relación a la selección de los antígenos, nuestro objetivo fue el de evaluar el potencial de una vacuna conteniendo un número pequeño de antígenos PCSs. Por lo tanto, en lugar de usar los doce péptidos inicialmente descritos, seleccionamos el péptido PCS5 usado en la evaluación en ratones, y los péptidos PCS2 y PCS12. Esta selección fue hecha en base a que se ha visto que mutaciones entorno a estas secuencias PCS son capaces de dificultar la replicación del VIH, dificultando la capacidad del virus para replicarse (resultados no mostrados).

Tras la formulación de las NPs con los tres PCSs, y de la adaptación del proceso de liofilización, se procedió al estudio de la eficacia de la prevención de la infección con VIS en primates. En este estudio también se evaluó la eficacia de la formulación de referencia, formada por NPs de CS/DS asociando los doce PCSs, junto con los vectores virales (virus de la estomatitis vesicular recombinante) codificando las secuencias de estos doce PCSs (rVSV + Nano, 12 PCSs) [61].

La combinación de las NPs de CS/DS y de CS/HA/pIC asociando los tres péptidos (Nano, 3 PCSs) fue administrada a ocho primates hembra. Cada animal recibió, en cada inmunización, las NPs de CS/DS por vía i.n. y las NPs de CS/HA/pIC por vía i.m., cada cuatro semanas, para un total de cuatro dosis de cada vacuna (**Fig. 5A**). En paralelo, la formulación de referencia formada por los doce péptidos contenidos en los vectores virales y en las NPs (rVSV + Nano, 12 PCSs) también fue administrada a ocho

primates hembra. En este grupo, cada animal recibió primero un *prime* con los rVSVs i.m., para luego ser inmunizados con una combinación de los vectores virales i.m. y las NPs i.n. (en los *boost* 1 y 3), de las NPs solas por vía i.n. (en el *boost* 2), o de los vectores virales solos por vía i.m. (en el *boost* 4). (**Fig. 5B**) [61]. En ambos casos, los animales fueron sometidos a desafíos con el VIS cada dos semanas, y los niveles virales en sangre monitorizados.

En la **Figura 5** se observa el número de animales vacunados no infectados tras cada desafío con el VIS, en comparación con los animales del grupo control. En el caso de la formulación de referencia a base de los doce péptidos (rVSV + Nano, 12 PCSs), tras siete desafíos intravaginales con el virus, el 75% de los primates permanecieron no infectados, frente al 25% del grupo control [61]. En el caso de la combinación de las NPs con los tres PCSs (Nano, 3 PCSs), un 50% de los animales no se infectaron tras estos siete desafíos con el virus.

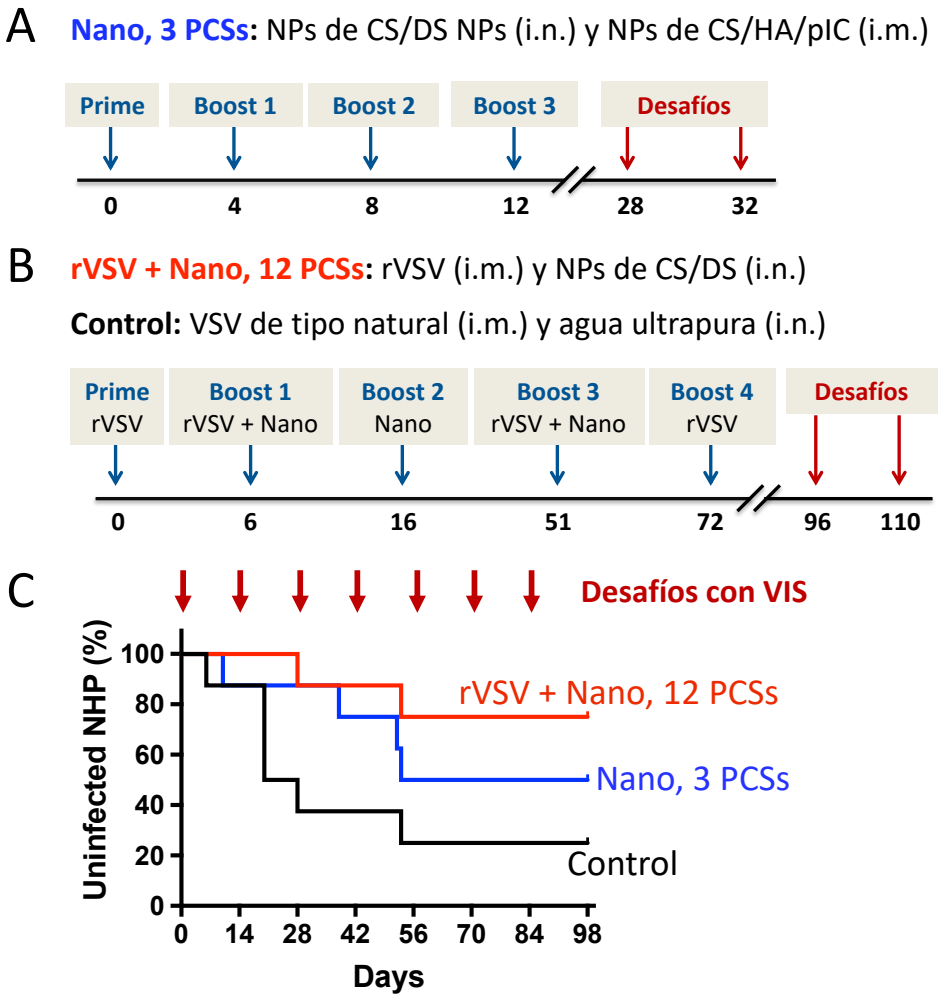

Figura 5. **Estudio de eficacia de protección frente a desafíos con el VIS de las vacunas descritas**. (A–B) Grupos de vacunación, esquema de la administración y de los desafíos para (A) la combinación de las nanopartículas de CS/DS y de CS/HA/pIC con los tres PCSs, administradas por vía intranasal e intramuscular, respectivamente; y de (B) la formulación de referencia formada por los vectores virales y las NPs de CS/DS con los doce PCSs, administradas por vía intramuscular e intranasal, respectivamente. (C) Primates no humanos fueron vacunados con las NPs de CS/DS y de CS/HA/pIC con los tres PCSs (Nano, 3 PCSs; en azul); con la formulación de referencia con los doce PCSs en vectores virales y nanopartículas de CS/DS (rVSV + Nano, 12 PCSs; en rojo) [61]; o con el control de los vectores virales naturales y agua (Control; en negro) [61]. Porcentaje de animales no infectados tras siete desafíos intravaginales con el VIS. CS, quitosano; DS, sulfato de dextrano; HA, ácido hialurónico; i.m., intramuscular; i.n., intranasal; NPs, nanopartículas; PCS, punto de corte de la proteasa; rVSV, virus de la estomatitis vesicular recombinante; VIS, virus de inmunodeficiencia en simios.

Estos resultados preliminares en primates apoyan la idea de que una vacuna conteniendo tres de los doce PCSs y con ninguna de las proteínas completas Env, Gag o Pol, es una estrategia que puede retrasar la adquisición del virus y prevenir la infección de forma moderada. Es importante destacar que esta formulación contiene péptidos poco inmunogénicos, y solo tres de los doce péptidos descritos para dificultar la maduración del virus [18,19]. De hecho, la formulación con los doce PCSs y con un vector muy inmunogénico (rVSV + 12PCSs), generaron prometedores resultados para la prevención del

VIS [61]. Por lo tanto, es posible que una mejor selección de los péptidos, o un aumento de su número, mejore la potencia de una esta vacuna basada en NPs. Además, la incorporación de adyuvantes adicionales podría ayudar a mejorar los niveles de protección. En conjunto, consideramos que hay un margen de mejora para optimizar esta formulación con el fin de obtener una potente vacuna contra el VIS basada en NPs asociando un bajo número de antígenos.

Teniendo en cuenta estos prometedores resultados en primates con las NPs de CS/DS, nuestro siguiente objetivo ha sido adaptar el proceso de fabricación de estas NPs a base de polisacáridos para su producción a nivel industrial en una planta piloto.

2. Desafíos tecnológicos en el desarrollo preclínico de una nanovacuna frente al VIH

En base a estos prometedores resultados en primates, el objetivo en esta parte del trabajo fue el de optimizar y adaptar la nanoformulación basada en interacciones iónicas entre el CS y el DS, con la finalidad de producirla en una planta piloto para su uso en preclínica y, posteriormente, en ensayos clínicos. La vacuna original está compuesta por doce antígenos peptídicos contra los doce PCSs del VIS, encapsulados dentro de NPs de CS/DS [22,23,61]. Dado que el proceso de formulación es el mismo para cada uno de los doce péptidos, uno de ellos (PCS5) fue seleccionado para su transferencia tecnológica, a modo de antígeno modelo.

Hoy en día, la complejidad de los nanosistemas, y la falta de métodos analíticos estandarizados que permitan su correcta y completa caracterización, ha frenado la llegada de más nanomedicinas al mercado [62]. De hecho, se han descrito importantes diferencias entre las mismas NPs preparadas en un laboratorio o a nivel industrial [63]. Por lo tanto, es importante emplear métodos analíticos que caractericen de forma exhaustiva y complementaria las NPs, garantizando su reproducibilidad. Así, nuestro objetivo fue establecer los requisitos más importantes para que una nanovacuna pueda llegar con mayor facilidad a la industria.

En primer lugar, empleamos una estrategia basada en la “calidad desde el diseño” (QbD, por sus siglas en inglés), a través de la cual se establecen tanto las especificaciones del producto final, como los atributos críticos para su calidad. Además, a través de un diagrama de Ishikawa también se identificaron los parámetros del proceso de fabricación de las NPs que podrían tener un mayor impacto en sus propiedades finales. Tal y como se ha descrito en la sección anterior, estas NPs son preparadas mediante la técnica de complejación iónica de los componentes de carga positiva (el CS y el péptido PCS5), con el polímero cargado negativamente (DS) (**Fig. 6A**). Estudiando la influencia de cada uno de

los parámetros del proceso de formulación, se pudo determinar que la etapa crítica en el proceso de formulación es la velocidad de adición de la disolución de DS sobre la fase de CS+PCS5.

Con respecto a los métodos analíticos para la caracterización de las NPs, las técnicas basadas en la dispersión dinámica de luz (DLS, por sus siglas en inglés) son métodos rápidos y sencillos para determinar el tamaño de partícula, pero presentan varias desventajas [64,65]. Por ello, su combinación con otras técnicas complementarias como la microscopía, o el análisis de seguimiento de nanopartículas (NTA, por sus siglas en inglés) es recomendado por las diferentes agencias regulatorias [65]. En nuestro caso, al aplicar todas estas técnicas para la caracterización de las NPs, se obtuvieron valores comparables de tamaño y dispersión de las NPs (**Fig. 6B–E**). En el caso de la formulación liofilizada, también se obtuvieron valores reproducibles con las distintas técnicas mencionadas. Además, se observó que la liofilización del nanosistema fue capaz de mantener la estabilidad a largo plazo de la formulación hasta 15 meses, tanto a temperatura ambiente como en nevera, en las diferentes condiciones de almacenamiento recomendadas por el Consejo Internacional de Armonización de los requisitos técnicos para el registro de medicamentos de uso humano (ICH).

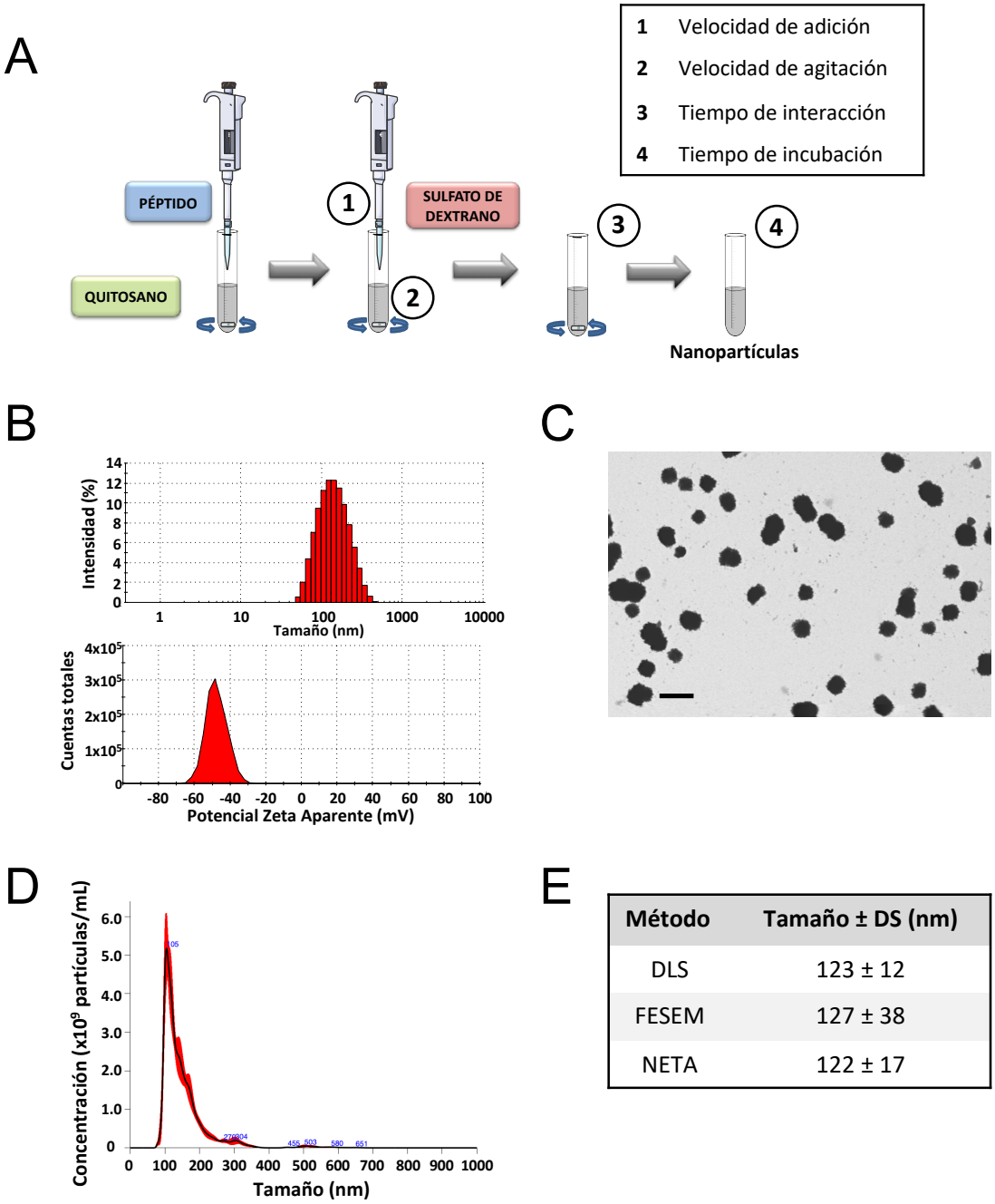

Figura 6. Preparación y caracterización de las nanopartículas. (A) Proceso de obtención de las nanopartículas. El antígeno peptídico es añadido sobre la solución de quitosano, dejándolos en agitación durante 5 min. Después, (1; velocidad de adición), la disolución de sulfato de dextrano se adiciona sobre la fase de carga positiva, (2; velocidad de agitación) bajo agitación magnética. (3; tiempo de interacción) Los componentes se dejan interactuar bajo agitación, para finalmente (4; tiempo de incubación) dejarlos incubar en ausencia de agitación (4). (B–D) Caracterización fisicoquímica de las nanopartículas usando técnicas complementarias. (B) Histogramas de intensidad del tamaño de partícula obtenido por DLS (imagen superior) y de los valores de la carga superficial (imagen inferior). (C) Imágenes de microscopía de las nanopartículas por FESEM (la barra de tamaño representa 200 nm). (D) Distribución de tamaño obtenido por NTA. (E) Resumen del tamaño de partícula medio obtenido por las tres técnicas complementarias. DLS, dispersión de luz dinámica; FESEM, microscopía electrónica de barrido de emisión de campo ; NTA, análisis de seguimiento de nanopartículas.

Como se indicó previamente, garantizar la reproducibilidad del proceso de fabricación de las NPs en diferentes laboratorios es un aspecto crítico para la correcta traslación del producto. En este sentido, el proceso de formulación de las NPs fue transferido a tres laboratorios diferentes con personal distinto, y los lotes de NPs producidos (de 1.65 a 200 mL) fueron caracterizados y comparados. En los tres centros, las propiedades fisicoquímicas de los lotes estaban dentro de las especificaciones previamente indicadas. Además, el escalado pudo realizarse a través de técnicas de microfluídica, y de producción discontinua en lotes. Finalmente, se llevó a cabo la preparación de un lote de 200 mL de formulación en la planta piloto, bajo condiciones de buenas prácticas de fabricación (BPF). En este sentido, tanto los procesos de producción, como los materiales y el flujo de trabajo del personal, fueron diseñados en condiciones cualificadas siguiendo las guías de BPF. Este lote de NPs fue liofilizado y caracterizado, y todas sus propiedades fisicoquímicas cumplieron con los atributos de calidad previamente establecidos (**Tabla 1**). Por lo tanto, la traslación de esta nanovacuna del laboratorio a un ambiente industrial fue realizada con éxito.

Tabla 1. Propiedades fisicoquímicas de la nanovacuna fabricada en la planta piloto.

Muestra	Tamaño (nm)	PDI	Potencial ζ (mV)	pH	Trasmitancia (%)	Osmolalidad (mosm/kg)
Formulación final	150 ± 1	0.13	-42 ± 1	6.6	7.2	186

PDI, índice de polidispersión.

En conclusión, hemos demostrado la posibilidad de producir esta nanovacuna contra el VIS en un ambiente industrial. Aplicando una estrategia de QbD, los aspectos con un mayor efecto sobre los atributos de la formulación fueron determinados. Además, hemos visto la importancia de combinar técnicas complementarias para garantizar una caracterización completa y realista del producto final. Finalmente, la reproducibilidad y escalabilidad de la formulación demuestran que esta nanomedicina estaría lista para ser trasladada a una fabricación industrial.

Por último, un objetivo diferente de esta tesis, pero en línea con nuestro interés por el potencial de la nanotecnología para la modulación del sistema inmune, fue la reactivación del sistema inmune para en el contexto del cáncer. Para ello, empleamos una molécula conocida, el agonista del receptor TLR3, poly(I:C). Esta molécula es un ARN de doble cadena que al interaccionar con su receptor aumenta la expresión de genes de IFN [66]. Esta activación genera estados proinflamatorios, que en el caso de los macrófagos asociados a tumores (TAMs, por sus siglas en inglés), son reactivados y pueden luchar de nuevo contra las células tumorales [67]. Así pues, el objetivo final de esta tesis fue el diseño y desarrollo de nanocomplejos de poly(I:C) con propiedades modulables, que permitan su direccionamiento a macrófagos, y su consiguiente polarización a estados proinflamatorios.

3. Nanocomplejos a base de arginina cargados con poly(I:C) para la reeducación de TAMs

A pesar del conocido potencial de poly(I:C) para polarizar macrófagos hacia un perfil M1, y su consecuente actividad antitumoral [68], su administración sistémica presenta importantes efectos secundarios [25]. En la actualidad, se ha descrito que el nanocomplejo del poly(I:C) con el polímero catiónico polietilenimina (PEI) ha resultado efectivo en diferentes modelos tumorales *in vivo* [69], y actualmente se encuentra en ensayos clínicos de fase I [70]. Sin embargo, la PEI también presenta cierta toxicidad sistémica [71]. Por lo tanto, el principal objetivo de este estudio ha sido desarrollar un nanotransportador para el poly(I:C), alternativo a la PEI, dotado con la capacidad de reeducar TAMs, y que podría ser adecuado para su administración sistémica.

3.1. Diseño y desarrollo de los nanocomplejos

Como primer paso para la formulación de poly(I:C), se partió de la nanotecnología recientemente descrita en nuestro grupo basada en la formación de complejos de octaarginina modificada hidrofóbicamente con polinucleótidos [72]. Para ello, se seleccionaron diferentes polímeros catiónicos ricos en arginina, con capacidad de interaccionar con polinucleótidos, a la vez que promover su penetración celular (CPPs, por sus siglas en inglés) [73,74]. Aunque inicialmente se seleccionaron la octaarginina (r8), un laurato de octaarginina (C12r8), y la poliarginina (pArg) para asociar el poly(I:C), solo los dos últimos generaron complejos con el poly(I:C). En el caso de la C12r8, es probable que su cadena hidrofóbica (C12) ayudase a mejorar la estabilidad de los nanocomplejos, en comparación con la r8 [75,76]. Para la pArg, es probable que sus largas cadenas positivas, con un gran número de puntos de interacción, permitiese una mejor interacción con el poly(I:C) que la r8 [77].

Con el fin de mejorar la estabilidad de los nanocomplejos, aplicamos la tecnología previamente descrita por nuestro grupo [78,79], para recubrir los nanocomplejos con ácido poliglutámico peguilado (PEG–PGA) o con HA, obteniendo así nanocomplejos recubiertos (ENCPs, *enveloped nanocomplexes*), con una estabilidad mejorada en medios fisiológicos. En el caso del PEG–PGA, se esperaba que la presencia de PEG en el exterior proporcionase una protección estérica a los ENCPs, aumentando así su estabilidad coloidal [80]. Al mismo tiempo, la combinación de PEG y PGA ya ha demostrado mejorar el acceso pasivo al tumor de NCs recubiertas con dicho polímero [81]. Como resultado de la evaluación de diferentes PEG–PGAs variando (*i*) su conformación (ramificada o dibloque), (*ii*) la longitud de la cadena de PGA, y (*iii*) la densidad de PEG, se observó que únicamente el polímero en forma de dibloque PEG_{20k}–PGA10 era capaz de mejorar la estabilidad de los nanocomplejos tras 24 h de incubación en medio celular. De hecho, este mismo PEG–PGA ya permtió mejorar la estabilidad de nanocomplejos similares a base de C12r8 en estudios previos [78,82]. Estos resultados confirman que esta

combinación particular de unas pocas unidades de PGA (10) con una larga cadena de PEG (de 20 kDa) es útil para conseguir una buena protección estérica.

En el caso del HA, este polímero de carga negativa fue seleccionado en base a sus propiedades *stealth*, aumentando su tiempo de circulación sistémica [83–85]. Además, se ha descrito que la presencia de HA recubriendo nanosistemas podría disminuir la adsorción de proteínas inmunogénicas [86]. En las condiciones estudiadas, los ENCPs de HA y C12r8 no fueron estables tras su incubación en medio celular durante 4 h, mientras que los de HA y pArg mantuvieron sus propiedades fisicoquímicas originales tras 24 h de incubación.

Así pues, los sistemas seleccionados para evaluación *in vitro* fueron los nanocomplejos de pArg y poly(I:C) sin cubierta (pArg:pIC), con cubierta de PEG–PGA (pArg:pIC/PEG–PGA) o de HA (pArg:pIC/HA); y los de C12r8 con cubierta de PEG–PGA (C12r8:pIC/PEG–PGA). Todos ellos presentaron propiedades fisicoquímicas adecuadas, con tamaños inferiores a 200 nm, índices de polidispersión bajos y cargas superficiales variables en función del polímero de la cubierta. En todos ellos los valores de carga de poly(I:C) fueron muy elevados (**Fig. 7A, B**). Además, el poly(I:C) estaba fuertemente unido a ellos, protegiéndolo así de la degradación enzimática en el medio celular (**Fig. 7C–E**).

A

Formulación	Ratio (p/p)	Tamaño (nm)	PDI	Potencial ζ (mV)	Carga de poly(I:C) (%)
pArg:pIC	1:1	163 ± 14	0.20	+44 ± 3	50
pArg:pIC /PEG–PGA	1:1 :3	190 ± 14	0.18	+26 ± 8	20
pArg:pIC /HA	1:1 :1.5	157 ± 10	0.16	-15 ± 7	29
C12r8:pIC /PEG–PGA	4:1 :3	165 ± 14	0.07	+5 ± 1	12.5

Media ± desviación estándar, n ≥ 12. C12r8, laurato de octaarginina; HA: ácido hialurónico; p/p: peso/peso; pArg, poliarginina; PDI, índice de polidispersión; PEG–PGA, ácido poliglutámico peguilado.

B

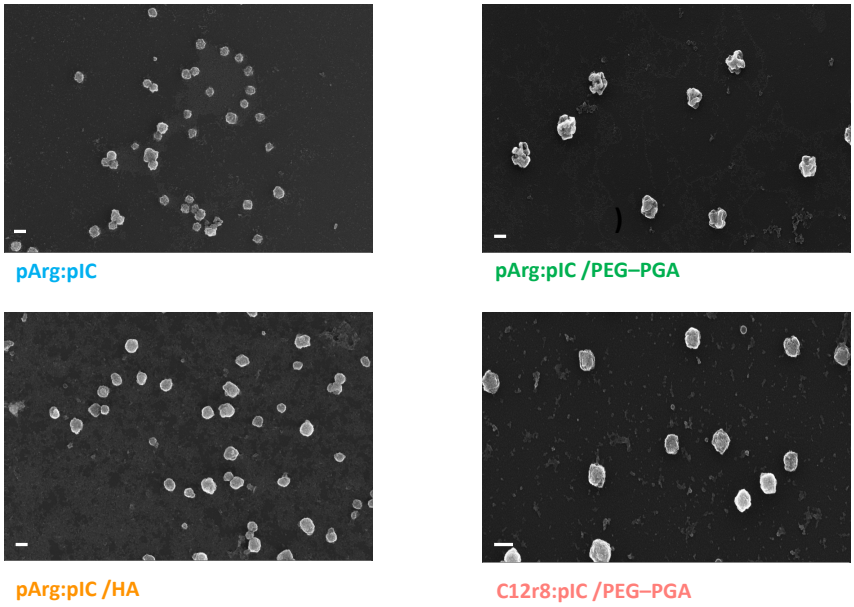

C

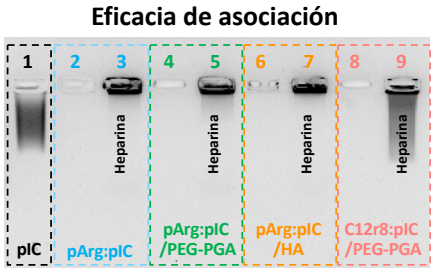

D

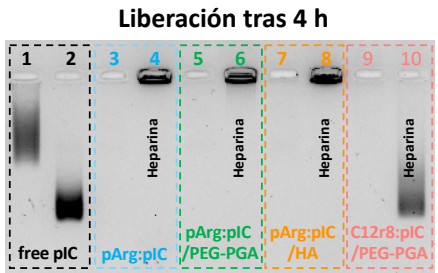

Figura 7. Propiedades fisicoquímicas y eficacia de asociación del poly(I:C) en los nanocomplejos seleccionados. (A) Resumen de las principales propiedades fisicoquímicas de los cuatro nanosistemas, y (B) imágenes de microscopía FESEM de cada uno. Los valores representan la media ± desviación estándar (n ≥ 12). Las barras de tamaño representan 200 nm. (C) Ensayo de desplazamiento en gel de agarosa para evaluar la capacidad de los nanocomplejos de asociar poly(I:C). Carriles: (1) poly(I:C) libre, (2, 4, 6, 8) son los nanocomplejos de pArg:pIC, pArg:pIC/PEG–PGA, pArg:pIC/HA y C12r8:pIC/PEG–PGA, respectivamente; y (3, 5, 7, 9) son los correspondientes nanocomplejos incubados con heparina. (D) Ensayo de desplazamiento en gel de agarosa para evaluar la liberación e integridad del poly(I:C) tras su incubación en medio de cultivo celular a 37 °C durante 4 h. Carriles: (1) poly(I:C) libre en disolución y (2) en medio de cultivo celular; (3, 5, 7, 9) son los nanocomplejos de pArg:pIC, pArg:pIC/PEG–PGA, pArg:pIC/HA y C12r8:pIC/PEG–PGA en medio de cultivo celular; y (4, 6, 8, 10) son los nanocomplejos en las mismas condiciones incubados con heparina. C12r8, laurato de octaarginina; HA, ácido hialurónico; p/p, peso/peso; pArg, poliarginina; PEG—PGA, ácido poliglutámico peguilado; PDI, índice de polidispersión; pIC, poly(I:C). FESEM, microscopía electrónica de barrido de emisión de campo.

3.2. Evaluación de la capacidad de los nanocomplejos de polarizar macrófagos

La diana de los complejos de poly(I:C) es el receptor endosomal TLR3. Para confirmar que el poly(I:C) asociado a los ENCPs alcanzaba este receptor, se realizaron estudios de co-localización para determinar la distribución intracelular de este polinucleótido. Para ello, se emplearon poly(I:C) marcado con el fluoróforo rodamina, y CellLight®, para visualizar la molécula y el endosoma, respectivamente. A través de microscopía confocal se pudo confirmar que, tras 8 h de incubación, una gran parte del poly(I:C) (en rojo) se encontraba en el interior del endosoma (en verde) (**Fig. 8A**).

Una vez confirmado que el receptor diana fue alcanzado, el siguiente paso fue determinar si el poly(I:C) era capaz de activarlo y, por lo tanto, de polarizar macrófagos. Para ello, primero se midió la expresión de diferentes marcadores de superficie asociados a fenotipos M1 proinflamatorios (CD80 y MHC II) o M2 protumorales (CD206 y CD163). En general, apenas se observaron cambios en los niveles de expresión de los receptores tanto en los macrófagos tratados con poly(I:C) libre o asociado al ENCP. Estos resultados están en línea con una publicación reciente sobre la evaluación del poly(I:C) y del imiquimod *in* vitro, en los que se vio una limitada capacidad del poly(I:C) para modular el ratio de receptores M1/M2 en la superficie de macrófagos M0 o M2 [68].

En base a estos datos, se evaluó la capacidad del poly(I:C) para polarizar macrófagos hacia fenotipos tipo M1 a través de ensayos funcionales. En primer lugar, se evaluó la habilidad de los macrófagos para secretar quimoquinas reclutadoras de células T citotóxicas, lo que finalmente favorece la eliminación del tumor [87,88]. En este caso, se observó que los macrófagos que habían sido tratados con los nanocomplejos de poly(I:C) secretaban altas cantidades de CXCL10 y CCL5, en comparación con macrófagos no tratados (**Fig. 8B**). Estos resultados demuestran que, aunque no se observaron cambios en la expresión de los receptores de superficie, otras propiedades antitumorales como el reclutamiento de células T citotóxicas a través de la secreción de quimoquinas, sí se mejoraron tras el tratamiento con los nanocomplejos. Por lo tanto, sería de esperar que, en el microambiente tumoral, y tras el tratamiento con los nanocomplejos, la secreción de estas quimoquinas por parte de los TAMs aumentase, atrayendo células T citotóxicas al tumor.

Además de esta capacidad de activar a otras células del sistema inmune para luchar contra las células cancerígenas, los macrófagos también pueden atacarlas directamente. Por lo tanto, en segundo lugar, se estudió si los nanocomplejos de poly(I:C) eran capaces de reactivar este rasgo característico de los macrófagos proinflamatorios *in vitro*. Para ello, los macrófagos fueron pretratados con los diferentes nanocomplejos, y posteriormente fueron coincubados con células de tumor de páncreas (PANC-1) durante 48 h. Tras este tiempo, la citotoxicidad hacia las células cancerígenas de

los macrófagos tratados con nanocomplejos (30–40%) fue mucho mayor que la de macrófagos M0 o M2 (0 y -15%, respectivamente), aunque ligeramente más baja que la de los macrófagos M1 (60%) (**Fig. 8C**). Estos resultados confirman el gran potencial de los nanocomplejos de poly(I:C) para reeducar macrófagos para luchar de nuevo contra las células tumorales.

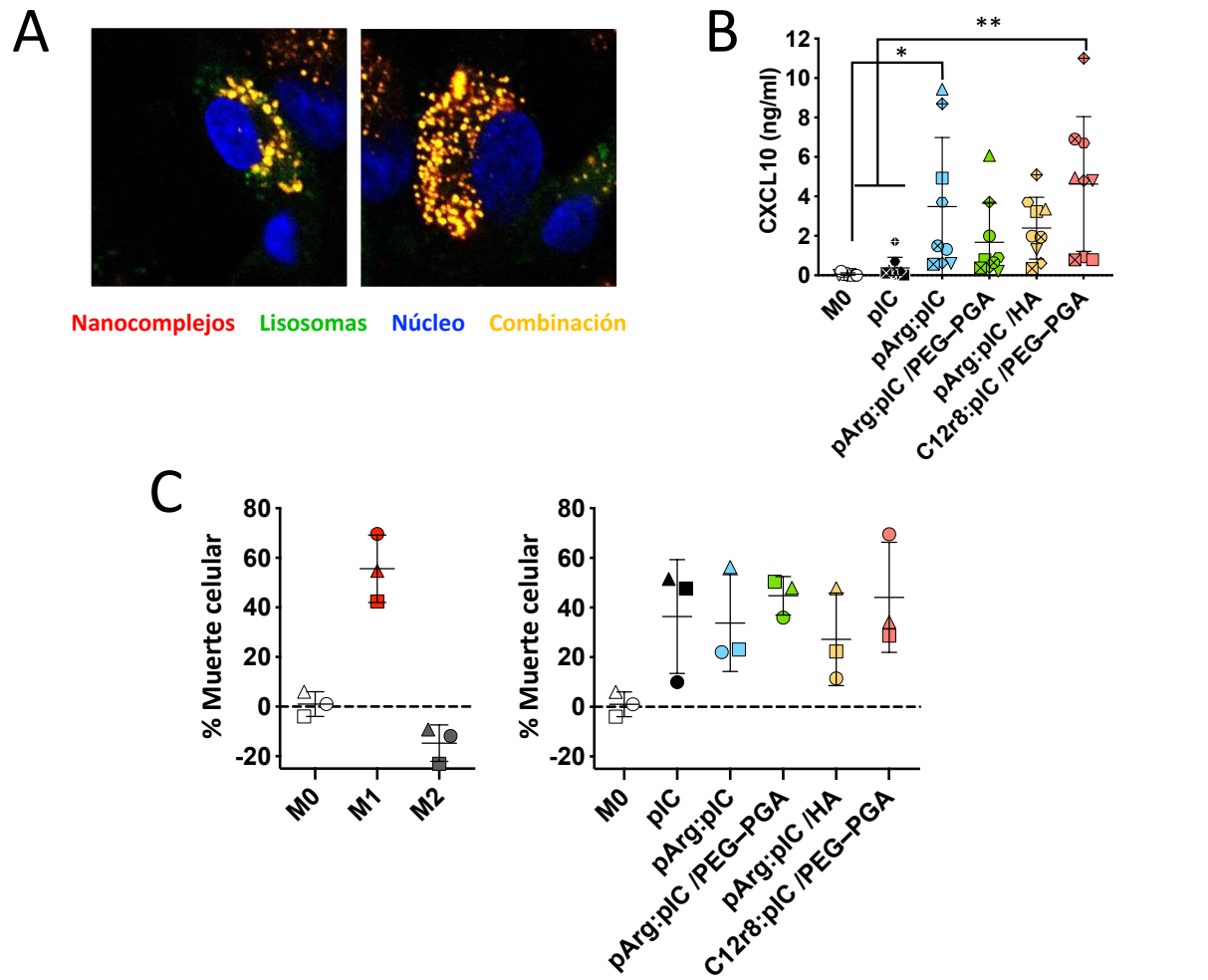

Figura 8. Distribución intracelular de los nanocomplejos de poly(I:C), y su capacidad *in vitro* para polarizar macrófagos hacia fenotipos M1. (A) Colocalización con el endosoma del poly(I:C) marcado con rodamina de los nanocomplejos de pArg:pIC tras 8 h de incubación (magnificación de 100x). (B) Secreción de la quimoquina CXCL10 en macrófagos tratados con los diferentes nanocomplejos. (C) Toxicidad de los macrófagos pretratados con los nanocomplejos hacia células cancerígenas, en comparación con macrófagos M0, M1 y M2. Cada forma representa un donante distinto. Los valores representan la media ± desviación estándar (n ≥ 3). El análisis estadístico fue hecho aplicando una prueba ANOVA unidireccional seguida por una prueba de comparación múltiple Tukey. Las diferencias significativas están representadas como $^{*}(p < 0.05)$ y $^{**}(p < 0.01)$. C12r8, laurato de octaarginina; HA, ácido hialurónico; PANC-1, células de cáncer de páncreas; pArg, poliarginina; PEG–PGA, ácido poliglutámico peguilado; PDI, índice de polispersión; pIC, poly(I:C).

Sin embargo, estos prometedores resultados *in vitro* no se trasladaron a una eficacia antitumoral *in vivo* en un modelo tumoral de ratón inmunocompetente. Aunque una correlación *in vitro*/*in vivo* no tendría necesariamente porqué observarse, hemos especulado sobre las posibles razones para esta

limitada actividad *in vivo* de los ENCPs. Una de nuestras hipótesis es una mayor dificultad de los ENCPs para difundir en el microambiente tumoral. Aunque se esperaría que la presencia de un polímero hidrofílico en la superficie de los nanotransportadores mejorase su difusión [81], el tamaño de los ENCPs podría haber dificultado su difusión dentro del tumor. Otra hipótesis estaría relacionada con la fuerte afinidad del poly(I:C) hacia los polímeros de arginina, que podría limitar su liberación y su disponibilidad para interaccionar con el receptor TLR3. Esta liberación lenta podría haber sido suficiente para estimular los macrófagos *in vitro*, pero no en condiciones *in vivo*. Por lo tanto, estudios de escalado de dosis serían necesarios para entender mejor el comportamiento mecanístico de los ENCPs.

En resumen, los nanocomplejos a base de arginina desarrollados en este trabajo fueron capaces de proteger y estabilizar el poly(I:C). Por un lado, el poly(I:C) llegó al endosoma, donde su receptor diana se encuentra, y fue capaz de polarizar macrófagos para secretar quimoquinas que atraigan a células T citotóxicas, además de mejorar sus propiedades citotóxicas. Sin embargo, estos prometedores resultados no encontraron correlación con la respuesta obtenida en un estudio exploratorio *in vivo* en el que se evaluaba la capacidad de los ENCPs para prevenir el crecimiento tumoral. Estas diferencias demuestran la necesidad de un mejor entendimiento de la biodistribución y la liberación intracelular del poly(I:C). Además, serán necesarios estudios de toxicidad *in vivo* tras una administración intravenosa para determinar el valor de esta estrategia. En este sentido, los ENCPs podrían presentar ventajas para la protección del fármaco.

Como conclusión, en esta tesis hemos demostrado que, aprovechando la versatilidad de las NPs, el sistema inmune puede ser modulado tanto en el contexto de una vacuna preventiva del VIH, como en el tratamiento del cáncer. Esta versatilidad de las NPs, que permite unir fármacos a través de diferentes mecanismos, personalizar la superficie de los nanosistemas, e incluir inmunomoduladores, entre otros, es una herramienta de gran potencial para el desarrollo de nuevos medicamentos. Finalmente, también hemos demostrado que la preparación de las NPs puede ser trasladada a una planta piloto trabajando de acuerdo con las normas de BPF, a través de una monitorización y análisis sistemático de los atributos críticos de la formulación.

Referencias

[1] D.J. Irvine, M.C. Hanson, K. Rakhra, T. Tokatlian, Synthetic nanoparticles for vaccines and immunotherapy, Chem. Rev. 115 (2015) 11109–11146. doi:10.1021/acs.chemrev.5b00109.

[2] T.G. Dacoba, A. Olivera, D. Torres, J. Crecente-Campo, M.J. Alonso, Modulating the immune system through nanotechnology, Semin. Immunol. 34 (2017) 78–102. doi:10.1016/j.smim.2017.09.007.

[3] M. Tobío, R. Gref, A. Sánchez, R. Langer, M.J. Alonso, Stealth PLA-PEG nanoparticles as protein carriers for nasal administration, Pharm. Res. 15 (1998) 270–275. doi:10.1023/A:1011922819926.

[4] A. Vila, A. Sánchez, C. Évora, I. Soriano, J.L. Vila Jato, M.J. Alonso, PEG-PLA nanoparticles as carriers for nasal vaccine delivery, J. Aerosol Med. 17 (2004) 174–185. doi:10.1089/0894268041457183.

[5] P. Calvo, C. Remuñán-López, J.L. Vila-Jato, M.J. Alonso, Novel hydrophilic chitosan-polyethylene oxide nanoparticles as protein carriers, J. Appl. Polym. Sci. 63 (1997) 125–132.

[6] C. Prego, P. Paolicelli, B. Díaz, S. Vicente, A. Sánchez, Á. González-Fernández, M.J. Alonso, Chitosan-based nanoparticles for improving immunization against hepatitis B infection, Vaccine. 28 (2010) 2607–2614. doi:10.1016/j.vaccine.2010.01.011.

[7] J.F. Correia-Pinto, N. Csaba, J. Schiller, M.J. Alonso, Chitosan-poly (I:C)-PADRE based nanoparticles as delivery vehicles for synthetic peptide vaccines, Vaccines. 3 (2015) 730–750. doi:10.3390/vaccines3030730.

[8] M. Peleteiro, E. Presas, J.V. González-Aramundiz, B. Sánchez-Correa, R. Simón-Vázquez, N. Csaba, M.J. Alonso, Á. González-Fernández, Polymeric nanocapsules for vaccine delivery: influence of the polymeric shell on the interaction with the immune system, Front. Immunol. 9 (2018). doi:10.3389/fimmu.2018.00791.

[9] A.S. Cordeiro, J. Crecente-Campo, B.L. Bouzo, S.F. González, M. de la Fuente, M.J. Alonso, Engineering polymeric nanocapsules for an efficient drainage and biodistribution in the lymphatic system, J. Drug Target. 27 (2019) 646–658. doi:10.1080/1061186X.2018.1561886.

[10] J. Crecente-Campo, J. Guerra-Varela, M. Peleteiro, C. Gutiérrez-Lovera, I. Fernández-Mariño, A. Diéguez-Docampo, Á. González-Fernández, L. Sánchez, M.J. Alonso, The size and composition of polymeric nanocapsules dictate their interaction with macrophages and biodistribution in zebrafish, J. Control. Release. 308 (2019) 98–108. doi:10.1016/j.jconrel.2019.07.011.

[11] J. Crecente-Campo, M.J. Alonso, Engineering, on-demand manufacturing, and scaling-up of polymeric nanocapsules, Bioeng. Transl. Med. 4 (2019) 38–50. doi:10.1002/btm2.10118.

[12] S. Vicente, M. Peleteiro, B. Díaz-Freitas, A. Sanchez, Á. González-Fernández, M.J. Alonso, Co-delivery of viral proteins and a TLR7 agonist from polysaccharide nanocapsules: a needle-free vaccination strategy, J. Control. Release. 172 (2013) 773–781. doi:10.1016/j.jconrel.2013.09.012.

[13] J.V. González-Aramundiz, E. Presas, I. Dalmau-Mena, S. Martínez-Pulgarín, C. Alonso, J.M. Escribano, M.J. Alonso, N.S. Csaba, Rational design of protamine nanocapsules as antigen delivery carriers, J. Control. Release. 245 (2017) 62–69. doi:10.1016/j.jconrel.2016.11.012.

[14] J. Crecente-Campo, S. Lorenzo-Abalde, A. Mora, J. Marzoa, N. Csaba, J. Blanco, Á. González-Fernández, M.J. Alonso, Bilayer polymeric nanocapsules: a formulation approach for a thermostable and adjuvanted E. coli antigen vaccine, J. Control. Release. 286 (2018) 20–32. doi:10.1016/j.jconrel.2018.07.018.

[15] A.M. Ledo, M.S. Sasso, V. Bronte, I. Marigo, B.J. Boyd, M. Garcia-Fuentes, M.J. Alonso, Co-delivery of RNAi and chemokine by polyarginine nanocapsules enables the modulation of myeloid-derived suppressor cells, J. Control. Release. 295 (2019) 60–73. doi:10.1016/j.jconrel.2018.12.041.

[16] HIV vaccines go to trial, Nat. Med. 25 (2019) 703. doi:10.1038/s41591-019-0460-0.

[17] Y. Liu, C. Chen, Role of nanotechnology in HIV/AIDS vaccine development, Adv. Drug Deliv. Rev. 103 (2016) 76–89. doi:10.1016/j.addr.2016.02.010.

[18] M. Luo, R. Capina, C. Daniuk, J. Tuff, H. Peters, M. Kimani, C. Wachihi, J. Kimani, T.B. Ball, F.A. Plummer, Immunogenicity of sequences around HIV-1 protease cleavage sites: potential targets and population

coverage analysis for a HIV vaccine targeting protease cleavage sites, Vaccine. 31 (2013) 3000–3008. doi:10.1016/j.vaccine.2013.04.057.

[19] H. Li, R.W. Omange, F.A. Plummer, M. Luo, A novel HIV vaccine targeting the protease cleavage sites, AIDS Res. Ther. 14 (2017) 51. doi:10.1186/s12981-017-0174-7.

[20] H. Li, R.W. Omange, C. Czarnecki, J.F. Correia-Pinto, J. Crecente-Campo, M. Richmond, L. Li, N. Schultz-Darken, M.J. Alonso, J.B. Whitney, F.A. Plummer, M. Luo, Mauritian cynomolgus macaques with M3M4 MHC genotype control SIVmac251 infection, J. Med. Primatol. 46 (2017) 137–143. doi:10.1111/jmp.12300.

[21] A.H. Kaplan, J.A. Zack, M. Knigge, D.A. Paul, D.J. Kempf, D.W. Norbeck, R. Swanstrom, Partial inhibition of the human immunodeficiency virus type 1 protease results in aberrant virus assembly and the formation of noninfectious particles, J. Virol. 67 (1993) 4050–4055.

[22] H. Li, M. Nykoluk, L. Li, L.R. Liu, R.W. Omange, G. Soule, L.T. Schroeder, N. Toledo, M.A. Kashem, J.F. Correia-Pinto, B. Liang, N. Schultz-Darken, M.J. Alonso, J.B. Whitney, F.A. Plummer, M. Luo, Natural and cross-inducible anti-SIV antibodies in Mauritian cynomolgus macaques, PLoS One. 12 (2017) 1–20. doi:10.1371/journal.pone.0186079.

[23] H. Li, Y. Hai, S.-Y. Lim, N. Toledo, J. Crecente-Campo, D. Schalk, L. Li, R.W. Omange, T.G. Dacoba, L.R.L.R. Liu, M.A. Kashem, Y. Wan, B. Liang, Q. Li, E. Rakasz, N. Schultz-Darken, M.J. Alonso, F.A. Plummer, J.B. Whitney, M. Luo, Mucosal antibody responses to vaccines targeting SIV protease cleavage sites or full-length Gag and Env proteins in Mauritian cynomolgus macaques, PLoS One. 13 (2018) e0202997. doi:10.1371/journal.pone.0202997.

[24] J.F. Correia-Pinto, M. Peleteiro, N. Csaba, Á. González-Fernández, M.J. Alonso, Multi-enveloping of particulated antigens with biopolymers and immunostimulant polynucleotides, J. Drug Deliv. Sci. Technol. 30 (2015) 424–434. doi:10.1016/j.jddst.2015.08.010.

[25] A.M. Hafner, B. Corthésy, H.P. Merkle, Particulate formulations for the delivery of poly(I:C) as vaccine adjuvant, Adv. Drug Deliv. Rev. 65 (2013) 1386–1399. doi:10.1016/j.addr.2013.05.013.

[26] H. Park, L. Adamson, T. Ha, K. Mullen, S.I. Hagen, A. Nogueron, A.W. Sylwester, M.K. Axthelm, A. Legasse, M. Piatak, J.D. Lifson, J.M. McElrath, L.J. Picker, R.A. Seder, Polyinosinic-polycytidylic acid is the most effective TLR adjuvant for SIV Gag protein-induced T cell responses in nonhuman primates, J. Immunol. 190 (2013) 4103–4115. doi:10.4049/jimmunol.1202958.

[27] A.S. Cordeiro, M.J. Alonso, M. de la Fuente, Nanoengineering of vaccines using natural polysaccharides, Biotechnol. Adv. 33 (2015) 1279–1293. doi:10.1016/j.biotechadv.2015.05.010.

[28] J. Shi, P.W. Kantoff, R. Wooster, O.C. Farokhzad, Cancer nanomedicine: progress, challenges and opportunities, Nat. Rev. Cancer. 17 (2017) 20–37. doi:10.1038/nrc.2016.108.

[29] F. Rose, J.E. Wern, F. Gavins, P. Andersen, F. Follmann, C. Foged, A strong adjuvant based on glycol-chitosan-coated lipid-polymer hybrid nanoparticles potentiates mucosal immune responses against the recombinant Chlamydia trachomatis fusion antigen CTH522, J. Control. Release. 271 (2018) 88–97. doi:10.1016/j.jconrel.2017.12.003.

[30] A. Vila, A. Sánchez, M. Tobío, P. Calvo, M.J. Alonso, Design of biodegradable particles for protein delivery, J. Control. Release. 78 (2002) 15–24. doi:10.1016/S0168-3659(01)00486-2.

[31] A. Vila, A. Sánchez, K. Janes, I. Behrens, T. Kissel, J.L. Vila-Jato, M.J. Alonso, Low molecular weight chitosan nanoparticles as new carriers for nasal vaccine delivery in mice, Eur. J. Pharm. Biopharm. 57 (2004) 123–131. doi:10.1016/j.ejpb.2003.09.006.

[32] S. Vicente, B. Diaz-Freitas, M. Peleteiro, A. Sanchez, D.W. Pascual, A. Gonzalez-Fernandez, M.J. Alonso, A polymer/oil based nanovaccine as a single-dose immunization approach, PLoS One. 8 (2013) 2–9. doi:10.1371/journal.pone.0062500.

[33] L. Cui, J.A. Cohen, K.E. Broaders, T.T. Beaudette, J.M.J. Fréchet, Mannosylated dextran nanoparticles: a pH-sensitive system engineered for immunomodulation through mannose targeting, Bioconjug. Chem.

22 (2011) 949–957. doi:10.1021/bc100596w.

[34] S. Sharma, T.K. Mukkur, H.A. Benson, Y. Chen, Enhanced immune response against Pertussis toxoid by IgA-loaded chitosan–dextran sulfate nanoparticles, J. Pharm. Sci. 101 (2012) 233–244. doi:10.1002/jps.22763.

[35] K. Perica, A. Tu, A. Richter, J.G. Bieler, M. Edidin, J.P. Schneck, Magnetic field-induced T cell receptor clustering by nanoparticles enhances T cell activation and stimulates antitumor activity, ACS Nano. 8 (2014) 2252–2260. doi:10.1021/nn405520d.

[36] B.J.G. Baaten, R. Tinoco, A.T. Chen, L.M. Bradley, Regulation of antigen-experienced T cells: lessons from the quintessential memory marker CD44, Front. Immunol. 3 (2012) 1–12. doi:10.3389/fimmu.2012.00023.

[37] C.C. Termeer, J. Hennies, U. Voith, T. Ahrens, J. M. Weiss, P. Prehm, J.C. Simon, Oligosaccharides of hyaluronan are potent activators of dendritic cells, J. Immunol. 165 (2000) 1863–1870. doi:10.4049/jimmunol.165.4.1863.

[38] C. Ke, D. Wang, Y. Sun, D. Qiao, H. Ye, X. Zeng, Immunostimulatory and antiangiogenic activities of low molecular weight hyaluronic acid, Food Chem. Toxicol. 58 (2013) 401–407. doi:10.1016/j.fct.2013.05.032.

[39] Y. Fan, P. Sahdev, L.J. Ochyl, J. J. Akerberg, J.J. Moon, Cationic liposome–hyaluronic acid hybrid nanoparticles for intranasal vaccination with subunit antigens, J. Control. Release. 208 (2015) 121–129. doi:10.1016/j.jconrel.2015.04.010.

[40] L. Liu, F. Cao, X. Liu, H. Wang, C. Zhang, H. Sun, C. Wang, X. Leng, C. Song, D. Kong, G. Ma, Hyaluronic acid-modified cationic lipid–PLGA hybrid nanoparticles as a nanovaccine induce robust humoral and cellular immune responses, ACS Appl. Mater. Interfaces. 8 (2016) 11969–11979. doi:10.1021/acsami.6b01135.

[41] J.V. González-Aramundiz, M. Peleteiro Olmedo, Á. González-Fernández, M.J. Alonso, N.S. Csaba, Protamine-based nanoparticles as new antigen delivery systems, Eur. J. Pharm. Biopharm. 97 (2015) 51–59. doi:10.1016/j.ejpb.2015.09.019.

[42] A.D. Baldwin, K.L. Kiick, Tunable degradation of maleimide-thiol adducts in reducing environments, Bioconjug. Chem. 22 (2011) 1946–1953. doi:10.1021/bc200148v.

[43] J.J. Moon, H. Suh, V. Li, C.F. Ockenhouse, A. Yadava, D.J. Irvine, Enhancing humoral responses to a malaria antigen with nanoparticle vaccines that expand Tfh cells and promote germinal center induction, Proc. Natl. Acad. Sci. 109 (2012) 1080–1085. doi:10.1073/pnas.1112648109.

[44] V. V. Temchura, D. Kozlova, V. Sokolova, K. Überla, M. Epple, Targeting and activation of antigen-specific B-cells by calcium phosphate nanoparticles loaded with protein antigen, Biomaterials. 35 (2014) 6098–6105. doi:10.1016/j.biomaterials.2014.04.010.

[45] J. Shao, J.P. Tam, Unprotected peptides as building blocks for the synthesis of peptide dendrimers with oxime, hydrazone, and thiazolidine linkages, J. Am. Chem. Soc. 117 (1995) 3893–3899. doi:10.1021/ja00119a001.

[46] H. Cho, T. Daniel, Y.J. Buechler, D.C. Litzinger, Z. Maio, A.-M.H. Putnam, V.S. Kraynov, B.-C. Sim, S. Bussell, T. Javahishvili, S. Kaphle, G. Viramontes, M. Ong, S. Chu, B. GC, R. Lieu, N. Knudsen, P. Castiglioni, T.C. Norman, D.W. Axelrod, A.R. Hoffman, P.G. Schultz, R.D. DiMarchi, B.E. Kimmel, Optimized clinical performance of growth hormone with an expanded genetic code, Proc. Natl. Acad. Sci. 108 (2011) 9060–9065. doi:10.1073/pnas.1100387108.

[47] C. Pifferi, N. Berthet, O. Renaudet, Cyclopeptide scaffolds in carbohydrate-based synthetic vaccines, Biomater. Sci. 5 (2017) 953–965. doi:10.1039/C7BM00072C.

[48] N.M. Molino, A.K.L. Anderson, E.L. Nelson, S.W. Wang, Biomimetic protein nanoparticles facilitate enhanced dendritic cell activation and cross-presentation, ACS Nano. 7 (2013) 9743–9752. doi:10.1021/nn403085w.

[49] J. Yang, J. Li, X. Li, X. Wang, Y. Yang, N. Kawazoe, G. Chen, Nanoencapsulation of individual mammalian cells with cytoprotective polymer shell, Biomaterials. 133 (2017) 253–262. doi:10.1016/j.biomaterials.2017.04.020.

[50] F. Meng, W.E. Hennink, Z. Zhong, Reduction-sensitive polymers and bioconjugates for biomedical applications, Biomaterials. 30 (2009) 2180–2198. doi:10.1016/j.biomaterials.2009.01.026.

[51] R. Cheng, F. Feng, F. Meng, C. Deng, J. Feijen, Z. Zhong, Glutathione-responsive nano-vehicles as a promising platform for targeted intracellular drug and gene delivery, J. Control. Release. 152 (2011) 2–12. doi:10.1016/j.jconrel.2011.01.030.

[52] G.K. Lewis, A.L. DeVico, R.C. Gallo, Antibody persistence and T-cell balance: two key factors confronting HIV vaccine development, Proc. Natl. Acad. Sci. 111 (2014) 15614–15621. doi:10.1073/pnas.1413550111.

[53] D.S. Watson, V.M. Platt, L. Cao, V.J. Venditto, F.C. Szoka, Antibody response to polyhistidine-tagged peptide and protein antigens attached to liposomes via lipid-linked nitrilotriacetic acid in mice, Clin. Vaccine Immunol. 18 (2011) 289–297. doi:10.1128/CVI.00425-10.

[54] R.D. Stout, J. Suttles, The many roles of CD40 in cell-mediated inflammatory responses, Immunol. Today. 17 (1996) 487–492. doi:10.1016/0167-5699(96)10060-I.

[55] I.S. Grewal, R.A. Flavell, CD40 and CD154 in cell-mediated immunity, Annu. Rev. Immunol. 16 (1998) 111–135. doi:10.1146/annurev.immunol.16.1.111.

[56] C.B. Thompson, Distinct roles for the costimulatory ligands B7-1 and B7-2 in T helper cell differentiation?, Cell. 81 (1995) 979–982. doi:10.1016/S0092-8674(05)80001-7.

[57] H. Song, P. Huang, J. Niu, G. Shi, C. Zhang, D. Kong, W. Wang, Injectable polypeptide hydrogel for dual-delivery of antigen and TLR3 agonist to modulate dendritic cells in vivo and enhance potent cytotoxic T-lymphocyte response against melanoma, Biomaterials. 159 (2018) 119–129. doi:10.1016/j.biomaterials.2018.01.004.

[58] N. Moyo, A.B. Vogel, S. Buus, S. Erbar, E.G. Wee, U. Sahin, T. Hanke, Efficient Induction of T cells against conserved HIV-1 regions by mosaic vaccines delivered as self-amplifying mRNA, Mol. Ther. - Methods Clin. Dev. 12 (2019) 32–46. doi:10.1016/j.omtm.2018.10.010.

[59] T. Hatziioannou, D.T. Evans, Animal models for HIV/AIDS research, Nat. Rev. Microbiol. 10 (2012) 852–867. doi:10.1038/nrmicro2911.

[60] T.G. Dacoba, R.W. Omange, H. Li, J. Crecente-Campo, M. Luo, M.J. Alonso, Polysaccharide nanoparticles can efficiently modulate the immune response against an HIV peptide antigen, ACS Nano. 13 (2019) 4947–4959. doi:10.1021/acsnano.8b07662.

[61] H. Li, R.W. Omange, B. Liang, N. Toledo, Y. Hai, L.R. Liu, D. Schalk, J. Crecente-Campo, T.G. Dacoba, A.B. Lambe, S.-Y. Lim, L. Li, M.A. Kashem, Y. Wan, J.F. Correia-Pinto, X.Q. Liu, R.F. Balshaw, Q. Li, E. Rakasz, N. Schultz-Darken, M.J. Alonso, J.B. Whitney, F.A. Plummer, M. Luo, A novel vaccine targeting the viral protease cleavage sites protects Mauritian cynomolgus macaques against vaginal SIVmac251 infection, BioRxiv. (2019). doi:10.1101/842955.

[62] H. Ragelle, F. Danhier, V. Préat, R. Langer, D.G. Anderson, Nanoparticle-based drug delivery systems: a commercial and regulatory outlook as the field matures, Expert Opin. Drug Deliv. 14 (2017) 851–864. doi:10.1080/17425247.2016.1244187.

[63] F. Dormont, M. Rouquette, C. Mahatsekake, F. Gobeaux, A. Peramo, R. Brusini, S. Calet, F. Testard, S. Lepetre-Mouelhi, D. Desmaële, M. Varna, P. Couvreur, Translation of nanomedicines from lab to industrial scale synthesis: the case of squalene-adenosine nanoparticles, J. Control. Release. 307 (2019) 302–314. doi:10.1016/j.jconrel.2019.06.040.

[64] C.M. Maguire, M. Rösslein, P. Wick, A. Prina-Mello, Characterisation of particles in solution – a perspective on light scattering and comparative technologies, Sci. Technol. Adv. Mater. 19 (2018) 732–745. doi:10.1080/14686996.2018.1517587.

[65] F. Caputo, J. Clogston, L. Calzolai, M. Rösslein, A. Prina-Mello, Measuring particle size distribution of nanoparticle enabled medicinal products, the joint view of EUNCL and NCI-NCL. A step by step approach combining orthogonal measurements with increasing complexity, J. Control. Release. 299 (2019) 31–43. doi:10.1016/j.jconrel.2019.02.030.

[66] B. Liu, Q. Liu, L. Yang, S.K. Palaniappan, I. Bahar, P.S. Thiagarajan, J.L. Ding, Innate immune memory and homeostasis may be conferred through crosstalk between the TLR3 and TLR7 pathways, Sci. Signal. 9 (2016) ra70–ra70. doi:10.1126/scisignal.aac9340.

[67] H. Shime, M. Matsumoto, H. Oshiumi, S. Tanaka, A. Nakane, Y. Iwakura, H. Tahara, N. Inoue, T. Seya, Toll-like receptor 3 signaling converts tumor-supporting myeloid cells to tumoricidal effectors, Proc. Natl. Acad. Sci. 109 (2012) 2066–2071. doi:10.1073/pnas.1113099109.

[68] A. Maeda, E. Digifico, F.T. Andon, A. Mantovani, P. Allavena, Poly(I:C) stimulation is superior than imiquimod to induce the antitumoral functional profile of tumor-conditioned macrophages, Eur. J. Immunol. 49 (2019) 801–811. doi:10.1002/eji.201847888.

[69] M.A. Aznar, L. Planelles, M. Perez-Olivares, C. Molina, S. Garasa, I. Etxeberría, G. Perez, I. Rodriguez, E. Bolaños, P. Lopez-Casas, M.E. Rodriguez-Ruiz, J.L. Perez-Gracia, I. Marquez-Rodas, A. Teijeira, M. Quintero, I. Melero, Immunotherapeutic effects of intratumoral nanoplexed poly I:C, J. Immunother. Cancer. 7 (2019) 116. doi:10.1186/s40425-019-0568-2.

[70] Exploratory study of BO-112 in adult patients with aggressive solid tumors, (2016). https://clinicaltrials.gov/ct2/show/NCT02828098 (accessed January 9, 2020).

[71] P. Chollet, M.C. Favrot, A. Hurbin, J.-L. Coll, Side-effects of a systemic injection of linear polyethylenimine-DNA complexes, J. Gene Med. 4 (2002) 84–91. doi:10.1002/jgm.237.

[72] J. DeRouchey, V.A. Parsegian, D.C. Rau, Cation charge dependence of the forces driving DNA assembly, Biophys. J. 99 (2010) 2608–2615. doi:10.1016/j.bpj.2010.08.028.

[73] T. Endoh, T. Ohtsuki, Cellular siRNA delivery using cell-penetrating peptides modified for endosomal escape, Adv. Drug Deliv. Rev. 61 (2009) 704–709. doi:10.1016/j.addr.2009.04.005.

[74] V.P. Torchilin, Cell penetrating peptide-modified pharmaceutical nanocarriers for intracellular drug and gene delivery, Biopolymers. 90 (2008) 604–610. doi:10.1002/bip.20989.

[75] C. Sun, T. Tang, H. Uludag, A molecular dynamics simulation study on the effect of lipid substitution on polyethylenimine mediated siRNA complexation, Biomaterials. 34 (2013) 2822–2833. doi:10.1016/j.biomaterials.2013.01.011.

[76] L. Pärnaste, P. Arukuusk, K. Langel, T. Tenson, Ü. Langel, The formation of nanoparticles between small interfering RNA and amphipathic cell-penetrating peptides, Mol. Ther. - Nucleic Acids. 7 (2017) 1–10. doi:10.1016/j.omtn.2017.02.003.

[77] D.J. Gary, N. Puri, Y.-Y. Won, Polymer-based siRNA delivery: perspectives on the fundamental and phenomenological distinctions from polymer-based DNA delivery, J. Control. Release. 121 (2007) 64–73. doi:10.1016/j.jconrel.2007.05.021.

[78] E. Samaridou, H. Walgrave, E. Salta, D.M. Álvarez, V. Castro-López, M. Loza, M.J. Alonso, Nose-to-brain delivery of enveloped RNA - cell permeating peptide nanocomplexes for the treatment of neurodegenerative diseases, Biomaterials. 230 (2020) 119657. doi:10.1016/j.biomaterials.2019.119657.

[79] E. Samaridou, N. Kalamidas, I. Santalices, J. Crecente-Campo, M.J. Alonso, Tuning the PEG surface density of the PEG-PGA enveloped octaarginine-peptide nanocomplexes, Drug Deliv. Transl. Res. (2019). doi:10.1007/s13346-019-00678-3.

[80] M.J. Santander-Ortega, A.B. Jódar-Reyes, N. Csaba, D. Bastos-González, J.L. Ortega-Vinuesa, Colloidal stability of pluronic F68-coated PLGA nanoparticles: a variety of stabilisation mechanisms, J. Colloid Interface Sci. 302 (2006) 522–529. doi:10.1016/j.jcis.2006.07.031.

[81] R. Abellan-Pose, M. Rodríguez-Évora, S. Vicente, N. Csaba, C. Évora, M.J. Alonso, A. Delgado, Biodistribution of radiolabeled polyglutamic acid and PEG-polyglutamic acid nanocapsules, Eur. J. Pharm.

Biopharm. 112 (2017) 155–163. doi:10.1016/j.ejpb.2016.11.015.

[82] Z. Niu, E. Samaridou, E. Jaumain, J. Coëne, G. Ullio, N. Shrestha, J. Garcia, M. Durán-Lobato, S. Tovar, M.J. Santander-Ortega, M.V. Lozano, M.M. Arroyo-Jimenez, R. Ramos-Membrive, I. Peñuelas, A. Mabondzo, V. Préat, M. Teixidó, E. Giralt, M.J. Alonso, PEG-PGA enveloped octaarginine-peptide nanocomplexes: an oral peptide delivery strategy, J. Control. Release. 276 (2018) 125–139. doi:10.1016/j.jconrel.2018.03.004.

[83] D. Peer, R. Margalit, Loading mitomycin C inside long circulating hyaluronan targeted nano-liposomes increases its antitumor activity in three mice tumor models, Int. J. Cancer. 108 (2004) 780–789. doi:10.1002/ijc.11615.

[84] K.Y. Choi, K.H. Min, J.H. Na, K. Choi, K. Kim, J.H. Park, I.C. Kwon, S.Y. Jeong, Self-assembled hyaluronic acid nanoparticles as a potential drug carrier for cancer therapy: synthesis, characterization, and in vivo biodistribution, J. Mater. Chem. 19 (2009) 4102. doi:10.1039/b900456d.

[85] X. Yang, Y. Li, M. Li, L. Zhang, L. Feng, N. Zhang, Hyaluronic acid-coated nanostructured lipid carriers for targeting paclitaxel to cancer, Cancer Lett. 334 (2013) 338–345. doi:10.1016/j.canlet.2012.07.002.

[86] A. Almalik, H. Benabdelkamel, A. Masood, I.O. Alanazi, I. Alradwan, M.A. Majrashi, A.A. Alfadda, W.M. Alghamdi, H. Alrabiah, N. Tirelli, A.H. Alhasan, Hyaluronic acid coated chitosan nanoparticles reduced the immunogenicity of the formed protein corona, Sci. Rep. 7 (2017) 1–9. doi:10.1038/s41598-017-10836-7.

[87] K. Franciszkiewicz, A. Boissonnas, M. Boutet, C. Combadiere, F. Mami-Chouaib, Role of chemokines and chemokine receptors in shaping the effector phase of the antitumor immune response, Cancer Res. 72 (2012) 6325–6332. doi:10.1158/0008-5472.CAN-12-2027.

[88] G. Arango Duque, A. Descoteaux, Macrophage cytokines: involvement in immunity and infectious diseases, Front. Immunol. 5 (2014) 1–12. doi:10.3389/fimmu.2014.00491.

Introduction

Nanotechnology, vaccines and cancer immunotherapy

Section 2 has been adapted/extracted from a recently published review entitled 'Modulating the immune system through nanotechnology' [1].

The modulation of the immune system is the base of new and promising therapies for some of the most prevalent and/or severe diseases of our time, such as cancer, HIV, or diabetes. The development of treatments based on this modulation is a field in expansion, where the contribution of nanotechnology is growing exponentially [2–4].

Based mainly on the molecular principles that govern the interaction between pathogens and immune cells, the use of nanotechnology represents a new way of communication with the immune system. By mimicking the size of microorganisms (bacteria and viruses) and incorporating key molecules involved in the immune processes (TLR agonists, cytokines, etc.), nanocarriers can be taken up by the immune cells and modulate their responses. Besides, the use of nanocarriers decorated with targeting moieties can favor their preferential access to specific immune cell populations [3,5–10]. Importantly, the versatility of nanotechnology also offers the possibility of reinforcing the desired aspect of the immune system, either by eliciting more prominent humoral or cellular responses, or by re-activating the immune system to fight cancer.

This introduction is intended to provide a general view of how nanotechnology is being used to modulate the immune system, and more specifically, in the topics addressed in this thesis: HIV and cancer. In the first section, nanoformulation strategies to target and modulate different types of immune cells are discussed. In a second section, the specific use of nanosystems for the development of vaccines against some important infectious diseases, with a special mention to HIV, is covered. In the third section, the advances accomplished in cancer immunotherapy thanks to the use of nanotechnology are also described. This introduction finishes with the hurdles that nanomedicine is facing to get to the market.

1. Nanotechnology and the immune system

The immune system is a complex network of organs and cells that play different and important roles. The crosstalk among these cells influences the different responses the immune system provides to external and self-antigens. Therefore, by specifically delivering antigens, drugs or immunomodulators to these cells, we can alter how they respond or react in different diseases [11,12]. In this section, a small overview regarding some immune cells that are currently being targeted for the modulation of the immune response, and the different nanotechnology-based approaches employed for this end, is provided.

1.1. Innate immune cells

1.1.1. Macrophages

Macrophages are innate immune cells that, in a simplistic manner, can be further divided in M1 macrophages, with inflammatory properties, or M2 macrophages, with a tolerogenic phenotype [13,14]. These different populations are involved in infections, inflammation or in tumor development. For example, macrophages that have been exposed to the immunosuppressive tumor microenvironment are polarized towards an M2 state, thus facilitating the spreading of tumor cells [15]. Oppositely, during inflammatory diseases, macrophages are continuously activated with an M1 phenotype [16]. Therefore, modulating macrophages has a great interest from a therapeutic perspective.

Macrophages can be targeted following different nanotechnology approaches. The optimal particle size for the efficient passive targeting of macrophages is still a controversial issue [1]. Early studies suggested a preference for micrometric sizes to improve macrophage uptake [17,18], although more recent studies have reported a preferential uptake for small nanometric sizes [19,20]. For example, a recent work using both, *in vitro* cell cultures and an *in vivo* zebrafish model, showed that small nanocapsules (NCs) (100 nm) were taken up more efficiently by macrophages than the medium-size ones (200 nm) [21], a tendency that was later corroborated in healthy mice [22]. With regard to the effect of the surface charge, contradictory results have also been reported [1]. However, the general trend points out to a preferable uptake of positively charged nanosystems as compared to the negatively charged or neutral ones. As an example, we recently observed an enhanced uptake of chitosan NCs as compared to the one of negatively charged inulin NCs [21]. It is to note that the value of the uptake data observed in the *in vitro* studies should not be overestimated as the biodistribution and diffusion across tissues are determinant barriers for the access of the particles to the cells.

The NP's composition can also play an important role in the interaction with macrophages. Some works have proposed the use of hyaluronic acid (HA) to improve the uptake by macrophages, through their interaction with the CD44 receptor [23,24]. In this sense, a systematic study aimed at evaluating the expression of CD44 by M0, M1 and M2 macrophages concluded that the expression of this receptor varies within the different phenotypes (M1 > M0 ≥ M2) [25]. However, a more efficient internalization was observed for the lower CD44 expression [25]. Therefore, the relevance of the CD44 expression from the targeting perspective remains questionable. On the other hand, it has been reported that high molecular weight (MW) HA (over 1 MDa, similar to the endogenous) is non-immunogenic and rather anti-inflammatory, while low MW HA (<200 Da) is able to activate macrophages [26]. This effect has been attributed to the potential interaction of hyaluronan fragments with TLR2 and 4 [27–29].

Indeed, HA-conjugated manganese NPs (MW 40 kDa) were shown to polarize macrophages *in vitro* towards M1 pro-inflammatory phenotypes, process that was mediated by the HA [30]. At the same time, liposomes coated with a high MW HA (1.5 MDa) were able to decrease the production of M1-like cytokines *in vitro* [31,32]. These polarization effects of low MW HA towards M1 states and high MW towards M2 phenotypes have also been reported for soluble HA [33,34]. On the contrary, Peer and collaborators studied a library of polystyrene NPs coated with different HA MWs (ranging from 6 to 1500 kDa), and observed no effect of the MW of HA on macrophage viability nor in cytokine secretion [35]. This absence of stimulatory properties of HA are in agreement with other studies claiming the capacity of HA to enhance the circulation time of NPs [36–38]. These stealth properties of HA are also in relation with the observed protein corona formed over HA-coated NPs, which contained some anti-inflammatory proteins rather than immune-activating proteins [39]. Overall, these data suggest that the macrophage-polarizing properties of HA, if existing, are rather limited. In this sense, it could be speculated that the combination with active compounds that are able to drive more efficiently these polarizations are key to elicit significant therapeutic effects.

Dextran is another polysaccharide known to be recognized by the scavenger receptors in macrophages. The conjugation of methotrexate to a 5-kDa dextran sulfate led to an improved uptake by macrophages, biodistribution to inflamed joints, and therapeutic effect *versus* the non-conjugated drug, both *in vitro* and *in vivo* [40,41]. Additionally, dextran sulfate improved the *in vivo* biodistribution to inflamed joints of the conjugates, in comparison to dextran [41]. Macrophage uptake was also reported to be dependent of dextran MW (10, 70 and 500 kDa), where the higher MWs were better taken up by macrophages in obese mice [42]. Furthermore, a conjugate of the 70-kDa dextran with an anti-inflammatory drug was more effective than the free drug alone [42].

Small sugar molecules, notably mannose, have been extensively used for active targeting to macrophages [43]. Indeed, mannose modification of solid lipid NPs improved their uptake by alveolar macrophages, in comparison to the plain NPs [44]. Conjugating mannose to liposomes was able to increase the presence of the NPs in lung tumors, which was associated to a great uptake by macrophages [45]. Other studies have decorated dendrimers with this sugar to direct an anti-atherosclerotic agent to macrophages over hepatocytes, reducing the atherosclerotic plaque development [46]. Similarly, exploiting the overexpression of galactose specific C-type lectins in tumor-associated macrophages has also generated promising therapeutic results [47].

1.1.2. Dendritic cells

Dendritic cells (DCs) are the most important antigen presenting cells (APCs), and can be described as the bridge between innate and adaptive immune responses [48,49]. These cells capture antigens and present them to T cells, together with other co-stimulatory signals, triggering different immune responses (**Fig. 1**) [49].

With regard to the properties of the particles that determine their interaction with DCs, it has been reported, both *in vitro* and *in vivo*, that nanometric particle sizes are preferable than micrometric sizes, [1], and that small NPs (100 nm) are better internalized than medium size NPs (200 nm) [22,50]. As in the case of macrophages, positively charged nanoparticles are also more efficiently taken-up than negative or neutral-charge nanoparticles (NPs) [1].

Different strategies have been described in the literature to actively target DCs, these including the functionalization with mannose and also with antibodies (Abs) against specific DCs receptors [51,52]. In fact, conjugating ovalbumin (OVA) or a *Plasmodium falciparum* antigen to mannose and a TLR7 agonist, increased the uptake by DCs by mannose-binding C-type lectins, and at the same time generated important humoral and cellular responses against the antigens [52]. On the other hand, the decoration of pegylated poly(lactic-co-glycolic) acid (PEG–PLGA) NPs, containing TLR agonists, with Abs targeting different surface receptors (CD40, CD11c or DEC-205) resulted in an efficient CD8 T cell activation, both *in vitro* and *in vivo* [53].

1.1.3. Myeloid-derived suppressor cells

An heterogeneous group of cells of myeloid origin is included under the name of myeloid-derived suppressor cells (MDSCs) [54]. In general, MDSCs have a suppressive effect over T cell responses, and they expand during the course of cancer, inflammation or infections [54]. Therefore, impairing MDSCs development, decreasing their numbers or depleting them will partially prevent the suppression of the immune response against tumors. Based on the capacity of 25 nm pegylated poly-propylene sulfide micelles to self-drain to the lymph nodes and interact with MDSCs, loading them with the anti-tumoral drug thioguanine was able to deplete MDSCs and improve the therapeutic efficacy of adoptive T cell therapy [55]. In a different study, the combination of gemcitabine-loaded lipid NCs with adoptive T cell therapy resulted in a slight improve of the *in vivo* effect of the T cell therapy [56]. Recently, an innovative approach involving the attraction of MDSCs with the chemokine CCL2, together with an RNA interference strategy, was also recently reported by our lab [57].

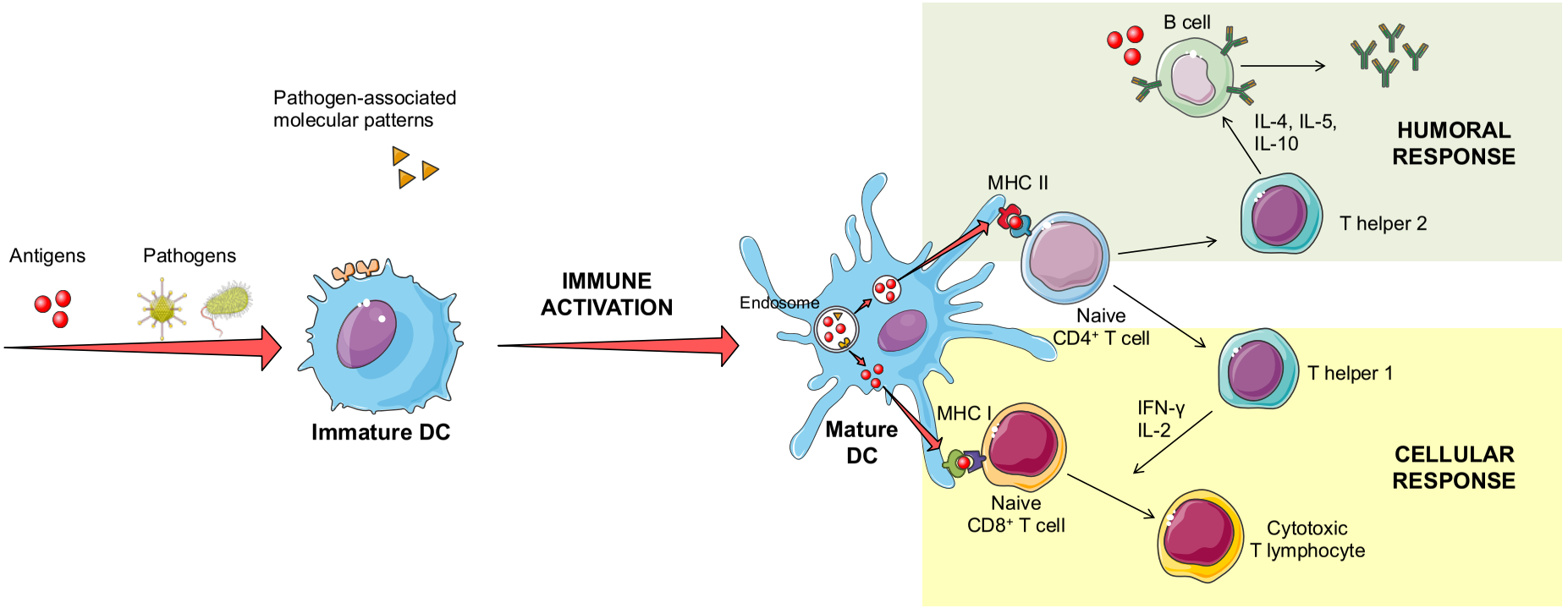

Figure 1. Immune cell network. Schematic overview of the generation of different immune responses by dendritic cells (DC). Antigens, pathogens and other molecules are taken up by immature dendritic cells. In the case of pathogens or systems expressing pathogen-associated molecular patterns (PAMPs), their internalization by dendritic cells leads to their presentation by class II major histocompatibility complexes (MHC II) to naïve CD4 T cells, which activate T helper cells (Th). Th2 cells produce IL-4, IL-5 and IL-10, which stimulate B cells to produce antibodies against the antigen. At the same time, antigens themselves can interact directly with B cells and activate them. Antigens can also be found in the cytosol of dendritic cells, which allows them to be presented by class I major histocompatibility complexes (MHC I), directly activating cytotoxic T lymphocytes. In this case, Th1 cells produce IFN-γ and IL-2, which favor cellular activation and hence, cytotoxic T cell responses. Co-stimulatory signals, not shown in the figure, are necessary for the final activation of T cells. Adapted with permission from [1].

1.1.4. Natural killer cell and natural killer T cells

Natural killer (NK) cells are innate lymphoid cells known due to their cytotoxic functions [58]. They can be divided in two main groups, one of them specialized on the secretion of inflammatory cytokines and the other one on cell-mediated killing. In parallel, there is another cell group under the name of natural killer T (NKT) cells, that are T cells with innate-like properties, that recognize lipidic antigens and that can have inflammatory or immunosuppressive properties [59].

To this date, not many nanotechnology approaches have been focused on specifically targeting these cells, but on activating them through the expression of the glycolipid α-galactosylceramide, known to stimulate NKT subsets [60,61]. Indeed, both studies showed an increased number of infiltrating NK and NKT cells upon treatment with the NPs containing α-galactosylceramide [60,61]. Similarly, trying to modulate the different immune cells found in the tumor microenvironment, lipid-coated silica NPs loaded with doxorubicin (as chemotherapeutic agent), all-trans retinoic acid (as both a chemo-sensitizer and MDSC modulator) and IL-2 (to increase the proliferation of T and NK cells), were shown to reduce the number of MDSC, while increasing the infiltrated NK and T cells in the tumor microenvironment [62].

1.1.5. Neutrophils

Neutrophils are circulating leukocytes that, during tissue damage or infection, are recruited to secret inflammatory cytokines [63,64]. An exacerbated activation of these cells is often associated to inflammatory diseases [63]. In cancer, neutrophils, like macrophages, suffer the Th1/Th2 paradigm, making them potential targets for immune modulation [64].

Currently, only a few reports have used NP-based systems to target neutrophils, and mainly in the context of inflammatory diseases. For example, cationic lipid NPs were employed to deliver a CRISP-Cas9 plasmid to hepatic neutrophils, aiming at decreasing the expression of neutrophil elastase, and as a result, diminish neutrophil infiltration and insulin resistance [65]. These cationic NPs were actually highly taken up by hepatic neutrophils *in vivo*, and induced anti-inflammatory effects in obese and diabetic mice [65]. Others have shown an increased uptake of albumin NPs only by activated neutrophils, in comparison to inactivated neutrophils or activated monocytes [66].

1.2. Adaptive immune cells

1.2.1. T cells

T cells are part of the adaptive arm of the immune system [49]. CD4 T cells are involved in the crosstalk with B cells, helping them in the generation of Abs (**Fig. 1**) [49]. On the other hand, CD8 T

cells are able to directly kill pathogens, infected cells and cancer cells (**Fig. 1**) [49]. Nevertheless, especially in the tumor microenvironment, these CD8 T cells might remain unresponsive towards cancer cells, a fact that makes them an interesting population to target. As shown in **Figure 1**, T cells are mainly activated by DCs, therefore many therapeutic strategies that ultimately activate T cells are focused on targeting DCs, as previously described.

Other approaches have explored strategies to directly interact with T cells. For example, some authors developed artificial antigen presenting cells (aAPCs), displaying both major histocompatibility complex molecules and co-stimulatory signals on their surface [67]. These aAPCs, alone or in combination with other anti-PD-1 mAbs, efficiently activated CD8 T cells [68–70]. Other studies have functionalized NPs with PD-1 ligands, in order to take advantage of the expression of this protein on the surface of the CD8 T cells present in the tumor microenvironment (further described in section 3).

T-cell targeting NPs have also shown advantages for the chimeric antigen receptor (CAR)-T cell therapies. CAR-T cells are the only adoptive T cell therapies that have been so far approved by the FDA. The manufacturing of these cells is based on isolating T cells from patients and genetically modify them through an *ex vivo* viral transfection, so they express the receptor that targets a specific cancer protein [71]. Then, the re-engineered T cells are expanded and transplanted back to the patients [71]. It has been reported that, by using CD3-targeted polymeric NPs loading an mRNA cargo during this *ex vivo* viral transfection, the efficacy and safety of the manufactured CAR-T cells was improved [72]. In parallel, the same NPs, but this time carrying a CAR-coding DNA, had the ability to generate CAR-T cells *in vivo*, as an alternative to the current *ex vivo* viral transfection [73].

1.2.2. B cells

B cells are in charge of the Ab production and, therefore, the humoral response. In general, B cells interact directly with the antigens, and upon their co-stimulation by CD4 T cells, they secrete Abs against the antigen (**Fig. 1**, top panel) [74]. Most of the classical vaccines against infectious diseases are based on eliciting important humoral responses. Indeed, it has been shown that alum, the most common adjuvant found in vaccines, has the capacity to generate important Ab responses, although the exact mechanism has not yet been elucidated [75].

So far, B-cell targeting strategies have been pursued mostly for the improvement of vaccines against infectious diseases. Examples of nanotechnology applied with this end related on a display of the antigens on the surface of NPs, following a repetitive pattern, for an augmented activation of B cells [76,77]. More examples of B cell activation and germinal center targeting are mentioned in section 2.

2. Nanovaccines and infectious diseases

During the last decades, significant efforts have been made to develop nanosystems capable of inducing protective immune responses against a variety of antigens. This section starts with a summary of the first reports about the potential of nanotechnology for the development of new vaccines. Next, an overview of the work done for those infective diseases that still remain elusive to vaccination, such as Hepatitis B, malaria or, in an extensive manner, HIV, is presented. For these diseases, where strong cellular responses are needed, nanotechnology might be a promising solution to obtain effective vaccines. Finally, the current nanotechnology-based adjuvants in the market are described.

2.1. The early steps of nanovaccinology

The potential of nanotechnology for vaccine application was first described by Birrenbanch and Speiser, who reported increased IgG levels against tetanus toxoid when polyacrylamide NPs were used as adjuvants [78]. Later, Preis and Langer introduced the concept of "single-dose vaccines" while they developed polymeric microparticles for long-term controlled protein release [79]. Following this trend, in the 90's, the World Health Organization started the initiative of single-dose vaccines for tetanus toxoid. Despite initial good results with PLGA-based systems, the acidification caused by the polymer degradation led to the partial loss of the antigen activity [80]. The inclusion of poloxamers, oily components, the decrease in particle size and pegylation of the systems were some of the approaches that our group explored with the idea of enhancing the performance of these antigen delivery systems [81–84].

Following this initial trend, many others have oriented their work to the development of nanotechnology-based vaccines. In general, the vast majority of the nanovaccines reported in the literature are based on using model proteins and peptides, such as OVA or its derivatives (e.g., SIINFEK). Although of great interest for vaccine design, optimization and validation, in the next sections we have aimed at highlighting those works employing antigens for preventing some of the most devastating infectious diseases of our time: Hepatitis B, malaria and HIV.

2.2. Hepatitis B

Our group has been involved in the development of nanoformulations of the recombinant hepatitis B surface antigen (rHBsAg). In particular, rHBsAg was associated to chitosan NPs and NCs and administered by the intramuscular route. The results showed an robust IgG response, that was higher than the one observed for the reference standard alum [85–87]. Moreover, more balanced Th1/Th2 profiles were obtained [86].

The tendency in the last years has been to design nanosystems that combine the intrinsic targeting properties of nanocarriers with the encapsulation of adjuvants. For example, our group developed CS NCs containing adjuvants such as squalene and imiquimod (TLR7 agonist) [88]. The results of the response attained after intranasal administration of this formulation showed its capacity to generate enhanced and long-lasting IgG levels [88]. More recently, a layer-by-layer approach was used to envelop the rHBSAg viral particles with a cationic polymer (protamine or polyarginine), followed by an anionic layer of poly(I:C) [89]. These nanostructures were able to elicit a more balanced Th1/Th2 ratio after both, intranasal and intramuscular administrations [89].

2.3. Malaria

The development of an effective vaccine against malaria has also attracted a lot of attention in the last decades. In 2015, GSK licensed a vaccine under the name of Mosquirix™, that contains the circumsporozoite protein of *Plasmodium falciparum* and the liposome-based adjuvant AS01, composed by monophosphoryl lipid A (MPLA) and the saponin QS21 [90]. This new vaccine has shown good safety profiles and an efficacy rate of 50% [91], leaving the door open for new improved systems. In this regard, some critical advances have been made thanks to the use of nanotechnology. For example, Moon *et al.* developed two different formulations of the VMP001-malaria antigen. One of them consisted of PLGA NPs with a phospholipidic coating [92], and the other one of multilamellar vesicles [77], both of them carrying the malaria antigen on the surface. The subcutaneous administration of both formulations in the presence of the adjuvant MPLA led to strong humoral and cellular responses, as well as a more balanced Th1/Th2 profile [77,92]. More recently, the conjugation of the circumsporozoite protein to mannose and a TLR7 molecule outperformed the gold standard AS01, both in the elicited IgG levels and in the CD8 T cell activation extent [52].

2.4. HIV

The development of an HIV vaccine is another global challenge. According to the World Health Organization, AIDS continues to kill over 1 million people per year [93]. Currently, the most promising vaccine evaluated in clinical trials was based on the combination of a viral vector expressing the group antigens (Gag) and the protease, together with the HIV gp120 envelope (Env) recombinant glycoprotein adsorbed onto alum, which demonstrated a modest 31% efficacy [94]. These results highlight the importance of continuing the search for new HIV nanovaccines. Overall, the major obstacles for an HIV vaccine are the choice of an effective immunogen, and the development of a nanosystem with the capacity to generate a potent immune response [95,96].

Briefly, the two main current strategies for the development of an effective HIV vaccine are: (*i*) a B-cell and germinal center focused therapy involving the generation of broadly-neutralizing (bN)Abs (**Fig. 2A*i***) [97]; or (*ii*) a therapy involving the stimulation of a combination of cellular and humoral responses, as those reported in the RV144 study (**Fig. 2A*ii***) [98,99]. Additionally, vaccination schedule is also an important aspect to consider for developing an efficient vaccine. For example, it has been recently shown that, in humans, priming with a DNA vector, followed by the administration of a recombinant poxvirus vector (NYVAC), induces a rapid Ab and T cell activation [100]. In any case, whether one of the previous strategies, or a combination of them, will lead to an effective vaccine is still under debate [99]. Nevertheless, the knowledge generated through all these studies will certainly bring us closer to an effective vaccine.

With regard to the use of nanotechnology to enhance the generation of antibodies against HIV, a strategy adopted by several authors has involved the use of liposomes displaying HIV Env-trimers on their surface in order to target B cells. As a result, an enhancement on the IgG titers and neutralizing Abs in mice was observed [101–103]. In another study, multilamellar liposomes were evaluated as a potential carrier for the Env gp140 trimers [104]. This new composition resulted in Th1/Th2 balanced profiles and increased titers against the antigens in the vaccinated mice [104]. Interesting results were also reported when mixing the soluble immunogens Env and Gag, with PLGA-based NPs loaded with TLR 4/7/8 adjuvants [105]. This combination led to an enhanced protection of non-human primates (NHPs) against twelve intravaginal challenges [105]. In an approach more focused to directly generate bNAbs, the administration of lipid NPs containing a mRNA encoding for the light and heavy chains of an anti-HIV bNAb was able to elicit high levels of the Abs in the treated mice [106]. Furthermore, humanized mice vaccinated with this mRNA vaccine were protected against an HIV intravenous challenge [106].

Another strategy aimed at stimulating both, B and T cells, has made use of two liposomal formulations, one of them displaying an Env-derived peptide and encapsulating a T-helper peptide, and another one loaded with cyclic di-GMP. This combination resulted in enhanced CD4 and CD8 T cell responses, and high-titer and more durable humoral responses in mice. However, the immune sera did not neutralize HIV [107]. Another exploratory study has made use of gold NPs functionalized with mannose and carrying HIV-derived peptides. This vaccine candidate led to increased CD4 and CD8 T cell responses *in vitro* [108]. DNA vaccination using synthetic nanocarriers has also been explored for HIV. For example, an HIV DNA vaccine complexed with a mannosylated cationic lipid was found to improve the B and T cell responses against the Env protein in mice [109]. Whether these designs will

indeed be able to protect against HIV in larger animal models, and ultimately in humans, is still to be defined.

The HIV protease cleavage sites (PCSs) have been presented as an alternative to the above-mentioned immunogens (**Fig. 2A*iii***). The correct and sequential cleavage of the proteins Gag, Pol and Nef in twelve specific sites is crucial for the correct maturation of the virus [110–112] (**Fig. 2B**). Therefore, it has been proposed that the interruption of this process will be able to stop HIV infection [110,111,113]. Furthermore, since these PCSs are highly conserved sequences among HIV-1 viruses, problems related to the high mutation of HIV could also be overcome. Following this approach, NHPs were vaccinated with both, the recombinant viral vectors containing the plasmids encoding for the twelve sequences, and with antigen-loaded chitosan/dextran sulfate NPs. Overall, high IgG levels were elicited after vaccination [114]. A different study showed a significantly higher level of protection in NHPs vaccinated with the same formulations after several challenges with low doses of an SIV strain, in comparison to the group vaccinated with the empty viral vectors [115]. Therefore, these alternative antigens represent an interesting strategy in the development of an HIV vaccine.

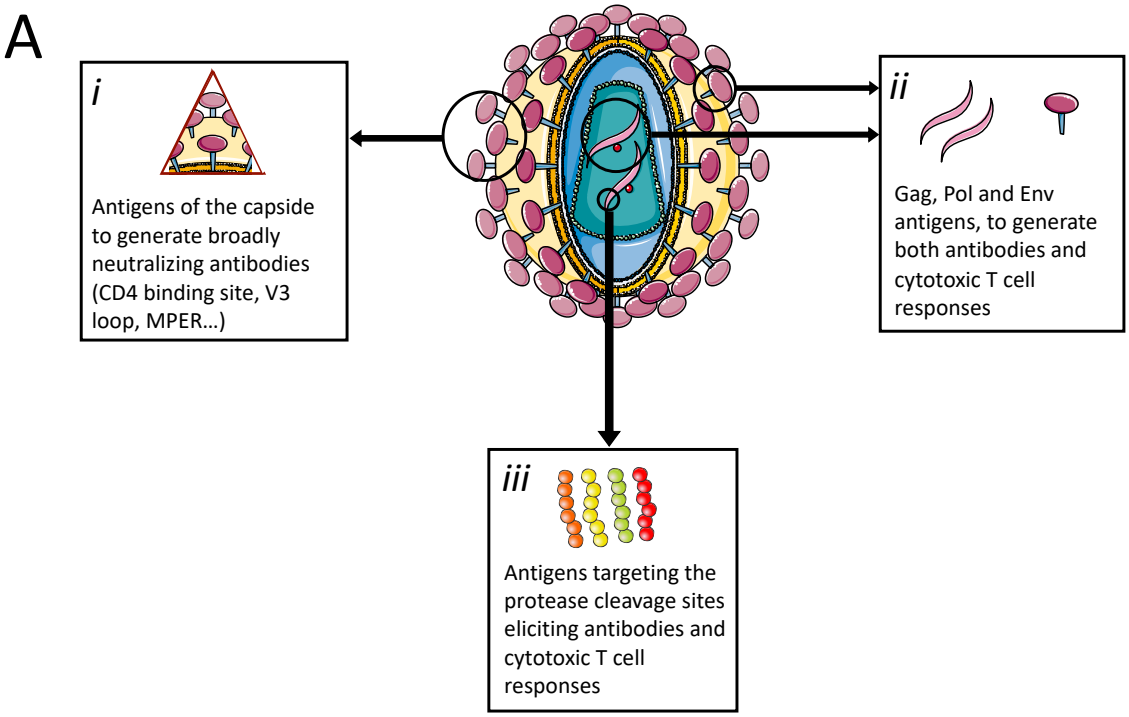

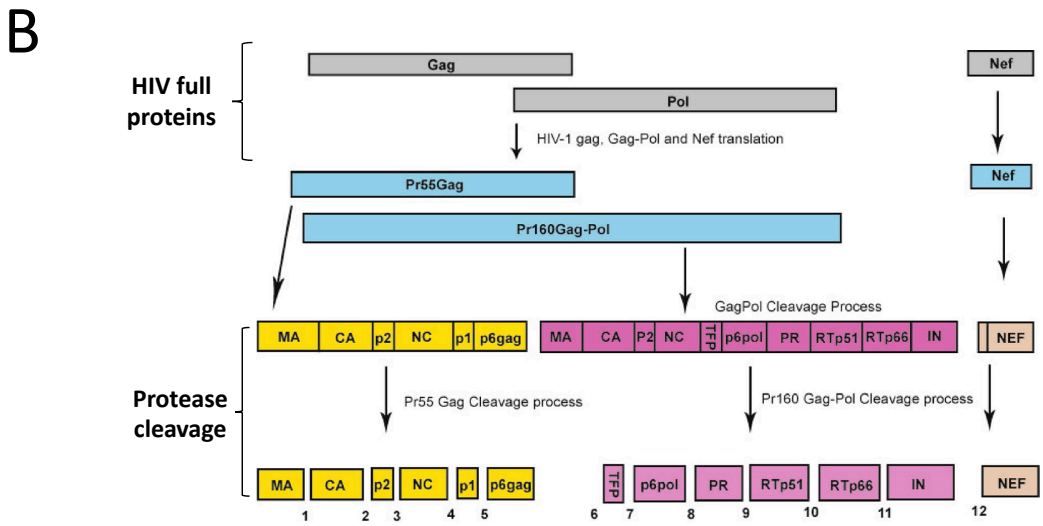

Figure 2. Overall summary of the main antigens currently under investigation for the development of an HIV vaccine. (A) (*i*) Different structures of the surface of the HIV virus have been employed in order to elicit broadly neutralizing antibodies (Env, CD4 binding site, V3 loop and surrounding glycans, membrane proximal region (MPER)…). (*ii*) Full-length proteins Gag and Pol, together with some Env proteins or peptides, have been used in the quest for generating both antibodies and cellular responses. (*iii*) The protease cleavage sites, highly conserved regions of the viruses, have been employed in order to generate antibodies and cellular responses. (B) HIV protease cleavage sites location in the Gag, Pol and Nef proteins, and fragments generated after the cleavage. The twelve peptide antigens are twenty amino acid sequences that overlap each of these twelve sequences (ten amino acids before and ten after each cleavage site). Images from (A) are reproduced and adapted from Servier Medical Art under a Creative Commons Attribution 3.0 Unported License. https://creativecommons.org/licenses/by/3.0. (B) was modified from [111] and reproduced under a Creative Commons Attribution 4.0 International License. http://creativecommons.org/licenses/by/4.0/.

2.5. Marketed adjuvants

As a result of all these investigations, some nanotechnology-based adjuvants are already commercialized (**Table 1**). This is the case of MF59, a nanoemulsion of squalene, Span 85® and Tween 80®, which can be found as part of a flu vaccine owned by Novartis [116]. Similarly, GSK has the adjuvant AS03, made of squalene, tocopherol and Tween 80®, as also part of the flu vaccine Pandemrix [117]. Finally, the adjuvant AS01 found in the malaria vaccine described in section 2.3, is a liposome-based nanosystem. Overall, so far, synthetic lipidic-based systems are the ones that have made their way to the patients.

Table 1. Commercialized nanotechnology-based adjuvants for human use

Adjuvant / Company	Composition	Disease	Licensing year
MF59 / Novartis	Squalene, Span 85® and Tween 80®	Influenza	1997
AS03 / GSK	Squalene, tocopherol and Tween 80®	Influenza	2009
AS01 / GSK	Monophosphoryl lipid A and QS21 (saponin)	Malaria Herpez zoster	2015 2017

Besides these adjuvants, some current vaccines against the human papilloma virus (HPV) and hepatitis B are based on virus-like particles (VLPs) [118].

3. Nanoimmunotherapies in cancer

The importance of the immune system in cancer progression, and the subsequent exploitation of this information, is just beginning. Although the concept of cancer immunotherapy dates from the late XIX century, its impact was only materialized in the last decades [119]. Understanding the role and the potential interventions over the immune system in order to potentiate its response against cancer, is the base of these therapies [120]. As illustrated in **Figure 3**, there are numerous factors involved in the immune response against cancer. At each point, different molecular cues can enhance or inhibit these steps, biasing the final outcome towards either cancer progression or elimination [121]. From a therapeutic perspective, by boosting or blocking the factors involved in the cancer-immunity cycle, the immune system can be redirected towards preventing tumor progression, and ultimately leading to tumor elimination.

It is interesting to note the increasing number of immunotherapies on the market (**Table 2**), using different pharmacological strategies, that will be described in the following sections. Unfortunately, many other immunotherapies have not reached the market due to their significant side effects [122]. This important drawback has opened the door for nanotechnology, since it offers strategies to facilitate the accumulation of active compounds in the target site, thereby reducing their off-target

effects [123,124]. Furthermore, even for local administration, the use of NPs to increase the retention in the injection site has proved to be advantageous in comparison to the use of the soluble forms [124].

Table 2. Summary of the immunotherapies currently approved for cancer treatment.

Type	Therapies	Mechanism	Cancer
Checkpoint blockade			
CTLA4 mAb	Ipilimumab	CTLA4 blockade	Melanoma
PD-1 mAb	Pembrolizumab Nivolumab	PD-1 blockade	Melanoma, NSCLC, Hodgkin lymphoma, advanced gastric cancer, head and neck cancer, advanced urothelial bladder cancer, colorectal cancer and hepatocellular cancer
PD-L1 mAb	Atezolizumab Avelumab Durvalumab	PD-L1 blockade	Urothelial cancer, NSCLC, Merkel cell carcinoma
Cytokines			
Recombinant IFN-α2a / IFN-α2b	Roferon A Intron A	Lymphocyte stimulation	HCL, CML, melanoma, follicular lymphoma and Kaposi sarcoma
Recombinant IL-2	Aldesleukin	Lymphocyte stimulation	Melanoma and kidney cancer
TLR agonists			
TLR7 agonist[a]	Imiquimod	Stimulates production of TNF, IL-12 and IFN-γ	Basal cell carcinoma
TLR2, 4 and 9 agonist[b]	Bacillus Calmette–Guérin	Activation of TLR2, 4 and 9	Bladder cancer
TLR4 agonist[c]	Monophosphoryl lipid A (MPLA)	Boosts response against antigen (as part of AS04)	Prevention of cervical cancer
Vaccines			
PBMCs pre-activated with GM-CSF and PAP	Sipuleucel T	Activates immune response against PAP	Prostate cancer
Engineered T cells			
CAR-T cells	Tisagenlecleucel Axicabtagene ciloleucel	C19-specific T cells	B-cell ALL and non-Hodgkin lymphoma Large B-cell lymphoma
Others			
Oncolytic virus	Talimogene laherparepvec	Modified HSV that replicates inside tumors and produces GM-CSF	Melanoma
Bispecific Ab	Blinatumomab	CD19 + CD3 bispecific Ab	B-cell ALL

[a]Not well stablished whether the mechanism of action depends only on a direct TLR7 activation.

[b]Normally included in the group of vaccines (TLR activation mechanism).

[c]MPLA is approved as part of the adjuvant AS04. It is not considered an immunotherapy, but a preventive vaccine.

ALL, acute lymphoblastic leukemia; CML, chronic myelogenous leukemia; GM-CSF, granulocyte-macrophage colony-stimulating factor; HCL, hairy cell leukemia; HSV, herpes simplex virus; mAb, monoclonal antibody; NSCLC, non-small-cell lung cancer; PAP, prostatic acid phosphatase; PBMCs, peripheral blood mononuclear cells.

In the following lines, the benefits of the combination of nanotechnology and immunotherapies are underlined. We describe how the use of biomaterials and NPs can decrease the resistance towards checkpoint inhibitors, or the systemic toxicity of toll-like receptor agonists, with a special mention to poly(I:C). Finally, the use of mRNAs for cancer vaccines, and the exploitation of neoantigens is also commented.

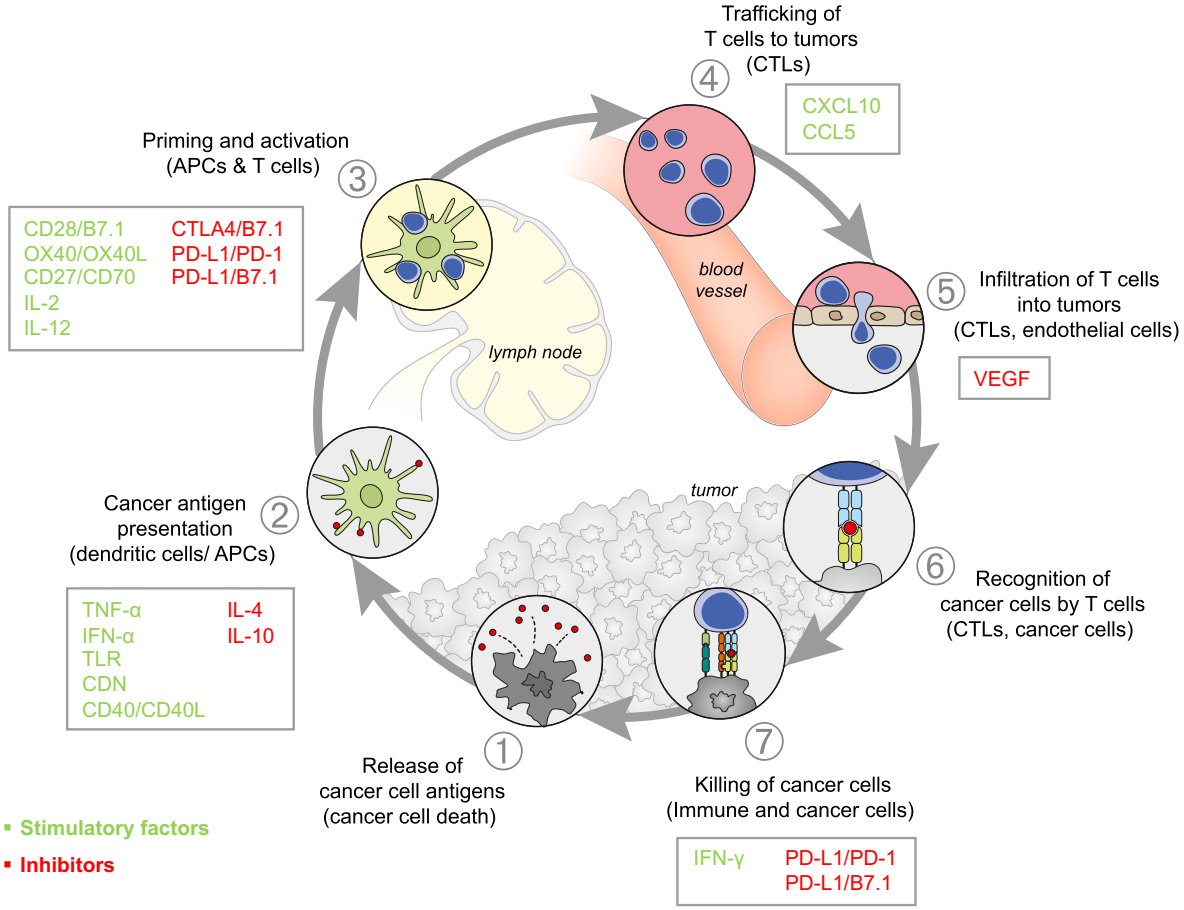

Figure 3. The cancer – immune cycle. The generation of immunity to cancer is a cyclic process that can be self-propagating. This cycle can be divided into seven major steps, starting with the release of antigens from the cancer cell and ending with the killing of cancer cells. Each step requires the coordination of numerous factors, both stimulatory and inhibitory in nature. Stimulatory factors (green) promote immunity, whereas inhibitors (red) help keeping the process in check and reduce immune activity and/or prevent autoimmunity. IL, interleukin; TNF, tumor necrosis factor; IFN, interferon; CDN, cyclic dinucleotide; TLR, Toll-like receptor; CTLA4, cytotoxic T-lymphocyte antigen-4; PD-L1, programmed death-ligand 1; CXCL/CCL, chemokine motif ligands; VEGF, vascular endothelial growth factor. Although not illustrated, it is important to note that intratumoral T regulatory cells, macrophages, and myeloid-derived suppressor cells are key sources of many of these inhibitory factors. This image has been minimally modified and reproduced with permission from [121].

3.1. Checkpoint blockade

So far, the use of monoclonal (m)Abs to target the immune checkpoints is the most common strategy followed in cancer immunotherapy. To this point, as shown in **Table 2**, six different mAbs against the cytotoxic T lymphocyte antigen 4 (CTLA4) and the programmed cell death 1 (PD-1) protein, or its ligand 1 (PD-L1), are already in the clinic [125]. CTLA4 is an membrane protein in activated T cells, that binds to CD80 and CD86 co-stimulatory molecules with a higher affinity than the natural CD28 receptor, therefore blocking one of the T cell stimulatory signals and leading to T cell attenuation [126,127]. PD-1 is also a membrane protein expressed in activated T cells, allowing them to recognize foreign structures that do not express its ligand PD-L1. As a scape mechanism, tumor cells are able to express PD-L1, avoiding their recognition by T cells [127]. Targeting and blocking any of these receptors (or their ligands) allows a continuous activation and proliferation of T cells, killing tumor cells. Unfortunately, these therapies carry some downsides, mainly due to important immune-related side effects [127,128], resistance mechanisms or lack of responsiveness in some patients [129]. As a consequence, more advanced therapies involving a combination of pharmacological entities are being considered as the next step in immunotherapy.

Within this context, NPs can be used to ameliorate this resistance or decrease toxicity. Indeed, the encapsulation of an anti-PD-1 mAb in pegylated PLGA NPs was able to decrease the drug dose necessary for an effective therapeutic effect in a murine melanoma model. This positive outcome was attributed to the accumulation of the NPs in the spleen, where a significant population of APCs expressing PD-1 can be found [130]. A different approach made use of microneedles with pH-sensitive dextran NPs containing an anti-PD-1 mAb and a pH-triggering molecule (glucose oxidase) [131]. The sustained release of the mAb from the patch applied over the tumour area was more efficacious in terms of tumor growth than the intratumoral administration of the free mAb [131]. Similarly, the sustained release of an anti-PD-1 peptide from PLGA NPs was more efficient than the single administration of the free peptide [132]. In this case, the combination with photothermal ablation was able to improve mice survival in comparison to the separated therapies, together with an increased anti-tumoral effect in distant tumors [132].

A combination therapy involving an anti-PD-L1 mAb and 4-1BB (a co-stimulatory receptor in effector T cells) has also been presented in the form of iron-dextran NPs [133]. This construct was found to block PD-L1 in tumor cells, while activating the co-stimulatory signal of CD8 T cells and, hence, inducing CD8 T cell expansion [133]. A different approach has relied on the use of siRNA-containing NPs for silencing the expression of the checkpoint inhibitors. For example, a CTLA-4 siRNA was

encapsulated in hybrid lipid pegylated-poly-glutamic acid NPs, increasing the level of CD8 T cell infiltrates in the tumor, together with an improved survival in tumor-bearing mice [134].

3.2. Pathogen-associated molecular patterns (PAMPs)

Toll-like receptors are the most well-known pattern recognition receptors, with the capacity to sense pathogen-associated cues. A total of ten TLRs have been identified in humans, and they can be found either on the external membrane of APCs (TLR1, 2, 4, 5, 6 and 10) or inside the endosomes (TLR3, 7, 8 and 9) [135]. Simplistically, external TLR recognize bacterial pathogens, while intracellular TLRs detect viral infections [135,136]. The activation of TLRs triggers MyD88 or TRIF cascades, which upregulate different inflammatory pathways [135,136]. As shown in **Table 2**, three different TLR agonists have been marketed for cancer therapy: the *bacillus* Calmette-Guérin, monophosphoryl lipid A (TLR4 agonist) and imiquimod (TLR7 agonist) [137]. In the case of the *bacillus* Calmette-Guérin, it is known that its therapeutic effect is through the activation of TLR2, TLR4 and TLR9 [137,138]. Imiquimod is a TLR7 activator, although its therapeutic effect in basal cell carcinoma could be dependent on other additional mechanisms [139]. Finally, for MPLA, included in the adjuvant AS04, the mechanism of action has not been fully elucidated. In addition to these marketed immunomodulators, in a preclinical setting, there are several agonists of TLR3, TLR7, TLR7/8, and TLR9 being evaluated [140]. An overview of their use in the form of NPs is provided below.

3.2.1. TLR3 agonists

Upon contact with double stranded (ds)RNA, TLR3 upregulates the TRIF pathway, ultimately stimulating the expression of IFN-I genes and generating pro-inflammatory features [141]. A synthetic dsRNA name as poly(I:C) is the most used TLR3 agonist at the preclinical level [141]. Currently, there are three derivatives of poly(I:C) in clinical trials: Ampligen®/Rintolimod® (polyI:C_{12}U), a poly(I:C) with an uridine residue every twelve cytosines in one of the RNA chains, that has demonstrated less toxicity and higher stability than the original poly(I:C) [142]; Hiltonol®, which is a poly(I:C) stabilized with poly-lysine and carboxymethylcellulose, known as poly-ICLC [143]; and BO-112, which is a polyplex of poly(I:C) and polyethyleneimine [144].

TLR3 agonists have been used as a single immunostimulant therapy and also in combination with tumor antigens. Besides the TRIF activation, some reports have claimed that the anti-tumor effect of poly(I:C) is due to the activation of the MDA5 and RIG-I intracellular receptors in tumor cells, with the subsequent apoptotic cell death [145,146]. Other recent works have been focused on the ability of this dsRNA to polarize tolerogenic M2 macrophages towards anti-tumoral M1 phenotypes in the tumor

microenvironment [147]. Despite these positive responses, this immunostimulant is known to cause important systemic side effects [148]. As a consequence, poly(I:C) needs to be administered by intratumoral injection. To solve this limitation, several tumor targeting approaches based on the use of nanocarriers have been reported. For example, the incorporation of poly(I:C) within liposomes was shown to increase the CD8 T cell response in vaccinated mice, while the systemic toxicity of the free form was decreased [149,150]. Similarly, it has been reported that the inclusion of poly(I:C) within chitosan NPs, or micelles, together with antigens and other modulators, may lead to important anti-tumor responses [151,152]. Alternatively, the association of poly(I:C) to iron oxide NPs resulted in an immune activation [153], and an improved therapeutic effect in different cancer models [154,155]. This still emerging activity has already led to the phase I clinical trials evaluation of a nanotechnology-based poly(I:C) formulation consisting of its complexation with polyethyleneimine [156].

The combination of several TLR agonists is also an approach that is gaining interest. For example, the association of a poly(I:C)–imiquimod (TLR7 agonist) complex onto magnetic NPs was able to delay tumor progression in mice [157].

3.2.2. TLR7 and TLR7/8 agonists

TLR7 and 8 are single-stranded (ss)RNAs that upregulate the MyD88 cascade [135]. So far, as mentioned earlier, imiquimod is the only marketed TLR7 agonist, indicated for the topical treatment of basal cell carcinomas and warts, however, there are other agonists that hold potential as immunotherapeutic molecules in cancer [158].

There are only a few examples on the use of nanotechnology to deliver these agonists. For example, the TLR7 agonist named as TMX–202, encapsulated in liposomes, was reported to increase the secretion of pro-inflammatory cytokines *in vitro* [159]. On the other hand, the use of a combination of TLR7 and 8, has resulted in the dual activation of DCs and T cells, ultimately decreasing the tumor burden in three different murine cancer models [160]. Following this trend, the dual TLR7/8 agonist resiquimod is also under investigation as a potential immunotherapeutic treatment. Recently, Weissleder and collaborators demonstrated an improved therapeutic performance of resiquimod when included in cyclodextrin NPs [161]. The anti-tumoral effect of these NPs was shown to be mediated by a polarization of the M2 pro-tumoral macrophages towards M1 phenotypes, and was more effective than the free resiquimod [161]. In fact, the conjunction of these NPs with an anti-PD-1 Ab in a non-responsive anti-PD-1 mice model decreased the tumor development in comparison to the separate approaches [161]. Similarly, the targeted delivery of resiquimod-loaded PLGA NPs to PD-1-expressing T cells extended the survival of the treated animals [162].

3.2.3. TLR9 agonists

TLR9 is activated by some DNA molecules, more specifically, unmethylated cytosine-phosphorothioester-guanine (CpG) dinucleotides, which are common in viruses and bacteria [163]. As artificial agonists, a great number of synthetic CpG oligodeoxynucleotide (ODN) have been developed for cancer therapy [163].

With regards to the formulation of CpG in the form of a nanostructure, it is worth mentioning the formation of lipid-modified CpGs with the capacity to self-assemble into micelles, which were shown to activate DCs *in vivo* [164]. In addition, the combination of CpGs with OVA as antigen, either through the complexation with polyethyleneimine, or by their association to organosilica NPs, showed a synergistic effect in terms of reducing tumor growth [165,166]. Furthermore, the co-administration of a cholesterol-modified CpG and the TLR4 agonist MPLA into nanodiscs, with the E7 peptide antigen, was reported to increase the survival in an HPV-associated cancer model [167].

Overall, all TLR agonists have shown significant potential in the modulation of the tumor microenvironment, alone or in combination with other agonists, antigens or checkpoint inhibitors. One key aspect for their successful translation to the clinic will be to guarantee their specific delivery to the target site, thereby limiting the undesired side effects.

3.3. Cancer vaccines

Cancer vaccination is driven by the activation of the immune system to fight against specific tumor antigens. By presenting these antigens to APCs, CD4 and CD8 T cells responses might increase, mitigating tumor progression. Traditionally, the antigens exploited for anti-cancer vaccination have been tumor-associated antigens (TAAs). These antigens are known to be overexpressed in tumors, but they are also presented in healthy tissues. The use of mRNAs coding for these TAAs is one of the most novel delivery approaches.

Alternatively, in the last years, a new group of antigens has emerged for cancer vaccination, the so-called tumor-specific antigens or neoantigens. These molecules are uniquely expressed by tumor cells and not by normal tissues, thereby directing the immune response only to the cancer cells, and decreasing off-target side effects [168].

In the following lines, we have focused on the most novel approaches for cancer vaccination: the delivery of TAAS as mRNA vaccines, and the use of neoantigens.

3.3.1. Tumor-associated antigens in mRNA vaccines

The most common approaches for mRNA vaccines are focused on a direct administration of the polynucleotides into critical tissues (lymph nodes or tumors), where APCs can directly interact with the mRNA, expressing the antigen and eliciting an immune response against it [169–171]. Nevertheless, the limitations of this therapeutic approach are mainly related to the instability of mRNA and its indiscriminate biodistribution, a fact that makes their intratumoral or intranodal administration necessary. The formulation of mRNA vaccines in nanosystems is nowadays an approach to overcome these hurdles. For example, Anderson and collaborators, using a model luciferase mRNA, have worked on the development of nanosystems able to protect and increase the response against mRNAs [172,173]. Further studies with this lipid-based nanosystem containing an ionizable lipid, showed that it has the capacity to increase the CD8 T cell response against two melanoma antigens, with important survival benefit [174]. Similarly, Kranz *et al.* showed that mRNA lipoplexes were able to increase the T cell response against the encoding tumor antigen in patients [175].

Furthermore, combination therapies of mRNA vaccines and checkpoint inhibitors have shown to synergistically improve cancer survival [169]. For example, lipid/calcium/phosphate NPs functionalized with mannose for a targeted delivery to DCs, and containing an mRNA for MUC1 antigen, were administered to an orthotopic triple negative breast cancer model [176]. Although the NPs alone were able to decrease tumor progression, only the combination with an anti-CTLA-4 mAb improved the infiltration of CD8 T cells, and further reduced tumor development [176].

3.3.2. Neoantigens

Somatic mutations can lead to the expression of tumor-specific proteins, solely presented by cancer cells [168]. These proteins can be employed as antigens, preventing the autoimmunity or immune tolerance of other non-specific antigens, like TAAs [168,177]. In this regard, clinical trials have already shown the capacity of neoantigens to induce satisfactory immune responses against them [178,179]. Preclinically, neoantigens have been delivered as long peptides, naked polynucleotides, within pulsed DCs, or in nanosystems [180].

In terms of the application of nanotechnology to improve the immune response against neoantigens, Zhu *et al.* have reported the development of self-assembled intertwining DNA-RNA NCs, that synergistically delivered CpG, a Stat3 short hairpin RNA, and a peptide neoantigen, that presented good therapeutic results [181]. Other approaches using ultra-pH-sensitive NPs, associating OVA or neoantigens, were able to decrease tumor development in different cancer models [182]. The

combination of nanodiscs loaded with CpG and a cocktail of melanoma neoantigens, together with checkpoint inhibitors, was able to eradicate tumor development in 85% of the treated animals [183].

Collectively, although a huge number of nanotechnological approaches have been implemented to improve cancer immunotherapy, it seems that the future tendencies are focused on the development of combined therapies, harnessing different and synergistic routes to overcome resistance [119].

4. On the road to the market

Despite the promising approaches where the application of nanotechnology for modulating the immune response has shown a therapeutic benefit, the number of nanotechnology-based drug products in the market is still scarce. This restricted translation to the clinic has been attributed to different factors [184]. For example, there is a limited knowledge about the influence of the physiopathology of diseases on the biodistribution of different nanocarriers. Indeed, the dogma of the enhanced permeability and retention (EPR) effect, which has been employed as one of the main reasons behind the potential of nanotechnology, is now known to occur only in some specific tumors [185]. Hence, a more personalized characterization of the tumors would permit patient stratification and selection of the potential responders to the nanomedicines, thereby allowing a more efficient clinical translation [186,187]. More importantly, the identification of tissue and cell targets that may be used to selectively guide the biodistribution of targeted carriers needs to be further expanded [188]. Additionally, as for all therapies, the results obtained in rodent animals used as preclinical models for the evaluation of the nanosystems are difficult to translate into a clinical setting, and this is mainly due to the obvious enormous differences in the biodistribution [185]. Finally, one could say that, often, *in vivo* studies reported in the literature lack of the appropriate controls that would help to comparatively understand the behavior of the therapies.

Other difficulties are related to the translation of the manufacturing processes from the bench side to an industrial environment. It has been reported that the scale-up of complex formulations can lead to reproducibility problems, and that consistent methods for an adequate characterization are necessary [189]. In this regard, significant advances have been made by specialized organizations in terms of standardizing the techniques for the characterization of nanomedicines [190], and defining appropriate methods for a more realistic characterization of the nanomedicine candidates [191,192]. This advances will certainly help to improve the safety and biocompatibility of the nanomedicine [184]. Ultimately, all these advances in developing unified methods and protocols, and in better

understanding relation between diseases and NPs properties, will contribute to a more successful translation of nanomedicines.

Although this is still an emerging field, we already have examples of immuno-based nanomedicines that have reached the market, or that are under clinical evaluation. These examples are described below.

4.1. Nanovaccines in the market and under evaluation

As already mentioned in section 2, some NP-based adjuvants have already reached the market (MF59, AS03 and AS01). Besides, the commercialized HPV and hepatitis B vaccines are based on VLPs [118]. In addition, a great number of vaccine nanoformulations are now in clinical trials (**Table 3**) [193]. The most advanced nanovaccines in clinical trials are currently in phase III. One is a combination of NanoFlu™ (NPs made of protein antigens) and Matrix M™ (a lipidic-based adjuvant). The other also contains the antigen proteins self-assembled into NPs. The rest of the nanovaccines under clinical evaluation are mainly composed by lipidic systems, similar to the marketed adjuvants (**Table 2**). A different approach is the one making use of inulin microparticles (Advax®), currently in Phase I/II clinical trials for hepatitis B and Influenza.

Table 3. **Most relevant nanovaccine for infectious diseases in clinical trials**

Name / Company	Nanomedicine	Disease	Clinical Phase	Ref.
NanoFlu™ + Matrix M™ / Novavax	NanoFlu: recombinant hemagglutinin protein NP + Matrix M™: saponin-based particles (saponins, synthetic Chol and phospholipids)	Influenza	Phase III	[194,195]
RSV F Vaccine / Novavax	RSV F Vaccine: recombinant F-proteins from RSV that self-assemble into NPs	RSV	Phase III	[196,197]
CTH522-CAF01 / Statens Serum Institut	CAF01: cationic liposomal adjuvant	Chlamydia (*C. trachomatis*)	Towards Phase II	[198]
HBV003 / Vaxine Pty Ltd.	Advax: D-inulin MPs	Hepatitis B	Phase I/II	[199,200]
R21 + Matrix M™ / University of Oxford & Novavax	Antigen + Matrix M™	Malaria	Phase I/II	[194,201]
MAS-1 / Nova Immunotherapeutics Ltd.	Nanoparticular emulsion-based adjuvant	Seasonal Influenza	Phase I	[202,203]
Advax - CpG55.2 / US NIAID	Advax: D-inulin MPs	Seasonal Influenza	Phase I	[204]
1790GAHB / GSK	GMMA: outer membrane particles from bacteria	Dysentery (*Shigella sonnei*)	Phase I	[205]
DPX-RSV / IMV Inc.	LNPs containing RSV SHe antigen	RSV	Phase I	[206]

Chol, cholesterol; CpG, cytosine-phosphorothioester-guanine GMMA, generalized modules of membrane antigen; MP, microparticle; NIAID, National Institute of Allergy and Infectious Diseases; NP, nanoparticle; LNP, lipid nanoparticle; RSV, respiratory syncital virus.

4.2. Nanoimmunotherapies in clinical trials

Currently, probably due to the limited number of marketed immunotherapies, the number of nanotechnology-based immunotherapies in clinical development is not extensive [123]. These potential nanomedicine candidates are summarized in **Table 4** [193]. The majority of them are in the form of liposomes containing tumor antigens. Moreover, many of these nanoformulation contain additional immunomodulators, such as MPLA, CpG or IL-2. A quite exceptional nanocomposition is the one named as BO-112 (from the Spanish company Bioncotech), which has no antigen nor lipid in its composition, but is based on the complexation of the positively charged polyethyleneimine with the negatively charged poly(I:C).

Overall, it seems clear that cancer vaccines and combinatory therapies are demonstrating a promising effectiveness in cancer treatment.

Table 4. **Clinical trials of some relevant nanoimmunotherapeutics**

Name / Company	Nanomedicine	Disease	Clinical Phase	Ref.
MAGE-A3 ASCI / GSK and Oncovir Inc.	AS15 adjuvant (liposomes of MPLA, QS21 and CpG) + recMAGE-A3	Melanoma	Phase II	[207]
L-BLP25 / ECOG-ACRIN Cancer Research Group	Liposome with tecemotide (lipopeptide targeting MUC1) and adjuvant MPLA	Lung cancer	Phase II	[208]
Oncoquest™-L / XEME Biopharma Inc.	Aggregon® liposomes: neoantigen + IL-2	Lymphoma	Phase II	[209]
DPX-Survivac / IMV Inc. & Merck	LNPs with TAA (Survivin)	Diffuse large B-cell lymphoma	Phase II	[210]
DPX-Survivac / IMV Inc. & Merck	LNPs with TAA (Survivin)	Advanced ovarian, primary peritoneal and fallopian tube cancer	Phase II	[211]
DPX-Survivac / IMV Inc. & Merck	LNPs with TAA (Survivin)	Ovarian, hepatocellular, non-small cell lung and bladder cancers	Phase II	[212]
DPX-Survivac / IMV Inc.	LNPs with TAA (Survivin)	Recurrent ovarian, peritoneal and fallopian tube cancers	Phase I/II	[213]
DPX-E7 / Dana Farber Cancer Institute	LNPs with an HPV antigen	Head, neck, cervix and anus cancer	Phase I/II	[214]
BO-112 / Bioncotech	Polyplex of poly(I:C) and polyethyleneimine	Aggressive solid tumors	Phase I	[144]
BNT111 / Biontech	FixVac®: mRNA lipoplex (4 MAAs)	Melanoma	Phase I	[215]
BNT114 / Biontech	FixVac®: liposomes + mRNA (neoantigens)	Triple negative breast cancer	Phase I	[216]
Oncoquest™-CLL / XEME Biopharma Inc.	Aggregon® liposomes: neoantigen + IL-2	Chronic lymphocytic leukemia	Phase I	[217]
AS15 + MAG-Tn3 / Institute Pasteur	AS15 adjuvant (liposomes of MPLA, QS21 and CpG) + MAG-Tn3 synthetic vaccine	Breast neoplasms	Phase I	[218]
WDVAX / Dana-Farber Cancer Institute	PLGA scaffold with GM-CSF, CpG and melanoma tumor lysate	Melanoma	Phase I	[219]

CpG, cytosine-phosphorothioester-guanine; DCs, dendritic cells; GM-CSF, granulocyte-macrophage colony-stimulating factor; HPV, human papilloma virus; IMV, ImmunoVaccine; LNPs, lipid nanoparticles; MAAs, melanoma-associated antigens; MPLA, monophosphoryl lipid A; MUC1: Mucin 1, cell surface associated; PLGA, poly-lactic-co-glycolic acid; recMAGE-A3: recombinant melanoma-associated antigen 3; TAA, tumor-associated antigen.

5. Conclusions and future perspectives

Overall, nanotechnology is nowadays considered as a powerful strategy to modulate the immune system and the different players involved in its regulation. In the vaccine field, nanotechnology has led to the development and commercialization of modern adjuvants that may increase the immune response against new and very poorly immunogenic antigens. In the area of cancer immunotherapies, nanotechnology has been shown to enable the accumulation of immunomodulating compounds in the target site, thus decreasing their undesired side effects. At the same time, as therapies advance and the knowledge of the molecular basis governing diseases grows, it becomes clear that the future steps are being directed towards the definition of combination of therapies. Although there are still some challenges to overcome in order to have more robust nanomedicines, considerable advances have been achieved in the last years. It is likely that thanks to all the research efforts currently ongoing, more advanced nanotechnology-based therapies will soon be improving patients' lives.

References

[1] T.G. Dacoba, A. Olivera, D. Torres, J. Crecente-Campo, M.J. Alonso, Modulating the immune system through nanotechnology, Semin. Immunol. 34 (2017) 78–102. doi:10.1016/j.smim.2017.09.007.

[2] M.F. Bachmann, G.T. Jennings, Vaccine delivery: a matter of size, geometry, kinetics and molecular patterns, Nat. Rev. Immunol. 10 (2010) 787–796. doi:10.1038/nri2868.

[3] D.M. Smith, J.K. Simon, J.R. Baker, Applications of nanotechnology for immunology, Nat. Rev. Immunol. 13 (2013) 592–605. doi:10.1038/nri3488.

[4] D.J. Irvine, M.C. Hanson, K. Rakhra, T. Tokatlian, Synthetic nanoparticles for vaccines and immunotherapy, Chem. Rev. 115 (2015) 11109–11146. doi:10.1021/acs.chemrev.5b00109.

[5] A.S. Cordeiro, M.J. Alonso, Recent advances in vaccine delivery, Pharm. Pat. Anal. 5 (2015) 49–73. doi:10.4155/ppa.15.38.

[6] A.S. Cordeiro, M.J. Alonso, M. de la Fuente, Nanoengineering of vaccines using natural polysaccharides, Biotechnol. Adv. 33 (2015) 1279–1293. doi:10.1016/j.biotechadv.2015.05.010.

[7] D. Van Duin, R. Medzhitov, A.C. Shaw, Triggering TLR signaling in vaccination, Trends Immunol. 27 (2006) 49–55. doi:10.1016/j.it.2005.11.005.

[8] A. Gutjahr, G. Tiraby, E. Perouzel, B. Verrier, S. Paul, Triggering intracellular receptors for vaccine adjuvantation, Trends Immunol. 37 (2016) 573–587. doi:10.1016/j.it.2016.07.001.

[9] D.R. Getts, L.D. Shea, S.D. Miller, N.J.C. King, Harnessing nanoparticles for immune modulation, Trends Immunol. 36 (2015) 419–427. doi:10.1016/j.it.2015.05.007.

[10] K.T. Gause, A.K. Wheatley, J. Cui, Y. Yan, S.J. Kent, F. Caruso, Immunological principles guiding the rational design of particles for vaccine delivery, ACS Nano. 11 (2017) 54–68. doi:10.1021/acsnano.6b07343.

[11] E. Ben-Akiva, S. Est Witte, R.A. Meyer, K.R. Rhodes, J.J. Green, Polymeric micro- and nanoparticles for immune modulation, Biomater. Sci. 7 (2019) 14–30. doi:10.1039/C8BM01285G.

[12] D.C. Hinshaw, L.A. Shevde, The tumor microenvironment innately modulates cancer progression, Cancer Res. 79 (2019) 4557–4566. doi:10.1158/0008-5472.CAN-18-3962.

[13] A. Mantovani, S. Sozzani, M. Locati, P. Allavena, A. Sica, Macrophage polarization: tumor-associated macrophages as a paradigm for polarized M2 mononuclear phagocytes, Trends Immunol. 23 (2002) 549–555. doi:10.1016/S1471-4906(02)02302-5.

[14] A. Mantovani, A. Sica, S. Sozzani, P. Allavena, A. Vecchi, M. Locati, The chemokine system in diverse forms of macrophage activation and polarization, Trends Immunol. 25 (2004) 677–686. doi:10.1016/j.it.2004.09.015.

[15] R. Noy, J.W. Pollard, Tumor-associated macrophages: from mechanisms to therapy, Immunity. 41 (2014) 49–61. doi:10.1016/j.immuni.2014.06.010.

[16] T. Krausgruber, K. Blazek, T. Smallie, S. Alzabin, H. Lockstone, N. Sahgal, T. Hussell, M. Feldmann, I.A. Udalova, IRF5 promotes inflammatory macrophage polarization and TH1-TH17 responses, Nat. Immunol. 12 (2011) 231–238. doi:10.1038/ni.1990.

[17] J.A. Champion, A. Walker, S. Mitragotri, Role of particle size in phagocytosis of polymeric microspheres, Pharm. Res. 25 (2008) 1815–1821. doi:10.1007/s11095-008-9562-y.

[18] N. Doshi, S. Mitragotri, Macrophages recognize size and shape of their targets, PLoS One. 5 (2010) 1–6. doi:10.1371/journal.pone.0010051.

[19] C. He, Y. Hu, L. Yin, C. Tang, C. Yin, Effects of particle size and surface charge on cellular uptake and biodistribution of polymeric nanoparticles, Biomaterials. 31 (2010) 3657–3666. doi:10.1016/j.biomaterials.2010.01.065.

[20] P. Pacheco, D. White, T. Sulchek, Effects of microparticle size and Fc density on macrophage phagocytosis, PLoS One. 8 (2013) 1–9. doi:10.1371/journal.pone.0060989.

[21] J. Crecente-Campo, J. Guerra-Varela, M. Peleteiro, C. Gutiérrez-Lovera, I. Fernández-Mariño, A. Diéguez-Docampo, Á. González-Fernández, L. Sánchez, M.J. Alonso, The size and composition of polymeric

nanocapsules dictate their interaction with macrophages and biodistribution in zebrafish, J. Control. Release. 308 (2019) 98–108. doi:10.1016/j.jconrel.2019.07.011.

[22] A.S. Cordeiro, J. Crecente-Campo, B.L. Bouzo, S.F. González, M. de la Fuente, M.J. Alonso, Engineering polymeric nanocapsules for an efficient drainage and biodistribution in the lymphatic system, J. Drug Target. 27 (2019) 646–658. doi:10.1080/1061186X.2018.1561886.

[23] J. Lesley, R. Hyman, P.W. Kincade, CD44 and its interaction with extracellular matrix, Adv. Immunol. 54 (1993) 271–335. doi:10.1016/S0065-2776(08)60537-4.

[24] R.A. Clark, R. Alon, T.A. Springer, CD44 and hyaluronan-dependent rolling interactions of lymphocytes on tonsillar stroma, J. Cell Biol. 134 (1996) 1075–1087. doi:10.1083/jcb.134.4.1075.

[25] J.M. Rios de la Rosa, A. Tirella, A. Gennari, I.J. Stratford, N. Tirelli, The CD44-mediated uptake of hyaluronic acid-based carriers in macrophages, Adv. Healthc. Mater. 6 (2017) 1601012. doi:10.1002/adhm.201601012.

[26] C. Ke, D. Wang, Y. Sun, D. Qiao, H. Ye, X. Zeng, Immunostimulatory and antiangiogenic activities of low molecular weight hyaluronic acid, Food Chem. Toxicol. 58 (2013) 401–407. doi:10.1016/j.fct.2013.05.032.

[27] L.Y.W. Bourguignon, G. Wong, C.A. Earle, W. Xia, Interaction of low molecular weight hyaluronan with CD44 and toll-like receptors promotes the actin filament-associated protein 110-actin binding and MyD88-NFκB signaling leading to proinflammatory cytokine/chemokine production and breast tumor invasion, Cytoskeleton. 68 (2011) 671–693. doi:10.1002/cm.20544.

[28] D. Jiang, J. Liang, J. Fan, S. Yu, S. Chen, Y. Luo, G.D. Prestwich, M.M. Mascarenhas, H.G. Garg, D.A. Quinn, R.J. Homer, D.R. Goldstein, R. Bucala, P.J. Lee, R. Medzhitov, P.W. Noble, Regulation of lung injury and repair by Toll-like receptors and hyaluronan, Nat. Med. 11 (2005) 1173–1179. doi:10.1038/nm1315.

[29] K.A. Scheibner, M.A. Lutz, S. Boodoo, M.J. Fenton, J.D. Powell, M.R. Horton, Hyaluronan fragments act as an endogenous danger signal by engaging TLR2, J. Immunol. 177 (2006) 1272–1281. doi:10.4049/jimmunol.177.2.1272.

[30] M. Song, T. Liu, C. Shi, X. Zhang, X. Chen, Bioconjugated manganese dioxide nanoparticles enhance chemotherapy response by priming tumor-associated macrophages toward M1-like phenotype and attenuating tumor hypoxia, ACS Nano. 10 (2016) 633–647. doi:10.1021/acsnano.5b06779.

[31] Y. Glucksam-Galnoy, T. Zor, R. Margalit, Hyaluronan-modified and regular multilamellar liposomes provide sub-cellular targeting to macrophages, without eliciting a pro-inflammatory response, J. Control. Release. 160 (2012) 388–393. doi:10.1016/j.jconrel.2011.10.008.

[32] T. Ben-Mordechai, D. Kain, R. Holbova, N. Landa, L.-P. Levin, I. Elron-Gross, Y. Glucksam-Galnoy, M.S. Feinberg, R. Margalit, J. Leor, Targeting and modulating infarct macrophages with hemin formulated in designed lipid-based particles improves cardiac remodeling and function, J. Control. Release. 257 (2017) 21–31. doi:10.1016/j.jconrel.2017.01.001.

[33] C.M. McKee, M.B. Penno, M. Cowman, M.D. Burdick, R.M. Strieter, C. Bao, P.W. Noble, Hyaluronan (HA) fragments induce chemokine gene expression in alveolar macrophages: the role of HA size and CD44., J. Clin. Invest. 98 (1996) 2403–2413. doi:10.1172/JCI119054.

[34] J.E. Rayahin, J.S. Buhrman, Y. Zhang, T.J. Koh, R.A. Gemeinhart, High and low molecular weight hyaluronic acid differentially influence macrophage activation, ACS Biomater. Sci. Eng. 1 (2015) 481–493. doi:10.1021/acsbiomaterials.5b00181.

[35] S. Mizrahy, S.R. Raz, M. Hasgaard, H. Liu, N. Soffer-Tsur, K. Cohen, R. Dvash, D. Landsman-Milo, M.G.E.G. Bremer, S.M. Moghimi, D. Peer, Hyaluronan-coated nanoparticles: The influence of the molecular weight on CD44-hyaluronan interactions and on the immune response, J. Control. Release. 156 (2011) 231–238. doi:10.1016/j.jconrel.2011.06.031.

[36] D. Peer, R. Margalit, Loading mitomycin C inside long circulating hyaluronan targeted nano-liposomes increases its antitumor activity in three mice tumor models, Int. J. Cancer. 108 (2004) 780–789.

doi:10.1002/ijc.11615.

[37] K.Y. Choi, K.H. Min, J.H. Na, K. Choi, K. Kim, J.H. Park, I.C. Kwon, S.Y. Jeong, Self-assembled hyaluronic acid nanoparticles as a potential drug carrier for cancer therapy: synthesis, characterization, and in vivo biodistribution, J. Mater. Chem. 19 (2009) 4102. doi:10.1039/b900456d.

[38] X. Yang, Y. Li, M. Li, L. Zhang, L. Feng, N. Zhang, Hyaluronic acid-coated nanostructured lipid carriers for targeting paclitaxel to cancer, Cancer Lett. 334 (2013) 338–345. doi:10.1016/j.canlet.2012.07.002.

[39] A. Almalik, H. Benabdelkamel, A. Masood, I.O. Alanazi, I. Alradwan, M.A. Majrashi, A.A. Alfadda, W.M. Alghamdi, H. Alrabiah, N. Tirelli, A.H. Alhasan, Hyaluronic acid coated chitosan nanoparticles reduced the immunogenicity of the formed protein corona, Sci. Rep. 7 (2017) 1–9. doi:10.1038/s41598-017-10836-7.

[40] M. Yang, J. Ding, X. Feng, F. Chang, Y. Wang, Z. Gao, X. Zhuang, X. Chen, Scavenger receptor-mediated targeted treatment of collagen-induced arthritis by dextran sulfate-methotrexate prodrug, Theranostics. 7 (2017) 97–105. doi:10.7150/thno.16844.

[41] R. Heo, D.G. You, W. Um, K.Y. Choi, S. Jeon, J.-S. Park, Y. Choi, S. Kwon, K. Kim, I.C. Kwon, D.-G. Jo, Y.M. Kang, J.H. Park, Dextran sulfate nanoparticles as a theranostic nanomedicine for rheumatoid arthritis, Biomaterials. 131 (2017) 15–26. doi:10.1016/j.biomaterials.2017.03.044.

[42] L. Ma, T.-W.W. Liu, M.A. Wallig, I.T. Dobrucki, L.W. Dobrucki, E.R. Nelson, K.S. Swanson, A.M. Smith, Efficient targeting of adipose tissue macrophages in obesity with polysaccharide nanocarriers, ACS Nano. 10 (2016) 6952–6962. doi:10.1021/acsnano.6b02878.

[43] Y. Singh, V.K. Pawar, J.G. Meher, K. Raval, A. Kumar, R. Shrivastava, S. Bhadauria, M.K. Chourasia, Targeting tumor associated macrophages (TAMs) via nanocarriers, J. Control. Release. 254 (2017) 92–106. doi:10.1016/j.jconrel.2017.03.395.

[44] A. Costa, B. Sarmento, V. Seabra, Mannose-functionalized solid lipid nanoparticles are effective in targeting alveolar macrophages, Eur. J. Pharm. Sci. 114 (2018) 103–113. doi:10.1016/j.ejps.2017.12.006.

[45] L.W. Locke, M.W. Mayo, A.D. Yoo, M.B. Williams, S.S. Berr, PET imaging of tumor associated macrophages using mannose coated 64Cu liposomes, Biomaterials. 33 (2012) 7785–7793. doi:10.1016/j.biomaterials.2012.07.022.

[46] H. He, Q. Yuan, J. Bie, R.L. Wallace, P.J. Yannie, J. Wang, M.G. Lancina, O.Y. Zolotarskaya, W. Korzun, H. Yang, S. Ghosh, Development of mannose functionalized dendrimeric nanoparticles for targeted delivery to macrophages: use of this platform to modulate atherosclerosis, Transl. Res. 193 (2018) 13–30. doi:10.1016/j.trsl.2017.10.008.

[47] L. Liu, H. Yi, H. He, H. Pan, L. Cai, Y. Ma, Tumor associated macrophage-targeted microRNA delivery with dual-responsive polypeptide nanovectors for anti-cancer therapy, Biomaterials. 134 (2017) 166–179. doi:10.1016/j.biomaterials.2017.04.043.

[48] P. Guermonprez, J. Valladeau, L. Zitvogel, C. Théry, S. Amigorena, Antigen presentation and T cell stimulation by dendritic cells, Annu. Rev. Immunol. 20 (2002) 621–667. doi:10.1146/annurev.immunol.20.100301.064828.

[49] J.M.M. den Haan, R. Arens, M.C. van Zelm, The activation of the adaptive immune system: cross-talk between antigen-presenting cells, T cells and B cells, Immunol. Lett. 162 (2014) 103–112. doi:10.1016/j.imlet.2014.10.011.

[50] J. Crecente-Campo, T. Virgilio, D. Morone, C. Calviño-Sampedro, I. Fernández-Mariño, A. Olivera, R. Varela-Calvino, S.F. González, M.J. Alonso, Design of polymeric nanocapsules to improve their lympho-targeting capacity, Nanomedicine. (2019). doi:10.2217/nnm-2019-0206.

[51] J. Conniot, A. Scomparin, C. Peres, E. Yeini, S. Pozzi, A.I. Matos, R. Kleiner, L.I.F. Moura, E. Zupančič, A.S. Viana, H. Doron, P.M.P. Gois, N. Erez, S. Jung, R. Satchi-Fainaro, H.F. Florindo, Immunization with mannosylated nanovaccines and inhibition of the immune-suppressing microenvironment sensitizes melanoma to immune checkpoint modulators, Nat. Nanotechnol. 14 (2019) 891–901. doi:10.1038/s41565-019-0512-0.

[52] D.S. Wilson, S. Hirosue, M.M. Raczy, L. Bonilla-Ramirez, L. Jeanbart, R. Wang, M. Kwissa, J.-F. Franetich, M.A.S. Broggi, G. Diaceri, X. Quaglia-Thermes, D. Mazier, M.A. Swartz, J.A. Hubbell, Antigens reversibly conjugated to a polymeric glyco-adjuvant induce protective humoral and cellular immunity, Nat. Mater. 18 (2019) 175–185. doi:10.1038/s41563-018-0256-5.

[53] L.J. Cruz, R.A. Rosalia, J.W. Kleinovink, F. Rueda, C.W.G.M. Löwik, F. Ossendorp, Targeting nanoparticles to CD40, DEC-205 or CD11c molecules on dendritic cells for efficient CD8+ T cell response: a comparative study, J. Control. Release. 192 (2014) 209–218. doi:10.1016/j.jconrel.2014.07.040.

[54] D.I. Gabrilovich, S. Nagaraj, Myeloid-derived suppressor cells as regulators of the immune system, Nat. Rev. Immunol. 9 (2009) 162–174. doi:10.1038/nri2506.

[55] L. Jeanbart, I.C. Kourtis, A.J. van der Vlies, M.A. Swartz, J.A. Hubbell, 6-Thioguanine-loaded polymeric micelles deplete myeloid-derived suppressor cells and enhance the efficacy of T cell immunotherapy in tumor-bearing mice, Cancer Immunol. Immunother. 64 (2015) 1033–1046. doi:10.1007/s00262-015-1702-8.

[56] M.S. Sasso, G. Lollo, M. Pitorre, S. Solito, L. Pinton, S. Valpione, G. Bastiat, S. Mandruzzato, V. Bronte, I. Marigo, J.-P. Benoit, Low dose gemcitabine-loaded lipid nanocapsules target monocytic myeloid-derived suppressor cells and potentiate cancer immunotherapy, Biomaterials. 96 (2016) 47–62. doi:10.1016/j.biomaterials.2016.04.010.

[57] A.M. Ledo, M.S. Sasso, V. Bronte, I. Marigo, B.J. Boyd, M. Garcia-Fuentes, M.J. Alonso, Co-delivery of RNAi and chemokine by polyarginine nanocapsules enables the modulation of myeloid-derived suppressor cells, J. Control. Release. 295 (2019) 60–73. doi:10.1016/j.jconrel.2018.12.041.

[58] H. Stabile, C. Fionda, A. Gismondi, A. Santoni, Role of distinct natural killer cell subsets in anticancer response, Front. Immunol. 8 (2017) 1–8. doi:10.3389/fimmu.2017.00293.

[59] S. Nair, M. V. Dhodapkar, Natural killer T cells in cancer immunotherapy, Front. Immunol. 8 (2017) 1–18. doi:10.3389/fimmu.2017.01178.

[60] V. Sainz, L.I.F. Moura, C. Peres, A.I. Matos, A.S. Viana, A.M. Wagner, J.E. Vela Ramirez, T. S. Barata, M. Gaspar, S. Brocchini, M. Zloh, N.A. Peppas, R. Satchi-Fainaro, H. F. Florindo, α-Galactosylceramide and peptide-based nano-vaccine synergistically induced a strong tumor suppressive effect in melanoma, Acta Biomater. 76 (2018) 193–207. doi:10.1016/j.actbio.2018.06.029.

[61] R. Verbeke, I. Lentacker, K. Breckpot, J. Janssens, S. Van Calenbergh, S.C. De Smedt, H. Dewitte, Broadening the message: a nanovaccine co-loaded with messenger RNA and α-galcer induces antitumor immunity through conventional and natural killer TcCells, ACS Nano. 13 (2019) 1655–1669. doi:10.1021/acsnano.8b07660.

[62] M. Kong, J. Tang, Q. Qiao, T. Wu, Y. Qi, S. Tan, X. Gao, Z. Zhang, Biodegradable hollow mesoporous silica nanoparticles for regulating tumor microenvironment and enhancing antitumor efficiency, Theranostics. 7 (2017) 3276–3292. doi:10.7150/thno.19987.

[63] H.L. Wright, R.J. Moots, R.C. Bucknall, S.W. Edwards, Neutrophil function in inflammation and inflammatory diseases, Rheumatology. 49 (2010) 1618–1631. doi:10.1093/rheumatology/keq045.

[64] E. Uribe-Querol, C. Rosales, Neutrophils in cancer: two sides of the same coin, J. Immunol. Res. 2015 (2015) 1–21. doi:10.1155/2015/983698.

[65] Y. Liu, Z.-T. Cao, C.-F. Xu, Z.-D. Lu, Y.-L. Luo, J. Wang, Optimization of lipid-assisted nanoparticle for disturbing neutrophils-related inflammation, Biomaterials. 172 (2018) 92–104. doi:10.1016/j.biomaterials.2018.04.052.

[66] Z. Wang, J. Li, J. Cho, A.B. Malik, Prevention of vascular inflammation by nanoparticle targeting of adherent neutrophils, Nat. Nanotechnol. 9 (2014) 204–210. doi:10.1038/nnano.2014.17.

[67] J.C. Sunshine, J.J. Green, Nanoengineering approaches to the design of artificial antigen-presenting cells, Nanomedicine. 8 (2013) 1173–89. doi:10.2217/nnm.13.98.

[68] J.C. Sunshine, K. Perica, J.P. Schneck, J.J. Green, Particle shape dependence of CD8+ T cell activation by

artificial antigen presenting cells, Biomaterials. 35 (2014) 269–277. doi:10.1016/j.biomaterials.2013.09.050.

[69] R.A. Meyer, J.C. Sunshine, K. Perica, A.K. Kosmides, K. Aje, J.P. Schneck, J.J. Green, Biodegradable nanoellipsoidal artificial antigen presenting cells for antigen specific T-cell activation, Small. 11 (2015) 1519–1525. doi:10.1002/smll.201402369.

[70] A.K. Kosmides, R.A. Meyer, J.W. Hickey, K. Aje, K.N. Cheung, J.J. Green, J.P. Schneck, Biomimetic biodegradable artificial antigen presenting cells synergize with PD-1 blockade to treat melanoma, Biomaterials. 118 (2017) 16–26. doi:10.1016/j.biomaterials.2016.11.038.

[71] S.A. Rosenberg, N.P. Restifo, Adoptive cell transfer as personalized immunotherapy for human cancer, Science. 348 (2015) 62–68. doi:10.1126/science.aaa4967.

[72] H.F. Moffett, M.E. Coon, S. Radtke, S.B. Stephan, L. McKnight, A. Lambert, B.L. Stoddard, H.P. Kiem, M.T. Stephan, Hit-and-run programming of therapeutic cytoreagents using mRNA nanocarriers, Nat. Commun. 8 (2017) 389. doi:10.1038/s41467-017-00505-8.

[73] T.T. Smith, S.B. Stephan, H.F. Moffett, L.E. McKnight, W. Ji, D. Reiman, E. Bonagofski, M.E. Wohlfahrt, S.P.S. Pillai, M.T. Stephan, In situ programming of leukaemia-specific T cells using synthetic DNA nanocarriers, Nat. Nanotechnol. 12 (2017) 813–820. doi:10.1038/nnano.2017.57.

[74] F.D. Batista, N.E. Harwood, The who, how and where of antigen presentation to B cells., Nat. Rev. Immunol. 9 (2008) 15–27. doi:10.1038/nri2454.

[75] E. De Gregorio, E. Caproni, J.B. Ulmer, Vaccine adjuvants: mode of action, Front. Immunol. 4 (2013) 1–6. doi:10.3389/fimmu.2013.00214.

[76] V. V. Temchura, D. Kozlova, V. Sokolova, K. Überla, M. Epple, Targeting and activation of antigen-specific B-cells by calcium phosphate nanoparticles loaded with protein antigen, Biomaterials. 35 (2014) 6098–6105. doi:10.1016/j.biomaterials.2014.04.010.

[77] J.J. Moon, H. Suh, V. Li, C.F. Ockenhouse, A. Yadava, D.J. Irvine, Enhancing humoral responses to a malaria antigen with nanoparticle vaccines that expand Tfh cells and promote germinal center induction, Proc. Natl. Acad. Sci. 109 (2012) 1080–1085. doi:10.1073/pnas.1112648109.

[78] G. Birrenbach, P.P. Speiser, Polymerized micelles and their use as adjuvants in immunology, J. Pharm. Sci. 65 (1976) 1763–1766. doi:10.1002/jps.2600651217.

[79] I. Preis, R.S. Langer, A single-step immunization by sustained antigen release, J. Immunol. Methods. 28 (1979) 193–197. doi:10.1016/0022-1759(79)90341-7.

[80] M.J. Alonso, R.K. Gupta, C. Min, G.R. Siber, R. Langer, Biodegradable microspheres as controlled-release tetanus toxoid delivery systems, Vaccine. 12 (1994) 299–306. doi:10.1016/0264-410X(94)90092-2.

[81] A. Sánchez, R.K. Gupta, M.J. Alonso, G.R. Siber, R. Langer, Pulsed controlled-released system for potential use in vaccine delivery, J Pharm Sci. 85 (1996) 547–52. doi:10.1021/js960069y.

[82] M. Tobío, J. Nolley, Y. Guo, J. McIver, M.J. Alonso, A novel system based on a poloxamer/PLGA blend as a tetanus toxoid delivery vehicle, Pharm. Res. 16 (1999) 682–688. doi:10.1023/a:1018820507379.

[83] A.J. Almeida, H.O. Alpar, M.R.W. Brown, Immune response to nasal delivery of antigenically intact tetanus toxoid associated with poly(L-lactic acid) microspheres in rats, rabbits and guinea-pigs, J. Pharm. Pharmacol. 45 (1993) 198–203. doi:10.1111/j.2042-7158.1993.tb05532.x.

[84] A. Vila, A. Sánchez, M. Tobío, P. Calvo, M.J. Alonso, Design of biodegradable particles for protein delivery, J. Control. Release. 78 (2002) 15–24. doi:10.1016/S0168-3659(01)00486-2.

[85] C. Prego, P. Paolicelli, B. Díaz, S. Vicente, A. Sánchez, Á. González-Fernández, M.J. Alonso, Chitosan-based nanoparticles for improving immunization against hepatitis B infection, Vaccine. 28 (2010) 2607–2614. doi:10.1016/j.vaccine.2010.01.011.

[86] S. Vicente, B. Diaz-Freitas, M. Peleteiro, A. Sanchez, D.W. Pascual, A. Gonzalez-Fernandez, M.J. Alonso, A polymer/oil based nanovaccine as a single-dose immunization approach, PLoS One. 8 (2013) 2–9. doi:10.1371/journal.pone.0062500.

[87] C. Prego, D. Torres, M.J. Alonso, Chitosan nanocapsules: a new carrier for nasal peptide delivery, J. Drug Deliv. Sci. Technol. 16 (2006) 331–337. doi:10.1016/S1773-2247(06)50061-9.

[88] S. Vicente, M. Peleteiro, B. Díaz-Freitas, A. Sanchez, Á. González-Fernández, M.J. Alonso, Co-delivery of viral proteins and a TLR7 agonist from polysaccharide nanocapsules: a needle-free vaccination strategy, J. Control. Release. 172 (2013) 773–781. doi:10.1016/j.jconrel.2013.09.012.

[89] J.F. Correia-Pinto, M. Peleteiro, N. Csaba, Á. González-Fernández, M.J. Alonso, Multi-enveloping of particulated antigens with biopolymers and immunostimulant polynucleotides, J. Drug Deliv. Sci. Technol. 30 (2015) 424–434. doi:10.1016/j.jddst.2015.08.010.

[90] A.M. Didierlaurent, B. Laupèze, A. Di Pasquale, N. Hergli, C. Collignon, N. Garçon, Adjuvant system AS01: helping to overcome the challenges of modern vaccines, Expert Rev. Vaccines. 16 (2017) 55–63. doi:10.1080/14760584.2016.1213632.

[91] C.T.P. RTS, S, Efficacy and safety of RTS,S/AS01 malaria vaccine with or without a booster dose in infants and children in Africa: final results of a phase 3, individually randomised, controlled trial, Lancet. 386 (2015) 31–45. doi:10.1016/S0140-6736(15)60721-8.

[92] J.J. Moon, H. Suh, M.E. Polhemus, C.F. Ockenhouse, A. Yadava, D.J. Irvine, Antigen-displaying lipid-enveloped PLGA nanoparticles as delivery agents for a Plasmodium vivax malaria vaccine, PLoS One. 7 (2012). doi:10.1371/journal.pone.0031472.

[93] UNAIDS Data 2018, (n.d.). http://www.unaids.org/sites/default/files/media_asset/unaids-data-2018_en.pdf (accessed September 19, 2018).

[94] S. Rerks-Ngarm, P. Pitisuttithum, S. Nitayaphan, J. Kaewkungwal, J. Chiu, R. Paris, N. Premsri, C. Namwat, M. de Souza, E. Adams, M. Benenson, S. Gurunathan, J. Tartaglia, J.G. McNeil, D.P. Francis, D. Stablein, D.L. Birx, S. Chunsuttiwat, C. Khamboonruang, P. Thongcharoen, M.L. Robb, N.L. Michael, P. Kunasol, J.H. Kim, Vaccination with ALVAC and AIDSVAX to prevent HIV-1 infection in Thailand, N. Engl. J. Med. 361 (2009) 2209–2220. doi:10.1056/NEJMoa0908492.

[95] B.F. Haynes, New approaches to HIV vaccine development, Curr. Opin. Immunol. 35 (2015) 39–47. doi:10.1016/j.coi.2015.05.007.

[96] Y. Liu, C. Chen, Role of nanotechnology in HIV/AIDS vaccine development, Adv. Drug Deliv. Rev. 103 (2016) 76–89. doi:10.1016/j.addr.2016.02.010.

[97] M. Caskey, F. Klein, M.C. Nussenzweig, Broadly neutralizing anti-HIV-1 monoclonal antibodies in the clinic, Nat. Med. 25 (2019) 547–553. doi:10.1038/s41591-019-0412-8.

[98] HIV vaccines go to trial, Nat. Med. 25 (2019) 703. doi:10.1038/s41591-019-0460-0.

[99] S.J. Kent, M.P. Davenport, Moving the HIV vaccine field forward: concepts of protective immunity, Lancet HIV. 6 (2019) e406–e410. doi:10.1016/S2352-3018(19)30134-1.

[100] G. Pantaleo, H. Janes, S. Karuna, S. Grant, G.L. Ouedraogo, M. Allen, G.D. Tomaras, N. Frahm, D.C. Montefiori, G. Ferrari, S. Ding, C. Lee, M.L. Robb, M. Esteban, R. Wagner, P.-A. Bart, N. Rettby, M.J. McElrath, P.B. Gilbert, J.G. Kublin, L. Corey, Safety and immunogenicity of a multivalent HIV vaccine comprising envelope protein with either DNA or NYVAC vectors (HVTN 096): a phase 1b, double-blind, placebo-controlled trial, Lancet HIV. 6 (2019) e737–e749. doi:10.1016/S2352-3018(19)30262-0.

[101] J. Ingale, A. Stano, J. Guenaga, S.K. Sharma, D. Nemazee, M.B. Zwick, R.T. Wyatt, High-density array of well-ordered HIV-1 spikes on synthetic liposomal nanoparticles efficiently activate B cells, Cell Rep. 15 (2016) 1986–1999. doi:10.1016/j.celrep.2016.04.078.

[102] J.M. Steichen, D.W. Kulp, T. Tokatlian, A. Escolano, P. Dosenovic, R.L. Stanfield, L.E. McCoy, G. Ozorowski, X. Hu, O. Kalyuzhniy, B. Briney, T. Schiffner, F. Garces, N.T. Freund, A.D. Gitlin, S. Menis, E. Georgeson, M. Kubitz, Y. Adachi, M. Jones, A.A. Mutafyan, D.S. Yun, C.T. Mayer, A.B. Ward, D.R. Burton, I.A. Wilson, D.J. Irvine, M.C. Nussenzweig, W.R. Schief, HIV vaccine design to target germline precursors of glycan-dependent broadly neutralizing antibodies, Immunity. 45 (2016) 483–496. doi:10.1016/j.immuni.2016.08.016.

[103] S. Bale, G. Goebrecht, A. Stano, R. Wilson, T. Ota, K. Tran, J. Ingale, M.B. Zwick, R.T. Wyatt, Covalent linkage of HIV-1 trimers to synthetic liposomes elicits improved B cell and antibody responses, J. Virol. 91 (2017) e00443-17. doi:10.1128/JVI.00443-17.

[104] S. Pejawar-Gaddy, J.M. Kovacs, D.H. Barouch, B. Chen, D.J. Irvine, Design of lipid nanocapsule delivery vehicles for multivalent display of recombinant Env trimers in HIV vaccination, Bioconjug. Chem. 25 (2014) 1470–1478. doi:10.1021/bc5002246.

[105] S.P. Kasturi, P.A. Kozlowski, H.I. Nakaya, M.C. Burger, P. Russo, M. Pham, Y. Kovalenkov, E.L. V. Silveira, C. Havenar-Daughton, S.L. Burton, K.M. Kilgore, M.J. Johnson, R. Nabi, T. Legere, Z.J. Sher, X. Chen, R.R. Amara, E. Hunter, S.E. Bosinger, P. Spearman, S. Crotty, F. Villinger, C.A. Derdeyn, J. Wrammert, B. Pulendran, Adjuvanting a simian immunodeficiency virus vaccine with toll-like receptor ligands encapsulated in nanoparticles induces persistent antibody responses and enhanced protection in TRIM5α restrictive macaques, J. Virol. 91 (2017) e01844-16. doi:10.1128/JVI.01844-16.

[106] N. Pardi, A.J. Secreto, X. Shan, F. Debonera, J. Glover, Y. Yi, H. Muramatsu, H. Ni, B.L. Mui, Y.K. Tam, F. Shaheen, R.G. Collman, K. Karikó, G.A. Danet-Desnoyers, T.D. Madden, M.J. Hope, D. Weissman, Administration of nucleoside-modified mRNA encoding broadly neutralizing antibody protects humanized mice from HIV-1 challenge, Nat. Commun. 8 (2017) 14630. doi:10.1038/ncomms14630.

[107] M.C. Hanson, M.P. Crespo, W. Abraham, K.D. Moynihan, G.L. Szeto, S.H. Chen, M.B. Melo, S. Mueller, D.J. Irvine, Nanoparticulate STING agonists are potent lymph node-targeted vaccine adjuvants, J. Clin. Invest. 125 (2015) 2532–2546. doi:10.1172/JCI79915.

[108] N. Climent, I. García, M. Marradi, F. Chiodo, L. Miralles, M.J. Maleno, J.M. Gatell, F. García, S. Penadés, M. Plana, Loading dendritic cells with gold nanoparticles (GNPs) bearing HIV-peptides and mannosides enhance HIV-specific T cell responses, Nanomedicine Nanotechnology, Biol. Med. 14 (2018) 339–351. doi:10.1016/j.nano.2017.11.009.

[109] C. Qiao, J. Liu, J. Yang, Y. Li, J. Weng, Y. Shao, X. Zhang, Enhanced non-inflammasome mediated immune responses by mannosylated zwitterionic-based cationic liposomes for HIV DNA vaccines, Biomaterials. 85 (2016) 1–17. doi:10.1016/j.biomaterials.2016.01.054.

[110] M. Luo, R. Capina, C. Daniuk, J. Tuff, H. Peters, M. Kimani, C. Wachihi, J. Kimani, T.B. Ball, F.A. Plummer, Immunogenicity of sequences around HIV-1 protease cleavage sites: potential targets and population coverage analysis for a HIV vaccine targeting protease cleavage sites, Vaccine. 31 (2013) 3000–3008. doi:10.1016/j.vaccine.2013.04.057.

[111] H. Li, R.W. Omange, F.A. Plummer, M. Luo, A novel HIV vaccine targeting the protease cleavage sites, AIDS Res. Ther. 14 (2017) 51. doi:10.1186/s12981-017-0174-7.

[112] H. Li, R.W. Omange, C. Czarnecki, J.F. Correia-Pinto, J. Crecente-Campo, M. Richmond, L. Li, N. Schultz-Darken, M.J. Alonso, J.B. Whitney, F.A. Plummer, M. Luo, Mauritian cynomolgus macaques with M3M4 MHC genotype control SIVmac251 infection, J. Med. Primatol. 46 (2017) 137–143. doi:10.1111/jmp.12300.

[113] A.H. Kaplan, J.A. Zack, M. Knigge, D.A. Paul, D.J. Kempf, D.W. Norbeck, R. Swanstrom, Partial inhibition of the human immunodeficiency virus type 1 protease results in aberrant virus assembly and the formation of noninfectious particles, J. Virol. 67 (1993) 4050–4055.

[114] H. Li, M. Nykoluk, L. Li, L.R. Liu, R.W. Omange, G. Soule, L.T. Schroeder, N. Toledo, M.A. Kashem, J.F. Correia-Pinto, B. Liang, N. Schultz-Darken, M.J. Alonso, J.B. Whitney, F.A. Plummer, M. Luo, Natural and cross-inducible anti-SIV antibodies in Mauritian cynomolgus macaques, PLoS One. 12 (2017) 1–20. doi:10.1371/journal.pone.0186079.

[115] H. Li, R.W. Omange, B. Liang, N. Toledo, Y. Hai, L.R. Liu, D. Schalk, J. Crecente-Campo, T.G. Dacoba, A.B. Lambe, S.-Y. Lim, L. Li, M.A. Kashem, Y. Wan, J.F. Correia-Pinto, X.Q. Liu, R.F. Balshaw, Q. Li, E. Rakasz, N. Schultz-Darken, M.J. Alonso, J.B. Whitney, F.A. Plummer, M. Luo, A novel vaccine targeting the viral protease cleavage sites protects Mauritian cynomolgus macaques against vaginal SIVmac251 infection,

BioRxiv. (2019). doi:10.1101/842955.

[116] D.T. O'Hagan, G.S. Ott, E. De Gregorio, A. Seubert, The mechanism of action of MF59 – An innately attractive adjuvant formulation, Vaccine. 30 (2012) 4341–4348. doi:10.1016/j.vaccine.2011.09.061.

[117] G. Ledet, L.A. Bostanian, T.K. Mandal, Nanoemulsions as a vaccine adjuvant, in: A. Tiwari, A. Tiwari (Eds.), Bioeng. Nanomater., CRC press: Boca Raton, 2013: pp. 125–148.

[118] A. Roldão, M.C.M. Mellado, L.R. Castilho, M.J. Carrondo, P.M. Alves, Virus-like particles in vaccine development, Expert Rev. Vaccines. 9 (2010) 1149–1176. doi:10.1586/erv.10.115.

[119] J. Nam, S. Son, K.S. Park, W. Zou, L.D. Shea, J.J. Moon, Cancer nanomedicine for combination cancer immunotherapy, Nat. Rev. Mater. 4 (2019) 398–414. doi:10.1038/s41578-019-0108-1.

[120] T.A. Waldmann, Immunotherapy: past, present and future, Nat. Med. 9 (2003) 269–277. doi:10.1038/nm0303-269.

[121] D.S. Chen, I. Mellman, Oncology meets immunology: the cancer-immunity cycle, Immunity. 39 (2013) 1–10. doi:10.1016/j.immuni.2013.07.012.

[122] L. Milling, Y. Zhang, D.J. Irvine, Delivering safer immunotherapies for cancer, Adv. Drug Deliv. Rev. 114 (2017) 79–101. doi:10.1016/j.addr.2017.05.011.

[123] R.S. Riley, C.H. June, R. Langer, M.J. Mitchell, Delivery technologies for cancer immunotherapy, Nat. Rev. Drug Discov. 18 (2019) 175–196. doi:10.1038/s41573-018-0006-z.

[124] M.S. Goldberg, Improving cancer immunotherapy through nanotechnology, Nat. Rev. Cancer. 19 (2019) 587–602. doi:10.1038/s41568-019-0186-9.

[125] A. Ribas, J.D. Wolchok, Cancer immunotherapy using checkpoint blockade, Science. 359 (2018) 1350–1355. doi:10.1126/science.aar4060.

[126] C.A. Chambers, M.S. Kuhns, J.G. Egen, J.P. Allison, CTLA-4-mediated inhibition in regultation of T cell responses: mechanisms and manipulation in tumor immunotherapy, Annu. Rev. Immunol. 19 (2001) 565–594. doi:10.1146/annurev.immunol.19.1.565.

[127] S.C. Wei, C.R. Duffy, J.P. Allison, Fundamental mechanisms of immune checkpoint blockade therapy, Cancer Discov. 8 (2018) 1069–1086. doi:10.1158/2159-8290.CD-18-0367.

[128] J.J. Moslehi, J.-E. Salem, J.A. Sosman, B. Lebrun-Vignes, D.B. Johnson, Increased reporting of fatal immune checkpoint inhibitor-associated myocarditis, Lancet. 391 (2018) 933. doi:10.1016/S0140-6736(18)30533-6.

[129] R.W. Jenkins, D.A. Barbie, K.T. Flaherty, Mechanisms of resistance to immune checkpoint inhibitors, Br. J. Cancer. 118 (2018) 9–16. doi:10.1038/bjc.2017.434.

[130] F. Ordikhani, M. Uehara, V. Kasinath, L. Dai, S.K. Eskandari, B. Bahmani, M. Yonar, J.R. Azzi, Y. Haik, P.T. Sage, G.F. Murphy, N. Annabi, T. Schatton, I. Guleria, R. Abdi, Targeting antigen-presenting cells by anti–PD-1 nanoparticles augments antitumor immunity, JCI Insight. (2018). doi:10.1172/jci.insight.122700.

[131] C. Wang, Y. Ye, G.M. Hochu, H. Sadeghifar, Z. Gu, Enhanced cancer immunotherapy by microneedle patch-assisted delivery of anti-PD1 antibody, Nano Lett. 16 (2016) 2334–2340. doi:10.1021/acs.nanolett.5b05030.

[132] L. Luo, J. Yang, C. Zhu, M. Jiang, X. Guo, W. Li, X. Yin, H. Yin, B. Qin, X. Yuan, Q. Li, Y. Du, J. You, Sustained release of anti-PD-1 peptide for perdurable immunotherapy together with photothermal ablation against primary and distant tumors, J. Control. Release. 278 (2018) 87–99. doi:10.1016/j.jconrel.2018.04.002.

[133] A.K. Kosmides, J.-W. Sidhom, A. Fraser, C.A. Bessell, J.P. Schneck, Dual targeting nanoparticle stimulates the immune system to inhibit tumor growth, ACS Nano. 11 (2017) 5417–5429. doi:10.1021/acsnano.6b08152.

[134] S.-Y. Li, Y. Liu, C.-F. Xu, S. Shen, R. Sun, X.-J. Du, J.-X. Xia, Y.-H. Zhu, J. Wang, Restoring anti-tumor functions of T cells via nanoparticle-mediated immune checkpoint modulation, J. Control. Release. 231 (2016) 17–28. doi:10.1016/j.jconrel.2016.01.044.

[135] H. Kanzler, F.J. Barrat, E.M. Hessel, R.L. Coffman, Therapeutic targeting of innate immunity with Toll-like

receptor agonists and antagonists, Nat. Med. 13 (2007) 552–559. doi:10.1038/nm1589.

[136] X. Cen, S. Liu, K. Cheng, The role of Toll-like receptor in inflammation and tumor immunity, Front. Pharmacol. 9 (2018) 1–8. doi:10.3389/fphar.2018.00878.

[137] K. Iribarren, N. Bloy, A. Buqué, I. Cremer, A. Eggermont, W.H. Fridman, J. Fucikova, J. Galon, R. Špíšek, L. Zitvogel, G. Kroemer, L. Galluzzi, Trial watch: immunostimulation with Toll-like receptor agonists in cancer therapy, Oncoimmunology. 5 (2016) e1088631. doi:10.1080/2162402X.2015.1088631.

[138] H. LaRue, C. Ayari, A. Bergeron, Y. Fradet, Toll-like receptors in urothelial cells —targets for cancer immunotherapy, Nat. Rev. Urol. 10 (2013) 537–545. doi:10.1038/nrurol.2013.153.

[139] A. Walter, M. Schäfer, V. Cecconi, C. Matter, M. Urosevic-Maiwald, B. Belloni, N. Schönewolf, R. Dummer, W. Bloch, S. Werner, H.-D. Beer, A. Knuth, M. van den Broek, Aldara activates TLR7-independent immune defence, Nat. Commun. 4 (2013) 1560. doi:10.1038/ncomms2566.

[140] T.H. Tran, T.T.P. Tran, D.H. Truong, H.T. Nguyen, T.T. Pham, C.S. Yong, J.O. Kim, Toll-like receptor-targeted particles: a paradigm to manipulate the tumor microenvironment for cancer immunotherapy, Acta Biomater. 94 (2019) 82–96. doi:10.1016/j.actbio.2019.05.043.

[141] B. Liu, Q. Liu, L. Yang, S.K. Palaniappan, I. Bahar, P.S. Thiagarajan, J.L. Ding, Innate immune memory and homeostasis may be conferred through crosstalk between the TLR3 and TLR7 pathways, Sci. Signal. 9 (2016) ra70–ra70. doi:10.1126/scisignal.aac9340.

[142] B.B. Gowen, M.-H. Wong, K.-H. Jung, A.B. Sanders, W.M. Mitchell, L. Alexopoulou, R.A. Flavell, R.W. Sidwell, TLR3 is essential for the induction of protective immunity against Punta Toro virus infection by the double-stranded RNA (dsRNA), poly(I:C12U), but not poly(I:C): differential recognition of synthetic dsRNA molecules, J. Immunol. 178 (2007) 5200–5208. doi:10.4049/jimmunol.178.8.5200.

[143] A.M. Salazar, H.B. Levy, S. Ondra, M. Kende, B. Scherokman, D. Brown, H. Mena, N. Martin, K. Schwab, D. Donovan, D. Dougherty, M. Pulliam, M. Ippolito, M. Graves, H. Brown, A. Ommaya, Long-term treatment of malignant gliomas with intramuscularly administered polyinosinic-polycytidylic acid stabilized with polylysine and carboxymethylcellulose: an open pilot study, Neurosurgery. 38 (1996) 1096–1103.

[144] Exploratory study of BO-112 in adult patients with aggressive solid tumors, (2016). https://clinicaltrials.gov/ct2/show/NCT02828098 (accessed January 9, 2020).

[145] R. Besch, H. Poeck, T. Hohenauer, D. Senft, G. Häcker, C. Berking, V. Hornung, S. Endres, T. Ruzicka, S. Rothenfusser, G. Hartmann, Proapoptotic signaling induced by RIG-I and MDA-5 results in type I interferon–independent apoptosis in human melanoma cells, J. Clin. Invest. 119 (2009) 2399–2411. doi:10.1172/JCI37155.

[146] T. Inao, N. Harashima, H. Monma, S. Okano, M. Itakura, T. Tanaka, Y. Tajima, M. Harada, Antitumor effects of cytoplasmic delivery of an innate adjuvant receptor ligand, poly(I:C), on human breast cancer, Breast Cancer Res. Treat. 134 (2012) 89–100. doi:10.1007/s10549-011-1930-3.

[147] Q. Zeng, C.M. Jewell, Directing toll-like receptor signaling in macrophages to enhance tumor immunotherapy, Curr. Opin. Biotechnol. 60 (2019) 138–145. doi:10.1016/j.copbio.2019.01.010.

[148] A.L. Engel, G.E. Holt, H. Lu, The pharmacokinetics of Toll-like receptor agonists and the impact on the immune system, Expert Rev. Clin. Pharmacol. 4 (2011) 275–289. doi:10.1586/ecp.11.5.

[149] P. Nordly, F. Rose, D. Christensen, H.M. Nielsen, P. Andersen, E.M. Agger, C. Foged, Immunity by formulation design: induction of high CD8+ T-cell responses by poly(I:C) incorporated into the CAF01 adjuvant via a double emulsion method, J. Control. Release. 150 (2011) 307–317. doi:10.1016/j.jconrel.2010.11.021.

[150] E.M. Varypataki, K. van der Maaden, J. Bouwstra, F. Ossendorp, W. Jiskoot, Cationic liposomes loaded with a synthetic long peptide and poly(I:C): a defined adjuvanted vaccine for induction of antigen-specific T cell cytotoxicity, AAPS J. 17 (2015) 216–226. doi:10.1208/s12248-014-9686-4.

[151] H.D. Han, Y. Byeon, J.-H. Jang, H.N. Jeon, G.H. Kim, M.G. Kim, C.-G. Pack, T.H. Kang, I.D. Jung, Y.T. Lim, Y.J.

Lee, J.-W. Lee, B.C. Shin, H.J. Ahn, A.K. Sood, Y.-M. Park, In vivo stepwise immunomodulation using chitosan nanoparticles as a platform nanotechnology for cancer immunotherapy, Sci. Rep. 6 (2016) 38348. doi:10.1038/srep38348.

[152] Z. Luo, C. Wang, H. Yi, P. Li, H. Pan, L. Liu, L. Cai, Y. Ma, Nanovaccine loaded with poly I:C and STAT3 siRNA robustly elicits anti-tumor immune responses through modulating tumor-associated dendritic cells in vivo, Biomaterials. 38 (2015) 50–60. doi:10.1016/j.biomaterials.2014.10.050.

[153] M. Cobaleda-Siles, M. Henriksen-Lacey, A.R. de Angulo, A. Bernecker, V.G. Vallejo, B. Szczupak, J. Llop, G. Pastor, S. Plaza-Garcia, M. Jauregui-Osoro, L.K. Meszaros, J.C. Mareque-Rivas, An iron oxide nanocarrier for dsRNA to target lymph nodes and strongly activate cells of the immune system, Small. 10 (2014) 5054–5067. doi:10.1002/smll.201401353.

[154] M. Ramani, M.C. Mudge, R.T. Morris, Y. Zhang, S.A. Warcholek, M.N. Hurst, J.E. Riviere, R.K. DeLong, Zinc oxide nanoparticle–poly I:C RNA complexes: implication as therapeutics against experimental melanoma, Mol. Pharm. 14 (2017) 614–625. doi:10.1021/acs.molpharmaceut.6b00795.

[155] J. Zhao, Z. Zhang, Y. Xue, G. Wang, Y. Cheng, Y. Pan, S. Zhao, Y. Hou, Anti-tumor macrophages activated by ferumoxytol combined or surface-functionalized with the TLR3 agonist poly (I : C) promote melanoma regression, Theranostics. 8 (2018) 6307–6321. doi:10.7150/thno.29746.

[156] M.A. Aznar, L. Planelles, M. Perez-Olivares, C. Molina, S. Garasa, I. Etxeberría, G. Perez, I. Rodriguez, E. Bolaños, P. Lopez-Casas, M.E. Rodriguez-Ruiz, J.L. Perez-Gracia, I. Marquez-Rodas, A. Teijeira, M. Quintero, I. Melero, Immunotherapeutic effects of intratumoral nanoplexed poly I:C, J. Immunother. Cancer. 7 (2019) 116. doi:10.1186/s40425-019-0568-2.

[157] A.I. Bocanegra Gondan, A. Ruiz-de-Angulo, A. Zabaleta, N. Gómez Blanco, B.M. Cobaleda-Siles, M.J. García-Granda, D. Padro, J. Llop, B. Arnaiz, M. Gato, D. Escors, J.C. Mareque-Rivas, Effective cancer immunotherapy in mice by polyIC-imiquimod complexes and engineered magnetic nanoparticles, Biomaterials. 170 (2018) 95–115. doi:10.1016/j.biomaterials.2018.04.003.

[158] H. Chi, C. Li, F.S. Zhao, L. Zhang, T.B. Ng, G. Jin, O. Sha, Anti-tumor activity of toll-like receptor 7 agonists, Front. Pharmacol. 8 (2017) 1–10. doi:10.3389/fphar.2017.00304.

[159] T.C.B. Klauber, J.M. Laursen, D. Zucker, S. Brix, S.S. Jensen, T.L. Andresen, Delivery of TLR7 agonist to monocytes and dendritic cells by DCIR targeted liposomes induces robust production of anti-cancer cytokines, Acta Biomater. 53 (2017) 367–377. doi:10.1016/j.actbio.2017.01.072.

[160] H. Kim, L. Niu, P. Larson, T.A. Kucaba, K.A. Murphy, B.R. James, D.M. Ferguson, T.S. Griffith, J. Panyam, Polymeric nanoparticles encapsulating novel TLR7/8 agonists as immunostimulatory adjuvants for enhanced cancer immunotherapy, Biomaterials. 164 (2018) 38–53. doi:10.1016/j.biomaterials.2018.02.034.

[161] C.B. Rodell, S.P. Arlauckas, M.F. Cuccarese, C.S. Garris, R. Li, M.S. Ahmed, R.H. Kohler, M.J. Pittet, R. Weissleder, TLR7/8-agonist-loaded nanoparticles promote the polarization of tumour-associated macrophages to enhance cancer immunotherapy, Nat. Biomed. Eng. 2 (2018) 578–588. doi:10.1038/s41551-018-0236-8.

[162] D. Schmid, C.G. Park, C.A. Hartl, N. Subedi, A.N. Cartwright, R.B. Puerto, Y. Zheng, J. Maiarana, G.J. Freeman, K.W. Wucherpfennig, D.J. Irvine, M.S. Goldberg, T cell-targeting nanoparticles focus delivery of immunotherapy to improve antitumor immunity, Nat. Commun. 8 (2017) 1747. doi:10.1038/s41467-017-01830-8.

[163] A.M. Krieg, Therapeutic potential of Toll-like receptor 9 activation, Nat. Rev. Drug Discov. 5 (2006) 471–484. doi:10.1038/nrd2059.

[164] J.-O. Jin, H. Park, W. Zhang, J.W. de Vries, A. Gruszka, M.W. Lee, D.-R. Ahn, A. Herrmann, M. Kwak, Modular delivery of CpG-incorporated lipid-DNA nanoparticles for spleen DC activation, Biomaterials. 115 (2017) 81–89. doi:10.1016/j.biomaterials.2016.11.020.

[165] X. Guan, J. Chen, Y. Hu, L. Lin, P. Sun, H. Tian, X. Chen, Highly enhanced cancer immunotherapy by

combining nanovaccine with hyaluronidase, Biomaterials. 171 (2018) 198–206. doi:10.1016/j.biomaterials.2018.04.039.

[166] Y. Lu, Y. Yang, Z. Gu, J. Zhang, H. Song, G. Xiang, C. Yu, Glutathione-depletion mesoporous organosilica nanoparticles as a self-adjuvant and co-delivery platform for enhanced cancer immunotherapy, Biomaterials. 175 (2018) 82–92. doi:10.1016/j.biomaterials.2018.05.025.

[167] R. Kuai, X. Sun, W. Yuan, L.J. Ochyl, Y. Xu, A. Hassani Najafabadi, L. Scheetz, M.-Z. Yu, I. Balwani, A. Schwendeman, J.J. Moon, Dual TLR agonist nanodiscs as a strong adjuvant system for vaccines and immunotherapy, J. Control. Release. 282 (2018) 131–139. doi:10.1016/j.jconrel.2018.04.041.

[168] M. Yarchoan, B.A. Johnson, E.R. Lutz, D.A. Laheru, E.M. Jaffee, Targeting neoantigens to augment antitumour immunity, Nat. Rev. Cancer. 17 (2017) 209–222. doi:10.1038/nrc.2016.154.

[169] N. Pardi, M.J. Hogan, F.W. Porter, D. Weissman, mRNA vaccines — a new era in vaccinology, Nat. Rev. Drug Discov. 17 (2018) 261–279. doi:10.1038/nrd.2017.243.

[170] R. Verbeke, I. Lentacker, S.C. De Smedt, H. Dewitte, Three decades of messenger RNA vaccine development, Nano Today. 28 (2019) 100766. doi:10.1016/j.nantod.2019.100766.

[171] P.S. Kowalski, A. Rudra, L. Miao, D.G. Anderson, Delivering the messenger: advances in technologies for therapeutic mRNA delivery, Mol. Ther. 27 (2019) 710–728. doi:10.1016/j.ymthe.2019.02.012.

[172] U. Capasso Palmiero, J.C. Kaczmarek, O.S. Fenton, D.G. Anderson, Poly(β-amino ester)- co -poly(caprolactone) terpolymers as nonviral vectors for mRNA delivery in vitro and in vivo, Adv. Healthc. Mater. 7 (2018) 1800249. doi:10.1002/adhm.201800249.

[173] P.S. Kowalski, U. Capasso Palmiero, Y. Huang, A. Rudra, R. Langer, D.G. Anderson, Ionizable amino-ooolyesters synthesized via ring opening polymerization of tertiary amino-alcohols for tissue selective mRNA delivery, Adv. Mater. 30 (2018) 1801151. doi:10.1002/adma.201801151.

[174] M.A. Oberli, A.M. Reichmuth, J.R. Dorkin, M.J. Mitchell, O.S. Fenton, A. Jaklenec, D.G. Anderson, R. Langer, D. Blankschtein, Lipid nanoparticle assisted mRNA delivery for potent cancer immunotherapy, Nano Lett. 17 (2017) 1326–1335. doi:10.1021/acs.nanolett.6b03329.

[175] L.M. Kranz, M. Diken, H. Haas, S. Kreiter, C. Loquai, K.C. Reuter, M. Meng, D. Fritz, F. Vascotto, H. Hefesha, C. Grunwitz, M. Vormehr, Y. Hüsemann, A. Selmi, A.N. Kuhn, J. Buck, E. Derhovanessian, R. Rae, S. Attig, J. Diekmann, R.A. Jabulowsky, S. Heesch, J. Hassel, P. Langguth, S. Grabbe, C. Huber, Ö. Türeci, U. Sahin, Systemic RNA delivery to dendritic cells exploits antiviral defence for cancer immunotherapy, Nature. 534 (2016) 396–401. doi:10.1038/nature18300.

[176] L. Liu, Y. Wang, L. Miao, Q. Liu, S. Musetti, J. Li, L. Huang, Combination immunotherapy of MUC1 mRNA nano-vaccine and CTLA-4 blockade effectively inhibits growth of triple negative breast cancer, Mol. Ther. 26 (2018) 45–55. doi:10.1016/j.ymthe.2017.10.020.

[177] T.N. Schumacher, R.D. Schreiber, Neoantigens in cancer immunotherapy, Science. 348 (2015) 69–74. doi:10.1126/science.aaa4971.

[178] B.M. Carreno, V. Magrini, M. Becker-Hapak, S. Kaabinejadian, J. Hundal, A.A. Petti, A. Ly, W.-R. Lie, W.H. Hildebrand, E.R. Mardis, G.P. Linette, A dendritic cell vaccine increases the breadth and diversity of melanoma neoantigen-specific T cells, Science. 348 (2015) 803–808. doi:10.1126/science.aaa3828.

[179] P.A. Ott, Z. Hu, D.B. Keskin, S.A. Shukla, J. Sun, D.J. Bozym, W. Zhang, A. Luoma, A. Giobbie-Hurder, L. Peter, C. Chen, O. Olive, T.A. Carter, S. Li, D.J. Lieb, T. Eisenhaure, E. Gjini, J. Stevens, W.J. Lane, I. Javeri, K. Nellaiappan, A.M. Salazar, H. Daley, M. Seaman, E.I. Buchbinder, C.H. Yoon, M. Harden, N. Lennon, S. Gabriel, S.J. Rodig, D.H. Barouch, J.C. Aster, G. Getz, K. Wucherpfennig, D. Neuberg, J. Ritz, E.S. Lander, E.F. Fritsch, N. Hacohen, C.J. Wu, An immunogenic personal neoantigen vaccine for patients with melanoma, Nature. 547 (2017) 217–221. doi:10.1038/nature22991.

[180] Y. Guo, K. Lei, L. Tang, Neoantigen vaccine delivery for personalized anticancer immunotherapy, Front. Immunol. 9 (2018) 1–8. doi:10.3389/fimmu.2018.01499.

[181] G. Zhu, L. Mei, H.D. Vishwasrao, O. Jacobson, Z. Wang, Y. Liu, B.C. Yung, X. Fu, A. Jin, G. Niu, Q. Wang, F.

Zhang, H. Shroff, X. Chen, Intertwining DNA-RNA nanocapsules loaded with tumor neoantigens as synergistic nanovaccines for cancer immunotherapy, Nat. Commun. 8 (2017). doi:10.1038/s41467-017-01386-7.

[182] M. Luo, H. Wang, Z. Wang, H. Cai, Z. Lu, Y. Li, M. Du, G. Huang, C. Wang, X. Chen, M.R. Porembka, J. Lea, A.E. Frankel, Y.-X. Fu, Z.J. Chen, J. Gao, A STING-activating nanovaccine for cancer immunotherapy, Nat. Nanotechnol. 12 (2017) 648–654. doi:10.1038/nnano.2017.52.

[183] R. Kuai, L.J. Ochyl, K.S. Bahjat, A. Schwendeman, J.J. Moon, Designer vaccine nanodiscs for personalized cancer immunotherapy, Nat. Mater. 16 (2017) 489–496. doi:10.1038/nmat4822.

[184] S. Hua, M.B.C. de Matos, J.M. Metselaar, G. Storm, Current trends and challenges in the clinical translation of nanoparticulate nanomedicines: pathways for translational development and commercialization, Front. Pharmacol. 9 (2018) 1–14. doi:10.3389/fphar.2018.00790.

[185] J.I. Hare, T. Lammers, M.B. Ashford, S. Puri, G. Storm, S.T. Barry, Challenges and strategies in anti-cancer nanomedicine development: an industry perspective, Adv. Drug Deliv. Rev. 108 (2017) 25–38. doi:10.1016/j.addr.2016.04.025.

[186] T. Lammers, F. Kiessling, M. Ashford, W. Hennink, D. Crommelin, G. Storm, Cancer nanomedicine: is targeting our target?, Nat. Rev. Mater. 1 (2016) 16069. doi:10.1038/natrevmats.2016.69.

[187] R. Van Der Meel, E. Sulheim, Y. Shi, F. Kiessling, W.J.M. Mulder, T. Lammers, Smart cancer nanomedicine, Nat. Nanotechnol. 14 (2019) 1007–1017. doi:10.1038/s41565-019-0567-y.

[188] R.-F. Wang, H.Y. Wang, Immune targets and neoantigens for cancer immunotherapy and precision medicine, Cell Res. 27 (2017) 11–37. doi:10.1038/cr.2016.155.

[189] F. Dormont, M. Rouquette, C. Mahatsekake, F. Gobeaux, A. Peramo, R. Brusini, S. Calet, F. Testard, S. Lepetre-Mouelhi, D. Desmaële, M. Varna, P. Couvreur, Translation of nanomedicines from lab to industrial scale synthesis: the case of squalene-adenosine nanoparticles, J. Control. Release. 307 (2019) 302–314. doi:10.1016/j.jconrel.2019.06.040.

[190] F. Caputo, J. Clogston, L. Calzolai, M. Rösslein, A. Prina-Mello, Measuring particle size distribution of nanoparticle enabled medicinal products, the joint view of EUNCL and NCI-NCL. A step by step approach combining orthogonal measurements with increasing complexity, J. Control. Release. 299 (2019) 31–43. doi:10.1016/j.jconrel.2019.02.030.

[191] N. Desai, Challenges in development of nanoparticle-based therapeutics, AAPS J. 14 (2012) 282–295. doi:10.1208/s12248-012-9339-4.

[192] V. Sainz, J. Conniot, A.I. Matos, C. Peres, E. Zupančič, L. Moura, L.C. Silva, H.F. Florindo, R.S. Gaspar, Regulatory aspects on nanomedicines, Biochem. Biophys. Res. Commun. 468 (2015) 504–510. doi:10.1016/j.bbrc.2015.08.023.

[193] X. Feng, W. Xu, Z. Li, W. Song, J. Ding, X. Chen, Immunomodulatory nanosystems, Adv. Sci. 6 (2019) 1900101. doi:10.1002/advs.201900101.

[194] Matrix-M™ technology, (n.d.). http://novavax.com/page/10/matrix-m-adjuvant-technology (accessed July 4, 2017).

[195] Phase 3 Pivotal Trial of NanoFlu™ in Older Adults, (2019). https://clinicaltrials.gov/ct2/show/NCT04120194 (accessed November 8, 2019).

[196] Vaccine technology, (n.d.). http://novavax.com/page/8/vaccine-technology (accessed July 4, 2017).

[197] A study to determine the safety and efficacy of the RSV F vaccine to protect infants via maternal immunization, (2015). https://clinicaltrials.gov/ct2/show/NCT02624947 (accessed September 11, 2019).

[198] S. Abraham, H.B. Juel, P. Bang, H.M. Cheeseman, R.B. Dohn, T. Cole, M.P. Kristiansen, K.S. Korsholm, D. Lewis, A.W. Olsen, L.R. McFarlane, S. Day, S. Knudsen, K. Moen, M. Ruhwald, I. Kromann, P. Andersen, R.J. Shattock, F. Follmann, Safety and immunogenicity of the chlamydia vaccine candidate CTH522 adjuvanted with CAF01 liposomes or aluminium hydroxide: a first-in-human, randomised, double-blind, placebo-controlled, phase 1 trial, Lancet Infect. Dis. 3099 (2019) 1–10. doi:10.1016/S1473-

3099(19)30279-8.

[199] M. Hayashi, T. Aoshi, Y. Haseda, K. Kobiyama, E. Wijaya, N. Nakatsu, Y. Igarashi, D.M. Standley, H. Yamada, Y. Honda-Okubo, H. Hara, T. Saito, T. Takai, C. Coban, N. Petrovsky, K.J. Ishii, Advax, a delta inulin microparticle, potentiates in-built adjuvant property of co-administered vaccines, EBioMedicine. 15 (2017) 127–136. doi:10.1016/j.ebiom.2016.11.015.

[200] A randomised controlled phase 1 study of vaccine therapy for control or cure of chronic hepatitis B virus infection (HBV003), (2017). https://clinicaltrials.gov/ct2/show/NCT03038802 (accessed September 11, 2019).

[201] A study to determine if a new malaria vaccine is safe and induces immunity among kenyan adults, young children and infants, (2018). https://clinicaltrials.gov/ct2/show/NCT03580824 (accessed September 11, 2019).

[202] L. Zhang, P. Londono, S. Grimes, P. Blackburn, P. Gottlieb, G.S. Eisenbarth, MAS-1 adjuvant immunotherapy generates robust Th2 type and regulatory immune responses providing long-term protection from diabetes in late-stage pre-diabetic NOD mice, Autoimmunity. 47 (2014) 341–350. doi:10.3109/08916934.2014.910768.

[203] The safety, tolerance, and immunogenicity of MAS-1-adjuvanted seasonal inactivated influenza vaccine (MER4101), (2015). https://clinicaltrials.gov/ct2/show/NCT02500680?term=NCT02500680&rank=1 (accessed September 11, 2019).

[204] Safety, reactogenicity and immunogenicity of two quadrivalent Seasonal Influenza vaccines (Fluzone(R) or Flublok(R)) with or without one of two adjuvants (AF03 or Advax-CpG55.2) in healthy adults, (2019). https://clinicaltrials.gov/ct2/show/NCT03945825 (accessed September 11, 2019).

[205] O. Launay, A.G.W. Ndiaye, V. Conti, P. Loulergue, A.S. Sciré, A.M. Landre, P. Ferruzzi, N. Nedjaai, L.D. Schütte, J. Auerbach, E. Marchetti, A. Saul, L.B. Martin, A. Podda, Booster vaccination with GVGH Shigella sonnei 1790GAHB GMMA vaccine compared to single vaccination in unvaccinated healthy european adults: results from a phase 1 clinical trial, Front. Immunol. 10 (2019) 1–10. doi:10.3389/fimmu.2019.00335.

[206] Study to evaluate the safety and reactogenicity of DPX-RSV(A), a respiratory syncytial virus vaccine, (2015). https://clinicaltrials.gov/ct2/show/NCT02472548 (accessed January 9, 2020).

[207] Phase II study to assess the safety and immunogenicity of recMAGE-A3+AS15 ASCI with or without poly IC:LC, (2011). https://clinicaltrials.gov/ct2/show/NCT01437605 (accessed January 9, 2020).

[208] BLP25 liposome vaccine and bevacizumab after chemotherapy and radiation therapy in treating patients with newly diagnosed stage IIIa or stage IIIb non-small cell lung cancer that cannot be removed by surgery, (2009). https://clinicaltrials.gov/ct2/show/record/NCT00828009 (accessed November 13, 2019).

[209] Oncoquest-L vaccine in patients with previously untreated stage III or IV, asymptomatic, non-bulky follicular lymphoma, (2014). https://clinicaltrials.gov/ct2/show/NCT02194751 (accessed November 13, 2019).

[210] DPX-Survivac and checkpoint inhibitor in DLBCL (SPiReL), (2017). https://clinicaltrials.gov/ct2/show/NCT03349450 (accessed January 9, 2020).

[211] Phase 2 study of pembrolizumab, DPX-Survivac vaccine and cyclophosphamide in advanced ovarian, primary peritoneal or fallopian tube cancer, (2017). https://www.clinicaltrials.gov/ct2/show/NCT03029403 (accessed November 13, 2019).

[212] Study of an immunotherapeutic, DPX-Survivac, in combination with low dose cyclophosphamide & pembrolizumab, in subjects with selected advanced & recurrent solid tumors, (2019). https://clinicaltrials.gov/ct2/show/NCT03836352 (accessed January 9, 2020).

[213] Study of DPX-Survivac therapy in patients with recurrent ovarian cancer, (2016). https://clinicaltrials.gov/ct2/show/NCT02785250 (accessed January 9, 2020).

[214] Trial to test safety and efficacy of vaccination for incurable HPV 16-related oropharyngeal, cervical and anal cancer, (2016). https://clinicaltrials.gov/ct2/show/NCT02865135 (accessed January 9, 2020).

[215] Evaluation of the safety and tolerability of i.v. administration of a cancer vaccine in patients with advanced melanoma (Lipo-MERIT), (2015). https://clinicaltrials.gov/ct2/show/NCT02410733 (accessed November 13, 2019).

[216] RNA-Immunotherapy of IVAC_W_bre1_uID and IVAC_M_uID (TNBC-MERIT), (2014). https://clinicaltrials.gov/ct2/show/NCT02316457 (accessed November 13, 2019).

[217] Vaccine therapy for treating patients with previously untreated chronic lymphocytic leukemia, (2013). https://clinicaltrials.gov/ct2/show/NCT01976520 (accessed November 13, 2019).

[218] A phase I study of a therapeutic vaccine candidate in patients with localized breast cancer at high-risk of relapse (MAGTRIVACSEIN), (2015). https://clinicaltrials.gov/ct2/show/NCT02364492 (accessed January 9, 2020).

[219] Dendritic cell activating scaffold in melanoma, (2012). https://clinicaltrials.gov/ct2/show/NCT01753089.

Background, Hypothesis and Objectives

Background

The immune system plays an important role in several illnesses, such as infectious diseases and cancer, either by favoring their progression or by promoting their elimination. Although in the last century we have witnessed a great progress in the development of vaccines, some infectious diseases remain elusive to vaccination [1–3]. In the particular case of cancer, the discovery of new therapies that re-activate the immune system towards fighting tumor progression has revolutionized the field, however, there are still many side effects associated to these treatments that need to be overcome in order to adequately exploit these new treatments [4,5].

Nanotechnology, through the design of vaccines and immunotherapies, allows the modulation of the activity of the immune system [6,7]. Additionally, nanosystems can specifically target some subsets of immune cells, and favor the arrival of the cargos to the lymph nodes, the tumor microenvironment or other tissues of interest [6,7].

In the case of vaccines, the newest antigens are based on low immunogenic biomolecules, such as peptides. Therefore, it is necessary to combine them with nanocarriers, which can mimic the size of microorganisms and co-deliver stimulatory molecules (e.g., cytokines, pathogen-associated molecular patterns), thereby enhancing the immunogenic response against the delivered antigen [8–14]. Indeed, some nanotechnology-based adjuvants have already been marketed [15,16], recently, one of them for the prevention of malaria [17]. Our group has three decades of expertise in designing nanocarriers adapted specifically to the nature of the antigen. In this regard, in the early 90's, the group started using poly-lactic acid-based polymers [18,19], while over the last decades, it has moved towards the use of polysaccharides and polypeptides [20–22], biocompatible and biodegradable polymers which offer important opportunities from an engineering perspective [23–26]. The nanosystems developed so far by our group have shown the capacity to protect and deliver a great variety of antigens, such as tetanus toxoid, Hepatitis B surface antigen, among others [27–30]. In some cases, adjuvants were also included in the composition to generate more robust immune responses [31,32]. Moreover, joining efforts with Canadian and American research groups, our first works against HIV resulted in the development of polysaccharide-based nanoparticles associating HIV peptide antigens with improved humoral responses in primates [33,34].

In the context of cancer, the availability of therapies that modify the immune response is relatively new [4]. Nevertheless, these new therapies have limited application and/or present important systemic toxicities [35–38]. Therefore, the use of nanosystems to modify the systemic biodistribution of the therapies towards the tumor site, and to favor their uptake by specific cell subtypes (e.g.,

dendritic cells, T cells, macrophages), holds great potential [39–41]. All these advantages have already taken several nanoimmunotherapies to clinical trials [42].

Further understanding on how the design of the nanoparticles affects the final immune response, and how to optimize the current available therapies, is critical in order to progress in the development of advanced new therapies. Additionally, manufacturing and characterization aspects that guarantee the correct development of new nanomedicines need to be considered as early as possible along the preclinical stages. Defining all these critical processes will ensure the translatability of the nanomedicines towards the industry.

Based on this background information, we have elaborated the following hypothesis:

Hypothesis

1. Polysaccharide-based nanoparticles are potential carriers for HIV peptide antigens. The type of attachment of a peptide antigen to its carrier, and the presence of adjuvants, have an effect in the elicited immune response.

2. The manufacturing process of polysaccharide-based nanoparticles can be translated to an industrial environment.

3. The formulation of immunomodulators, i.e. poly(I:C), in the form of nanocomplexes is a strategy to improve their stability and to target the tumor site. Upon contact with these nanocomplexes, macrophages will be polarized towards M1 phenotypes and will mediate tumor cell killing.

Objectives

Taking into consideration the background and hypothesis previously stated, the main goals of this thesis were oriented into two main directions:

A. To design and develop a prototype consisting of polysaccharide-based nanoparticles, with the capacity to carry HIV peptide antigens. This objective was the continuation of previous efforts where the same antigens were included into chitosan/dextran nanoparticles with increased humoral responses in non-human primates.

B. To design and develop nanocomplexes loaded with the immunomodulator poly(I:C), in order to facilitate its transport to tumor-associated macrophages and their subsequent polarization towards anti-tumoral phenotypes.

To achieve these objectives, the following experimental activities were performed:

1. Development of polysaccharide-based nanoparticles associating an HIV peptide antigen, that improves the elicited immune response. This activity has involved:
    a. The design of different association approaches of the antigen to the nanocarriers, including poly(I:C) as an adjuvant.
    b. The characterization of the physicochemical properties of the developed nanoparticles and their formulation in a freeze-dried powder aiming at increasing their stability.
    c. The evaluation of the capacity of each nanosystem to generate humoral and cellular responses in vaccinated mice.
    d. The optimization of the most promising prototypes to load three different PCSs and the determination of their efficacy in terms of SIV prevention in non-human primates

    The results corresponding to this objective are presented in Chapter 1 “Development of an SIV vaccine candidate based on polysaccharide nanoparticles loading peptide antigens”.

2. Adaptation of the manufacturing process of polysaccharide-based nanoparticles to be implemented in a pilot plant. This activity has involved:
    a. The application of a quality-by-design approach to the fabrication of the nanoparticles and of a risk analysis to underline the most important parameters to be controlled.
    b. The characterization of the formulation through several complementary orthogonal techniques, while developing methods to measure the content uniformity.
    c. The evaluation of the long-term colloidal stability under ICH conditions.

d. The scaling-up of the nanoparticle fabrication using continuous and discontinuous methods.

The results corresponding to this objective are presented in Chapter 2 “Technological challenges in the preclinical development of an HIV nanovaccine candidate”.

3. Design and development of poly(I:C) nanocomplexes with the adequate properties to target and polarize tumor-associated macrophages. This activity has involved:
   a. The evaluation of the capacity of arginine-rich polymers to form nanocomplexes with poly(I:C), and the study of their subsequent envelopment with anionic polymers in order to improve their stability.
   b. The evaluation of the *in vitro* toxicity, internalization and intracellular trafficking of the nanocomplexes in macrophages.
   c. The study of the capacity of the nanocomplexed poly(I:C) to polarize macrophages towards M1 phenotypes and, subsequently, to secret attracting chemokines and to directly destroy tumor cells.
   d. The evaluation of the poly(I:C) nanocomplexes capacity to prevent tumor development in an immunocompetent murine model.

   The results corresponding to this goal are presented in Chapter 3 “Arginine-based poly(I:C)-loaded nanocomplexes for the re-education of tumor-associated macrophages”.

References

[1] B.D. Walker, D.R. Burton, Toward an AIDS vaccine, Science. 320 (2008) 760–764. doi:10.1126/science.1152622.

[2] S.G. Reed, M.T. Orr, C.B. Fox, Key roles of adjuvants in modern vaccines, Nat. Med. 19 (2013) 1597–1608. doi:10.1038/nm.3409.

[3] I. Delany, R. Rappuoli, E. De Gregorio, Vaccines for the 21st century, EMBO Mol. Med. 6 (2014) 708–720. doi:10.1002/emmm.201403876.

[4] J. Couzin-Frankel, Cancer immunotherapy, Science. 342 (2013) 1432–1433. doi:10.1126/science.342.6165.1432.

[5] P. Sharma, S. Hu-Lieskovan, J.A. Wargo, A. Ribas, Primary, adaptive, and acquired resistance to cancer immunotherapy, Cell. 168 (2017) 707–723. doi:10.1016/j.cell.2017.01.017.

[6] D.J. Irvine, M.C. Hanson, K. Rakhra, T. Tokatlian, Synthetic nanoparticles for vaccines and immunotherapy, Chem. Rev. 115 (2015) 11109–11146. doi:10.1021/acs.chemrev.5b00109.

[7] T.G. Dacoba, A. Olivera, D. Torres, J. Crecente-Campo, M.J. Alonso, Modulating the immune system through nanotechnology, Semin. Immunol. 34 (2017) 78–102. doi:10.1016/j.smim.2017.09.007.

[8] A.S. Cordeiro, M.J. Alonso, Recent advances in vaccine delivery, Pharm. Pat. Anal. 5 (2015) 49–73. doi:10.4155/ppa.15.38.

[9] A.S. Cordeiro, M.J. Alonso, M. de la Fuente, Nanoengineering of vaccines using natural polysaccharides, Biotechnol. Adv. 33 (2015) 1279–1293. doi:10.1016/j.biotechadv.2015.05.010.

[10] D. Van Duin, R. Medzhitov, A.C. Shaw, Triggering TLR signaling in vaccination, Trends Immunol. 27 (2006) 49–55. doi:10.1016/j.it.2005.11.005.

[11] A. Gutjahr, G. Tiraby, E. Perouzel, B. Verrier, S. Paul, Triggering intracellular receptors for vaccine adjuvantation, Trends Immunol. 37 (2016) 573–587. doi:10.1016/j.it.2016.07.001.

[12] D.R. Getts, L.D. Shea, S.D. Miller, N.J.C. King, Harnessing nanoparticles for immune modulation, Trends Immunol. 36 (2015) 419–427. doi:10.1016/j.it.2015.05.007.

[13] K.T. Gause, A.K. Wheatley, J. Cui, Y. Yan, S.J. Kent, F. Caruso, Immunological principles guiding the rational design of particles for vaccine delivery, ACS Nano. 11 (2017) 54–68. doi:10.1021/acsnano.6b07343.

[14] D.M. Smith, J.K. Simon, J.R. Baker, Applications of nanotechnology for immunology, Nat. Rev. Immunol. 13 (2013) 592–605. doi:10.1038/nri3488.

[15] D.T. O'Hagan, G.S. Ott, E. De Gregorio, A. Seubert, The mechanism of action of MF59 – An innately attractive adjuvant formulation, Vaccine. 30 (2012) 4341–4348. doi:10.1016/j.vaccine.2011.09.061.

[16] G. Ledet, L.A. Bostanian, T.K. Mandal, Nanoemulsions as a vaccine adjuvant, in: A. Tiwari, A. Tiwari (Eds.), Bioeng. Nanomater., CRC press: Boca Raton, 2013: pp. 125–148.

[17] A.M. Didierlaurent, B. Laupèze, A. Di Pasquale, N. Hergli, C. Collignon, N. Garçon, Adjuvant system AS01: helping to overcome the challenges of modern vaccines, Expert Rev. Vaccines. 16 (2017) 55–63. doi:10.1080/14760584.2016.1213632.

[18] A. Vila, A. Sánchez, M. Tobío, P. Calvo, M.J. Alonso, Design of biodegradable particles for protein delivery, J. Control. Release. 78 (2002) 15–24. doi:10.1016/S0168-3659(01)00486-2.

[19] A. Vila, A. Sánchez, C. Évora, I. Soriano, J.L. Vila Jato, M.J. Alonso, PEG-PLA nanoparticles as carriers for nasal vaccine delivery, J. Aerosol Med. 17 (2004) 174–185. doi:10.1089/0894268041457183.

[20] P. Calvo, C. Remuñán-López, J.L. Vila-Jato, M.J. Alonso, Novel hydrophilic chitosan-polyethylene oxide nanoparticles as protein carriers, J. Appl. Polym. Sci. 63 (1997) 125–132.

[21] J.F. Correia-Pinto, N. Csaba, J. Schiller, M.J. Alonso, Chitosan-poly (I:C)-PADRE based nanoparticles as delivery vehicles for synthetic peptide vaccines, Vaccines. 3 (2015) 730–750. doi:10.3390/vaccines3030730.

[22] J.V. González-Aramundiz, E. Presas, I. Dalmau-Mena, S. Martínez-Pulgarín, C. Alonso, J.M. Escribano, M.J. Alonso, N.S. Csaba, Rational design of protamine nanocapsules as antigen delivery carriers, J. Control.

Release. 245 (2017) 62–69. doi:10.1016/j.jconrel.2016.11.012.

[23] M. Peleteiro, E. Presas, J.V. González-Aramundiz, B. Sánchez-Correa, R. Simón-Vázquez, N. Csaba, M.J. Alonso, Á. González-Fernández, Polymeric nanocapsules for vaccine delivery: influence of the polymeric shell on the interaction with the immune system, Front. Immunol. 9 (2018). doi:10.3389/fimmu.2018.00791.

[24] A.S. Cordeiro, J. Crecente-Campo, B.L. Bouzo, S.F. González, M. de la Fuente, M.J. Alonso, Engineering polymeric nanocapsules for an efficient drainage and biodistribution in the lymphatic system, J. Drug Target. 27 (2019) 646–658. doi:10.1080/1061186X.2018.1561886.

[25] J. Crecente-Campo, J. Guerra-Varela, M. Peleteiro, C. Gutiérrez-Lovera, I. Fernández-Mariño, A. Diéguez-Docampo, Á. González-Fernández, L. Sánchez, M.J. Alonso, The size and composition of polymeric nanocapsules dictate their interaction with macrophages and biodistribution in zebrafish, J. Control. Release. 308 (2019) 98–108. doi:10.1016/j.jconrel.2019.07.011.

[26] J. Crecente-Campo, M.J. Alonso, Engineering, on-demand manufacturing, and scaling-up of polymeric nanocapsules, Bioeng. Transl. Med. 4 (2019) 38–50. doi:10.1002/btm2.10118.

[27] A. Vila, A. Sánchez, K. Janes, I. Behrens, T. Kissel, J.L. Vila-Jato, M.J. Alonso, Low molecular weight chitosan nanoparticles as new carriers for nasal vaccine delivery in mice, Eur. J. Pharm. Biopharm. 57 (2004) 123–131. doi:10.1016/j.ejpb.2003.09.006.

[28] C. Prego, P. Paolicelli, B. Díaz, S. Vicente, A. Sánchez, Á. González-Fernández, M.J. Alonso, Chitosan-based nanoparticles for improving immunization against hepatitis B infection, Vaccine. 28 (2010) 2607–2614. doi:10.1016/j.vaccine.2010.01.011.

[29] J.V. González-Aramundiz, M. Peleteiro Olmedo, Á. González-Fernández, M.J. Alonso, N.S. Csaba, Protamine-based nanoparticles as new antigen delivery systems, Eur. J. Pharm. Biopharm. 97 (2015) 51–59. doi:10.1016/j.ejpb.2015.09.019.

[30] J. Crecente-Campo, S. Lorenzo-Abalde, A. Mora, J. Marzoa, N. Csaba, J. Blanco, Á. González-Fernández, M.J. Alonso, Bilayer polymeric nanocapsules: a formulation approach for a thermostable and adjuvanted E. coli antigen vaccine, J. Control. Release. 286 (2018) 20–32. doi:10.1016/j.jconrel.2018.07.018.

[31] S. Vicente, M. Peleteiro, B. Díaz-Freitas, A. Sanchez, Á. González-Fernández, M.J. Alonso, Co-delivery of viral proteins and a TLR7 agonist from polysaccharide nanocapsules: a needle-free vaccination strategy, J. Control. Release. 172 (2013) 773–781. doi:10.1016/j.jconrel.2013.09.012.

[32] J.F. Correia-Pinto, M. Peleteiro, N. Csaba, Á. González-Fernández, M.J. Alonso, Multi-enveloping of particulated antigens with biopolymers and immunostimulant polynucleotides, J. Drug Deliv. Sci. Technol. 30 (2015) 424–434. doi:10.1016/j.jddst.2015.08.010.

[33] H. Li, M. Nykoluk, L. Li, L.R. Liu, R.W. Omange, G. Soule, L.T. Schroeder, N. Toledo, M.A. Kashem, J.F. Correia-Pinto, B. Liang, N. Schultz-Darken, M.J. Alonso, J.B. Whitney, F.A. Plummer, M. Luo, Natural and cross-inducible anti-SIV antibodies in Mauritian cynomolgus macaques, PLoS One. 12 (2017) 1–20. doi:10.1371/journal.pone.0186079.

[34] H. Li, Y. Hai, S.-Y. Lim, N. Toledo, J. Crecente-Campo, D. Schalk, L. Li, R.W. Omange, T.G. Dacoba, L.R.L.R. Liu, M.A. Kashem, Y. Wan, B. Liang, Q. Li, E. Rakasz, N. Schultz-Darken, M.J. Alonso, F.A. Plummer, J.B. Whitney, M. Luo, Mucosal antibody responses to vaccines targeting SIV protease cleavage sites or full-length Gag and Env proteins in Mauritian cynomolgus macaques, PLoS One. 13 (2018) e0202997. doi:10.1371/journal.pone.0202997.

[35] L. Milling, Y. Zhang, D.J. Irvine, Delivering safer immunotherapies for cancer, Adv. Drug Deliv. Rev. 114 (2017) 79–101. doi:10.1016/j.addr.2017.05.011.

[36] J.J. Moslehi, J.-E. Salem, J.A. Sosman, B. Lebrun-Vignes, D.B. Johnson, Increased reporting of fatal immune checkpoint inhibitor-associated myocarditis, Lancet. 391 (2018) 933. doi:10.1016/S0140-6736(18)30533-6.

[37] S.C. Wei, C.R. Duffy, J.P. Allison, Fundamental mechanisms of immune checkpoint blockade therapy,

Cancer Discov. 8 (2018) 1069–1086. doi:10.1158/2159-8290.CD-18-0367.

[38] R.W. Jenkins, D.A. Barbie, K.T. Flaherty, Mechanisms of resistance to immune checkpoint inhibitors, Br. J. Cancer. 118 (2018) 9–16. doi:10.1038/bjc.2017.434.

[39] R.S. Riley, C.H. June, R. Langer, M.J. Mitchell, Delivery technologies for cancer immunotherapy, Nat. Rev. Drug Discov. 18 (2019) 175–196. doi:10.1038/s41573-018-0006-z.

[40] M.S. Goldberg, Improving cancer immunotherapy through nanotechnology, Nat. Rev. Cancer. 19 (2019) 587–602. doi:10.1038/s41568-019-0186-9.

[41] J. Nam, S. Son, K.S. Park, W. Zou, L.D. Shea, J.J. Moon, Cancer nanomedicine for combination cancer immunotherapy, Nat. Rev. Mater. 4 (2019) 398–414. doi:10.1038/s41578-019-0108-1.

[42] X. Feng, W. Xu, Z. Li, W. Song, J. Ding, X. Chen, Immunomodulatory nanosystems, Adv. Sci. 6 (2019) 1900101. doi:10.1002/advs.201900101.

Chapter 1

Development of an SIV vaccine candidate based on polysaccharide nanoparticles loading peptide antigens

Chapter 1.A

Engineering polysaccharide nanoparticles for the modulation of the immune response against an SIV peptide antigen

Chapter 1.A

Engineering polysaccharide nanoparticles for the modulation of the immune response against an SIV peptide antigen

This work has been done in collaboration with the University of Manitoba (Canada). The results from this chapter have already been published in [1].

Abstract

The development of an effective HIV vaccine continues to be a major health challenge since, so far, only the RV144 trial has demonstrated a modest clinical efficacy. Recently, the targeting of the twelve highly conserved protease cleavage sites (PCS1–12) has been presented as a strategy seeking to hamper the maturation and infectivity of HIV. To pursue this line of research, and because peptide antigens have low immunogenicity, we have included these peptides in engineered nanoparticles, aiming at overcoming this limitation. More specifically, we investigated whether the covalent attachment of a PCS peptide (PCS5) to polysaccharide-based nanoparticles, and their coadministration with polyinosinic:polycytidylic acid (poly(I:C)), improved the generated immune response. To this end, PCS5 was first conjugated to two different polysaccharides (chitosan and hyaluronic acid), through either a stable or a cleavable bond, and then associated to an oppositely charged polymer (dextran sulfate and chitosan) and poly(I:C) to form the nanoparticles. Nanoparticles associating PCS5 by ionic interactions were used in this study as the control formulation. *In vivo*, all nanosystems elicited high anti-PCS5 antibodies. Nanoparticles containing PCS5 conjugated and poly(I:C) seemed to induce the strongest activation of antigen presenting cells. Interestingly, T cell activation presented different kinetics depending on the prototype. These findings show that both, the nanoparticle composition and the conjugation of the peptide antigen, may play an important role in the generation of humoral and cellular responses.

Graphical abstract

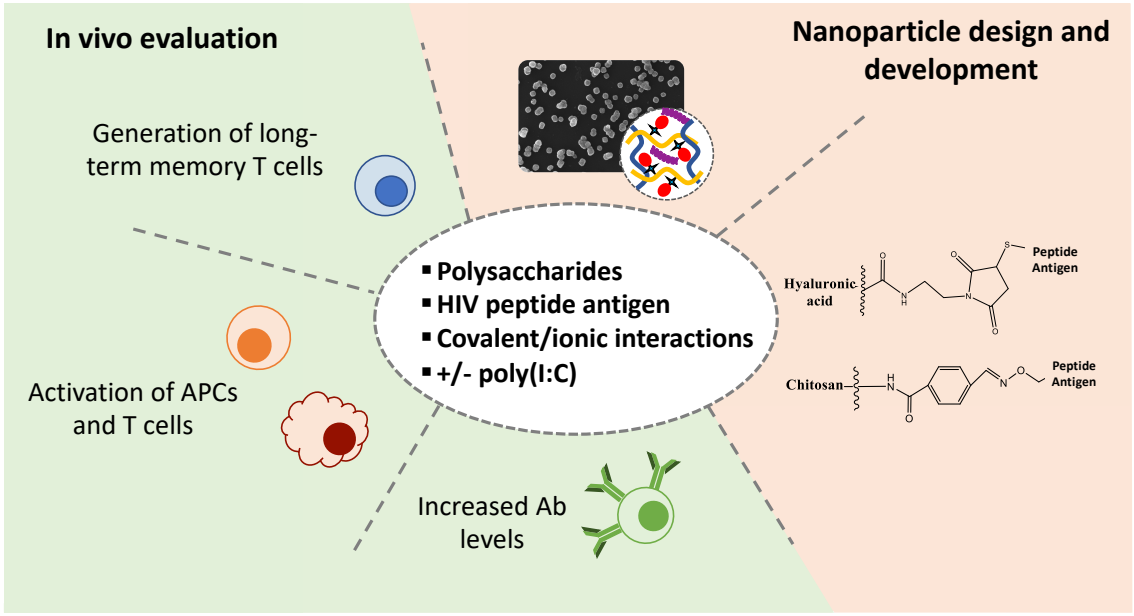

1. Introduction

With almost 2 million newly infected individuals per year, HIV continues to be one of the most important global health challenges [2]. Despite the efforts dedicated to the discovery of an effective vaccine against this virus, the most positive results achieved so far are those reported in the RV144 vaccine (Phase III clinical trial), which conferred a modest 30% protection against the infection [3]. This protection was associated with the ability of the vaccine to generate weakly neutralizing and non-neutralizing antibody responses [4]. It is also worth noting that the efficacy of this trial declined from 60 to 30% from 42 to 60 months after administration, which further underscores the need for HIV vaccine designs that would efficiently induce protective and long-lasting immune responses. This efficiency depends, to a great extent, on the adequate combination of antigen and adjuvant [5,6].

Considering how the natural immunity to HIV-1 works, the peptide sequences around the protease cleavage sites (PCSs) have been proposed as the targets for a candidate vaccine against HIV. The protease is an essential enzyme for the HIV virus because its function is to cleave specific proteins, such as Gag, Gag-Pol and Nef, that are essential for the maturation of HIV virions, and thus, crucial to its infectivity [7–9]. The proteolysis of these proteins must take place on the twelve cleavage sites in a controlled and sequential way, and the interruption of this process, even in one single site, may interrupt virus maturation and, therefore, stop virus infection [7,8,10]. In addition, these sites are highly conserved among HIV-1 viruses, which could help overcome the problems associated with the HIV virus high sequence diversity and rapid mutation rates.

A wide variety of nanosystems are currently under evaluation for their ability to deliver vaccine immunogens, to protect the antigens from degradation and to facilitate their internalization by the target immune cells [11]. In addition, it has been reported that the response to antigen-loaded nanocarriers may be influenced by their composition and physicochemical properties [11–13]. Among these nanocarriers, chitosan (CS)-based nanosystems have been widely employed as antigen carriers through both, parenteral and mucosal routes [14]. In fact, CS is a biodegradable and biocompatible polymer, with a FDA GRAS status, which has already been approved for dietary use and as a wound dressing material [15,16]. Our group has originally reported the development of CS nanoparticles (NPs) [17] and nanocapsules (NCs) [18], and assessed their potential to generate humoral responses against different antigens, such as the recombinant hepatitis B surface antigen (rHBsAg), the tetanus toxoid and the IutA antigen from *E. coli* [19–22]. Other studies have also shown promising results when using CS-based nanosystems in order to enhance T cell responses [23,24].

A critical aspect that has not been completely elucidated is the influence of the antigen-nanocarrier interaction on the nature of the immune response generated. In some studies, the association of antigens to nanocarriers has relied on simple physical entrapment techniques, or the establishment of ionic or hydrophobic forces [25–27]; whereas in others the association has involved the chemical conjugation of the antigens to the nanosystems [28–38]. In the later studies, chemical conjugation was shown to increase the humoral response when compared to other types of antigen association [30,33,34,38]. More specifically, a study performed for a malaria antigen showed that these improved humoral responses were caused by an increased interaction of the antigen with the B-cell receptor when the antigen was covalently attached to the surface of lipid NCs [34]. Similarly, the covalent attachment of an HIV protein antigen to virus-like particles resulted in an efficient generation of specific humoral and CD8 T-cell responses [32].

On the other hand, over the last decade, it has become evident that the co-encapsulation of antigens and adjuvants, such as the toll-like receptor (TLR) agonists, further improves the performance of antigen-loaded nanosystems in vaccination [11]. Furthermore, it has been reported that these TLR molecules are able to direct the immune response towards either humoral or cellular profiles [21,27,39].

Based on this background information, the primary objective of this work was to evaluate if the chemical linkage of an SIV (the simian HIV) PCS peptide antigen (PCS5) to polysaccharide NPs, and the inclusion of poly(I:C), could improve its immunogenicity over the association by ionic forces to NPs. We hypothesized that the conjugation of the antigen to the polysaccharides might prevent its release until the particles are internalized and processed by antigen presenting cells (APCs), thereby dually improving and prolonging the induced immune responses. CS and hyaluronic acid (HA) were the polysaccharides of choice to conjugate the peptide antigen PCS5. Also, the TLR3 agonist poly(I:C) was included in these two nanosystems to stimulate a cellular response against the antigen. As the control formulation, PCS5 was entrapped by ionic forces in NPs of CS and dextran sulfate (DS), which were previously reported as good antigen carriers for the PCS peptide antigens [40]. Polymer–PCS5 conjugates and the resulting NPs were characterized in terms of their chemical composition and structural organization. Finally, their capacity to activate the immune system, regarding antibody production, T cell and APCs activation and generation of central and effector memory T cells in mice, was studied.

2. Materials and Methods

2.1. Materials

Chitosan (CS) (hydrochloride salt, molecular weight (MW) 42.7 KDa and 88% deacetylation degree) was obtained from HMC^{+} (Halle, Germany). Dextran sulfate (DS), (sodium salt, MW 8 KDa) was purchased from Sigma-Aldrich SAFC® (MO, USA). Sodium hyaluronate (HA) (MW 57 kDa) was purchased from Lifecore Biomedical (MN, USA). High MW poly(I:C) was acquired from Invivogen (CA, USA) and high purity α,α–Trehalose dihydrate was purchased from Pfanstiehl (IL, USA). SIV PCS5 peptide (GPWGKKPRNFPMAQVHQGLM, MW 2280 Da and >95% purity), with or without a terminal cysteine residue, was purchased from GenScript (NJ, USA). MES hydrate, N-(2-aminoethyl)maleimide trifluoroacetate salt (ASEM), N-hydroxysuccinimide (NHS) and N-(3-Dimethylaminopropyl)-N´-ethylcarbodiimide hydrochloride (EDC) were obtained from Sigma-Aldrich (MI, USA).

Bio-Plex Pro™ Magnetic COOH Beads and Bio-Plex Amine Coupling Kit were purchased from Bio-Rad (CA, USA). Phycoerythrin-labelled mouse anti-monkey IgG were obtained from Southern Biotech (AL, USA) and PCS5 monoclonal antibody was donated by National Microbiology Laboratory (Winnipeg, MB, Canada).

2.2. Screening of blank NPs

The preparation method for all the NPs in this study was ionic complexation, based on the interactions between the oppositely charged polymers: CS and DS, or CS and HA.

For CS/DS NPs, mass ratios from 3:1 to 1:3 were screened. Equal volumes (0.825 mL) of an aqueous solution of CS (concentration from 1.875 to 0.625 mg/mL), and aqueous solution of DS (concentration from 0.625 to 1.875 mg/mL) were mixed under mild magnetic stirring. The solutions were kept under magnetic stirring for 10 min.

In the case of CS/HA NPs, mass ratios from 1.5:1 to 1:4 were screened. Equal volumes (0.550 mL) of an aqueous solution of CS (concentrations from 2.40 to 0.80 mg/mL) and aqueous solution of HA (concentration from 1.60 to 3.20 mg/mL) were mixed under mild magnetic stirring. The solution was stirred for 10 additional minutes.

2.3. Preparation of CS/DS + PCS5 NPs

CS/DS NPs at a 1:3 mass ratio were prepared as previously described [40], but with materials of a higher quality grade. Briefly, 0.055 mL of PCS5 in aqueous solution (4 mg/mL) were added to 0.770 mL of a CS aqueous solution (0.67 mg/mL) under mild magnetic stirring. After stirring for 5 min, 0.825 mL

of a DS aqueous solution (1.875 mg/mL) were also added. The solution was stirred for 5 additional minutes, and the formulation was kept for 10 min without stirring prior to characterization.

2.4. Determination of PCS5 association efficiency

CS/DS + PCS5 NPs were isolated by size exclusion chromatography (SEC) using CentriPure P10 Gel Filtration Columns (emp Biotech GmbH, Berlin, Germany). The columns were first washed and stabilized with 15 mL of ultrapure water. Then, 1 mL of NPs was transferred to the column and allowed to enter the gel bed completely. After the void volume was discarded, 2 mL of ultrapure water were added to the column and the isolated NPs collected. The association efficiency (AE) was calculated by comparing the amount of PCS5 associated to the NPs with the initial amount added to prepare the NPs (**Eq. 1**). For this purpose, isolated NPs from SEC were treated to a final KCl concentration of 2M to break the ionic interactions between the components of the NPs. Samples were analyzed by Ultra Performance Liquid Chromatography (UPLC) on an Acquity H-UPLC Class system with a Tunable UV (TUV) detector (Waters Corporation, MA, USA) equipped with an Aeris 3.6 µm Widepore XB-C18 LC 100 x 2.1 mm Column (Phenomenex, CA, USA). The mobile Phase A consisted of 0.1% trifluoroacetic acid (v/v) in ultrapure water and the Phase B of 0.1% trifluoroacetic acid (v/v) in acetonitrile HPLC gradient. The column temperature was set at 30 °C and the run from 10% to 100% of phase B in 5 min. The amount of PCS5 in each sample was calculated using a standard curve generated with known concentrations of the peptide (6.5–100 µg/mL, $R^2 = 0.99$).

$$\mathrm{AE}\ (\%) = \frac{Amount\ of\ PCS5\ recovered\ from\ SEC}{Amount\ of\ PCS5\ added\ during\ preparation} \times 100 \qquad \textbf{Eq. 1}$$

2.5. Preparation of CS–PCS5/DS/pIC NPs

The conjugate CS–PCS5 was purchased from Pepscan. PAoa-Ahx-PCS5-OH was synthesized using standard solid phase peptide chemistry through Fmoc/tBu chemistry, and subsequently purified to specifications using reversed phase preparative HPLC.

On the other hand, CS was dissolved in buffer (10 mM phosphate buffer at pH 6.5); while N-succinimidyl 4-formylbenzoate (S-4FB) was dissolved in dry dimethylsulfoxide (DMSO) to generate a stock of 30 mg/mL. A volume of 50 µL of the S-4FB stock were added dropwise to the CS solution (10 mg/mL in phosphate buffer), and the reaction mixture was stirred overnight to allow for the coupling of the S-4FB linker to the free amine residues of the CS. This derivatized CS was then desalted using dialysis against phosphate buffer. Next, a PCS5 aqueous solution at pH 6, was added to the activated

CS solution and allowed to conjugate overnight with agitation. The resulting conjugate was then subjected to dialysis against phosphate buffer to remove the unbound peptide.

Ratio PCS5/CS was determined by a colorimetric assay. First, 2-hydrazinopyridine was added to react with the S-4FB incorporated to CS. Following incubation at 37 °C for 30 min, the chromophoric bis-arylhydrazone obtained was quantified at 350 nm. The difference between the amount of free linker before and after PCS5 conjugation was considered the value of the substitution degree. CS, PCS5 and CS–PCS5 samples were diluted in D_2O water and analyzed in a Spectrometer Varian Inova 750 for ^1H NMR, processed using MestreNova (MESTRELAB, Santiago de Compostela, Spain).

For the preparation of these NPs, a mass ratio 2:1 CS/DS was selected. A volume of 0.0385 mL of an aqueous solution of the modified CS (8.8 mg/mL) were added to a CS aqueous solution of 0.909 mg/mL to obtain a solution containing 2 mg/mL of CS and 0.2 µg/mL of PCS5. Simultaneously, 2.5 µL of poly(I:C) (1 mg/mL) were, then, added to 0.250 mL of an aqueous solution of DS (1 mg/mL), and this solution was poured over 0.250 mL of the previous CS solution (2 mg/mL CS and 0.2 µg/mL of PCS5) under magnetic stirring, and left under agitation for 10 min.

2.6. Preparation of CS/HA–PCS5/pIC NPs

The PCS5 peptide was linked to HA by a thiol-maleimide conjugation reaction, adapting a recently described protocol [41]. First, HA was diluted in MES buffer (0.1 N, pH 6) to a concentration of 2 mg/mL, and ASEM, NHS and EDC in the same buffer solution were added at a concentration 6-, 14- and 143-fold times higher than HA, respectively. The solution was kept under magnetic stirring for 4 h at room temperature, and then dialyzed for 24 h to remove free reactives (SnakeSkin, cellulose membrane MW 7 KDa, Thermo Fisher, MA, USA). In a second step, 0.228 mL of PCS5 with a terminal cysteine residue in aqueous solution (5 mg/mL) were poured over 5 mL of the solution of HA–ASEM (1 mg/mL) in buffer (MES 0.1N, NaCl 100mM), under magnetic stirring. The solution was kept under stirring for 4 h, and then dialyzed for 24 h. Finally, the modified HA solution was frozen at -20 °C and freeze-dried.

NMR analyses of HA, PCS5 and HA–PCS5 were conducted to characterize the link, determine the substitution degree and the yield. For this purpose, freeze-dried samples were resuspended in D_2O, and analyzed using a Spectrometer Varian Inova 750 for ^1H NMR and diffusion-ordered spectroscopy (DOSY). Then, the NMR spectra were processed using MestreNova (MESTRELAB, Santiago de Compostela, Spain). The degree of substitution (DS) was calculated as the amount of PCS5 conjugated per amount of HA, while yield was determined by comparing the amount of PCS5 conjugated to the total amount added to the reaction (**Equation 2**).

$$Yield\ (\%) = \frac{Amount\ of\ PCS5\ conjugated\ to\ HA}{Intial\ amount\ of\ PCS5} \times 100 \qquad \textbf{Eq. 2}$$

NPs were formed at a 1:1 CS/HA mass ratio. Aqueous solutions of either HA or HA–PCS5 at 2 mg/mL were prepared, and the ratio between the two solutions adjusted to a final PCS5 peptide concentration of 0.20 mg/mL. Poly(I:C) was also added as a 1 mg/mL aqueous solution to a final concentration of 2 µg/mL. Later, 0.55 mL of this HA and poly(I:C) solution (2 mg/mL, 2 µg/mL) were poured over 0.55 mL of a CS aqueous solution (2 mg/mL) under magnetic stirring, and kept stirring for 10 min.

2.7. Nanoparticle characterization

The mean size (Z-average) and polydispersity index (PDI) of the NPs were characterized by Dynamic Light Scattering (DLS). The zeta potential values of the NPs were determined by Laser Doppler Anemometry (LDA), measuring the mean electrophoretic mobility after a 10-times dilution of the NPs in ultrapure water. Both properties were measured using a Zetasizer® NanoZS using the software Zetasizer v7.13 (Malvern Panalytical Ltd., Malvern, UK). The measurements were performed at 25 °C with a detection angle of 173.

The PCS5 peptide loading capacity was determined by calculating the real amount of PCS5 associated to the NPs (theoretical mass x AE%) relative to the real mass of the formulation, represented in **equation 3**. Poly(I:C) loading values were calculated according to **equation 4**.

$$Peptide\ loading\ (\%) = \frac{Theoretical\ mass\ of\ PCS5\ \times \mathrm{AE}\%}{Real\ mass\ of\ the\ formulation} \times 100 \qquad \textbf{Eq. 3}$$

$$Poly(I{:}C)\ loading\ (\%) = \frac{Theoretical\ mass\ of\ poly(I{:}C)}{Real\ mass\ of\ the\ formulation} \times 100 \qquad \textbf{Eq. 4}$$

2.8. Morphological analysis

Morphological analysis of the suspension of NPs was conducted by Field Emission Scanning Electron Microscopy (FESEM) (Zeiss Gemini Ultra Plus, Oberkochen, Germany). NPs were diluted 1:100 in water, and then with the same volume of phosphotungstic acid (2% in water). A volume of 1 µL of sample was placed on a copper grid with carbon films and allow to dry. Then, the grids were washed with water and analyzed under the microscope once dried. STEM and immersion lens (InLens) detectors were used to observe the samples.

2.9. Nanoparticle surface analysis by X-ray Photoelectron Spectroscopy (XPS)

The surface of CS/HA/pIC and CS/HA–PCS5/pIC NPs was analyzed to confirm the presence of PCS5. For this purpose, a droplet of each NP suspension was placed on a silicon wafer, used as sample holder, and then allowed to dry in a desiccator overnight. For the reference materials (CS, HA and PCS5), a small quantity of powder was pressed onto a conductive double side adhesive tape on the standard sample holder.

Samples were analyzed by angle resolved XPS using the ESCALAB 250 iXL instrument (Thermo Scientific K-Alpha ESCA, Thermo Scientific, MA, USA), and photoelectrons were collected from a take-off angle of 45 relative to the sample surface. Monochromatic X-ray source Al Kα (1486.6 eV) was used for experiments and spectra were acquired at 10^{-10} mbar. Surface elemental composition was determined using the standard Scofield photoemission cross section. The binding energies (BEs) positions on unsputtered surfaces were calibrated by setting the C1s photopeak corresponding to aliphatic carbon at 285.0 eV. The atomic concentrations were determined from the XPS peak areas using the Shirley background subtraction technique and the Scofield sensitivity factors.

2.10. PCS5 release in glutathione-rich media

CS/HA–PCS5/pIC NPs were incubated at 37 °C, up to 8 h in PBS with a 10 mM concentration of reduced glutathione (GSH). In parallel, as a control, NPs were incubated in PBS under the same conditions. At the different time points, NPs were centrifuged for 10 min at 16000 g to break the NPs and collect the HA–PCS5 from the supernatant. Later, 1 N HCl was added to the supernatant to bring it to pH 2, in order to avoid interactions between the free peptide (pI 11) and the conjugate HA–PCS5 (pKa 3), and to prevent that any remaining GSH kept reacting. Samples were analyzed by UPLC, as described for PCS5, but with a run from 10% to 50% of phase B in 20 min. The amount of free PCS5 peptide and conjugated PCS5 in each sample was calculated using a standard curve generated with known concentrations of the peptide and conjugate (6–50 µg/mL, $R^2 = 0.99$).

2.11. Freeze-drying

Nanoparticles were frozen in the presence of the cryoprotectant agent trehalose at -80 °C for at least 2 h, and then freeze-dried (Genesis™ 25 EL, S.P Industries, PA, USA). Samples were first left in the freeze-drier at -40 °C for 4 h to guarantee that they were completely frozen, with a vacuum of 200 mTorr. Then, the first drying phase was done at a temperature ranging from -40 °C to +20 °C, applying a progressive vacuum to 20 mTorr for a period of 43 h. Finally, the secondary drying phase was done

for 3 h at +22 °C and 20 mTorr. After this process, NPs were resuspended in ultrapure water and their physicochemical properties determined by DLS and LDA as previously described.

2.12. Animal care

Female BALB/c mice 6-8 weeks old were obtained from Charles River Laboratories (Wilmington, MA, USA) and housed at the Veterinary Technical Service unit of National Microbiology Laboratory (Winnipeg, MB, Canada). A maximum of 5 animals were housed per cage, in a level 2 facility. All animals used in the project were treated in a humane manner in accordance with the Principles of the Canadian Council on Animal Care contained in the "Guide to the Care and Use of Experimental Animals". All animal procedures were performed by highly trained personnel using approved techniques. All mice were anaesthetized by inhalation of 3–5% isofluorane, and all possible efforts were made to minimize the pain and discomfort of the animals. Euthanization of animals was conducted using an excess amount of the anesthetic.

2.13. Murine experiments

Eighty female BALB/c mice were divided into four categories. Five unvaccinated mice (week 0) were used as a control. The rest of the mice were divided into three groups of twenty-five animals each. Mice were intramuscularly injected with 50 µL of the resuspended freeze-dried NPs (CS/DS + PCS5, CS/HA–PCS5/pIC and CS–PCS5/DS/pIC) at 0, 4, and 8 weeks. Each group of vaccinated animals was kept in a separate cage and monitored every 24 h for feeding, water drinking, and weight loss.

2.14. Plasma antibody quantification

Plasma was separated from whole blood collected from mice using saphenous bleeding, by centrifugation at 2000 g for 10 min. Mouse plasma samples were collected at 2, 4, 8, 9, 10, 12, 14, and 16 weeks following vaccination, and the concentrations of PCS5-specific plasma IgG antibodies were quantified using a previously published protocol [40]. Briefly, 20 µg of PCS5 was coupled to 1.25 x 10^6 Bio-Plex Pro™ Magnetic COOH Beads (BioRad Laboratories, CA, USA) using a Bio-Plex Amine Coupling Kit (BioRad Laboratories, CA, USA). Then, 50 µL of plasma (1:80 diluted) were incubated with 2,500 beads. SIV-specific IgG was detected with phycoerythrin-labelled mouse anti-monkey IgG at 5 µg/mL (BioRad Laboratories, CA, USA). Bead fluorescence intensities were acquired on the Bio-Plex 200 system (BioRad Laboratories, CA, USA) and converted to concentrations as previously described [40].

2.15. Splenocytes responses quantification

Five mice per group were sacrificed at 0 (naïve mice) 9, 10, 12, 14, and 16 weeks (vaccinated mice), and their spleens were collected. Splenocytes were purified by straining of spleens through a 40 µm nylon mesh (BD Falcon, CA, USA). The resulting mixtures were suspended in R10 media containing RPMI-1640 (Hyclone) complemented with 10% Fetal Bovine Serum (FBS) and 2% antibiotic-antimycotic solutions (Invitrogen, CA, USA). The splenocytes were then frozen in freezing media consisting of 9% FBS and 5% DMSO. Half a million splenocytes were transferred into 12 x 75 mm polypropylene BD Falcon tubes for flow cytometry antibody labeling. Alternatively, 5.0×10^5 splenocytes were stimulated separately with a 5 µg/ml suspension of a pool of PCS5 peptides: PCS5-1 (GPWGKKPRNFPMAQVHQGLM), PCS5-2 (YGQMPRQTGGFFRPWSMGKE), or PCS5-3 (KPRNFPMAQVHQGLM) peptides. Peptide stimulated and unstimulated splenocytes were washed using PBS with 2% FBS at 1500 rpm for 5 minutes. The washed splenocytes were surface stained with either a T-cell or monocyte/macrophage cocktails of antibodies for 30 minutes in the dark and at room temperature. The stained cells were washed using 5% PBS followed by addition of 150 µL of BD Cytofix/Cytoperm™ (BD Biosciences, CA, USA) and a 10 min incubation in the dark. Following the incubation, permeabilized cells were washed using 1x BD Permwash™ solution, followed by intracellular cytokine staining (ICS) for 30 min in the dark. After ICS, cells were washed using 1x BD PermWash™ then ran on LSRII flow cytometer. Data acquisition was done using BD FACSDiva™ software and analyzed using FlowJo™ (Treestar Inc, OR, USA).

2.16. Statistical analysis

Data analysis was performed using GraphPad Prism version 7.0 (GraphPad Inc). Comparison of group data was performed with a Mann-Whitney test. Data are expressed as the mean ± standard error of the mean (SEM). *p* values of 0.05 or less were considered statistically significant.

3. Results and Discussion

Developing an effective HIV vaccine has proved to be particularly challenging due to the special characteristics of this virus. On the one hand, the virus infects CD4 T cells, which have an important role in the development of the adaptive immune response. On the other hand, it mutates rapidly, leading to a deleterious activation of the immune system, which results in the generation of ineffective humoral and cellular responses. In addition, the different virus strains are highly variable, a fact that complicates the generation of broad and protective immune responses [6]. Our approach for the

design of an HIV vaccine has been to use the peptide sequences that overlap the twelve SIV PCSs as antigens. For the generation of infective virions, these HIV PCSs have to be cleaved sequentially, thus, if a single proteolytic reaction is disrupted, the whole process could fail. An additional advantage of the PCS peptide antigens relies on the fact that these PCSs are highly conserved regions among HIV-1 viruses and, therefore, the mutation of the virus will not diminish the activity of the vaccine [7–10]. In a prior approach, these peptide antigens were entrapped into CS/DS NPs and administered to non-human primates, which had already been primed with the PCS1-12 encoding plasmids cloned into viral vectors. The results showed a significant increase in the IgG responses against the PCS peptide antigens after nasal boosting with the nanoparticles [40].

Based on these preliminary findings, we sought to further improve the immunogenicity of our PCS antigens, by exploring different NPs-based formulation strategies to deliver the peptide antigen. For this purpose, the PCS5 peptide antigen was selected for its association to the nanosystems, based on the premise that one cleavage error could interrupt virus maturation. PCS5 was first conjugated to two different polysaccharides, CS and HA, and the resulting conjugate was used to form NPs by ionic interaction with an oppositely-charged polymer (CS–PCS5/DS and CS/HA–PCS5 NPs). The TLR3 agonist, poly(I:C), was also associated to these NPs in order to evaluate its effect on the cellular immune response generated by the NPs. The already reported CS/DS NPs with PCS5 physically entrapped were used as the control formulation [40]. These strategies were based on the hypothesis that conjugation of PCS5 peptide antigen to the matrix-forming polymer would facilitate the intracellular delivery of the antigen with the subsequent improvement of the humoral and cellular immune responses. In addition, poly(I:C) was expected to boost the activation of APCs, effector and memory T cells.

3.1. Development of peptide-loaded polysaccharide NPs

Polysaccharides, particularly CS, have attracted significant attention as biomaterials for the design of antigen delivery carriers [14,42,43]. Our group has originally reported the development of NPs and NCs made of CS [17,18] for the delivery of a variety of antigens (*e.g.,* tetanus toxoid, rHBsAg, influenza, *E. coli* antigen, and also peptide antigens) through different routes of administration [19,20,25,44,45]. Other authors have also disclosed the utility of nanosystems made of DS [14,46–48], or HA [49–54], both negatively charged polysaccharides, to induce immune responses. In most of these reports, the association of the antigen to the polymeric nanocarrier was based on a simple entrapment process, normally driven by ionic interactions between the polymers and the antigen. However, in this work our objective was to covalently conjugate the PCS5 peptide antigen to the NPs in order to achieve a more sustained and improved presentation of the antigen to the immune cells.

Apart from selecting the biomaterials to form the antigen nanocarriers, we also chose an adjuvant, the TLR3 agonist poly(I:C). This molecule mimics viral dsRNA, and activates TLR3 inducing robust cytokine and chemokine responses [45,55–57]. With these components, we designed three different nanosized systems, where the peptide antigen PCS5 was either (*i*) entrapped into the CS/DS NPs, as the control formulation, (*ii*) covalently linked to CS, or (*iii*) covalently linked to HA; prior to the formation of the NPs by adjusting the ionic interaction of CS with DS or HA (**Fig. 1**).

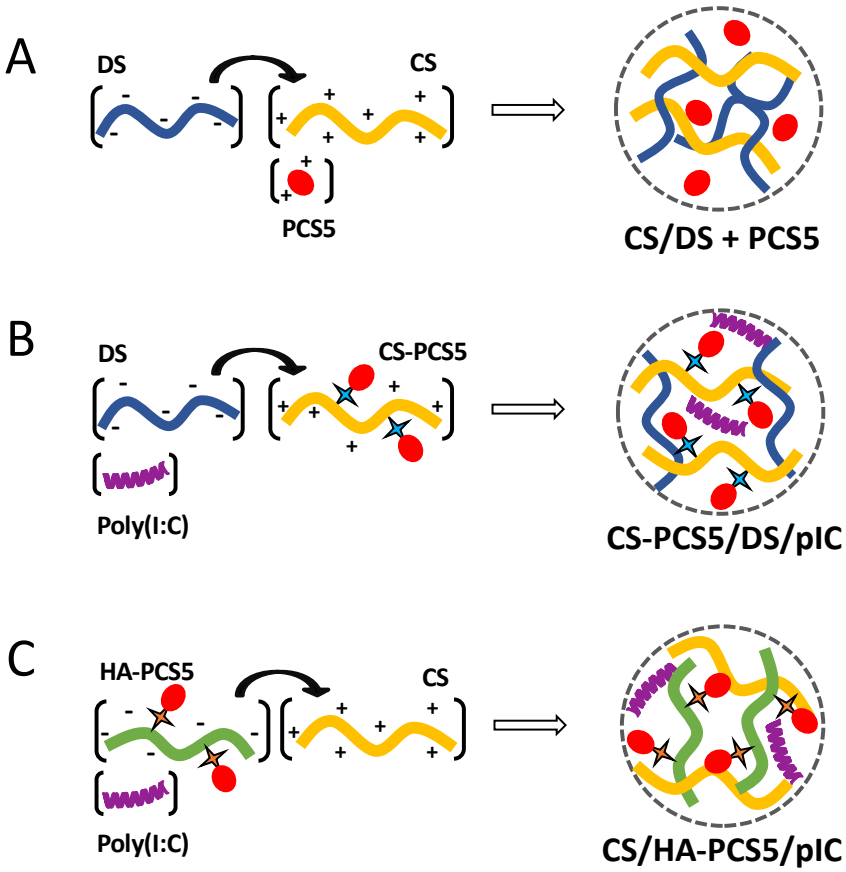

Figure 1. Composition of the different prototypes developed in this work. Schematic representation of the preparation process for the three developed nanosystems. (A) CS/DS + PCS5 NPs, (B) CS–PCS5/DS/pIC NPs, and (C) CS/HA–PCS5/pIC NPs. CS, chitosan; DS, dextran sulfate; HA, hyaluronic acid; PCS5, protease cleavage site 5; pIC, poly(I:C); NPs, nanoparticles.

3.2. Preparation of CS/DS + PCS5 NPs

Using the preparation method for CS/DS NPs previously described by our laboratory [40], PCS5 was easily entrapped within CS/DS nanoparticles by simply adjusting the ionic interaction of the cationic peptide (PCS5) and the cationic polysaccharide (CS) with the negatively charged polysaccharide (DS) (**Fig. 1A**). The mass ratio 1:3 CS:DS resulted in adequate physicochemical properties, association efficiency (80 ± 8%), and antigen loading (8%). This apparent excess of DS was required to complex

efficiently the cationic peptide. The resulting NPs had a particle size of approximately 120 nm, low polydispersity and a negative ζ-potential (**Table 1**).

3.3. Preparation of CS–PCS5/DS/pIC NPs

PCS5 peptide was conjugated to CS by an oxime bond, as schematically represented in **Figure 2Ai**. ^{1}H NMR analysis led to the identification of the signal peaks of the aromatic rings and isopropyl groups of PCS5 (in blue), together with specific signal peaks of CS's glucosamine units (orange arrows), which confirms the chemical conjugation of peptide and polymer. The substitution degree, assessed using a colorimetric assay, was of 2.6 mol of PCS5 per mol of CS (14% in weight).

The CS–PCS5 conjugate was then used to form NPs through ionic interaction with DS. In addition, poly(I:C) was also incorporated into the NPs to increase its immunostimulatory properties. NPs with adequate final antigen loading (5%), and poly(I:C) loading (0.3%) could be obtained when the CS:DS (w/w) ratio was 2:1 (**Fig. 1B**). The resulting NPs had a particle size of 140 nm, with low polydispersity and positive surface charge (**Table 1**). This positive charge was attributed to a certain excess of CS conjugated with the peptide, since increasing amounts of DS caused a decrease in the surface charge (**Supporting Information, Fig. S1A**).

3.4. Preparation of CS/HA–PCS5/pIC NPs

The conjugation of PCS5 to HA was achieved through the formation of a thioether bond, which has been reported to be cleaved in glutathione-rich environments, such as the cytosol [58]. In this case, thiol-maleimide chemistry was employed to link PCS5 to HA (**Supporting Information, Fig. S2**). The results of the ^{1}H NMR and DOSY analyses allowed us to evaluate the peptide conjugation reaction and its yield. As shown in **Figure 2Bii**, the NMR spectrum of the conjugate exhibits the characteristic peaks of PCS5 (blue arrows), and those corresponding to the acetyl groups of HA (orange arrows). The substitution degree calculated by NMR was of 3.8 mol of PCS5 per mol of HA (15.9% in weight). On the other hand, DOSY analysis showed a diffusion coefficient for the conjugate of 9.5 x 10^{-8} cm^2/s, similar to the one for HA (8.8 x 10^{-8} cm^2/s), and much lower than the one observed for the free PCS5 (8.4 x 10^{-7} cm^2/s) (**Supporting Information, Fig. S3**); confirming the conjugation of the peptide to the polymer.

Prior to the formation of the NPs using the HA–PCS5 conjugate, a screening of blank CS/HA NPs was conducted to select the most adequate polymer ratio combination (**Supporting Information, Fig. S1B**). A surface charge switch from positive to negative values was observed when the mass ratio CS:HA

decreased. For this reason, a mass ratio CS/HA 1:1 was selected to form these NPs, since their positive surface charge was expected to allow the association of the negatively charged poly(I:C) to the system (**Fig. 1C**). The final NPs had a particle size of approximately 200 nm and a positive surface charge of +30 mV (**Table 1**). Adequate loading values for PCS5 (5%) and poly(I:C) (0.05%) were also achieved (**Table 1**).

Table 1. Physicochemical characterization of the three PCS5-loaded nanosystems.[a]

Nanosystems	Particle size (nm)	PDI	ζ-Potential (mV)	Antigen loading (%)	pIC loading (%)
CS/DS + PCS5	119 ± 7	0.15	-50 ± 3	7.9	N/A
CS–PCS5/DS/pIC	141 ± 6	0.17	+29 ± 3	4.9	0.3
CS/HA–PCS5/pIC	211 ± 15	0.07	+30 ± 1	4.6	0.05

[a]Mean ± S.D., n ≥ 3. CS, chitosan; DS, dextran sulfate; HA, hyaluronic acid; PCS5, protease cleavage site 5; PDI, polydispersity index; pIC, poly(I:C); NPs, nanoparticles.

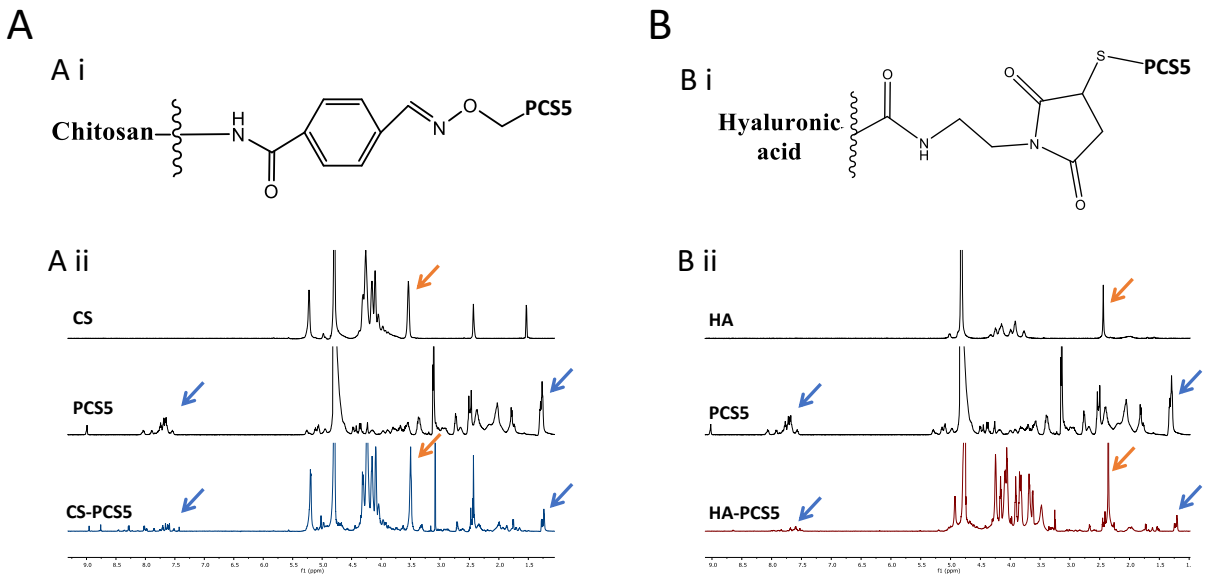

Figure 2. Chemical characterization of polymer–PCS5 conjugates. (A) CS–PCS5 final conjugate, (i) schematically represented, (ii) ^{1}H NMR of CS, PCS5, and CS–PCS5 conjugate. Blue arrows indicate the signals from the aromatic rings and isopropyl groups of PCS5, and orange arrows the glucosamine units of CS, both observed in the NMR of the conjugate. (B) HA–PCS5 conjugate (i) schematically represented, (ii) ^{1}H NMR of HA, PCS5 and HA–PCS5 conjugate. These results corroborated the presence of both the PCS5 characteristic signals (blue arrows), and the acetyl groups of HA (orange arrows) in the conjugate. CS, chitosan; HA, hyaluronic acid; PCS5, protease cleavage site 5.

3.5. Morphological analysis of the nanosystems

Field emission scanning electron microscopy (FESEM) images from the NPs were taken for each nanosystem using the STEM and InLens detectors (**Fig. 3**). In all cases, a spherical particle shape could be observed, as well as diameters similar to the ones reported by DLS analysis (**Table 1**).

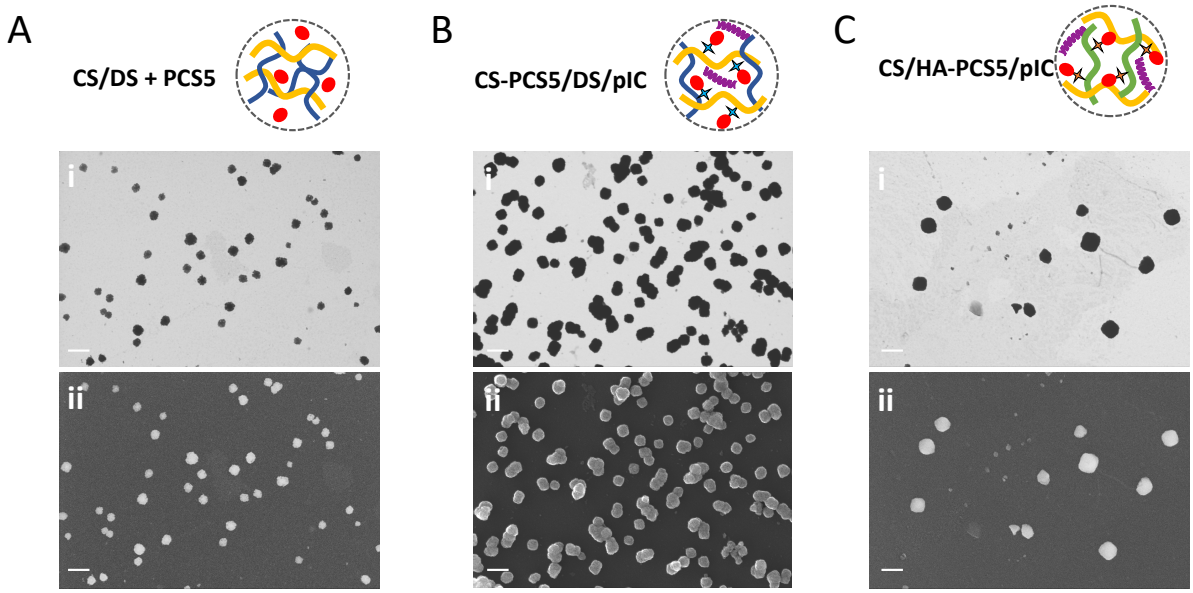

Figure 3. Morphological characterization of the developed nanosystems. Field Emission Scanning Electron Microscopy (FESEM) images of (A) CS/DS + PCS5 NPs, (B) CS–PCS5/DS/pIC NPs and (C) CS/HA–PCS5/pIC NPs with the (i) STEM and (ii) InLens detectors. Scale bar 200 nm. CS, chitosan; DS, dextran sulfate; HA, hyaluronic acid; InLens, immersion lens; PCS5, protease cleavage site 5; pIC, poly(I:C); STEM, scanning transmission electron microscopy.

3.6. Structural distribution of PCS5 in CS/HA–PCS5/pIC NPs

XPS analysis was also used to characterize the surface composition of this nanocarrier. The amount of sulfur present on CS/HA–PCS5/pIC NPs (1.15%) was higher than the one observed in blank CS/HA/pIC NPs (0.28%), which indicates that PCS5 (2.05% of sulfur) must be present on the external layers of the NPs (**Supporting Information, Table S1**). Similarly, the ratios C/O and C/N determined for CS/HA–PCS5/pIC NPs (3.19 and 9.31, respectively) were closer to those of PCS5 (3.50 and 3.66) than to those observed in the blank CS/HA/pIC NPs (1.87 and 12.86), further confirming the prevalent presence of PCS5 on the surface of the NPs.

On the other hand, the binding energy of an element is very sensitive to its chemical environment, and it can be used as the fingerprint of a compound. Thus, we compared the required energy to extract one electron from the carbon 1s orbital of PCS5, CS/HA/pIC and CS/HA–PCS5/pIC NPs (**Supporting Information, Fig. S4**). The obtained profiles indicated that the binding energies of PCS5 alone and CS/HA–PCS5/pIC were very similar, as additional proof that PCS5 was present on the surface of the

NPs. This structural organization could facilitate the presentation of the antigen to B cells, and increase the humoral response against it, as already reported for similar antigen presentations [34,36].

3.7. PCS5 release when covalently attached to NPs

In the present work, we also compared the influence of different covalent attachments in the generation of the immune response. In this regard, a non-cleavable bond (oxime bond, in CS–PCS5 conjugate) and a cleavable one (thioether bond, in HA–PCS5 conjugate) were evaluated. In the case of the CS–PCS5 conjugate (**Fig. 2Ai**), the oxime bonds have been reported as highly-stable linkages at physiological pHs [59–61]. Therefore, this linkage would be the model for a long-lasting attachment of the peptide antigen, which would only be released after being processed by APCs.

On the other hand, thioether bonds are known to undergo retro-Michael reactions in the presence of free thiols [35,58,62], which are presented in great amounts in the cytosol of cells as part of glutathione (GSH) molecules. To demonstrate this hypothesis, NPs were incubated in phosphate buffered saline (PBS), alone or with a 10 mM GSH concentration for up to 8 h at 37 °C. As shown in **Figure 4**, almost no PCS5 was detected upon incubation in PBS, however, upon incubation in a GSH-rich medium, PCS5 was immediately released from the NPs. These results indicate that the release of the peptide is triggered by GSH and led us to speculate that the peptide will not be released in the extracellular medium, but only in the intracellular compartments where high concentrations of GSH are present [63,64].

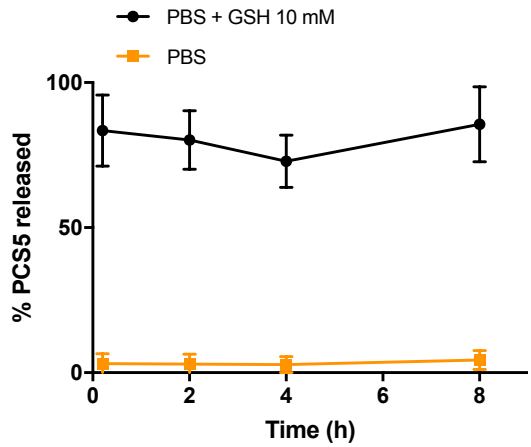

Figure 4. **PCS5 release from CS/HA–PCS5/pIC NPs in** a thiol-rich PBS solution (GSH 10 mM), in comparison to only PBS. GSH, glutathione; PBS, phosphate buffer saline; PCS5, protease cleavage site 5.

3.8. Freeze-drying preserves NPs properties and allows long-term storage

A key feature of vaccine formulations is their stability during storage. Thus, in order to improve the long-term stability of the antigen-loaded NPs, the different formulations were freeze-dried using different cryoprotectants. The results of the screening of the freeze-drying conditions led to the selection of a 7% of trehalose, for both CS/DS + PCS5 and CS/HA–PCS5/pIC NPs, and a 4% for the CS–PCS5/DS/pIC NP formulation. These conditions guaranteed the preservation of the original properties of the formulations (**Fig. 5**). When stored at 4 °C, these freeze-dried formulations maintained PDI and surface charge stable for at least 18 months, while particle size slightly increased.

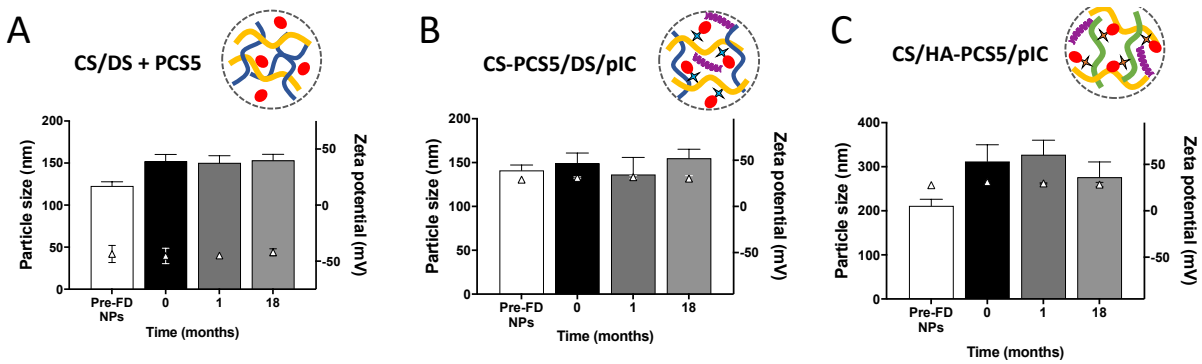

Figure 5. Freeze-dried stability of the developed nanosystems. Evolution of the particle size and the surface charge of the freeze-dried (A) CS/DS + PCS5 NPs, (B) CS–PCS5/DS/pIC NPs and (C) CS/HA–PCS5/pIC NPs during storage. CS, chitosan; DS, dextran sulfate; FD, freeze-dried; HA, hyaluronic acid; PCS5, protease cleavage site 5; pIC, poly(I:C); NPs, nanoparticles.

3.9. *In vivo* antibody responses

To evaluate the *in vivo* activity of the different PCS5-loaded prototypes, freeze-dried formulations were resuspended in water, and 50 µL of this suspension (containing a PCS5 dose of 5 µg) were intramuscularly injected to BALB/c mice. A group of non-vaccinated animals was used as control. Animals were vaccinated 3 times, as shown in **Figure 6A**.

Figure 6B shows the evolution of the anti-PCS5 IgG levels over time. Overall, the IgG responses elicited by the three different NP formulations increased significantly over time, reaching their maximum values at the latest time point in the experiment (week 16). At this time point, the amount of anti-PCS5 antibodies detected in all NPs was 3 times higher than the levels detected in unvaccinated mice. This increasing and prolonged immunogenic response is of particular interest in the design of an HIV vaccine, because persistent levels of antibodies seem to be important for an effective vaccination [65]. This response is also in agreement with previous data reported by our group that showed the capacity of the antigen-loaded NPs to induce significant IgG levels up to 28 or 37 weeks after

immunization [21,26]. Considering these previous results, it is possible that the antigen-loaded NPs could still produce important levels of antibodies beyond the 16 weeks considered in our study.

In addition to eliciting a strong and maintained immune response, the results of this study also indicate that the covalent linkage between the peptide and the NPs does not have an effect on the humoral responses. This is in contrast with previous findings where antigen conjugation improved humoral response when compared to simple ionic interactions [33,34].

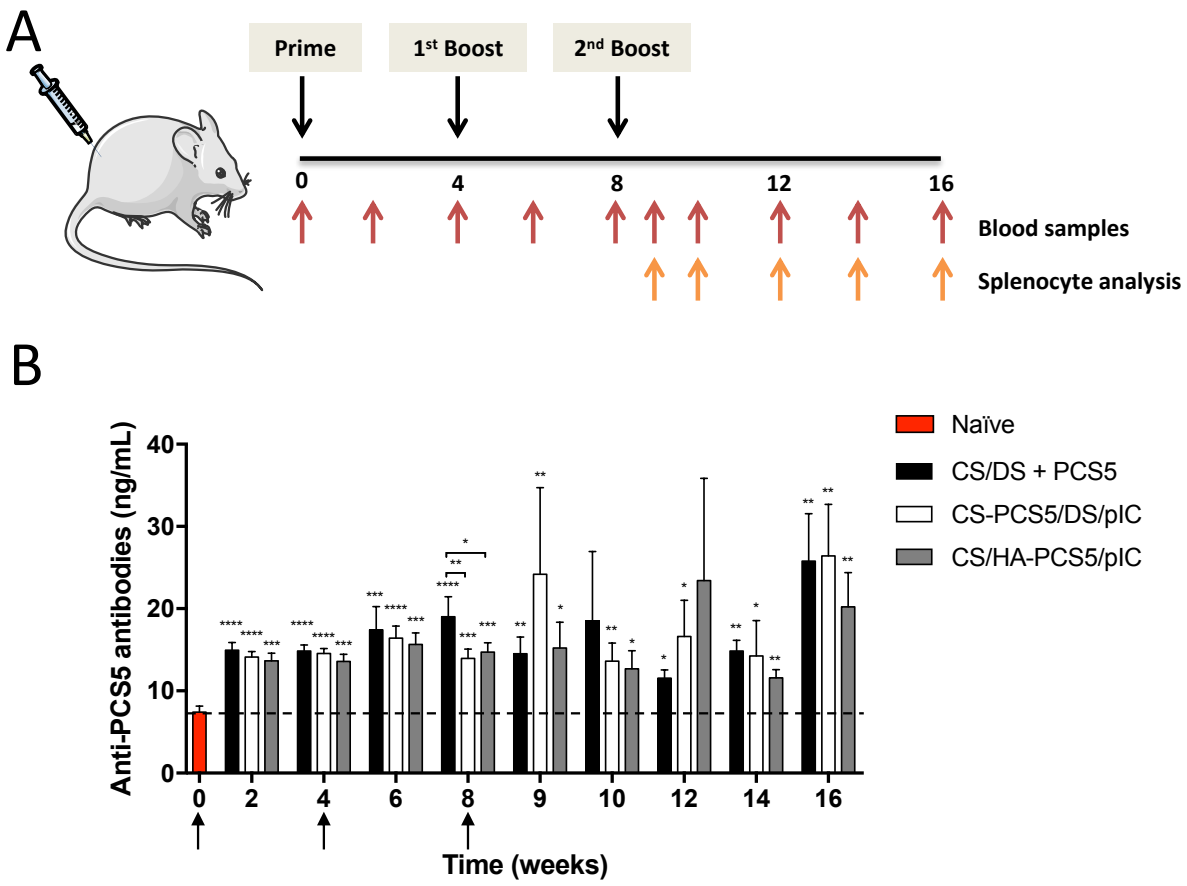

Figure 6. *In vivo* studies in mice. (A) Schematic representation of the study design and timeline of the analysis. (B) Anti-PCS5 antibody levels after the intramuscular administration of the three nanoformulations CS/DS + PCS5 (black bars), CS–PCS5/DS/pIC (white bars), and CS/HA–PCS5/pIC (gray bars) to 50 mice per group. Values represent mean ± SEM (n ≥ 5). Statistical comparison between groups was done using a Mann-Whitney test. Significant statistical differences are represented as * ($p < 0.05$), ** ($p < 0.01$), *** ($p < 0.001$) and **** ($p < 0.0001$) for comparison between groups and to naïve mice. Mouse and syringe images in (A) were reproduced from Servier Medical Art under a Creative Commons Attribution 3.0 Unported License. https://creativecommons.org/licenses/by/3.0. CS, chitosan; DS, dextran sulfate; HA, hyaluronic acid; PCS5, protease cleavage site 5; pIC, poly(I:C); NPs, nanoparticles.

3.10. *In vivo* cellular activation

To evaluate the changes in T cell subsets, and the cellular activation of different immune cells upon vaccination, splenocytes from naïve or NP-vaccinated mice were stained and analyzed for different T cell and monocyte/macrophage phenotyping markers. Multicolor flow cytometry gating strategy used for phenotyping is summarized in **Supporting Information, Figure S5.**

Monocytes and macrophages are APCs that process and present pathogen-derived antigens to T cells. Depending on their function, murine monocytes can be further divided as Ly6c^{hi} and Ly6c^{low}, being the former the classical pro-inflammatory and phagocytic monocytes, and the latter the non-classical or patrolling monocytes [66–68]. Thus, the greater the activation of these APCs, the higher the capacity to recall other cellular populations and to stimulate the immune system. Splenocytes were stained with markers for phenotyping monocytes subsets Ly6c^{hi} and Ly6c^{low}, and markers for characterizing macrophages (CD11b^{+} CD11c^{-} F4/80^{+}) to identify the different subsets (**Supporting Information, Fig. S5A**). To investigate whether the nanosystems were able to activate these subpopulations, the expression of the co-stimulatory signals CD40 and CD86, both involved in the T-cell activation process [69–71], was measured. Regarding CD40 expression, the highest activation of Ly6c^{hi}, Ly6c^{low} and macrophages by CS/HA–PCS5/pIC NPs took place 9 weeks post prime (**Fig. 7**). However, this expression decreased slightly during the subsequent weeks (**Supporting Information, Fig. S6**). For CS/DS + PCS5 and CS–PCS5/DS/pIC NPs the number of monocytes and macrophages expressing CD40 was lower than in the prototype containing HA, but the response remained for a longer period of time. In the case of CD86 monocytes and macrophages, the values mirrored the ones for CD40, with the difference that at later time points the values were similar to those found in naïve mice (**Supporting Information, Fig. S6**). Overall, the prototypes of CS/HA–PCS5/pIC NPs and CS–PCS5/DS/pIC NPs elicited the highest stimulation of the monocyte/macrophage lineage (**Fig. 7** and **Supporting Information, Fig. S6**), which might be caused by the covalent conjugation of the peptide antigen, in accordance with our hypothesis. In addition, we cannot discard the potential role of poly(I:C) in the stimulation process [72].

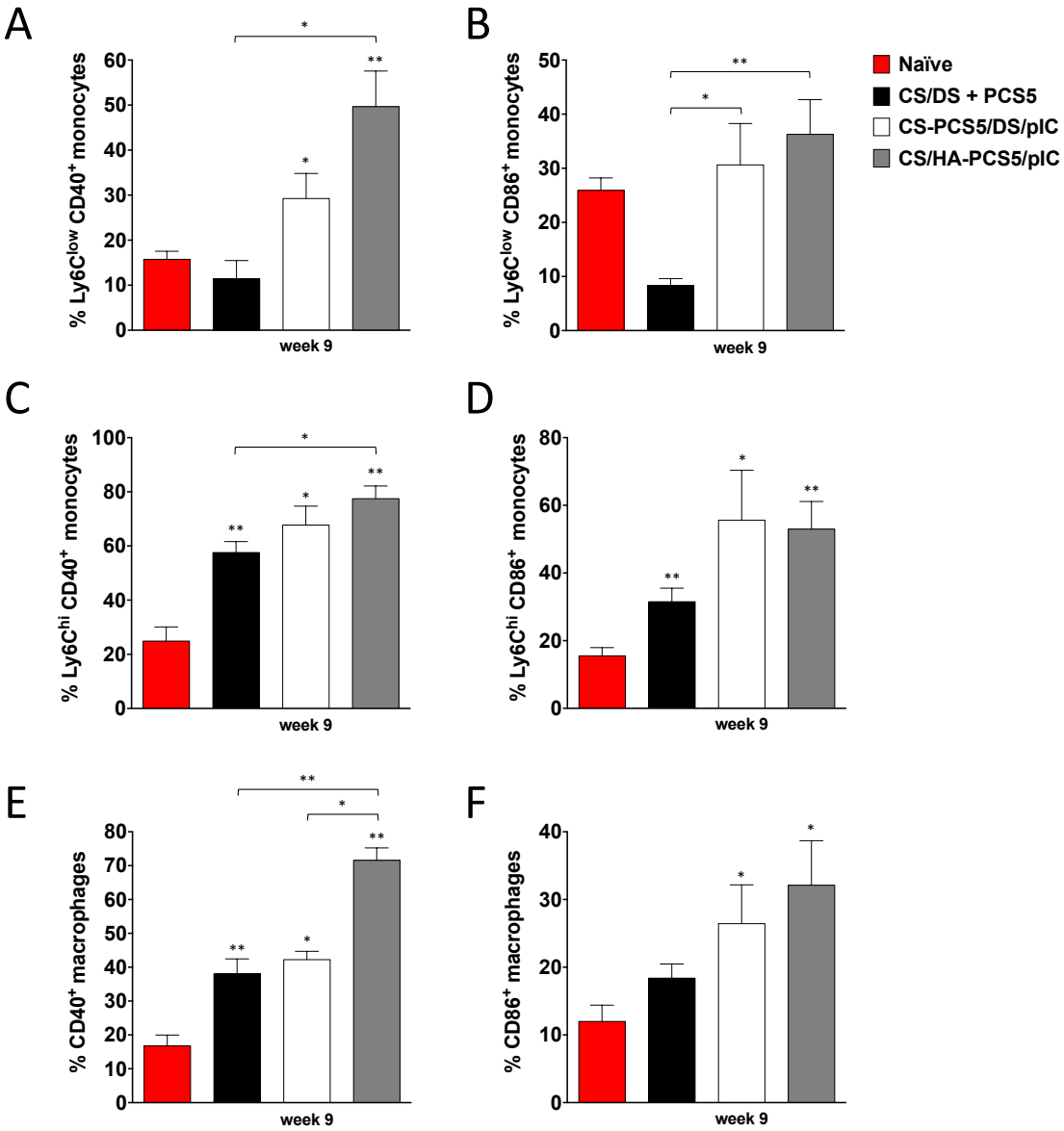

Figure 7. Monocyte and macrophage expression of co-stimulatory factors. CD40 and CD86 expression in (A-B) Ly6C^{low} monocytes; (C-D) Ly6C^{high} monocytes and (E-F) macrophages at 9 weeks post prime was quantified by multicolor flow cytometry of splenocytes obtained from non-treated naïve (red bars) and NP-vaccinated mice: CS/DS + PCS5 (black bars), CS–PCS5/DS/pIC (white bars) or CS/HA–PCS5/pIC (gray bars). Values represent mean ± SEM (n ≥ 3). Statistical comparison between groups was done using a Mann-Whitney test. Significant statistical differences are represented as * ($p < 0.05$) and ** ($p < 0.01$) for comparison between groups and to naïve mice. CS, chitosan; DS, dextran sulfate; HA, hyaluronic acid; PCS5, protease cleavage site 5; pIC, poly(I:C); NPs, nanoparticles.

In a second set of experiments and, in order to further assess the activation of T cells, the secretion of two cytokines that influence anti-HIV responses, *i.e.,* interleukin 2 (IL-2) and tumor necrosis factor alpha (TNFα) [73], was measured. IL-2 is involved in T-cell proliferation and expansion [74], while TNFα is a pro-inflammatory cytokine that participates in innate and adaptive immune responses [75–77].

We also aimed at evaluating the kinetics of T cell activation over time, bearing in mind that an immediate high T cell response would not necessary translate into the best protection. The results showed that the three prototypes were able to activate both CD4 and CD8 T cells with different cytokine secretion kinetics. The highest overall secretion was observed for CS/DS + PCS5 NPs at 10 weeks. In the case of CS–PCS5/DS/pIC NPs, the highest secretion of both IL-2 and TNFα was observed at 9 weeks and 16 weeks post prime (**Fig. 8**), whereas in the case of CS/HA–PCS5/pIC NPs, this activation was more sustained at 12–16 weeks (**Fig. 8**). This pattern could be caused by the different release profiles of the antigen from the NPs, as previously discussed. It is also worth mentioning that delayed T cell activation observed here has also been recently described for an mRNA-based vaccine [78], a result that raises questions regarding the ideal T cell activation profile that will guarantee an efficient protection.

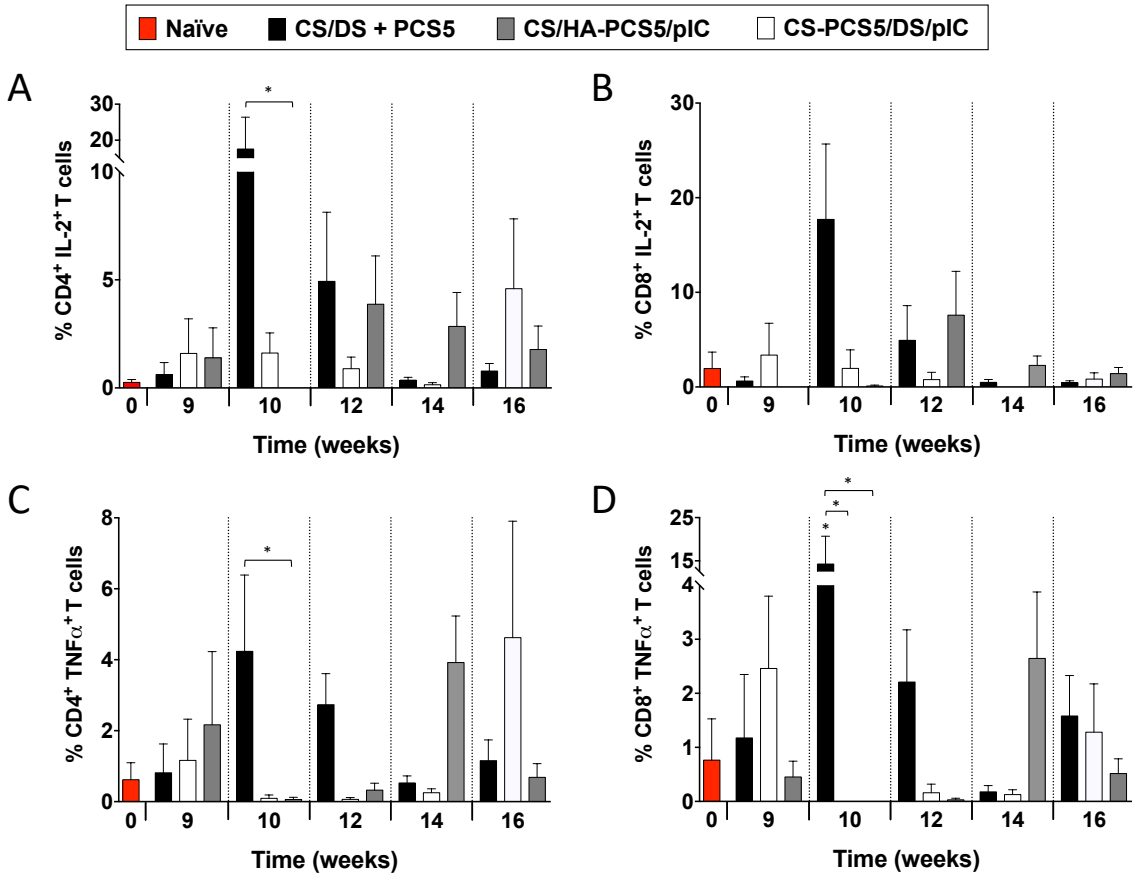

Figure 8. CD4 and CD8 T-cell activation. IL-2 and TNFα secretion in (A, C) CD4 and (B, D) CD8 T cells was quantified by multicolor flow cytometry of T-cells derived from splenocytes from non-treated naïve (red bars) and NP-vaccinated mice: CS/DS + PCS5 (black bars), CS–PCS5/DS/pIC (white bars) or CS/HA–PCS5/pIC (gray bars). Values represent mean ± SEM (n ≥ 3). Statistical comparison between groups was done using a Mann-Whitney test. Significant statistical differences are represented as * ($p < 0.05$) for comparison between groups and to naïve mice. CS, chitosan; DS, dextran sulfate; HA, hyaluronic acid; PCS5, protease cleavage site 5; pIC, poly(I:C); NPs, nanoparticles.

Besides effector T cells, the generation of memory T cells by vaccines is also important to guarantee long-term responses against infections [79]. Depending on the expression of the homing marker L-selectin (CD62L), CD4 and CD8 memory T cells can be further divided as central memory T cells (T_{CM}; $CD44^+$ $CD62L^+$) and effector memory T cells (T_{EM}; $CD44^+$ $CD62L^-$). Regarding their role in the immune response, T_{CM} are important for the stimulation of dendritic cells and B cells, and also because they help expand the effector T cell subsets once they have encountered the antigen. On the other hand, in the same situation, T_{EM} rapidly convert to effector cells to fight against the infection [80,81]. Hence, our objective was to assess if the three nanoformulations under study were able to increase both types of memory T cells, thereby ensuring a good immune response upon infection. The results in **Figure 9** indicate that the three prototypes generated a modest number of memory T cells for up to several weeks after the last boost. In general, the highest proportions of memory T cells corresponded to CS/HA–PCS5/pIC NPs and CS/DS + PCS5 NPs, both at shorter and later time points.

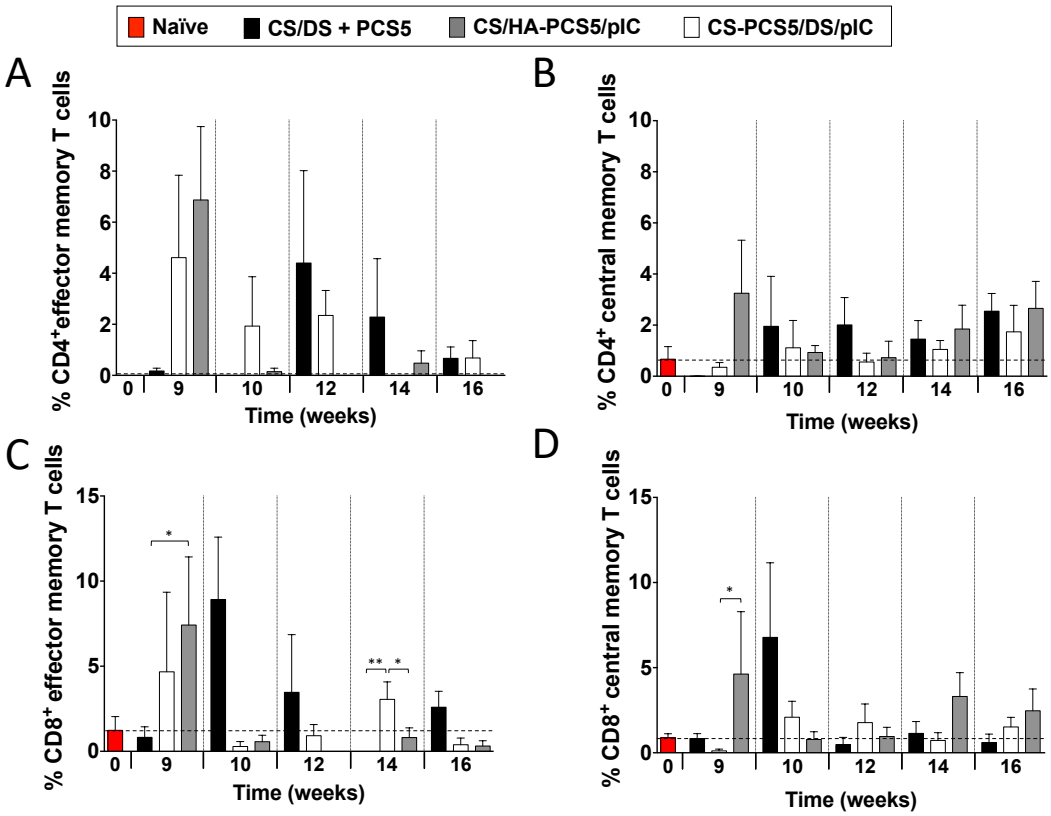

Figure 9. Change in CD4 and CD8 central memory and effector memory T cells. The amount of CD4 and CD8 T cell subsets expressing (A, C) $CD44^+$ $CD62L^-$ (T effector memory – T_{EM}) and (B, D) $CD44^+$ $CD62L^+$ (T central memory – T_{CM})) was quantified by multicolor flow cytometry of splenocytes from naïve (red bars) and NP-vaccinated mice: CS/DS + PCS5 (black bars), CS–PCS5/DS/pIC (white bars) or CS/HA–PCS5/pIC (gray bars). Values represent mean ± SEM (n ≥ 3). Statistical comparison between groups was done using a Mann-Whitney test. Significant statistical differences are represented as * ($p < 0.05$) and ** ($p < 0.01$) for comparison between groups and to naïve mice. CS, chitosan; DS, dextran sulfate; HA, hyaluronic acid; PCS5, protease cleavage site 5; pIC, poly(I:C); NPs, nanoparticles.

Overall, the three prototypes of NPs showed the ability to generate important antibody responses (**Fig. 6B**), whereas the ones containing PCS5 conjugated (CS/HA–PCS5/pIC NPs and CS–PCS5/DS/pIC NPs) activated APCs in a higher extent (**Fig. 7**). In terms of cellular activation, all prototypes were able to increase the secretion of important cytokines such as IL-2 and TNFα, although the production kinetics varied depending on the prototype (**Fig. 8**). The implications of these secretion patterns in the protection against infection is a subject that has to be further analyzed.

4. Conclusions

In the present study, we engineered different polysaccharide-based NPs loaded with an SIV peptide antigen candidate, PCS5. The results showed that different factors, such as the attachment of the antigen (ionic interactions, cleavable and non-cleavable conjugations), the presence of immunomodulatory molecules such as poly(I:C), or the nature of the polysaccharides (CS, DS or HA) could importantly influence the type of the elicited immune response. All the nanosystems showed the ability to induced humoral responses against the antigen, while for the kinetics of the effector T cell responses varied depending on the prototype. In summary, composition, antigen attachment and adjuvants are important design aspects that need to be considered when developing nanovaccines. Further *in vivo* studies would be needed to evaluate whether these humoral and cellular responses would translate into efficient protection in larger animal models.

References

[1] T.G. Dacoba, R.W. Omange, H. Li, J. Crecente-Campo, M. Luo, M.J. Alonso, Polysaccharide nanoparticles can efficiently modulate the immune response against an HIV peptide antigen, ACS Nano. 13 (2019) 4947–4959. doi:10.1021/acsnano.8b07662.

[2] UNAIDS Data 2018, (n.d.). http://www.unaids.org/sites/default/files/media_asset/unaids-data-2018_en.pdf (accessed September 19, 2018).

[3] S. Rerks-Ngarm, P. Pitisuttithum, S. Nitayaphan, J. Kaewkungwal, J. Chiu, R. Paris, N. Premsri, C. Namwat, M. de Souza, E. Adams, M. Benenson, S. Gurunathan, J. Tartaglia, J.G. McNeil, D.P. Francis, D. Stablein, D.L. Birx, S. Chunsuttiwat, C. Khamboonruang, P. Thongcharoen, M.L. Robb, N.L. Michael, P. Kunasol, J.H. Kim, Vaccination with ALVAC and AIDSVAX to prevent HIV-1 infection in Thailand, N. Engl. J. Med. 361 (2009) 2209–2220. doi:10.1056/NEJMoa0908492.

[4] J.H. Kim, J.-L. Excler, N.L. Michael, Lessons from the RV144 Thai phase III HIV-1 vaccine trial and the search for correlates of protection, Annu. Rev. Med. 66 (2015) 423–437. doi:10.1146/annurev-med-052912-123749.

[5] B.F. Haynes, New approaches to HIV vaccine development, Curr. Opin. Immunol. 35 (2015) 39–47. doi:10.1016/j.coi.2015.05.007.

[6] Y. Liu, C. Chen, Role of nanotechnology in HIV/AIDS vaccine development, Adv. Drug Deliv. Rev. 103 (2016) 76–89. doi:10.1016/j.addr.2016.02.010.

[7] M. Luo, R. Capina, C. Daniuk, J. Tuff, H. Peters, M. Kimani, C. Wachihi, J. Kimani, T.B. Ball, F.A. Plummer, Immunogenicity of sequences around HIV-1 protease cleavage sites: potential targets and population coverage analysis for a HIV vaccine targeting protease cleavage sites, Vaccine. 31 (2013) 3000–3008. doi:10.1016/j.vaccine.2013.04.057.

[8] H. Li, R.W. Omange, F.A. Plummer, M. Luo, A novel HIV vaccine targeting the protease cleavage sites, AIDS Res. Ther. 14 (2017) 51. doi:10.1186/s12981-017-0174-7.

[9] H. Li, R.W. Omange, C. Czarnecki, J.F. Correia-Pinto, J. Crecente-Campo, M. Richmond, L. Li, N. Schultz-Darken, M.J. Alonso, J.B. Whitney, F.A. Plummer, M. Luo, Mauritian cynomolgus macaques with M3M4 MHC genotype control SIVmac251 infection, J. Med. Primatol. 46 (2017) 137–143. doi:10.1111/jmp.12300.

[10] A.H. Kaplan, J.A. Zack, M. Knigge, D.A. Paul, D.J. Kempf, D.W. Norbeck, R. Swanstrom, Partial inhibition of the human immunodeficiency virus type 1 protease results in aberrant virus assembly and the formation of noninfectious particles, J. Virol. 67 (1993) 4050–4055.

[11] T.G. Dacoba, A. Olivera, D. Torres, J. Crecente-Campo, M.J. Alonso, Modulating the immune system through nanotechnology, Semin. Immunol. 34 (2017) 78–102. doi:10.1016/j.smim.2017.09.007.

[12] K.T. Gause, A.K. Wheatley, J. Cui, Y. Yan, S.J. Kent, F. Caruso, Immunological principles guiding the rational design of particles for vaccine delivery, ACS Nano. 11 (2017) 54–68. doi:10.1021/acsnano.6b07343.

[13] D.J. Irvine, M.C. Hanson, K. Rakhra, T. Tokatlian, Synthetic nanoparticles for vaccines and immunotherapy, Chem. Rev. 115 (2015) 11109–11146. doi:10.1021/acs.chemrev.5b00109.

[14] A.S. Cordeiro, M.J. Alonso, M. de la Fuente, Nanoengineering of vaccines using natural polysaccharides, Biotechnol. Adv. 33 (2015) 1279–1293. doi:10.1016/j.biotechadv.2015.05.010.

[15] M. Garcia-Fuentes, M.J. Alonso, Chitosan-based drug nanocarriers: where do we stand?, J. Control. Release. 161 (2012) 496–504. doi:10.1016/j.jconrel.2012.03.017.

[16] Z. Shariatinia, Pharmaceutical Applications of Chitosan, Adv. Colloid Interface Sci. 263 (2019) 131–194. doi:10.1016/j.cis.2018.11.008.

[17] P. Calvo, C. Remuñán-López, J.L. Vila-Jato, M.J. Alonso, Novel hydrophilic chitosan-polyethylene oxide nanoparticles as protein carriers, J. Appl. Polym. Sci. 63 (1997) 125–132.

[18] C. Prego, D. Torres, M.J. Alonso, Chitosan nanocapsules: a new carrier for nasal peptide delivery, J. Drug Deliv. Sci. Technol. 16 (2006) 331–337. doi:10.1016/S1773-2247(06)50061-9.

[19] C. Prego, P. Paolicelli, B. Díaz, S. Vicente, A. Sánchez, Á. González-Fernández, M.J. Alonso, Chitosan-based nanoparticles for improving immunization against hepatitis B infection, Vaccine. 28 (2010) 2607–2614. doi:10.1016/j.vaccine.2010.01.011.

[20] A. Vila, A. Sánchez, K. Janes, I. Behrens, T. Kissel, J.L. Vila-Jato, M.J. Alonso, Low molecular weight chitosan nanoparticles as new carriers for nasal vaccine delivery in mice, Eur. J. Pharm. Biopharm. 57 (2004) 123–131. doi:10.1016/j.ejpb.2003.09.006.

[21] S. Vicente, M. Peleteiro, B. Díaz-Freitas, A. Sanchez, Á. González-Fernández, M.J. Alonso, Co-delivery of viral proteins and a TLR7 agonist from polysaccharide nanocapsules: a needle-free vaccination strategy, J. Control. Release. 172 (2013) 773–781. doi:10.1016/j.jconrel.2013.09.012.

[22] J. Crecente-Campo, S. Lorenzo-Abalde, A. Mora, J. Marzoa, N. Csaba, J. Blanco, Á. González-Fernández, M.J. Alonso, Bilayer polymeric nanocapsules: a formulation approach for a thermostable and adjuvanted E. coli antigen vaccine, J. Control. Release. 286 (2018) 20–32. doi:10.1016/j.jconrel.2018.07.018.

[23] E. Zupančič, C. Curato, M. Paisana, C. Rodrigues, Z. Porat, A.S. Viana, C.A.M. Afonso, J. Pinto, R. Gaspar, J.N. Moreira, R. Satchi-Fainaro, S. Jung, H.F. Florindo, Rational design of nanoparticles towards targeting antigen-presenting cells and improved T cell priming, J. Control. Release. 258 (2017) 182–195. doi:10.1016/j.jconrel.2017.05.014.

[24] G.-N. Shi, C.-N. Zhang, R. Xu, J.-F. Niu, H.-J. Song, X.-Y. Zhang, W.-W. Wang, Y.-M. Wang, C. Li, X.-Q. Wei, D.-L. Kong, Enhanced antitumor immunity by targeting dendritic cells with tumor cell lysate-loaded chitosan nanoparticles vaccine, Biomaterials. 113 (2017) 191–202. doi:10.1016/j.biomaterials.2016.10.047.

[25] S. Vicente, B. Diaz-Freitas, M. Peleteiro, A. Sanchez, D.W. Pascual, A. Gonzalez-Fernandez, M.J. Alonso, A polymer/oil based nanovaccine as a single-dose immunization approach, PLoS One. 8 (2013) 2–9. doi:10.1371/journal.pone.0062500.

[26] J.V. González-Aramundiz, E. Presas, I. Dalmau-Mena, S. Martínez-Pulgarín, C. Alonso, J.M. Escribano, M.J. Alonso, N.S. Csaba, Rational design of protamine nanocapsules as antigen delivery carriers, J. Control. Release. 245 (2017) 62–69. doi:10.1016/j.jconrel.2016.11.012.

[27] A. V Li, J.J. Moon, W. Abraham, H. Suh, J. Elkhader, M.A. Seidman, M. Yen, E.-J. Im, M.H. Foley, D.H. Barouch, D.J. Irvine, Generation of effector memory T cell-based mucosal and systemic immunity with pulmonary nanoparticle vaccination, Sci. Transl. Med. 5 (2013) 1–11. doi:10.1126/scitranslmed.3006516.

[28] J.T. Wilson, S. Keller, M.J. Manganiello, C. Cheng, C.-C. Lee, C. Opara, A. Convertine, P.S. Stayton, pH-responsive nanoparticle vaccines for dual-delivery of antigens and immunostimulatory oligonucleotides, ACS Nano. 7 (2013) 3912–3925. doi:10.1021/nn305466z.

[29] B.R. Sloat, M.A. Sandoval, A.M. Hau, Y. He, Z. Cui, Strong antibody responses induced by protein antigens conjugated onto the surface of lecithin-based nanoparticles, J. Control. Release. 141 (2010) 93–100. doi:10.1016/j.jconrel.2009.08.023.

[30] S. Bale, G. Goebrecht, A. Stano, R. Wilson, T. Ota, K. Tran, J. Ingale, M.B. Zwick, R.T. Wyatt, Covalent linkage of HIV-1 trimers to synthetic liposomes elicits improved B cell and antibody responses, J. Virol. 91 (2017) e00443-17. doi:10.1128/JVI.00443-17.

[31] A. Jain, W. Yan, K.R. Miller, R. O'Carra, J.G. Woodward, R.J. Mumper, Tresyl-based conjugation of protein antigen to lipid nanoparticles increases antigen immunogenicity, Int. J. Pharm. 401 (2010) 87–92. doi:10.1016/j.ijpharm.2010.09.003.

[32] A. Caivano, N.A. Doria-Rose, B. Buelow, R. Sartorius, M. Trovato, L. D'Apice, G.J. Domingo, W.F. Sutton, N.L. Haigwood, P. De Berardinis, HIV-1 Gag p17 presented as virus-like particles on the E2 scaffold from Geobacillus stearothermophilus induces sustained humoral and cellular immune responses in the absence of IFNγ production by CD4+ T cells, Virology. 407 (2010) 296–305. doi:10.1016/j.virol.2010.08.026.

[33] D.S. Watson, V.M. Platt, L. Cao, V.J. Venditto, F.C. Szoka, Antibody response to polyhistidine-tagged

peptide and protein antigens attached to liposomes via lipid-linked nitrilotriacetic acid in mice, Clin. Vaccine Immunol. 18 (2011) 289–297. doi:10.1128/CVI.00425-10.

[34] J.J. Moon, H. Suh, V. Li, C.F. Ockenhouse, A. Yadava, D.J. Irvine, Enhancing humoral responses to a malaria antigen with nanoparticle vaccines that expand Tfh cells and promote germinal center induction, Proc. Natl. Acad. Sci. 109 (2012) 1080–1085. doi:10.1073/pnas.1112648109.

[35] N.M. Molino, A.K.L. Anderson, E.L. Nelson, S.W. Wang, Biomimetic protein nanoparticles facilitate enhanced dendritic cell activation and cross-presentation, ACS Nano. 7 (2013) 9743–9752. doi:10.1021/nn403085w.

[36] V. V. Temchura, D. Kozlova, V. Sokolova, K. Überla, M. Epple, Targeting and activation of antigen-specific B-cells by calcium phosphate nanoparticles loaded with protein antigen, Biomaterials. 35 (2014) 6098–6105. doi:10.1016/j.biomaterials.2014.04.010.

[37] Q. Liu, C. Zhang, X. Zheng, X. Shao, X. Zhang, Q. Zhang, X. Jiang, Preparation and evaluation of antigen/N-trimethylaminoethylmethacrylate chitosan conjugates for nasal immunization, Vaccine. 32 (2014) 2582–2590. doi:10.1016/j.vaccine.2014.03.041.

[38] Q. Liu, X. Zheng, C. Zhang, X. Shao, Q. Zhang, X. Jiang, Conjugating Influenza A (H1N1) antigen to N-trimethylaminoethylmethacrylate chitosan nanoparticles improves the immunogenicity of the antigen after nasal administration, J. Med. Virol. 87 (2015) 1807–1815. doi:10.1002/jmv.24253.

[39] S.P. Kasturi, P.A. Kozlowski, H.I. Nakaya, M.C. Burger, P. Russo, M. Pham, Y. Kovalenkov, E.L. V. Silveira, C. Havenar-Daughton, S.L. Burton, K.M. Kilgore, M.J. Johnson, R. Nabi, T. Legere, Z.J. Sher, X. Chen, R.R. Amara, E. Hunter, S.E. Bosinger, P. Spearman, S. Crotty, F. Villinger, C.A. Derdeyn, J. Wrammert, B. Pulendran, Adjuvanting a simian immunodeficiency virus vaccine with toll-like receptor ligands encapsulated in nanoparticles induces persistent antibody responses and enhanced protection in TRIM5α restrictive macaques, J. Virol. 91 (2017) e01844-16. doi:10.1128/JVI.01844-16.

[40] H. Li, M. Nykoluk, L. Li, L.R. Liu, R.W. Omange, G. Soule, L.T. Schroeder, N. Toledo, M.A. Kashem, J.F. Correia-Pinto, B. Liang, N. Schultz-Darken, M.J. Alonso, J.B. Whitney, F.A. Plummer, M. Luo, Natural and cross-inducible anti-SIV antibodies in Mauritian cynomolgus macaques, PLoS One. 12 (2017) 1–20. doi:10.1371/journal.pone.0186079.

[41] C. Teijeiro-Valiño, R. Novoa-Carballal, E. Borrajo, A. Vidal, M. Alonso-Nocelo, M. de la Fuente Freire, P.P. Lopez-Casas, M. Hidalgo, N. Csaba, M.J. Alonso, A multifunctional drug nanocarrier for efficient anticancer therapy, J. Control. Release. 294 (2019) 154–164. doi:10.1016/j.jconrel.2018.12.002.

[42] J. Shi, P.W. Kantoff, R. Wooster, O.C. Farokhzad, Cancer nanomedicine: progress, challenges and opportunities, Nat. Rev. Cancer. 17 (2017) 20–37. doi:10.1038/nrc.2016.108.

[43] F. Rose, J.E. Wern, F. Gavins, P. Andersen, F. Follmann, C. Foged, A strong adjuvant based on glycol-chitosan-coated lipid-polymer hybrid nanoparticles potentiates mucosal immune responses against the recombinant Chlamydia trachomatis fusion antigen CTH522, J. Control. Release. 271 (2018) 88–97. doi:10.1016/j.jconrel.2017.12.003.

[44] A. Vila, A. Sánchez, M. Tobío, P. Calvo, M.J. Alonso, Design of biodegradable particles for protein delivery, J. Control. Release. 78 (2002) 15–24. doi:10.1016/S0168-3659(01)00486-2.

[45] J.F. Correia-Pinto, N. Csaba, J. Schiller, M.J. Alonso, Chitosan-poly (I:C)-PADRE based nanoparticles as delivery vehicles for synthetic peptide vaccines, Vaccines. 3 (2015) 730–750. doi:10.3390/vaccines3030730.

[46] L. Cui, J.A. Cohen, K.E. Broaders, T.T. Beaudette, J.M.J. Fréchet, Mannosylated dextran nanoparticles: a pH-sensitive system engineered for immunomodulation through mannose targeting, Bioconjug. Chem. 22 (2011) 949–957. doi:10.1021/bc100596w.

[47] S. Sharma, T.K. Mukkur, H.A. Benson, Y. Chen, Enhanced immune response against Pertussis toxoid by IgA-loaded chitosan–dextran sulfate nanoparticles, J. Pharm. Sci. 101 (2012) 233–244. doi:10.1002/jps.22763.

[48] K. Perica, A. Tu, A. Richter, J.G. Bieler, M. Edidin, J.P. Schneck, Magnetic field-induced T cell receptor clustering by nanoparticles enhances T cell activation and stimulates antitumor activity, ACS Nano. 8 (2014) 2252–2260. doi:10.1021/nn405520d.

[49] B.J.G. Baaten, R. Tinoco, A.T. Chen, L.M. Bradley, Regulation of antigen-experienced T cells: lessons from the quintessential memory marker CD44, Front. Immunol. 3 (2012) 1–12. doi:10.3389/fimmu.2012.00023.

[50] C.C. Termeer, J. Hennies, U. Voith, T. Ahrens, J. M. Weiss, P. Prehm, J.C. Simon, Oligosaccharides of hyaluronan are potent activators of dendritic cells, J. Immunol. 165 (2000) 1863–1870. doi:10.4049/jimmunol.165.4.1863.

[51] C. Ke, D. Wang, Y. Sun, D. Qiao, H. Ye, X. Zeng, Immunostimulatory and antiangiogenic activities of low molecular weight hyaluronic acid, Food Chem. Toxicol. 58 (2013) 401–407. doi:10.1016/j.fct.2013.05.032.

[52] Y. Fan, P. Sahdev, L.J. Ochyl, J. J. Akerberg, J.J. Moon, Cationic liposome–hyaluronic acid hybrid nanoparticles for intranasal vaccination with subunit antigens, J. Control. Release. 208 (2015) 121–129. doi:10.1016/j.jconrel.2015.04.010.

[53] L. Liu, F. Cao, X. Liu, H. Wang, C. Zhang, H. Sun, C. Wang, X. Leng, C. Song, D. Kong, G. Ma, Hyaluronic acid-modified cationic lipid–PLGA hybrid nanoparticles as a nanovaccine induce robust humoral and cellular immune responses, ACS Appl. Mater. Interfaces. 8 (2016) 11969–11979. doi:10.1021/acsami.6b01135.

[54] J.V. González-Aramundiz, M. Peleteiro Olmedo, Á. González-Fernández, M.J. Alonso, N.S. Csaba, Protamine-based nanoparticles as new antigen delivery systems, Eur. J. Pharm. Biopharm. 97 (2015) 51–59. doi:10.1016/j.ejpb.2015.09.019.

[55] J.F. Correia-Pinto, M. Peleteiro, N. Csaba, Á. González-Fernández, M.J. Alonso, Multi-enveloping of particulated antigens with biopolymers and immunostimulant polynucleotides, J. Drug Deliv. Sci. Technol. 30 (2015) 424–434. doi:10.1016/j.jddst.2015.08.010.

[56] A.M. Hafner, B. Corthésy, H.P. Merkle, Particulate formulations for the delivery of poly(I:C) as vaccine adjuvant, Adv. Drug Deliv. Rev. 65 (2013) 1386–1399. doi:10.1016/j.addr.2013.05.013.

[57] H. Park, L. Adamson, T. Ha, K. Mullen, S.I. Hagen, A. Nogueron, A.W. Sylwester, M.K. Axthelm, A. Legasse, M. Piatak, J.D. Lifson, J.M. McElrath, L.J. Picker, R.A. Seder, Polyinosinic-polycytidylic acid is the most effective TLR adjuvant for SIV Gag protein-induced T cell responses in nonhuman primates, J. Immunol. 190 (2013) 4103–4115. doi:10.4049/jimmunol.1202958.

[58] A.D. Baldwin, K.L. Kiick, Tunable degradation of maleimide-thiol adducts in reducing environments, Bioconjug. Chem. 22 (2011) 1946–1953. doi:10.1021/bc200148v.

[59] J. Shao, J.P. Tam, Unprotected peptides as building blocks for the synthesis of peptide dendrimers with oxime, hydrazone, and thiazolidine linkages, J. Am. Chem. Soc. 117 (1995) 3893–3899. doi:10.1021/ja00119a001.

[60] H. Cho, T. Daniel, Y.J. Buechler, D.C. Litzinger, Z. Maio, A.-M.H. Putnam, V.S. Kraynov, B.-C. Sim, S. Bussell, T. Javahishvili, S. Kaphle, G. Viramontes, M. Ong, S. Chu, B. GC, R. Lieu, N. Knudsen, P. Castiglioni, T.C. Norman, D.W. Axelrod, A.R. Hoffman, P.G. Schultz, R.D. DiMarchi, B.E. Kimmel, Optimized clinical performance of growth hormone with an expanded genetic code, Proc. Natl. Acad. Sci. 108 (2011) 9060–9065. doi:10.1073/pnas.1100387108.

[61] C. Pifferi, N. Berthet, O. Renaudet, Cyclopeptide scaffolds in carbohydrate-based synthetic vaccines, Biomater. Sci. 5 (2017) 953–965. doi:10.1039/C7BM00072C.

[62] J. Yang, J. Li, X. Li, X. Wang, Y. Yang, N. Kawazoe, G. Chen, Nanoencapsulation of individual mammalian cells with cytoprotective polymer shell, Biomaterials. 133 (2017) 253–262. doi:10.1016/j.biomaterials.2017.04.020.

[63] F. Meng, W.E. Hennink, Z. Zhong, Reduction-sensitive polymers and bioconjugates for biomedical

applications, Biomaterials. 30 (2009) 2180–2198. doi:10.1016/j.biomaterials.2009.01.026.

[64] R. Cheng, F. Feng, F. Meng, C. Deng, J. Feijen, Z. Zhong, Glutathione-responsive nano-vehicles as a promising platform for targeted intracellular drug and gene delivery, J. Control. Release. 152 (2011) 2–12. doi:10.1016/j.jconrel.2011.01.030.

[65] G.K. Lewis, A.L. DeVico, R.C. Gallo, Antibody persistence and T-cell balance: two key factors confronting HIV vaccine development, Proc. Natl. Acad. Sci. 111 (2014) 15614–15621. doi:10.1073/pnas.1413550111.

[66] C. Auffray, M.H. Sieweke, F. Geissmann, Blood monocytes: development, heterogeneity, and relationship with dendritic cells, Annu. Rev. Immunol. 27 (2009) 669–692. doi:10.1146/annurev.immunol.021908.132557.

[67] C. Auffray, D. Fogg, M. Garfa, G. Elain, O. Join-Lambert, S. Kayal, S. Sarnacki, A. Cumano, G. Lauvau, F. Geissmann, Monitoring of blood vessels and tissues by a population of monocytes with patrolling behavior, Science. 317 (2007) 666–670. doi:10.1126/science.1142883.

[68] J. Yang, L. Zhang, C. Yu, X.-F. Yang, H. Wang, Monocyte and macrophage differentiation: circulation inflammatory monocyte as biomarker for inflammatory diseases, Biomark. Res. 2 (2014) 1. doi:10.1186/2050-7771-2-1.

[69] R.D. Stout, J. Suttles, The many roles of CD40 in cell-mediated inflammatory responses, Immunol. Today. 17 (1996) 487–492. doi:10.1016/0167-5699(96)10060-I.

[70] I.S. Grewal, R.A. Flavell, CD40 and CD154 in cell-mediated immunity, Annu. Rev. Immunol. 16 (1998) 111–135. doi:10.1146/annurev.immunol.16.1.111.

[71] C.B. Thompson, Distinct roles for the costimulatory ligands B7-1 and B7-2 in T helper cell differentiation?, Cell. 81 (1995) 979–982. doi:10.1016/S0092-8674(05)80001-7.

[72] H. Song, P. Huang, J. Niu, G. Shi, C. Zhang, D. Kong, W. Wang, Injectable polypeptide hydrogel for dual-delivery of antigen and TLR3 agonist to modulate dendritic cells in vivo and enhance potent cytotoxic T-lymphocyte response against melanoma, Biomaterials. 159 (2018) 119–129. doi:10.1016/j.biomaterials.2018.01.004.

[73] D.R. Lucey, M. Clerici, Type 1 and type 2 cytokine dysregulation in human infectious, neoplastic, and inflammatory diseases, Clin. Microbiol. Rev. 9 (1996) 532–562.

[74] M.A. Williams, A.J. Tyznik, M.J. Bevan, Interleukin-2 signals during priming are required for secondary expansion of CD8+ memory T cells, Nature. 441 (2006) 890–893. doi:10.1038/nature04790.

[75] G. Chen, D. V. Goeddel, TNF-R1 signaling: a beautiful pathway, Science. 296 (2002) 1634–1635. doi:10.1126/science.1071924.

[76] S. Vallabhapurapu, M. Karin, Regulation and function of NF-κB transcription factors in the immune system, Annu. Rev. Immunol. 27 (2009) 693–733. doi:10.1146/annurev.immunol.021908.132641.

[77] G. Arango Duque, A. Descoteaux, Macrophage cytokines: involvement in immunity and infectious diseases, Front. Immunol. 5 (2014) 1–12. doi:10.3389/fimmu.2014.00491.

[78] N. Moyo, A.B. Vogel, S. Buus, S. Erbar, E.G. Wee, U. Sahin, T. Hanke, Efficient Induction of T cells against conserved HIV-1 regions by mosaic vaccines delivered as self-amplifying mRNA, Mol. Ther. - Methods Clin. Dev. 12 (2019) 32–46. doi:10.1016/j.omtm.2018.10.010.

[79] M.A. Williams, M.J. Bevan, Effector and memory CTL differentiation, Annu. Rev. Immunol. 25 (2007) 171–192. doi:10.1146/annurev.immunol.25.022106.141548.

[80] M.T. Esser, R.D. Marchese, L.S. Kierstead, L.G. Tussey, F. Wang, N. Chirmule, M.W. Washabaugh, Memory T cells and vaccines, Vaccine. 21 (2003) 419–430. doi:10.1016/S0264-410X(02)00407-3.

[81] F. Sallusto, J. Geginat, A. Lanzavecchia, Central memory and effector memory T cell subsets: function, generation, and maintenance, Annu. Rev. Immunol. 22 (2004) 745–763. doi:10.1146/annurev.immunol.22.012703.104702.

Supporting Information

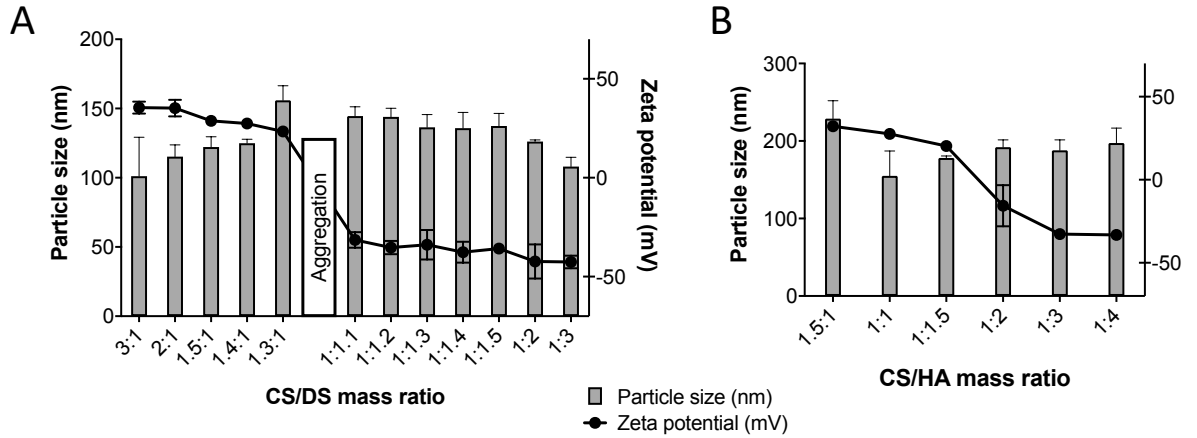

Supporting Figure S1. Evolution of particle size and zeta potential of blank (A) CS/DS NPs and (B) CS/HA NPs as the mass ratio of the negative polymer is increased. CS, chitosan; DS, dextran sulfate; HA, hyaluronic acid; NPs, nanoparticles.

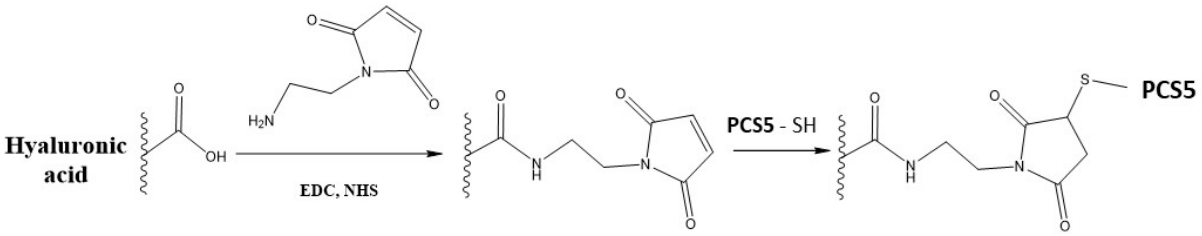

Supporting Figure S2. Preparation of the conjugate HA–PCS5 in a 2-step thiol-maleimide conjugation reaction.

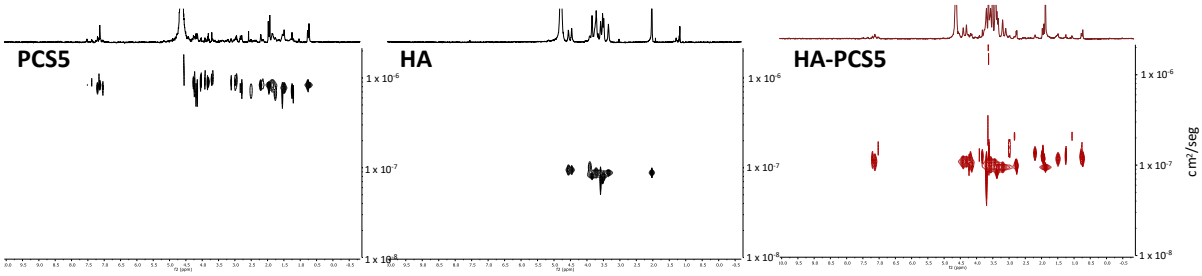

Supporting Figure S3. Diffusion-ordered spectroscopy (DOSY) spectra of PCS5, HA and HA–PCS5. HA, hyaluronic acid; PCS5, protease cleavage site 5.

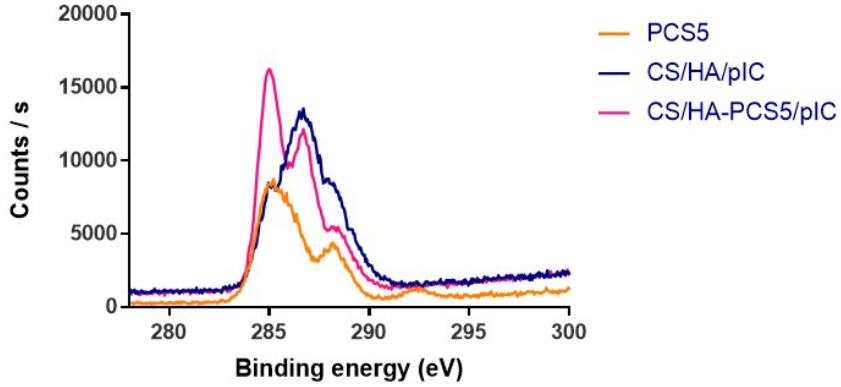

Supporting Figure S4. Carbon s1 binding energies of PCS5 (orange), CS/HA/pIC NPs (blue) and CS/HA–PCS5/pIC NPs (pink). CS, chitosan; HA, hyaluronic acid; PCS5, protease cleavage site 5; pIC, poly(I:C); NPs, nanoparticles.

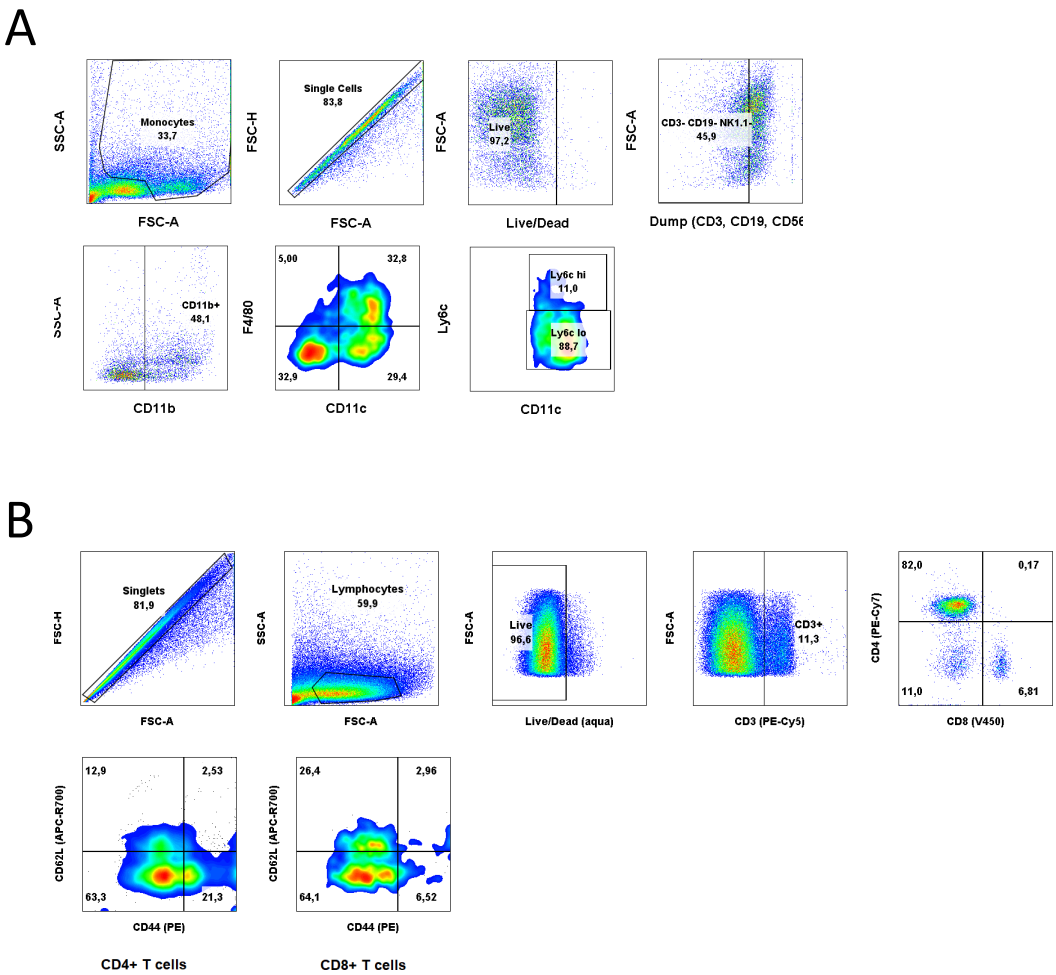

Supporting Figure S5. Multicolor flow gating of (A) monocytes Ly6c^{hi} and Ly6c^{low} and macrophages CD11b^{+} CD11c^{-} F4/80^{+} and (B) central memory and effector memory T cells (CD44^{+} CD62L^{+} and CD44^{+} CD62L^{-}).

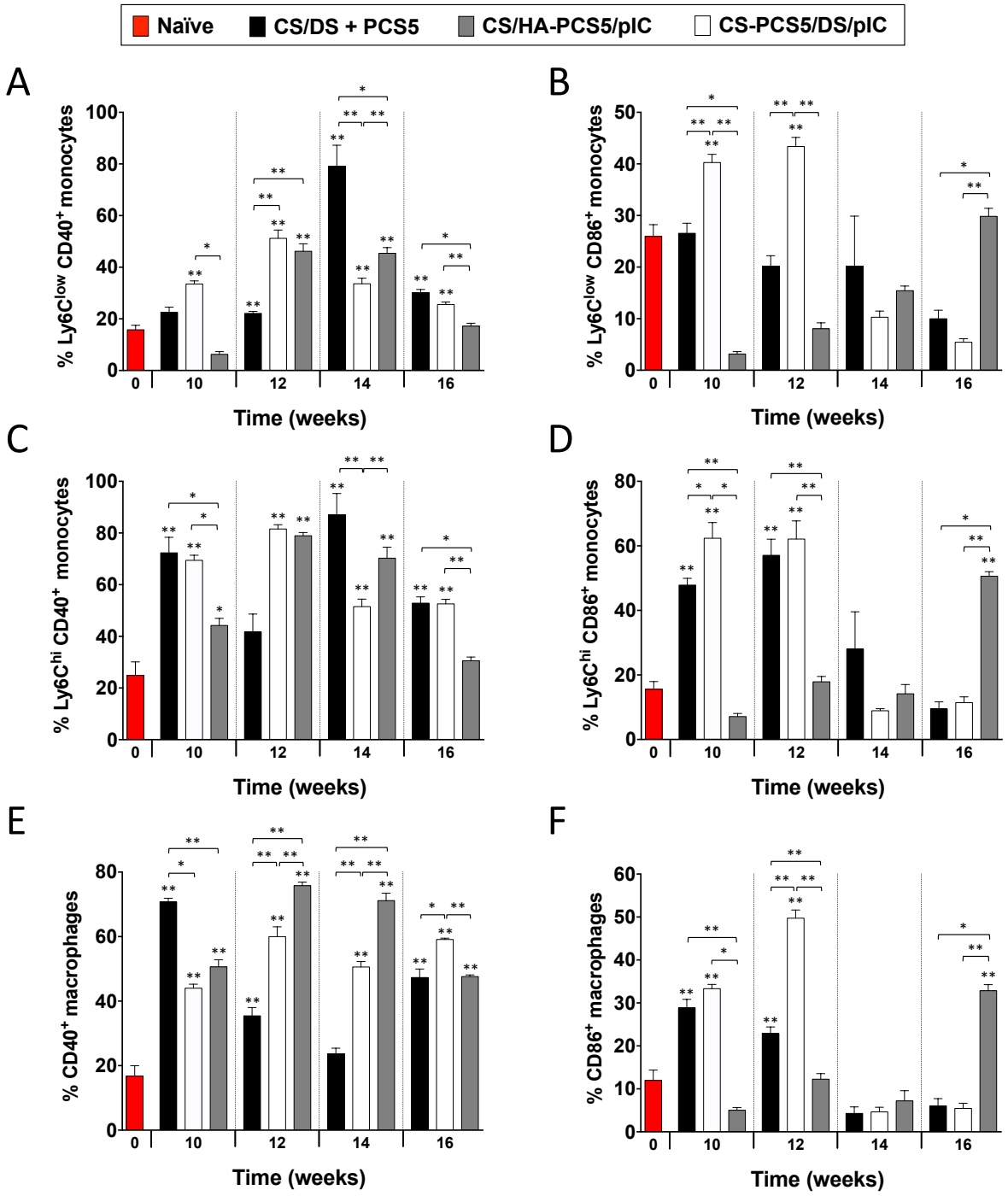

Supporting Figure S6. Monocyte and macrophage expression of co-stimulatory factors at 10, 12, 14 and 16 weeks post prime. CD40 and CD86 expression in (A–B) Ly6C^{low} monocytes; (C–D) Ly6C^{high} monocytes and (E–F) macrophages was quantified by multicolor flow cytometry of splenocytes obtained from non-treated naïve (red bars) and NP-vaccinated mice: CS/DS + PCS5 (black bars), CS–PCS5/DS/pIC (white bars) or CS/HA–PCS5/pIC (gray bars). Values represent mean ± SEM (n ≥ 3). Statistical comparison between groups was done using a Mann-Whitney test. Significant statistical differences are represented as * ($p < 0.05$) and ** ($p < 0.01$) for comparison between groups and to naïve mice.; CS, chitosan; DS, dextran sulfate; HA, hyaluronic acid; PCS5, protease cleavage site 5; pIC, poly(I:C); NPs, nanoparticles.

Supporting Table S1. Elemental composition (%) by XPS of the surface of CS, HA, PCS5, blank CS/HA/pIC NPs and loaded CS/HA–PCS5/pIC NPs.

Sample	C	O	N	Cl	Mg	F	Na	S	C/O	C/N
Chitosan	50.53	32.78	7.46	6.18	2.75	0.30	-	-	1.54	6.77
Hyaluronic acid	51.73	34.87	3.95	0.45	0.71	5.42	5.88	-	1.48	13.10
PCS5	58.49	16.72	15.96	-	-	6.79	-	2.05	3.50	3.66
CS/HA/pIC NPs	55.19	29.38	4.29	2.05	-	-	4.56	0.28	1.87	12.86
CS/HA–PCS5/pIC NPs	65.51	20.52	7.04	3.67	-	0.39	1.72	1.15	3.19	9.31

CS, chitosan; HA, hyaluronic acid; PCS5, protease cleavage site 5; pIC, poly(I:C); NPs, nanoparticles.

Chapter 1.B

Assessment of the efficacy of a tri-peptide nanoparticle-based SIV vaccine candidate

Chapter 1.B

Assessment of the efficacy of a tri-peptide nanoparticle-based SIV vaccine candidate

This work was done in collaboration with the University of Manitoba, Winnipeg (Canada) and the Wisconsin National Primate Research Center (USA).

Abstract

In the first part of this chapter we showed that the attachment of the PCS5 antigen to different nanoparticles (NPs) influenced the immune response generated in mice. Hence, in this second part of the chapter, the objective was to evaluate the potential of two of these NPs containing three protease cleavage site (PCS) peptides. The selected prototypes were chitosan/dextran sulfate (CS/DS) NPs with the PCSs associated by ionic interactions; and chitosan/hyaluronic acid/poly(I:C) (CS/HA–PCS/pIC) NPs, in which the PCSs were covalently linked to HA. The peptide antigens were separately associated to the NPs and a cocktail of each prototype containing the three PCSs was prepared. Furthermore, the physicochemical properties of the resulting prototype cocktails were similar to the ones of the NPs loading the individual PCSs. Finally, *in vivo* studies were conducted in non-human primates. Animals were immunized with the combination of the two selected prototypes of NPs containing the three PCSs, by intramuscular and intranasal administration. The performance of these prototypes was compared with that of a formulation previously reported, composed of CS/DS NPs loaded with the twelve PCSs in combination with specific viral vectors coding for these sequences. The results showed that the combination of NPs containing three PCSs was able to protect 50% of the animals upon seven SIV intravaginal challenges, compared to the control (25%). On the other hand, the combination of the twelve PCSs resulted in 75% protection. Overall, these results pave the way to develop an effective version of the reference PCS vaccine based only on NPs and a low number of PCSs.

Graphical abstract

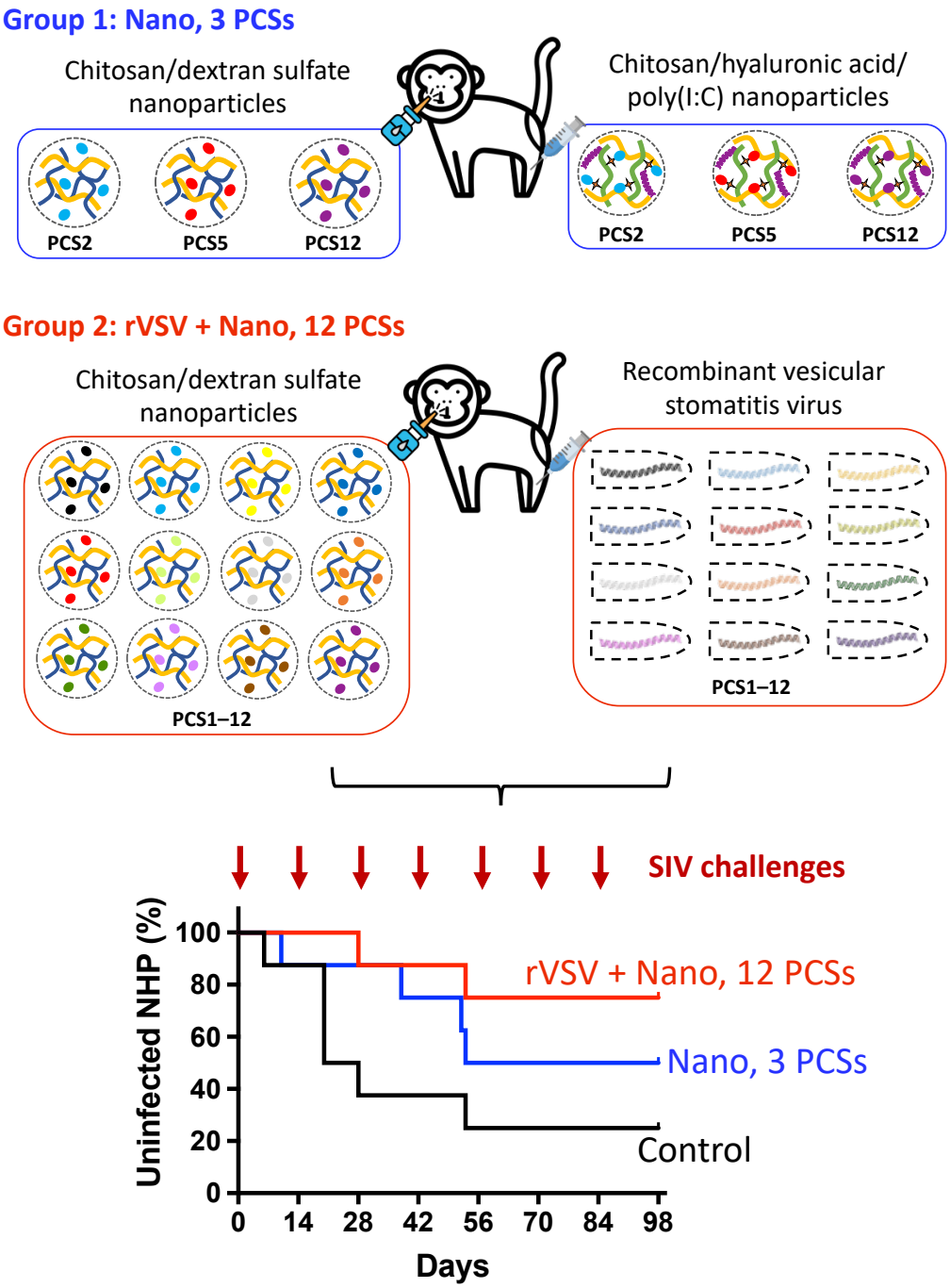

1. Introduction

Tremendous economic and scientific efforts have been made to develop a successful HIV vaccine. Up until now, six HIV vaccines have completed phase III clinical trials, however, none of them has reported an important protection against virus acquisition [1,2]. Overall, two main strategies are currently being pursued for developing an effective HIV vaccine. One of them is focused on generating a balanced activation of T and B cells, while the other one aims at stimulating an specific B cell immunity able to elicit broadly neutralizing antibodies [2,3]. Whether one of these approaches, or a combination of them, will be the solution for HIV prevention, is still unknown.

Most of the HIV vaccine prototypes developed so far consist of certain HIV antigens, such as Env, Gag, or Pol, administered as full-length proteins with adjuvants, and/or delivered by viral vectors [3,4]. In this context, it has been suggested that nanocarriers could be an alternative to these viral vectors, which are usually highly immunogenic. Indeed, nanosystems have been reported to protect antigens, while delivering them to specific immune cells, thereby enhancing the activity of the antigen [5–7]. Moreover, the nanosystem may also include one or more immunomodulators, the combination of which may result in an enhanced adjuvant effect [5–7]. The efficacy of this nanotechnological approach has been shown at the preclinical level [6], but also by the fact that a few nanotechnology-based formulations are already in the market [8,9] (**Introduction, Table 1**).

Apart from the classical Env, Gag and Pol immunogens, Luo and collaborators have described the twelve sequences surrounding the HIV protease cleavage sites (PCSs) as potent alternative antigens to these full-length proteins [10,11]. In this regard, good immune responses were recently described after the administration of these PCS vaccine to non-human primates (NHPs) [12,13]. This vaccine was composed of a combination of recombinant vesicular stomatitis virus (rVSV) coding for the twelve PCSs, together with a cocktail of CS/DS NPs associating the twelve PCS peptides [12,13].

Considering this background information, together with the results presented in Chapter 1.A, where the capacity of different PCS5-loaded NPs to activate the immune response in mice was shown [14], the objective of this work was to investigate the potential value of a NP-based vaccine candidate containing three PCS peptides as antigens. The vaccine efficacy of this new vaccine candidate was evaluated in non-human primates (NHPs) and compared to the one of the vaccine containing the twelve PCSs delivered both in NPs and in viral vectors [15].

2. Materials and methods

2.1. Materials

Chitosan (CS) (chlorhydrate salt, molecular weight (MW) 42.7 kDa and an 88% deacetylation degree) was purchased from HMC^{+} (Halle, Germany). Dextran sulfate (DS), (sodium salt, MW 8 kDa) was obtained from Sigma-Aldrich SAFC® (MO, USA). Research grade sodium hyaluronate (HA) (MW 57 kDa) was purchased from Lifecore Biomedical (MN, USA). Poly(I:C) HMW was acquired from InvivoGen (CA, USA) and high purity α,α–Trehalose dihydrate was purchased from Pfanstiehl (IL, USA). SIV peptides PCS2 (sequence: GGPGQKARLMAEALKEALAP, MW 2010 Da), PCS5 peptide (sequence: GPWGKKPRNFPMAQVHQGLM, MW 2280 Da), and PCS12 (sequence: NQGQYMNTPWRNPAEEREKL, MW 2460 Da)) with or without a terminal cysteine residue and >95% purity, were purchased from GenScript (NJ, USA). MES hydrate, N-(2-aminoethyl)maleimide trifluoroacetate salt (ASEM), N-hydroxysuccinimide (NHS) and N-(3-Dimethylaminopropyl)-N´-ethylcarbodiimide hydrochloride (EDC) were obtained from Sigma-Aldrich (MO, USA).

2.2. Preparation of CS/DS + PCS NPs

CS/DS NPs in a mass ratio 1:3, and associating each PCS separately, were prepared using the same protocol previously described for PCS5 [14]. Once prepared, 0.5 mL of each PCS-loaded nanosystem were mixed, and the individual formulations and the physical mixture were characterized by DLS (section 2.5). At last, 1.5 mL of the cocktail were freeze-dried with 0.6 mL of a trehalose aqueous solution (45% w/v). Just prior the immunization, the freeze-dried formulation was reconstituted in 1.3 mL of water for a final concentration of 0.05 mg/mL of each PCS.

2.3. Synthesis of HA–PCS conjugates

The peptide antigens (PCS2, PCS5 and PCS12) were separately linked to HA by a thiol-maleimide conjugation reaction following exactly the same procedure previously described for HA to PCS5 conjugation [14]. The resulting conjugates were characterized by ^{1}H NMR following a protocol already published [14].

2.4. Preparation of CS/HA–PCS/pIC NPs

For the preparation of these NPs, a mass ratio 1:1 CS/HA was employed. In all cases, a 2 mg/mL aqueous solution of HA was prepared, adjusting the final peptide concentration of 0.20 mg/mL. Besides, poly(I:C) was added as a 1 mg/mL aqueous solution to have a final concentration of 2 μg/mL.

The NPs containing each of the HA–PCS conjugates were prepared as described for the CS/HA–PCS5/pIC NPs [14]. Once the NPs containing each PCS conjugate were fabricated, all the PCS-loaded nanosystems were mixed in equal volumes and characterized before and after the process. Then, 0.9 mL of the cocktail was freeze-dried with 0.6 mL of a trehalose aqueous solution (22.5% w/v). Before the immunization, the freeze-dried formulation was reconstituted in 0.9 mL of water to a final trehalose concentration of 15%.

2.5. NP characterization

The mean size (Z-average) and polydispersity index (PDI) of the NPs were characterized by Dynamic Light Scattering (DLS). The zeta potential values of the NPs were determined by Laser Doppler Anemometry (LDA), measuring the mean electrophoretic mobility after a 10-times dilution of the NPs in ultrapure water. Both properties were measured using a Zetasizer® NanoZS, using the software Zetasizer v7.13 (Malvern Instruments, Malvern, UK). The measurements were performed at 25 °C with a detection angle of 173.

2.6. Freeze-drying

The freeze-drying process followed was the same described in another publication [14]. The resuspended NPs were characterized as described in section 2.5.

2.7. Preparation of the reference formulation

Both, the CS/DS NPs containing the twelve PCS and the recombinant vesicular stomatitis virus (rVSV) coding for the same PCS, were prepared as described in early reports [12,13,15].

2.8. Animal studies

All animal studies were conducted at the Wisconsin National Primate Research Center (USA). The experiments were approved by the University of Wisconsin (Institutional Animal Care and Use Committees, protocol number G005765), in accordance with the US Animal Welfare Act and following the recommendations of the National Research Council Guide for the Care and Use of Laboratory Animals (8^{th} Edition), and the Weatherall report for The Use of Nonhuman Primates in Research. The Wisconsin National Primate Research Center is fully accredited by Association for Assessment and Accreditation of Laboratory Animal Care International (AAALAC) under the University of Wisconsin, Division of Vice-Chancellor for Research and Graduate Education [15].

Vaccine evaluation was conducted using the Mauritian cynomolgus macaque (MCM)/SIVmac251 infection model [15].

Female *Mauritian cynomolgus* macaques were housed in pairs within the same experimental group during the immunization phase of the study, with visual and auditory access to the other animals. Paired animals lived in two adjacent standard stainless-steel primate cages. Rooms were maintained at 18–24 °C, 30–70% humidity, and on a 12:12 light-dark cycles. Standard non-human primate food with fruit or vegetables was provided daily. In addition, foraging activities and physical environmental enrichment were provided at least weekly, for both activities. All animals were observed at least twice daily for health or welfare issues. Sedation (ketamine alone, or ketamine/dexmedetomidine, atipamezole for reversal) was provided during the experimental procedures [15].

2.9. Administration scheme

In all cases, NPs were presented in a freeze-dried form and resuspended before administration. Each animal group was formed by eight female macaques. The administration protocol of the different formulations was as follows.

2.9.1. The combination of CS/DS and CS/HA/pIC NPs containing three PCSs (Nano, 3 PCSs)

Each animal in this group received two administrations at the same time: one of each NP prototype, one intranasally (i.n.) and the other one intramuscularly (i.m.). These administrations were done once every four weeks, for total of four times (one prime and three boosts) (**Fig. 1A**).

For the CS/DS NPs, 1 mL of the NP suspension (50 μg of each PCS/prototype/animal) was i.n. administered, half of the volume to each nostril. For the CS/HA/pIC NPs, 1.5 mL of these NPs were i.m. injected to the animal flank (50 μg of each PCS/prototype/animal) (**Fig. 1A**).

2.9.2. The combination of rVSV and CS/DS NPs delivering the twelve PCSs (rVSV + Nano, 12 PCSs)

Each animal in this group received one prime (with rVSVs) and four boosts (1^{st} boost: rVSV + NPs; 2^{nd} boost: NPs; 3^{rd} boost: rVSV + NPs; 4^{th} boost: rVSV). In all cases, the rVSVs were i.m. administered with a dose of $2x10^7$ pfu/animal (except in the 4^{th} boost, with $1x10^8$ pfu/animal). For the cocktail of CS/DS NPs with the twelve PCSs, a total volume of 0.5 mL was i.n. administered to each animal (50 μg of each PCS/prototype/animal) [15] (**Fig. 1B**).

2.9.3. The control group

The control group received ultrapure water i.n., and the wild type VSVs i.m., following the same administration scheme than the group of the twelve PCSs (section 2.9.2) [15] (**Fig. 1B**).

2.10. Intravaginal challenges

Intravaginal challenges were done every two weeks starting at 16 weeks (for the group of Nano, 3 PCS) or 24 weeks (for the control group and the group of rVSV + Nano, 12 PCSs) after the last vaccine administration; for a total of seven challenges (**Fig. 1**).

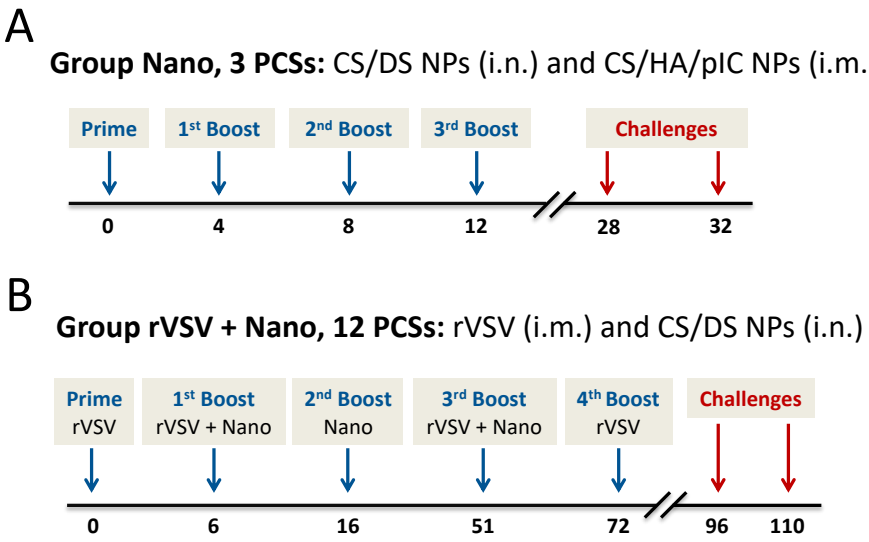

Figure 1. Vaccine administration and challenges schedule for (A) the combination of the CS/DS and CS/HA/pIC nanoparticles with the three PCSs, administered intranasally and intramuscularly, respectively; and (B) the reference formulation based on the viral vectors and CS/DS nanoparticles containing the twelve peptide antigens, administered intramuscularly and intranasally, respectively [15]. CS, chitosan; DS, dextran sulfate; HA, hyaluronic acid; i.m.; intramuscular; i.n., intranasal; NPs, nanoparticles; PCS, protease cleavage site; pIC, poly(I:C); rVSV, recombinant vesicular stomatitis virus.

Intravaginal challenges consisted of 250 times the 50% tissue culture infectious dose (TCID50) of SIVmac251, contained in 1 mL of saline [15]. The virus was delivered using a TB syringe without the needle, or with a rounded end gavage tube. The syringe was gently inserted into the vagina about 4 cm, then slightly withdrawn, and the dose slowly injected for 1 min. Then, the animal's pelvic region was kept elevated for about 30 min before returning the animal to its cage. At the moment of syringe withdraw, it was examined to ensure that no trauma to the vagina had been inflicted. For anesthesia, animals were immobilized against the front of the cage by a squeeze back mechanism, and anesthetized using up to 7 mg/kg ketamine (i.m.) and up to 0.03 mg/kg dexmedetomidine (i.m.). At the conclusion of the procedure, up to 0.3 mg/kg atipamezole (i.v. or i.m.) were used for the reversion

phase. Any additional anesthesia was administered only in consultation with a WNPRC veterinarian. Alternative anesthesia would only be used as directed by a WNPRC veterinarian. The duration of anesthesia was usually less than 45 min. Monitoring of anesthesia recovery was documented every 15 min until the animal was sitting upright, then every 30 min until the animal was fully recovered.

Plasma viral load was quantified on days 6, 10 and 14 of each challenge round. Furthermore, any animal found infected was not further challenged. Viral RNA was isolated from plasma samples using the Maxwell 16 Viral Total Nucleic Acid Purification kit on the Maxwell 16MDx instrument (Promega, WI, USA). Viral RNA was then quantified using a highly sensitive qRT-PCR assay based on a previously published protocol [15,16].

2.11. Statistical analysis

Data analysis was performed using GraphPad Prism version 7.0 (GraphPad Inc). Data are expressed as the mean ± standard deviation (SD).

3. Results and Discussion

Based on the promising *in vivo* responses in NHPs generated by the twelve PCS-based vaccine (composed by a combination of viral vectors and NPs delivering the twelve PCSs) [12,13], and considering the results described in Chapter 1.A [14], two types of NPs were selected for their combination in a preliminary efficacy study in NHPs. Namely, chitosan/dextran sulfate (CS/DS) NPs and chitosan/hyaluronic acid/poly(I:C) (CS/HA/pIC) NPs were the chosen prototypes.

More specifically, CS/DS NPs were selected due to their capacity to elicit cellular responses at short times after vaccination in mice [14]. Besides, this was the same composition as in the NPs employed in the previously reported twelve PCS-based vaccine [12,13]. Since these NPs had been administered intranasally targeting mucosal immunity, with important IgG levels detected at mucosal sites [13], the same route of administration was maintained in this new study.

In the case of the CS/HA/pIC NPs, the rationale behind their selection was based on their capacity to elicit a modest but sustained T cell activation in mice [14]. These NPs were administered intramuscularly in order to generate a broad systemic immune response.

With regard to the selection of the antigens, our goal was to evaluate the potential of a vaccine with a minimum amount of PCS antigens. Thus, rather than using the twelve peptides previously investigated, we selected the PCS5 peptide that was used for the initial evaluation in mice, as well as

the PCS2 and PCS12 peptides. The concept behind this selection was based on the fact that single mutations surrounding these particular sites were reported to significantly impair viral fitness, thus hampering the capacity of the virus to replicate (data not shown). With this idea in mind, the two selected NP prototypes were adapted to associate the three selected PCSs, separately. Finally, the two prototypes were administered, one intranasally and the other intramuscularly, to NHPs, with the final goal of evaluating their protection capacity against SIV infection.

3.1. Preparation of CS/DS + PCS NPs

The association of the three selected peptides to CS/DS NPs by ionic interactions was performed as described in Chapter 1.A for PCS5 peptide [14]. The resulting NPs had similar physicochemical properties, independently of the loaded PCS (**Table 1**). The three NP suspensions were mixed to obtain a cocktail containing the three peptide antigens. As observed in **Table 1**, the physicochemical properties of the cocktail suspension were similar to those of the individual prototypes, with a particle size around 120 nm, a low polydispersity and a high negative zeta-potential.

Table 1. Physicochemical properties of the CS/DS nanoparticles formulated with each PCS, before and after the physical mixture of the three nanosystems (cocktail).

CS/DS + PCS	Particle size (nm)	PDI	ζ-potential (mv)
PCS2	109 ± 6	0.14	-50 ± 4
PCS5	124 ± 8	0.15	-53 ± 3
PCS12	102 ± 5	0.15	-52 ± 4
Cocktail	117 ± 6	0.16	-50 ± 4

Values represent mean ± SD (n ≥ 3). CS, chitosan; DS, dextran sulfate; PCS, protease cleavage site; PDI, polydispersity index.

3.2. Preparation of CS/HA–PCS/pIC NPs

Firstly, HA–PCS conjugates were synthesized, then, this modified HA were used to prepare the NPs.

3.2.1. Synthesis of the HA–PCS conjugates

HA conjugates were prepared following a two-step maleimide reaction. Each peptide was separately linked to HA, and the resulting conjugates were characterized by ^{1}H NMR (**Fig. 2**). For PCS2, the NMR spectra of the conjugate exhibited the characteristic peaks of the isopropyl groups of the three leucine amino acids of the peptide, together with the acetyl groups of HA (**Fig. 2B**). The calculated substitution degree was 205 ± 21 μg PCS2/mg of HA, with a 90% yield. In the case of PCS12, both the isopropyl peaks of the leucine, and of the aromatic amino acids (tyrosine and tryptophan), could be

identified in the NMR spectrum of the HA–PCS12 (**Fig. 2C**). The substitution degree for PCS12 was of 119 ± 56 µg PCS12/mg of HA and the yield, 52%. As already described in Chapter 1.A, for PCS5 the substitution degree was of 159 ± 26 µg PCS5/mg of HA and a 70% yield (**Fig. 2B**) [14].

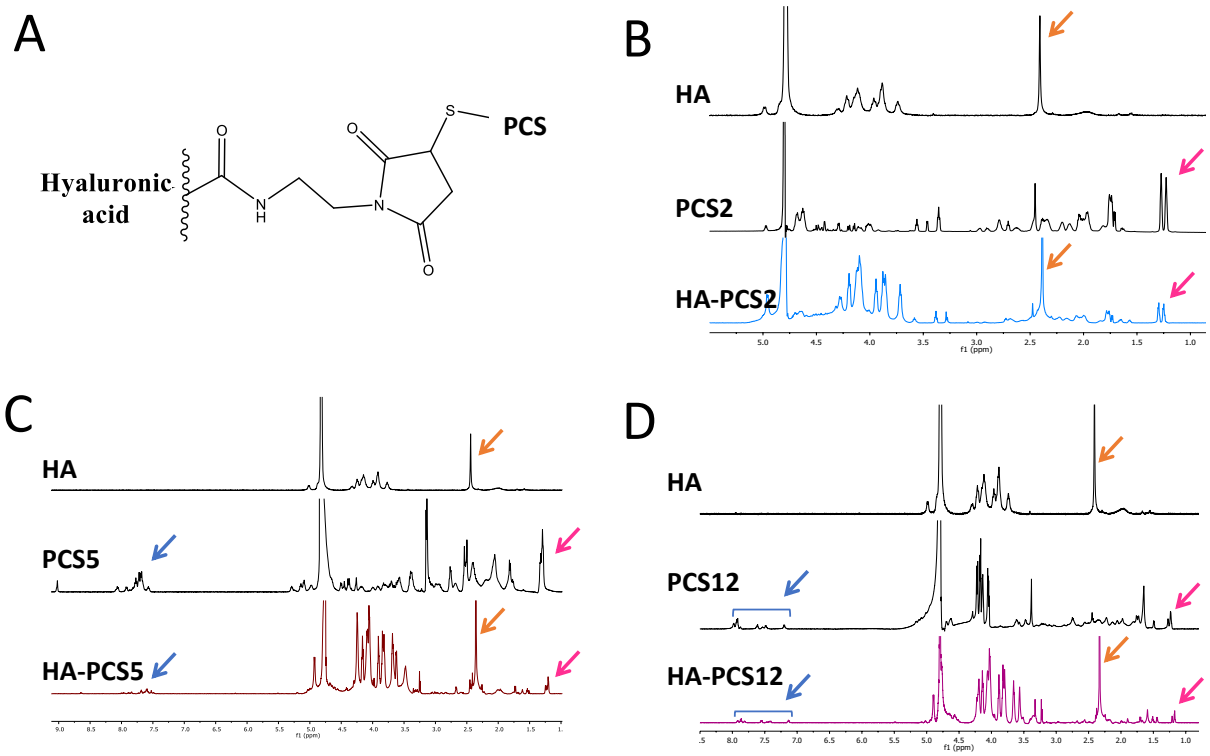

Figure 2. NMR characterization of the three HA-PCS conjugates. (A) Schematic representation of a HA–PCS conjugate. (B) ^{1}H-NMR of HA, PCS2 and HA–PCS2 conjugate. The PCS2 leucine peaks (pink arrows), and the acetyl groups of HA (orange arrows) are found in the conjugate. (C) ^{1}H-NMR of HA, PCS5 and HA–PCS5 conjugate. These results corroborated the presence of both the PCS5 leucine peaks (pink arrows) and aromatic signals (blue arrows); and the acetyl groups of HA (orange arrows) in the conjugate. (D) ^{1}H-NMR of HA, PCS12 and HA–PCS12 conjugate. The signal of both the leucine of PCS12 (pink arrows) and of the aromatic rings (blue arrows), can be detected in the NMR, together with the acetyl groups of HA (orange arrows). HA, hyaluronic acid; PCS, protease cleavage site.

3.2.2. Preparation of CS/HA–PCS/pIC NPs

Once the polymer–peptide conjugates were synthesized and characterized, NPs were prepared following the same procedure that for the HA–PCS5 conjugate in Chapter 1.A [14]. Depending on the substitution degree values, the amounts of unmodified and modified HA were adapted to have a final peptide concentration of 0.1 mg/mL, while maintaining the total amount of HA (1 mg/mL). As shown in **Table 2**, the physicochemical properties of the cocktail formulation were similar to those of the individual formulations of each PCS peptide, with a particle size around 170 nm, a very low PDI and a zeta-potential around +30 mV.

Table 2. Physicochemical properties of the CS/HA–PCS/pIC nanoparticles formulated with each PCS, before and after the physical mixture of the three nanosystems (cocktail).

CS/HA–PCS/pIC	Particle size (nm)	PDI	ζ-potential (mv)
PCS2	166 ± 13	0.07	+29 ± 2
PCS5	176 ± 11	0.08	+31 ± 1
PCS12	170 ± 12	0.08	+30 ± 2
Cocktail	175 ± 12	0.09	+31 ± 2

Values represent mean ± SD (n ≥ 3). CS, chitosan; HA, hyaluronic acid; PCS, protease cleavage site; PDI, polydispersity index; pIC, poly(I:C).

3.3. Development of two freeze-dried formulations containing three peptide antigens

The developed NPs were freeze-dried as a way to increase the long-term stability of the cocktail formulation. At the same time, this process allowed us to concentrate the formulation in order to reach the target dose of 50 µg of each PCS, per prototype and per animal. Considering this final dose and the different administration volumes required by the intranasal and intramuscular routes, the freeze-drying conditions for each prototype of NPs were adapted using trehalose as the cryoprotectant. The final colloidal properties of the NPs, before and after the freeze-drying process, are summarized in **Table 3**.

Table 3. Physicochemical properties of the developed nanoparticles containing the three PCSs, before and after the freeze-drying process.

Nanoparticles	FD	Trehalose concentration	Particle size (nm)	PDI	ζ-potential (mV)	Route of administration
CS/DS	Before	n/a	117 ± 6	0.16	-50 ± 4	Intranasal
	After	20%	177 ± 11	0.18	-56 ± 7	
CS/HA/pIC	Before	n/a	175 ± 12	0.09	+31 ± 2	Intramuscular
	After	15%	292 ± 25	0.10	+32 ± 2	

Values represent mean ± SD (n ≥ 3). CS, chitosan; DS, dextran sulfate; FD, freeze-drying; HA, hyaluronic acid; n/a, not applicable; PCS, protease cleavage site; PDI, polydispersity index; pIC, poly(I:C).

3.4. Evaluation of the nanovaccine capacity to prevent SIV infection

Finally, the efficacy of these formulations in terms of SIV prevention was assessed in NHPs. Additionally, the efficacy of the NPs described in this chapter was compared to that of the reference formulation, composed of CS/DS NPs associating the twelve PCSs, combined with the rVSV vectors coding for these sequences (rVSV + Nano, 12 PCSs).

The combination of the CS/DS and CS/HA/pIC NPs described in this chapter (Nano, 3 PCSs) were administered to eight female macaques. Each animal received both, at the same time, an i.n. instillation of the CS/DS + PCS cocktail of NPs and an i.m. injection of the CS/HA–PCS/pIC cocktail of NPs, every four weeks, for a total of four doses each (**Fig. 1A**). In parallel, the reference formulation containing the twelve PCSs delivered in viral vectors and in NPs (rVSV + Nano, 12 PCSs) was also administered to eight female macaques. In this group, each animal was first primed with the rVSVs i.m. and, then, boosted with a combination of the NPs i.n. and the rVSVs i.m. (in the 1st and 3rd boosts), only the NPs i.n. (in the 2nd boost) or the rVSVs i.m. alone (in the 4th boost) (**Fig. 1B**) [15]. In both cases, animals were challenged every two weeks, and viral loads monitored.

The results in **Figure 3** indicate that the combination of NPs containing three PCSs was able to delay the infection after subsequent intravaginal SIV challenges, and to protect 50% of the animals upon seven of these challenges, compared to the control (25%). On the other hand, the combination of the twelve peptides in NPs and viral vectors (reference formulation) resulted in 75% protection after seven challenges [15].

It is important to highlight that the formulation developed in this study contains only three of the twelve peptides that have been described as critical to prevent the virus maturation [10,11]. Indeed, the formulation with the twelve peptides and a highly immunogenic carrier (rVSV + Nano, 12 PCSs) showed very promising results in terms of SIV prevention [15]. Therefore, it is possible that a better selection of peptides or an increase of this number might improve the potency of the NP-based vaccine. Besides, the incorporation of additional adjuvants might help to increase the levels of protection. Altogether, we believe that there is still space to optimize the NP-based vaccine in order to generate a more potent SIV vaccine candidate based on NPs with a low number of antigens.

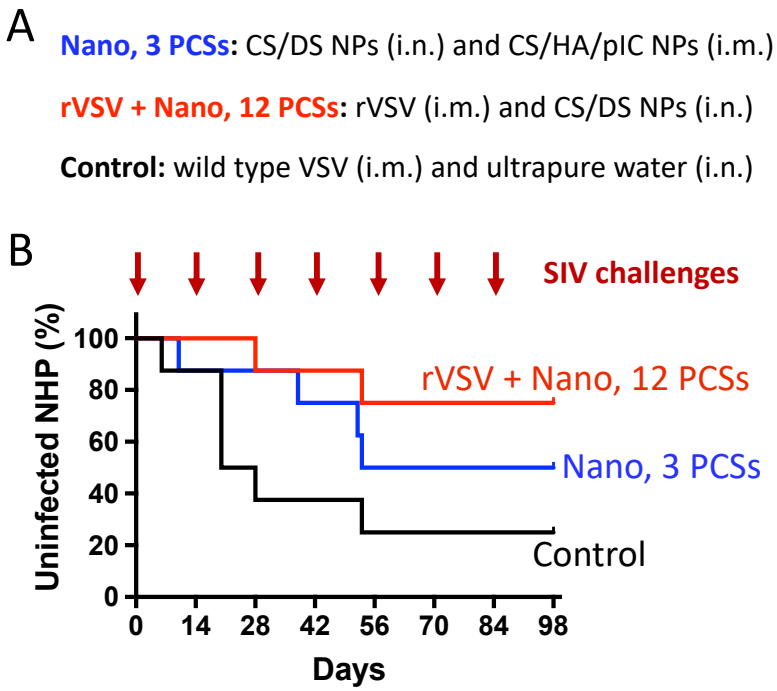

Figure 3. Preliminary *in vivo* study in NHPs. (A) Summary of the formulations administered in each vaccination group. (B) Non-human primates were vaccinated either with the CS/DS and CS/HA/pIC nanoparticles containing the three PCSs (Nano, 3 PCSs; in blue); the reference formulation based the twelve peptide antigens delivered in viral vectors and in CS/DS nanoparticles (rVSV + Nano, 12 PCSs; in red) [15]; or with the control VSVs without the peptides and ultrapure water (Control; in black). Percentage of uninfected animals after every intravaginal challenge with SIV, up to seven challenges. CS, chitosan; DS, dextran sulfate; HA, hyaluronic acid; i.m., intramuscular; i.n.; intranasal; NPs, nanoparticles; PCS, protease cleavage site; rVSV, recombinant vesicular stomatitis virus.

4. Conclusions

Overall, we have successfully loaded three PCSs peptides into two selected polysaccharide-based NPs protypes. This combination of two formulations, one of them administered intramuscularly and the other one intranasally, led to a 50% protection against seven SIV challenges, compared to the 25% of non-infected control animals. Although some adjustments in both, the NP carrier design and the peptide selection, could be necessary, the reported outcome of this study in primates supports that a vaccine based on PCSs peptides loaded into NPs, could be an interesting and alternative strategy to develop an effective HIV vaccine.

References

[1] B.F. Haynes, New approaches to HIV vaccine development, Curr. Opin. Immunol. 35 (2015) 39–47. doi:10.1016/j.coi.2015.05.007.

[2] HIV vaccines go to trial, Nat. Med. 25 (2019) 703. doi:10.1038/s41591-019-0460-0.

[3] S.J. Kent, M.P. Davenport, Moving the HIV vaccine field forward: concepts of protective immunity, Lancet HIV. 6 (2019) e406–e410. doi:10.1016/S2352-3018(19)30134-1.

[4] D.R. Burton, L. Hangartner, Broadly neutralizing antibodies to HIV and their role in vaccine design, Annu. Rev. Immunol. 34 (2016) 635–659. doi:10.1146/annurev-immunol-041015-055515.

[5] D.J. Irvine, M.C. Hanson, K. Rakhra, T. Tokatlian, Synthetic nanoparticles for vaccines and immunotherapy, Chem. Rev. 115 (2015) 11109–11146. doi:10.1021/acs.chemrev.5b00109.

[6] T.G. Dacoba, A. Olivera, D. Torres, J. Crecente-Campo, M.J. Alonso, Modulating the immune system through nanotechnology, Semin. Immunol. 34 (2017) 78–102. doi:10.1016/j.smim.2017.09.007.

[7] K.T. Gause, A.K. Wheatley, J. Cui, Y. Yan, S.J. Kent, F. Caruso, Immunological principles guiding the rational design of particles for vaccine delivery, ACS Nano. 11 (2017) 54–68. doi:10.1021/acsnano.6b07343.

[8] D.T. O'Hagan, G.S. Ott, E. De Gregorio, A. Seubert, The mechanism of action of MF59 – An innately attractive adjuvant formulation, Vaccine. 30 (2012) 4341–4348. doi:10.1016/j.vaccine.2011.09.061.

[9] G. Ledet, L.A. Bostanian, T.K. Mandal, Nanoemulsions as a vaccine adjuvant, in: A. Tiwari, A. Tiwari (Eds.), Bioeng. Nanomater., CRC press: Boca Raton, 2013: pp. 125–148.

[10] M. Luo, R. Capina, C. Daniuk, J. Tuff, H. Peters, M. Kimani, C. Wachihi, J. Kimani, T.B. Ball, F.A. Plummer, Immunogenicity of sequences around HIV-1 protease cleavage sites: potential targets and population coverage analysis for a HIV vaccine targeting protease cleavage sites, Vaccine. 31 (2013) 3000–3008. doi:10.1016/j.vaccine.2013.04.057.

[11] H. Li, R.W. Omange, F.A. Plummer, M. Luo, A novel HIV vaccine targeting the protease cleavage sites, AIDS Res. Ther. 14 (2017) 51. doi:10.1186/s12981-017-0174-7.

[12] H. Li, M. Nykoluk, L. Li, L.R. Liu, R.W. Omange, G. Soule, L.T. Schroeder, N. Toledo, M.A. Kashem, J.F. Correia-Pinto, B. Liang, N. Schultz-Darken, M.J. Alonso, J.B. Whitney, F.A. Plummer, M. Luo, Natural and cross-inducible anti-SIV antibodies in Mauritian cynomolgus macaques, PLoS One. 12 (2017) 1–20. doi:10.1371/journal.pone.0186079.

[13] H. Li, Y. Hai, S.-Y. Lim, N. Toledo, J. Crecente-Campo, D. Schalk, L. Li, R.W. Omange, T.G. Dacoba, L.R.L.R. Liu, M.A. Kashem, Y. Wan, B. Liang, Q. Li, E. Rakasz, N. Schultz-Darken, M.J. Alonso, F.A. Plummer, J.B. Whitney, M. Luo, Mucosal antibody responses to vaccines targeting SIV protease cleavage sites or full-length Gag and Env proteins in Mauritian cynomolgus macaques, PLoS One. 13 (2018) e0202997. doi:10.1371/journal.pone.0202997.

[14] T.G. Dacoba, R.W. Omange, H. Li, J. Crecente-Campo, M. Luo, M.J. Alonso, Polysaccharide nanoparticles can efficiently modulate the immune response against an HIV peptide antigen, ACS Nano. 13 (2019) 4947–4959. doi:10.1021/acsnano.8b07662.

[15] H. Li, R.W. Omange, B. Liang, N. Toledo, Y. Hai, L.R. Liu, D. Schalk, J. Crecente-Campo, T.G. Dacoba, A.B. Lambe, S.-Y. Lim, L. Li, M.A. Kashem, Y. Wan, J.F. Correia-Pinto, X.Q. Liu, R.F. Balshaw, Q. Li, E. Rakasz, N. Schultz-Darken, M.J. Alonso, J.B. Whitney, F.A. Plummer, M. Luo, A novel vaccine targeting the viral protease cleavage sites protects Mauritian cynomolgus macaques against vaginal SIVmac251 infection, BioRxiv. (2019). doi:10.1101/842955.

[16] L.E. Valentine, J.T. Loffredo, A.T. Bean, E.J. Leon, C.E. MacNair, D.R. Beal, S.M. Piaskowski, Y.C. Klimentidis, S.M. Lank, R.W. Wiseman, J.T. Weinfurter, G.E. May, E.G. Rakasz, N.A. Wilson, T.C. Friedrich, D.H. O'Connor, D.B. Allison, D.I. Watkins, Infection with "escaped" virus variants impairs control of simian immunodeficiency virus SIVmac239 replication in Mamu-B*08-positive macaques, J. Virol. 83 (2009) 11514–11527. doi:10.1128/jvi.01298-09.

Chapter 2

Technological challenges in the preclinical development of an HIV nanovaccine candidate

Chapter 2

Technological challenges in the preclinical development of an HIV nanovaccine candidate

This work has been done in collaboration with CIDETEC (Basque Research and Technology Alliance, Spain), with Ultra Trace Analyses Aquitaine (Technopôle Hélioparc Pau-Pyrénées, France); and with the University of Manitoba (Canada).

Abstract

Despite active research in the field of nanomedicine, only a few nano-based drug delivery systems have reached the market. The "death valley" between research and commercialization has been partially attributed to the limited characterization and reproducibility of the nanoformulations. Our group has previously reported the potential of a peptide-based nanovaccine candidate for the prevention of SIV infection in macaques. This vaccine candidate is composed of chitosan/dextran sulfate nanoparticles containing twelve SIV peptide antigens. The aim of this work was to rigorously characterize one of these nanoformulations containing a specific peptide, following a quality-by-design approach. The evaluation of the different quality attributes was performed by several complementary techniques, such as dynamic light scattering, nanoparticle tracking analysis and electron microscopy for particle size characterization. The inter-batch reproducibility was validated by three independent laboratories. Finally, the long-term stability and scalability of the manufacturing technique were assessed. Overall, these data, together with the *in vivo* efficacy results obtained in macaques, underline the promise this new vaccine holds with regard to its translation to clinical trials.

Graphical abstract

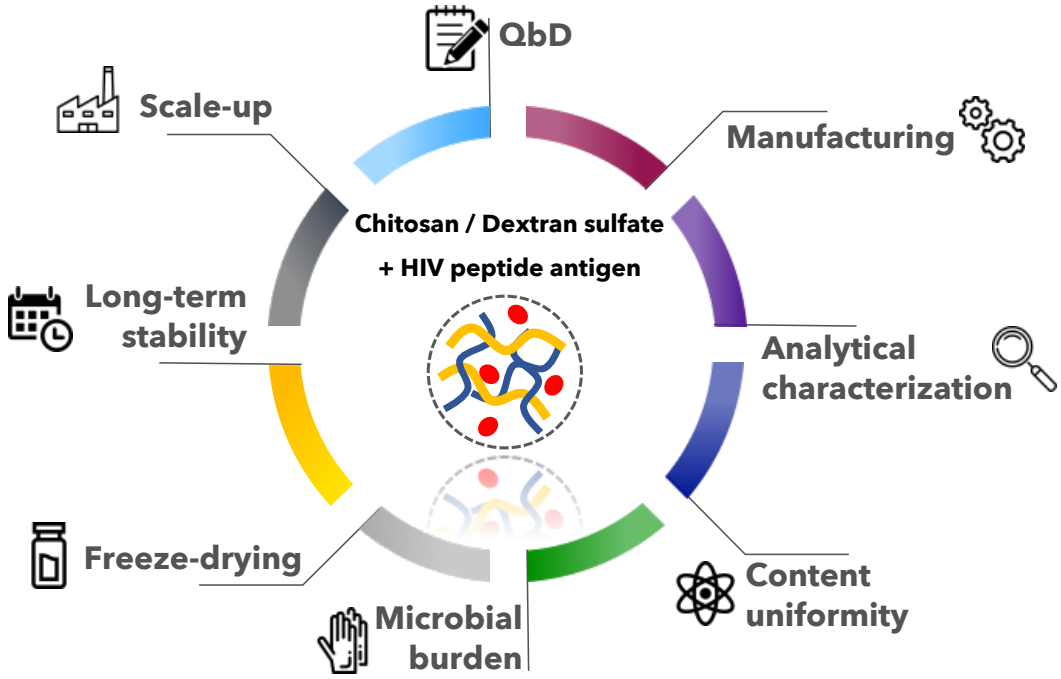

1. Introduction

In the last decades, nanotechnology has shown a great potential for the delivery of complex biomolecules [1–8] and particularly antigens [9–12]. Advances in this field have led to the clinical approval of a few tens of nanoformulations [13–15], and to the evaluation of many more in clinical trials [11,14]. Regardless of the type of formulation, nanomedicines are usually complex systems, where small changes in their production or composition can result in a decreased efficacy and, often, undesired side effects [16]. This complexity is also one of the main reasons that has hindered the commercialization of nanotechnology-based drugs [17,18]. For example, Couvreur *et al.* have recently reported the challenges faced during the scale-up of squalene-adenosine NPs and the important differences in the physicochemical properties of lab- and industrial-scale batches [19]. Therefore, a detailed analytical characterization of the nanomedicines is a critical step to identify their most important manufacturing features, and to ensure their reproducibility, therapeutic efficacy and safety [16,20].

Pharmaceutical quality-by-design (QbD) is a systematic approach that begins by predefining the characteristics of the targeted formulation. It is based on implementing statistical, analytical and risk-management methods in order to understand the product and the processes involved in its fabrication [21]. The application of QbD is essential to guarantee the safety and efficacy of a formulation [21–24]. In addition, the knowledge generated through these approaches represents critical information to be considered by the regulatory authorities. The increasing application of QbD approaches for the development of nanoformulations will certainly contribute to generate more robust formulations [25–30]. Additionally, as indicated by the MIRIBEL recommendations [31], the report of a minimum information about nano-delivery systems in terms of material and biological characterization, together with the experimental protocol details, will be another key aspect in the generation of more robust nanomedicines.

Despite the important advances achieved in vaccination through the use of nanotechnology, still many infectious diseases (*i.e.,* HIV, malaria or tuberculosis) remain elusive to vaccination [11]. Our group has dedicated significant efforts to the development of effective nanovaccines for different infectious diseases [32–35]. All this knowledge brought us to develop, in collaboration with investigators of the University of Manitoba, a potential HIV vaccine candidate based on polysaccharide nanoparticles (NPs) [36–38]. The vaccine is composed of twelve different small peptide antigens that overlap the protease cleavage sites (PCS) of the virus, that are associated to chitosan/dextran sulfate (CS/DS) NPs [36,38]. The promising results reported in macaques encouraged us to optimize and adapt the nanoformulation for its production in a pilot plant for preclinical and, potentially, future clinical

trials [36]. Considering that the formulation process for each of the peptides is the same, the technology transfer process was validated for the NPs containing only one peptide antigen (PCS5). For this purpose, and within the frame of the European Horizon 2020 project NANOPILOT, several research groups were involved in the development of the methods, techniques and a pilot plant to produce the nanovaccine. This work compiles part of the results generated within this consortium. Thus, in the following sections, we report the adaptation of the manufacturing procedure of an HIV nanovaccine candidate for its production in a pilot plant. The use of the QbD methodology involved the identification of the target product profile of the selected prototype, its critical quality attributes, and a risk analysis based on an Ishikawa diagram. Then, the influence of the manufacturing parameters on the final properties of the nanoformulation was assessed. A thorough characterization using orthogonal techniques was carried out in order to define the attributes of the nanoformulation. Finally, different scaling-up methodologies and an interlaboratory manufacturing transfer were conducted to study the translational potential of these polymeric NPs to an industrial environment.

2. Materials and Methods

2.1. Materials

Chitosan (CS) (hydrochloride salt, molecular weight (MW) 42.7 KDa and 88% deacetylation degree) was obtained from HMC$^+$ (Halle, Germany). Dextran sulfate (DS), (sodium salt, MW 8 KDa) was purchased from Dextran Products Ltd (ON, Canada). High purity α,α–trehalose dihydrate was purchased from Pfanstiehl (IL, USA). SIV PCS5 peptide (sequence GPWGKKPRNFPMAQVHQGLM, MW 2280 Da and >95% purity) was obtained from GenScript (NJ, USA).

2.2. Quality-by-design (QbD)

The quality target product profile (QTTP) and critical quality attributes (CQAs) of the nanoformulation were established based on previous knowledge, and recommendations from the International Conference on Harmonisation of Technical Requirements for Registration of Pharmaceuticals for Human Use (ICH), European Medicines Agency (EMA) and US Food and Drug Administration (FDA) [39,40]; and are summarized in **Table 1** and **Table 2**. For the risk analysis, experts in different fields agreed on the design of an Ishikawa diagram and identified the most critical parameters that could have an effect on the nanoformulation CQAs (**Fig. 1**) [40].

2.3. Nanoparticle preparation

CS/DS NPs were prepared as previously described [36,37]. Briefly, 0.770 mL of a CS aqueous solution (0.67 mg/mL) were added to a test tube under mild magnetic stirring. A volume of 0.055 mL of PCS5 in aqueous solution (4 mg/mL) was then added with a pipette. After 5 min of stirring, 0.825 mL of a DS aqueous solution (1.875 mg/mL) were added. The solution was stirred for 5 additional min, and the formulation was left standing for 10 min prior to characterization. For the preparation of blank NPs, the solution of PCS5 was replaced by ultrapure water.

2.4. Nanoparticle freeze-drying

A volume of 180 µL of trehalose 45% (w/v) was added to 900 µL of NPs, mixed by horizontal shaking for at least 20 min, frozen at -80 °C for 2 h, and then freeze-dried (Genesis™ 25 EL, S.P Industries, PA, USA). Samples were first left in the freeze-drier at -40 °C for 4 h to guarantee that they were completely frozen, with a vacuum of 200 mTorr. Then, the first drying phase was done at a temperature ranging from -40 °C to +20 °C, applying a progressive vacuum to 20 mTorr for a period of 43 h. Finally, the secondary drying phase was done for 3 h at +22 °C and 20 mTorr. At pre-determined times, the final cake was reconstituted in ultrapure water and NPs were conveniently characterized.

2.5. Nanoparticle characterization

2.5.1. Dynamic Light Scattering (DLS)

The mean particle size (Z-average) and polydispersity index (PDI) of the non-diluted samples were characterized by DLS, following ISO standards [41]. The zeta potential values were determined by Laser Doppler Anemometry (LDA), measuring the mean electrophoretic mobility after a 10-times dilution of the NPs in ultrapure water. Derived count rate represents the scattering intensity measured in the absence of a laser light attenuation filter, and it was calculated as the ratio between the measured count rate and the attenuation factor. At USC and CIDETEC, these properties were measured using a Zetasizer® NanoZS, using the software Zetasizer v7.13 (Malvern Panalytical Ltd., Malvern, UK), at 25 °C and a detection angle of 173. At UT2A, DLS measurements were done in a VASCO-2 particle size analyzer (Cordouan Technology, France) in combination with the software nanoQ v 6.2.2, at 25 °C and a detection angle of 135.

2.5.2. Electron microscopy

Field Emission Scanning Electron Microscopy (FESEM) (Zeiss Gemini Ultra Plus, Oberkochen, Germany) was used for morphology evaluation. Reconstituted freeze-dried NPs were diluted 1:100 in

water, and then diluted 1:1 with phosphotungstic acid (2% in water). A sample volume of 1 µL was placed on a copper grid with carbon films and, once dried, washed with 1 mL of ultrapure water. When dried, samples were analyzed under the microscope using a STEM detector. ImageJ software was used for NP counting and analysis (n ≈ 100), by employing the *Analyze/Analyze Particles* command, in accordance to an already described method [42].

2.5.3. Nanoparticle tracking analysis (NTA)

Reconstituted freeze-dried NPs were diluted 1:1000 in ultrapure water prior to analysis in a Nanosight NS300 (Malvern Panalytical Ltd., Malvern, UK) using the Nanosight NTA software v3.3. The camera gain was set at 11 or 13. Each sample was measured 5 times for 60 s each.

2.5.4. pH, osmolality, % of transmittance and moisture

A freshly calibrated Sartorius Docu-pH Benchtop Meters (Thermo Fisher Scientific, MA, USA) was employed for the determination of the pH of the formulation at USC. A GLP2 pH-meter (Crison Scharlab, Barcelona, Spain) was used in CIDETEC for the determination of the pH of the final product. Osmolality was measured in a Gonotec Osmomat 030 Cryoscopic Osmometer (Gonotec GmbH, Berlin, Germany) at USC, or in a vapor pressure osmometer model 5600 Vapor (Wescor Vapro, Utah, USA) at CIDETEC. The values of percentage of transmittance were obtained either from a DU®730 UV/Vis Spectrophotometer (Beckman-Coulter, CS, USA) at USC, or from a UV-Visible spectrophotometer Shimazdu UV-2401PC (Shimazdu, Kyoto, Japan) at CIDETEC, both at a wavelength of 236 nm. The water content was determined by Karl-Fischer titration (Metrohm 899, Herisau, Switzerland).

2.6. Filtration

Millex®-GV filters (Millipore Corporation, MA, USA), of 13- or 33-mm diameter and 0.22 µm pore size of polyvinylidene fluoride (PVDF), polyethylene sulfone (PES) or polytetrafluoroethylene (PTFE) were used to filter NPs or polymer solutions. A volume of 0.5 mL of nanoformulation or 20 mL of polymer solution was injected through the filters, discarding the first drops, following the supplier recommendation.

2.7. Peptide PCS5 quantification

2.7.1. Particle disassembling

For the particle disruption process, NPs were diluted in a 1:1 (v/v) ratio with the solution of KCl, and the derived count rate determined by DLS. As a control, NPs were diluted in the same proportion with water.

2.7.2. UPLC detection

At USC, samples were analyzed by Ultra Performance Liquid Chromatography (UPLC) on an Acquity H-UPLC Class system with a UV detector at 280 nm (Waters Corporation, MA, USA) equipped with an Aeris 3.6 µm Widepore XB-C18 LC 100 x 2.1 mm Column (Phenomenex, CA, USA), as previously described [37]. Briefly, mobile phases A and B consisted of 0.1 % trifluoroacetic acid (v/v) in either ultrapure water or acetonitrile HPLC grade, respectively. Column temperature was set at 30 ℃, and the run from 10% to 100% of phase B in 5 min, and 3 min to 10%. A calibration curve generated with known concentrations of the peptide, both in water and in the disassembled NPs (6.5 – 100 mg/L, R^2 = 0.99) was used to quantify the amount of PCS5 in each sample.

At CIDETEC, the quantification of the peptide was carried out using a High Performance Liquid Chromatography (HPLC), in an Agilent model 1100 series LC with UV detector, the ChemStation software (Agilent Technologies, CA, USA) and with a X Bridge BEH C18 2.5 µm 4.6 x 100 mm column (Waters Corporation, MA, USA). Mobile phases A and B consisted of 0.1% trifluoroacetic acid (v/v) in either ultrapure water or acetonitrile HPLC grade, respectively. Column temperature was set at 30 °C, and the run from 10% to 100% of phase B in 12 min at flow rate of 0.65 mL/min. A calibration curve generated with known concentrations of the peptide, in water and in the disassembled NPs (6.5–100 mg/L, R^2 = 0.99) was used to quantify the amount of PCS5 in each sample.

At UT2A, samples were analyzed with an Agilent 1260 series autosampler and a HPLC pump (Agilent Technologies, CA, USA) equipped with a Superdex peptide 10/300GL column (GE Healthcare, IL, USA) and an UV-Visible detector operating at 214 nm (VWD 1200 series, Agilent Technologies, CA, USA), as already reported [43]. In this case, peptide elution was done with 50 mM phosphate buffer and 150 mM sodium chloride, with flow rate of 0.7 mL/min for 35 min. Calibration was obtained with peptide concentrations ranging from 10 to 100 mg/L (R^2 >0.995), prepared in NaOH 0.1 M.

2.8. Scale-up

2.8.1. Microfluidics (continuous mode)

A NanoAssemblr microfluidics device (Precision nanosystems, Vancouver, Canada) was used for the preparation of the NPs. The cartridges used were 200 µm wide and 79 µm high, while the mixing area had a herringbone structure that was 31 µm high and 50 µm thick. To assess the influence of the total flow rate, flows ranging from 0.5 mL/min to 14 mL/min were used, with initial polymer concentrations of 0.63 mg/mL of CS and 1.875 mg/mL of DS, and a 1:1 flow ratio. For the loaded NPs, the CS solution had a PCS5 concentration of 0.27 mg/mL. NPs were characterized by DLS (section 2.5.1).

2.8.2. Batch-mode (discontinuous mode)

For the preparation of 200 mL batches, a propeller stirrer IKA RW 20 (Staufen, Germany; 4-blade, stir diameter 50 mm, shaft diameter 8 mm, and shaft length 350 mm) was used to mix the different solutions, and 250-mL beakers were employed for mixing the solutions. To 93.3 mL of an aqueous solution of CS (0.67 mg/mL), 6.7 mL of either ultrapure water or an aqueous solution of PCS5 (4 mg/mL) were added under stirring at 700 rpm, and left to mix for 5 min. Then, 100 mL of an aqueous solution of DS (1.875 mg/mL) were poured onto the CS/PCS5 solution, kept under stirring for 5 min and standing for 10 min. NPs were freeze-dried (section 2.4) and characterized by DLS (section 2.5.1)

2.9. Statistical analysis

Data analysis was performed with GraphPad Prism version 7.0 (GraphPad Inc). Statistical comparison was done using ANOVA, followed by a Dunnett's multiple comparison test. Data are expressed as the mean ± standard deviation (SD). *p* values of 0.05 or less were considered statistically significant.

3. Results and Discussion

The complexity of some nanoformulations and the lack of well-defined standard analytical methodologies for their complete characterization are some of the hurdles that have hampered the arrival of nanomedicines to the market [17]. In fact, these difficulties for the translation of NPs preparation technique from a lab to an industrial scale were recently described in a report by Couvreur *el al*. [19]. Therefore, it has become clear that the assessment of reproducibility and the selection of adequate characterization methods are critical steps to be considered in the scientific literature. Here, our aim was to transfer the development of a potential nanovaccine candidate from the bench to an

industrial environment, highlighting the critical requirements that all nanovaccine candidates should fulfill in order to progress towards commercialization.

3.1. Implementation of a quality-by-design approach

The aim of a QbD approach is to understand how the formulation and processing parameters affect the properties of the formulation. This knowledge is critical in order to generate more robust and reproducible nanomedicines [44]. Here, the quality target product profile (QTPP) of the nanoformulation was first established (**Table 1**), following ICH recommendations [40]. The QTPP was determined by the indication and the modality of administration. In this sense, based on the positive data obtained in macaques [36,38], the product was defined for vaccination against HIV and for intranasal administration (**Table 1**). In order to maintain the long-term stability, the product was formulated as a freeze-dried powder that could be rapidly dispersed in water at the moment of administration (**Table 1**).

Table 1. **Quality Target Product Profile (QTPP) of the HIV vaccine candidate.**

Parameter	Target	Justification
Indication	HIV vaccine	PCS5 has been reported to be one potential antigen in HIV [45]
Route of administration	Nasal	Good preliminary results through this route, improves patient compliance [36]
Dosage form	Freeze-dried powder	To increase long-term stability
API content	100 µg/mL	Required antigen dose for macaque studies
Packaging	Type I glass vials	Recommended by USP and Eur. Ph. for injectable formulations and able to resist thermal shocks (for freeze-drying)
Stability	At least 1 year at room temperature	To guarantee an acceptable stability
Dispersibility	In 10 s, by manual shaking	To facilitate self-preparation and administration – no need of training or specialized equipment
Moisture	< 3%	To avoid API degradation or bacterial growth

As a second step, the critical quality attributes (CQAs) were defined (**Table 2**). CQAs are the main physical, chemical and biological attributes, which are critical to guarantee the safety and efficacy of the nanoformulation (**Table 2**) [39]. These details were gathered from the knowledge our research group has from working on the development of this type of nanocarriers, from the specific recommendations from the FDA and the EMA, and also from the different Pharmacopeias. More precisely, both the composition of the CS/DS NPs and the antigen dose selected were already tested

in vivo, with promising results [36,38]. Indeed, CS and DS are two polysaccharides used in nanovaccines due to their biocompatibility, biodegradability, and low toxicity, and that have also shown to improve the immune response against many antigens [35,46–49]. Furthermore, CS has an FDA GRAS status. The values of the physicochemical properties of the NPs were based on the literature, where nanometric sizes have been shown to perform better than micrometric sizes for the delivery of biomolecules through the nasal route [50]. Within the nanometric range, medium size NPs (200 nm) elicited stronger responses than very small sizes (30 nm) [51]. In terms of the surface charge, it is important to find a balance between mucoadhesion and mucodiffusion [10]. Finally, values as osmolality, pH, moisture and microbiology have been selected from the literature and FDA recommendations [52–54].

Table 2. Critical quality attributes (CQAs) of the formulation.

CQAs	Target	Justification
Components	Dextran sulfate, sodium salt Chitosan, hydrochloride salt Peptide antigen (PCS5) Highly purified water (type I)	Materials of the original formulation; water for parenteral administration [36,38]
Content uniformity	82.25 mg ± 10%	Amount needed for an adequate dosing of API
API content	100 µg/mL	Dose used in macaques [36,38]
Particle size and distribution	100–300 nm D(10) 80–150 nm D(50) 150–250 nm D(90) 250–450 nm Span 0.4–3	Adequate size for nasal administration and for the interaction with immune cells [10]
Polydispersity	< 0.3	Physicochemical properties that guarantee reproducibility
Surface charge	-30 to -65 mV	Adequate values to prevent aggregation in the mucus, and to ensure a longer stability [10]
Osmolality	100–200 mOsm/Kg	Adequate for nasal administration
pH	5–7.5	Adequate for nasal administration [52]
Dispersibility	10 s	For an easy extemporaneous formulation preparation
Microbiology	TAMC: 10^2 CFU/g TYMC: 10^1 CFU/g *E. coli*: Absence/mL	Adequate for nasal administration [53]
Water content	≤3%	To avoid API degradation and bacterial growth [54]

TAMC, Total Aerobic Microbial Count; TYMC, Total Combined Yeast and Mold Count.

Once the CQAs of the product were selected, the subsequent step was to perform a risk analysis of the impact of different parameters in the CQAs of the formulation [40]. In general, these parameters are related to the characteristics of the starting materials (*i.e*., polymers, drug, solvents or ratios), the different steps in the manufacturing process (*i.e*., phase incorporation rates, incubation times or agitation speeds) and also the environmental factors. In this case, an Ishikawa diagram was sketched to illustrate which specific parameters could alter the CQAs of our nanoformulation (**Fig. 1**). This risk management tool allowed to identify the potential variables that could have a harmful effect on the formulation attributes. Overall, the factors related to the preparation process had to be further monitored and controlled, and their influence was rigorously analyzed as described in the following section.

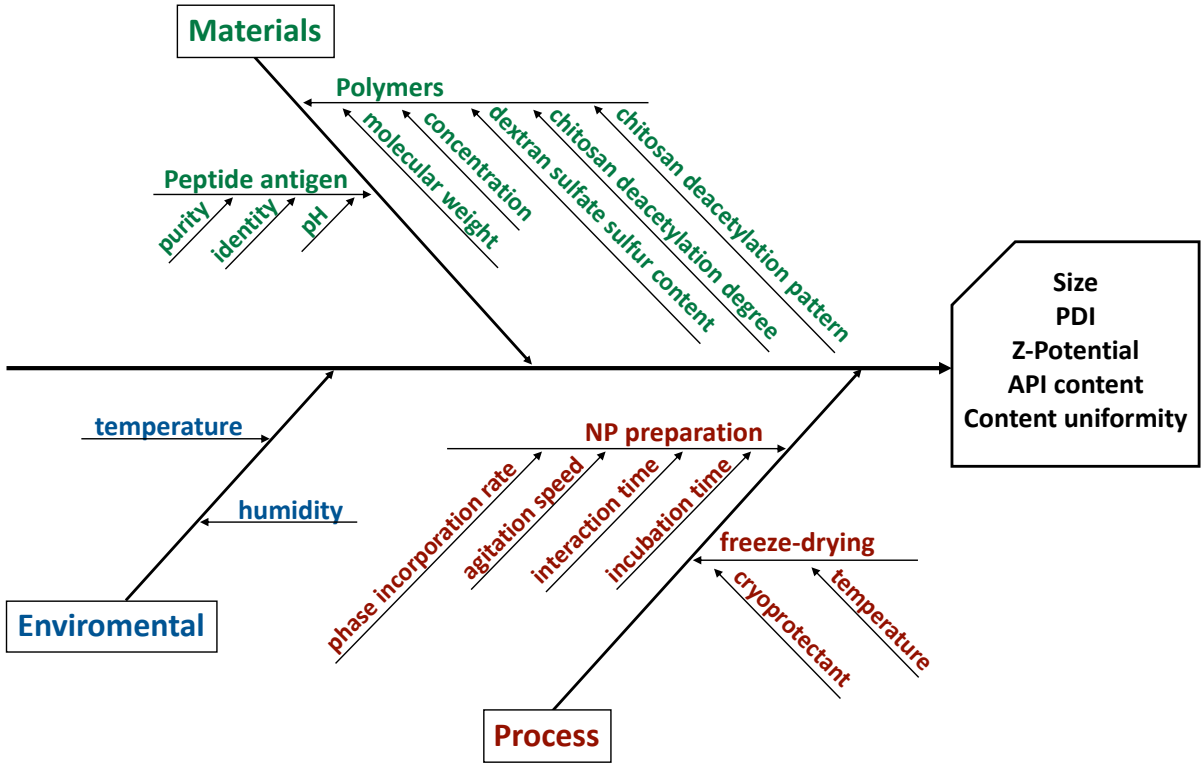

Figure 1. Ishikawa diagram of the composition and manufacturing factors that influence the quality attributes of the nanoformulation. Interaction time refers to the time that the components are interacting under stirring; while incubation time refers to the same condition, but in the absence of agitation (more details in Figure 2).

3.2. Nanoparticles fabrication. Determination of the critical process parameters

NPs were prepared by ionic complexation of the positively charged components (CS and the peptide PCS5) and the negatively charged DS, to a final concentration of 0.31 mg/ml of CS, 0.13 mg/mL of PCS5 and 0.94 mg/mL of DS. The fabrication process of the NPs is represented in **Figure 2A**. Accordingly, and following the Ishikawa diagram (**Fig. 1**), we studied how the different formulation steps influenced the final NP properties. Namely, we analyzed how the incorporation rate of DS solution over the CS/PCS5 solution affected the characteristics of the NPs. For this purpose, the DS solution was added dropwise (which would represent a low incorporation rate), with a pipette (medium incorporation rate, as in the original protocol) or using a syringe (to achieve high phase incorporation rates). As shown in **Figure 2B,C**, the dropwise incorporation (represented as "low") caused the aggregation of the NPs, with significant changes in particle size and PDI. However, the other two procedures led to particles of adequate physicochemical properties (particle size close to 150 nm, PDI lower than 0.2 and negative surface charges). Other parameters such as the agitation speed of the CS/PCS5 phase while adding DS, the time of interaction with DS, or the incubation time were also evaluated (**Fig. 2**). All procedures

yielded NPs with physicochemical properties similar to the ones produced following the original protocol.

Overall, the most critical parameter to monitor when translating this manufacturing process will be the incorporation rate of DS over the CS/PCS5 phase, because a low incorporation rate will cause the aggregation of the NPs.

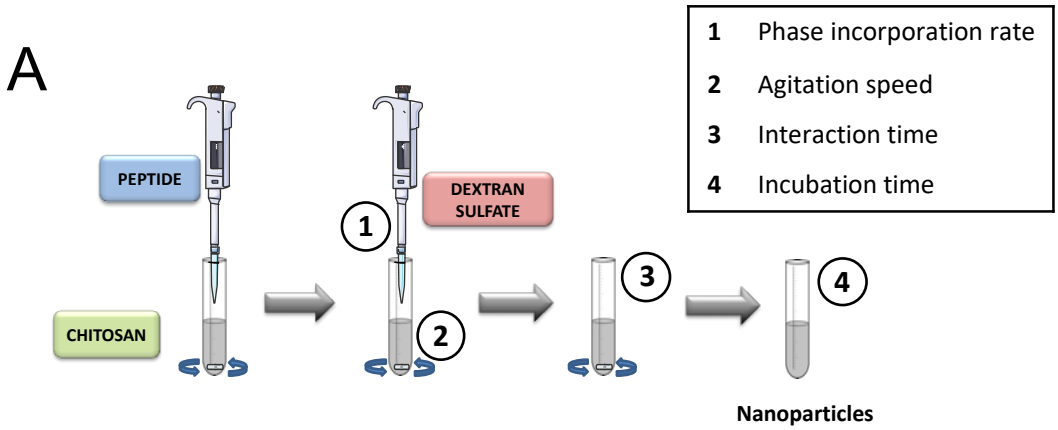
A
1 Phase incorporation rate
2 Agitation speed
3 Interaction time
4 Incubation time
PEPTIDE
DEXTRAN SULFATE
CHITOSAN
1
2
3
4
Nanoparticles

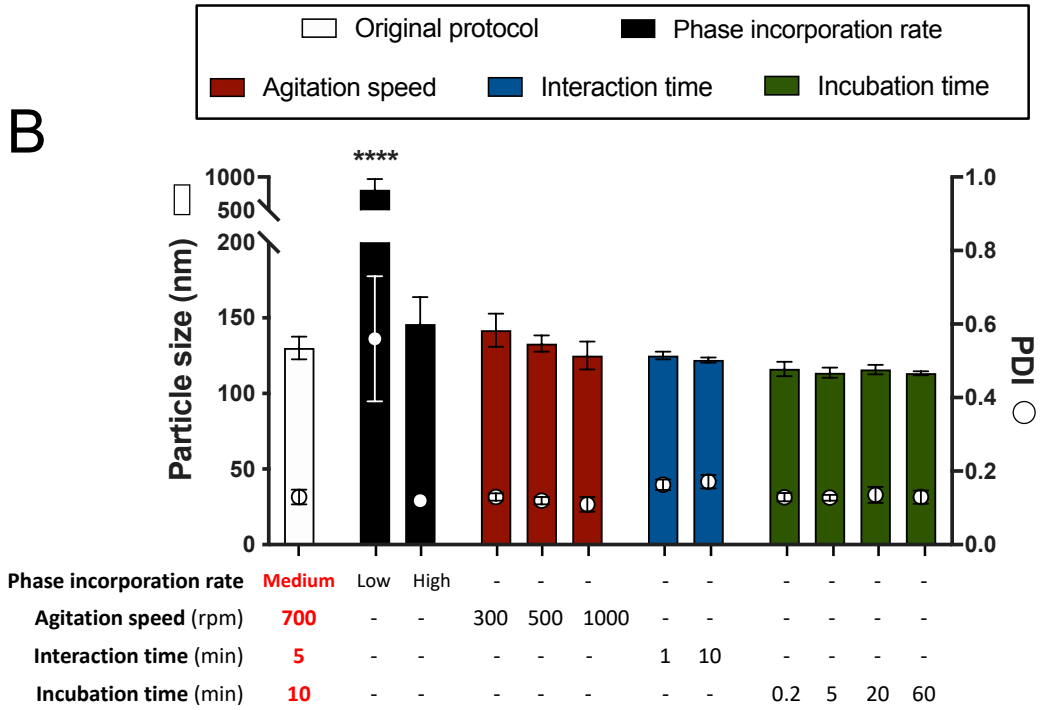
Original protocol
Phase incorporation rate
Agitation speed
Interaction time
Incubation time
B
****
Particle size (nm)
PDI
1000
500
200
150
100
50
0
1.0
0.8
0.6
0.4
0.2
0.0
Phase incorporation rate Medium Low High - - - - - - - - - -
Agitation speed (rpm) 700 - - 300 500 1000 - - - - - -
Interaction time (min) 5 - - - - - 1 10 - - - -
Incubation time (min) 10 - - - - - - - 0.2 5 20 60

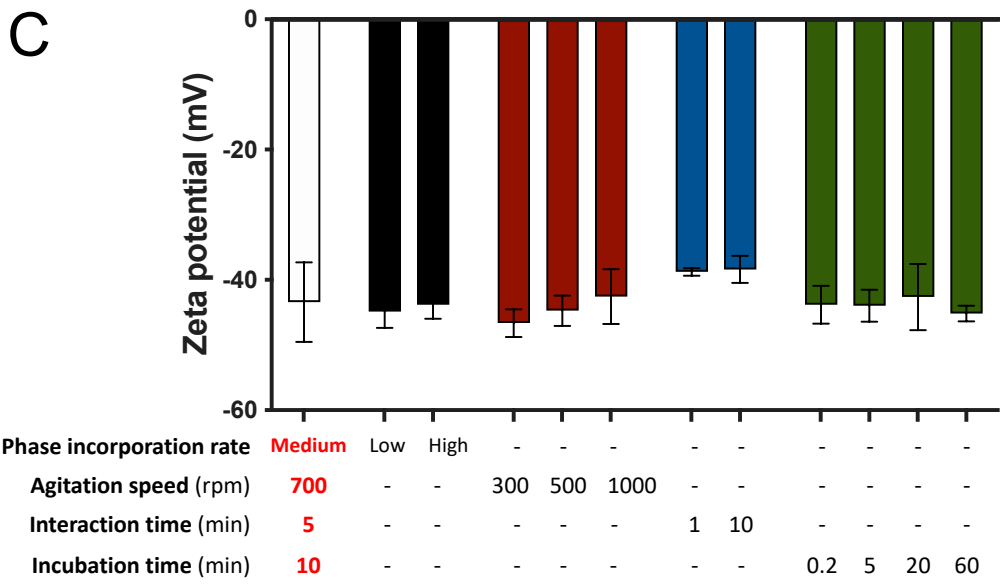
C
Zeta potential (mV)
0
-20
-40
-60
Phase incorporation rate Medium Low High - - - - - - - - - -
Agitation speed (rpm) 700 - - 300 500 1000 - - - - - -
Interaction time (min) 5 - - - - - 1 10 - - - -
Incubation time (min) 10 - - - - - - - 0.2 5 20 60

Figure 2. Nanoparticle manufacturing process and effect of the different steps on the physicochemical properties of the formulation. (A) Fabrication of the nanoparticles. The peptide antigen is added to the chitosan solution. Then, (1; phase incorporation rate) the solution of dextran sulfate is incorporated into the chitosan/peptide solution, (2; agitation speed) under magnetic stirring. (3; interaction time) Components are kept under agitation to allow their interaction, and then (4; incubation time) they are kept for 10 additional min in the absence of agitation. (B,C) Effect of the manufacturing parameters on the physicochemical properties of the nanoparticles. (B) Particle size and PDI, and (C) Zeta-potential values were monitored for the different processes: phase incorporation rate, agitation speed, interaction time and incubation time. Hyphens represent the values that are constant, as in the first column. Values represent mean ± SD ($n \geq 3$). A statistical comparison was done using a one-way ANOVA, followed by a Dunnett's multiple comparison test. Significant statistical differences are represented as **** ($p < 0.0001$) in comparison to the original protocol.

3.3. Characterization of particle size and size distribution

The selection of adequate analytical methods for the characterization of nanostructures is a key step in the development of a nanomedicine [16,55]. Dynamic light scattering (DLS) techniques are fast and easy methods to determine particle size and polydispersity [56]. For the particles here studied these values were about 120 nm for size, PDI of 0.2 and negative surface charge (**Fig. 3A,D**). Nevertheless, this method has several drawbacks, such as a bias towards detecting the larger particles of the sample, limited resolution between subpopulations with similar particle size, or the assumption that the particles are spherical [56]. To overcome these biases, the combination with other complementary orthogonal techniques is highly recommended by specialized organizations such as the European Nanomedicine Characterization Laboratory (EUNCL) or the US National Cancer Institute Nanotechnology Characterization Laboratory (NCI-NCL), that works jointly with the FDA [57]. Electron microscopy imaging can help to identify the shape and geometry of the NPs, as well as confirm their distribution and size in number [57]. Indeed, transmission electron microscopy studies corroborated that the developed NPs were spheres, with sizes in the 100–200 nm range (**Fig. 3B,D**). NTA analysis, although also based on light scattering, is able to track individual particles, allowing to better distinguish between subpopulations of particles with similar particle size [56]. Here, NTA analysis was used as a complementary technique, confirming the particle size values obtained with the previous methods (**Fig. 3C,D**).

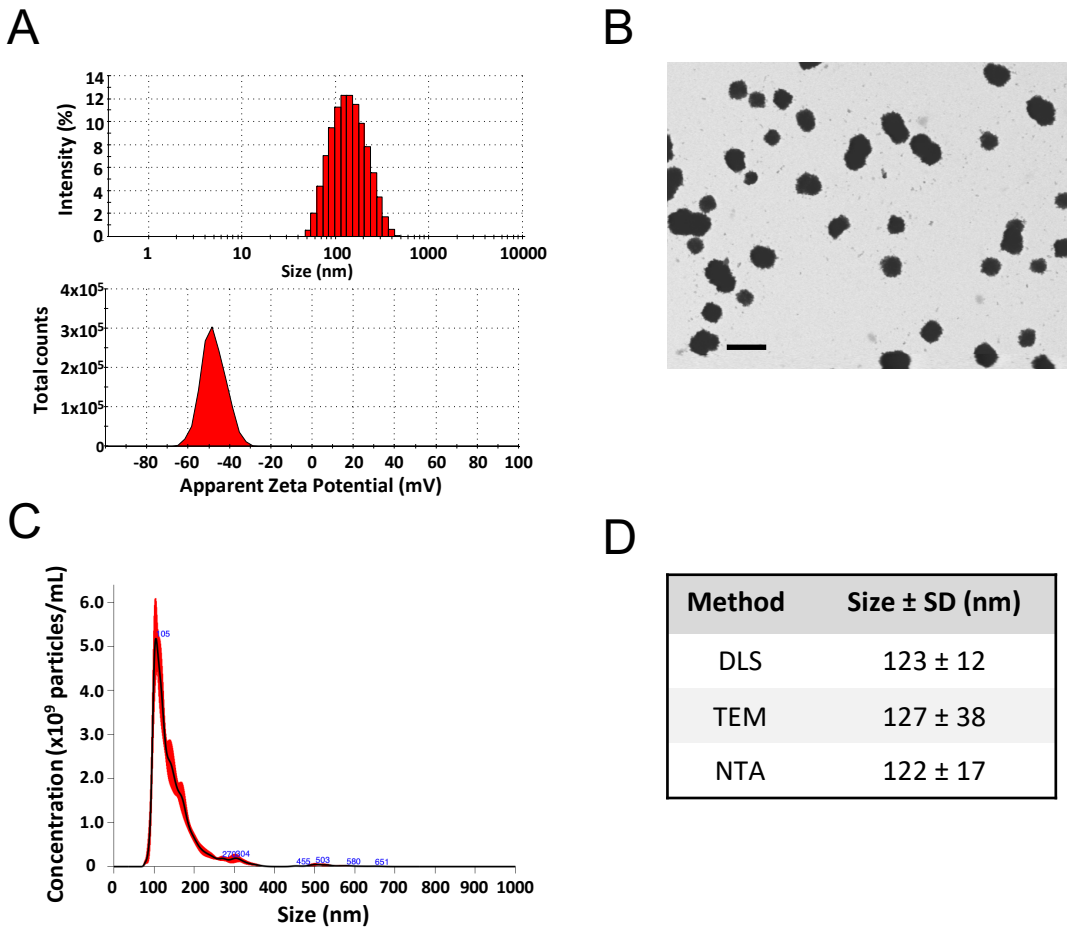

Method	Size ± SD (nm)
DLS	123 ± 12
TEM	127 ± 38
NTA	122 ± 17

Figure 3. Physicochemical characterization of the nanoformulation. (A) DLS particle size distribution based on intensity (top) and surface charge distribution (bottom), (B) Micrographs of the NPs by FESEM with the STEM detector (size bar represents 200 nm), and (C) NTA particle size distribution. (D) Summary of the mean size values of the nanoparticles measured by the three complementary techniques evaluated. DLS, dynamic light scattering; FESEM, field emission scanning electron microscopy; NTA, nanoparticle tracking analysis.

3.4. Content uniformity monitorization

The selection of adequate methods for the quantification of both the number of NPs and the quantity of drug associated to them is an essential step to guarantee the uniformity of the formulations and their batch-to-batch reproducibility.

3.4.1. Methods for particle content evaluation

Derived count rate is a parameter given by DLS measurement that represents the scattering intensity measured in the absence of a laser light attenuation filter, making it a convenient parameter to obtain the particle concentration [58,59]. Although it is not a direct measure of the number of particles within the formulation, it can be used as an indirect measurement for the purpose of comparison between batches, and its use is recommended by the EUNCL at prescreening phases [58]. It is important to bear in mind that in order for this parameter to be accurate, NP size has to remain

constant in the different particles concentrations tested [59]. In this case, different dilutions of the initial nanoformulation showed a linear correlation ($R^2 > 0.998$) with the values of the derived count rate (**Supporting Information, Fig. S1A**). Nevertheless, since the lasers of different devices are not identically calibrated, the overall values are not comparable among them (data not shown). Therefore, DLS was a suitable measurement of the content uniformity as an internal control.

The determination of the turbidimetry (values of transmittance) has classically been a way to have a gross estimation of the concentration of particles in suspension, with the premise that particle size also has to remain constant [59]. Using ultrapure water as a blank (100% transmittance), a linear correlation ($R^2 > 0.942$) between the percentage of transmittance and the concentration of the formulation was reported (**Supporting Information, Fig. S1B**). Furthermore, the fact that the transmittance values were similar between different laboratories, confirmed them as an interlaboratory validation method for the manufacturing process of the nanoformulation.

3.4.2. Evaluation of the API content

The determination of the drug content is a parameter that deserves special attention. In this case, an UPLC method to analyze the peptide antigen (PCS5) has already been described [37]. For PCS5 quantification, NPs were, first, disassembled in order to release the peptide. Since NPs were mainly formed through ionic interactions between the two polymers and the peptide (isoelectric point values of: 6.5 for CS; <2 for DS; 11 for PCS5), the use of a hypertonic medium was expected to disrupt the particles and allow the quantification of the peptide. Indeed, high concentrations of KCl (2 M) led to the disassociation of the particles, verified by a 100% recovery of the peptide. This was also confirmed by a dramatic decrease in the derived count rate values (**Supporting Information, Fig. S2A**).

Additionally, calibration curves of the peptide in water and in the matrix (blank NPs disrupted with 2M KCl) showed no influence of the matrix for the quantification of PCS5, confirming the specificity of the method. Additionally, linear calibration curves with $R^2 > 0.999$ were obtained in both cases (**Supporting Information, Fig. S2b**). The accuracy and precision of the method were also confirmed (data not shown).

3.5. Aseptic manufacturing

According to FDA regulations, nasal sprays do not need to be sterile for patient administration, nevertheless, the microbial content has to be controlled [53]. To do so, from the different sterilization methods available, we selected filtration as the one to guarantee a low microbial burden [60]. At the

same time, it is important to bear in mind that having reliable and reproducible methods to reduce the microbial burden is crucial to guarantee the safety of the product. In fact, problems related to the sterilization of Doxil®/Caelyx® were reported in 2011, and caused an important drug shortage [22,61].

The effect of the filter material (PVDF, PES or PTFE) over some CQAs (e.g., particle size and number of particles) was studied in order to select the most adequate filter. It has been described that for an effective filtration through a 0.22 µm mesh size filter, particle size should be smaller than 200 nm, preferably bellow 100 nm [62–64]. The assessment of the value of the filtration process was assayed for the nanoformulation and, although the results showed no significant changes in the particle size when using the different filters (**Fig. 4A**), a 15–30% decrease in the derived count rate was observed after filtration (**Fig. 4B**), indicating that a certain number of NPs did not pass through the filters.

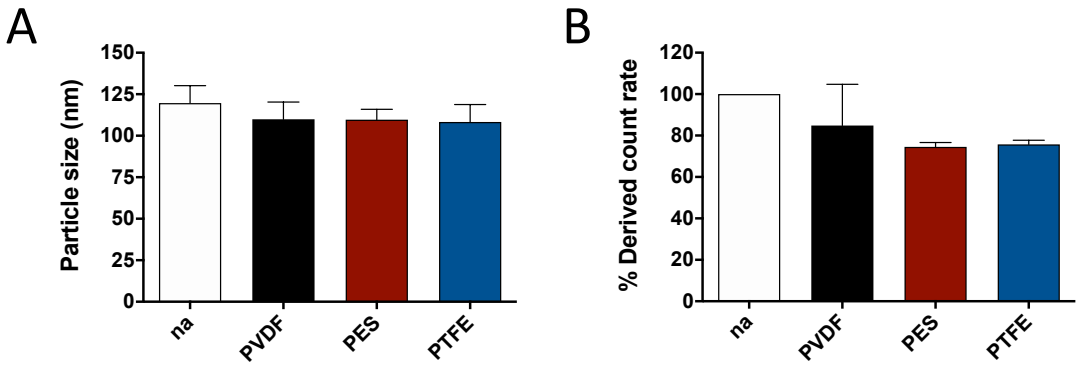

Figure 4. Effect of NP filtration through different 0.22 µm filters in terms of (A) particle size and (B) derived count rate after filtration, in comparison to the non-filtered particles (na). Values represent mean ± SD (n = 3).

An alternative procedure to decrease the potential impurities of the NPs would be the filtration of the starting materials. To determine the feasibility of this approach, solutions of CS and DS were filtered through 0.22 µm PVDF filters, and then freeze-dried to determine the yield of the process. The recovery yields obtained were 94 ± 5% for CS, and 100 ± 7% for DS. Furthermore, the NPs formulated with the filtered materials presented the same attributes as the ones with non-filtered components (**Supporting Information, Table S1**). Therefore, starting materials could also be filtered to minimize the microbial burden of the final formulation, without modifying any other attributes.

3.6. Long-term stability of the freeze-dried formulation

A long-term stability at room temperature is a highly desirable attribute for any vaccine. Having this feature would eliminate the need for the cold chain and would facilitate the accessibility of the vaccine to developing countries. For this purpose, NPs were freeze-dried in order to preserve the formulation

stability under storage for long periods of time. Trehalose was selected as a cryoprotectant, since its use has been proven to maintain the physicochemical properties of the NPs [37].

The characterization of the NPs by DLS, microscopy, and NTA confirmed that the particle size values of the nanoformulations were barely altered during the freeze-drying process (**Supporting Information, Fig. S3**). In fact, a modest increase in particle size by the three techniques was observed. An analysis of the content uniformity yielded transmittance values of 4 ± 2%; and a peptide recovery of 96 ± 13%, confirming the stability after the lyophilization process. The resuspended freeze-dried formulation also presented a pH of 6.5, appropriate for nasal administration [52]. Regarding the osmolality, values of approximately 149 mOsm/Kg were obtained. Finally, the residual moisture after freeze-drying was also tested, providing values lower than 3%, which have been reported to be adequate to avoid unwanted bacterial growth [54].

In agreement with the ICH guidelines, the evaluation of the long-term stability of the freeze-dried NPs [65], was performed at 5 °C, 25 °C/60% relative humidity (RH) for a general long-term stability study, and at 40 °C/75% RH for an accelerated stability study. Some physicochemical properties (particle size, PDI and Z-potential), API content and pH, were monitored over time. All these attributes were found within our specification values for up to 15 months in storage, both for the refrigerator and the general long-term stability conditions (**Fig. 5**). Only in the case of the accelerated study (40 °C/75% RH), the pH value was below the specification range (**Fig. 5D**), which could be related to the degradation of the components [66].

These results evidence the necessity of establishing and tracking all key attributes to guarantee a good characterization and understanding of the developed nanoformulations. They also underline that the nanovaccine here developed is stable for over a year without the need of the cold chain.

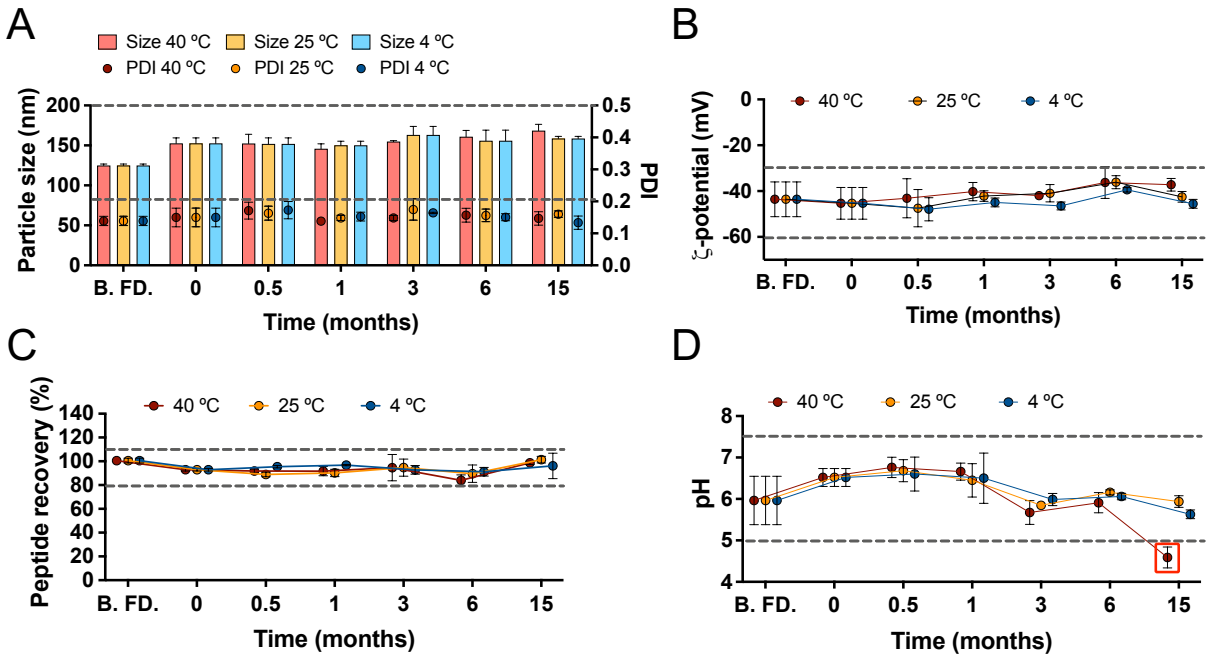

Figure 5. Long-term stability of the freeze-dried NPs at 5 °C; at 25 °C /60% RH; and at 40 °C /75% RH. Evolution of (A) particle size and PDI, (B) zeta-potential, (C) % of peptide recovery and (D) pH. The red box highlights the values that are not within the CQAs. Values represent mean ± SD (n ≥ 3).

3.7. Technology transfer

Another important requirement for the good manufacturing of a nanoformulation is to ensure that the production procedure is reproducible with different batches of the forming polymers, as well as across different people and laboratories. First, we compared the physicochemical properties of the NPs prepared with three different batches of CS, and two different batches of DS, confirming the reproducibility of the formulation (**Supporting Information, Table S2**). Additionally, the formulation process was transferred to three different laboratories (at the University of Santiago de Compostela, at CIDETEC Nanomedicine, and at UT2A laboratory), with different personnel, and the resulting batches of loaded NPs (from 1.65 to 200 mL) were thoroughly characterized and compared. In all three centers, the physicochemical properties of the different batches were found to be within the specification values previously established in the CQAs (**Supporting Information, Table S3**). These results further highlight the suitability of these polymeric NPs for a successful translation from the bench to an industrial level.

3.8. Scaling-up by a microfluidic-based and a batch-mode method

Bearing in mind that the ultimate goal of this nanoformulation development was an industrial translation, a scale-up from the original batch size (1.65 mL) to a more suitable size for preclinical and clinical studies was a fundamental step in this work. Thus, we studied both a continuous and

discontinuous scale-up procedure, by the adaptation of microfluidics for the production of the NPs and the preparation of a 200 mL batch. Finally, a 200-mL batch was produced in the pilot plant under GMP-like conditions.

3.8.1. Continuous production of the nanoparticles using microfluidics

Microfluidics has emerged as a potential tool to produce highly reproducible nanoformulations, with the additional advantage of scalability [67]. In this case, a staggered herringbone mixer was employed for the preparation of the NPs [68]. Most nanosystems prepared by this technique are based on the nanoprecipitation of the materials when the organic and aqueous phase meet, while in our case the particle formation relied on the ionic interactions between two oppositely charged phases. The satisfactory application of this technique for a solvent-free NP formation has been recently disclosed for the preparation of octaarginine/RNA nanocomplexes [69]. Considering that the process parameters have an important effect in the properties of the resulting NPs [70], here, we first conducted a screening of the influence of the flow rates over the production of blank NPs. Then, the method that provided the best result was applied to the loaded NPs. The cartridge employed consisted on two inlets, one for the positively charged phase and the other for the negative DS phase, followed by a mixing area and finally an outlet to collect the formed NPs (**Fig. 6A**). Solutions of CS and DS were prepared at the same concentrations as the ones used for smaller batches; the flow ratio was kept constant at 1:1, and the flow rate was the parameter of study (from 0.5 to 14 mL/min).

For the blank NPs, the particle size decreased as the flow rate values were increased, but at the same time, a higher variability was detected (**Fig. 6B**). Interestingly, the higher flow rates also yielded smaller derived count rate values (**Fig. 6C**). On the other hand, the lowest flow rate tested (0.5 mL/min) generated reproducible particles, with properties closer to our nanoformulation CQAs (**Fig. 6B,C**). In this regard, we have hypothesized that the high flow rates (of 3 mL/min or more) might hinder the adequate interaction time between the oppositely charged polymers. This incomplete interaction would lead to a higher amount of free components, resulting in low derived count rate values. When testing these conditions for the loaded NPs, similar physicochemical properties to the ones produced by a discontinuous method were obtained (**Fig. 6d**). Therefore, the nanoformulation of study could be produced with microfluidics, which allows to envisage a continuous and scaled-up production.

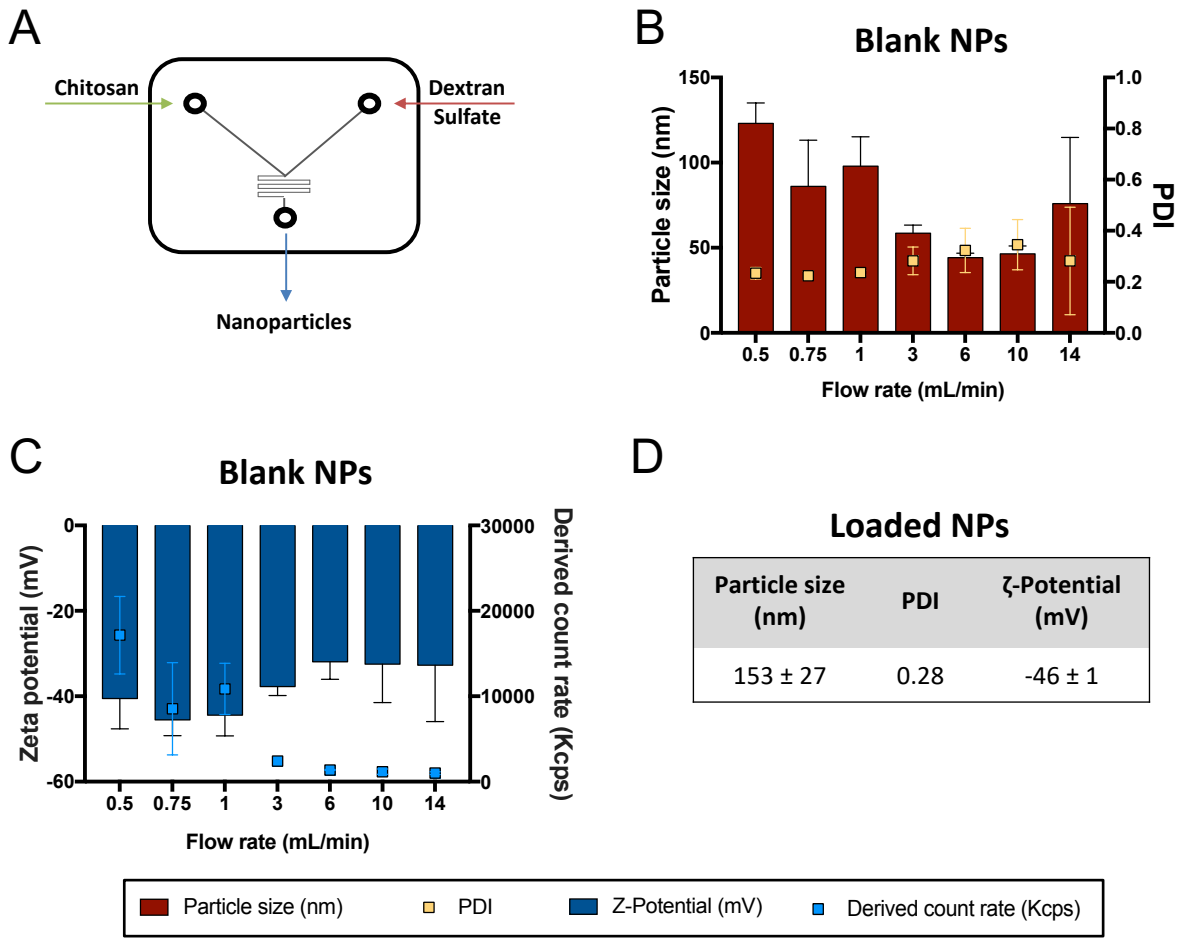

Figure 6. Scale-up of the nanoparticles fabrication using microfluidics. (A) Design of the cartridge used. Influence of the different flow rates in (B) particle size and PDI, and in (C) Z-potential and derived count rate. (D) Physicochemical properties of the loaded NPs prepared with a flow rate of 0.5 mL/min. Values represent mean ± SD (n = 3). NPs, nanoparticles; PDI, polydispersity index.

3.8.2. Batch mode production of the nanoformulation

The NPs were prepared by ionic complexation, a method that has been described as easily scalable [71]. In the particular case of the NPs here studied, the magnetic stirring of the small batches was substituted by a mechanical stirring with a blade agitator, more suitable for an accurate control when large volume solutions are mixed. As studied in section 3.2., the most critical parameter to obtain adequate NPs and prevent aggregation was the incorporation rate of the DS solution over the CS/PCS5 phase. Thus, for this scale-up, the mechanical stirring was kept at 700 rpm, and the DS solution was poured manually.

First, 200 mL batches of blank NPs were prepared to confirm the suitability of the procedure for a larger scale, and then the same procedure was applied to prepare the loaded NPs. Particle size, PDI, Z-potential and pH were monitored to evaluate the method performance. As shown in **Table 3**, all values

were found within the product specifications previously described. Therefore, this discontinuous method was proven to be suitable for the production of large volumes of NPs, with no important effects over any of their physicochemical properties.

Table 3. Physicochemical properties of the scaled-up blank and loaded nanoparticles, in comparison with the small-size batches.

Sample	Particle size (nm)	PDI	ζ-potential (mV)	pH	Transmittance (%)
Blank NPs (1.65 mL batch)	95 ± 8	0.16	-41 ± 4	7 ± 0.2	25 ± 4
Blank NPs (200 mL batch)	99 ± 8	0.14	-39 ± 1	7 ± 0.4	24 ± 5
Loaded NPs (1.65 mL batch)	130 ± 15	0.14	-45 ± 7	6 ± 0.6	6 ± 3
Loaded NPs (200 mL batch)	129 ± 4	0.15	-41 ± 6	6 ± 0.2	3 ± 2
FD NPs (1.65 mL batch)	160 ± 15	0.16	-43 ± 7	7 ± 0.6	4 ± 2
FD NPs (200 mL batch)	182 ± 11	0.19	-45 ± 3	6 ± 0.7	3 ± 2

Values represent mean ± SD (n ≥ 3; except for loaded and FD NPs 200 ml batch, where n=2)
FD, freeze-dried; NPs, nanoparticles; PDI, polydispersity index.

We have seen in this section that the formulation of CS/DS NPs can be translated to an industrial environment and fabricated either by discontinuous (batch-mode) or continuous (microfluidics) methods. In the case of the batch-mode preparation, it is a simple and fast method, that may need subsequent adaptations with the increase in the batch size. On the other hand, microfluidics is a very reproducible technique that can produce high NP volumes by using several cartridges in a row. Nevertheless, these cartridges are costly, and have a limited lifetime and re-usability, thus increasing the final cost of fabrication. These aspects have to be taken into consideration when selecting the methods for an industrial translation.

3.8.3. Production of a GMP-like batch in the pilot plant

As the last step on the road to the translation of the nanomedicine, a 200-mL formulation was prepared in the pilot plant. This batch size, equivalent to 220 doses of the vaccine candidate, was considered to be sufficient for an exploratory preclinical study with 50 non-human primates and four boosts per animal. Furthermore, all the procedures in the pilot plant were conducted under GMP-like conditions. In this regard, production processes, materials and personal flow were designed in qualified facilities according to GMP guidelines. All the components used to prepare the formulation were qualified as GMP grade materials, with the exception of the peptide antigen. To prepare the

GMP-like batch, the starting polymer solutions (CS and DS) were first filtered through 0.2 µm mesh size filters (more details in section 3.5). Then, the formulation was prepared under mechanical stirring with a blade agitator (more details in section 2.8.2). Subsequently, formulation and cryoprotectant were added to type I glass vials, to then be freeze-dried in the same conditions as the non-GMP batches (more details in section 2.4). The resulting formulation was re-dispersed in highly purified water and characterized. The physicochemical properties of the NPs were found within the CQAs previously described (**Table 4**). Therefore, the translation of the nanovaccine from the bench to an industrial environment has been successfully achieved.

Table 4. Physicochemical properties of the nanovaccine fabricated in the pilot plant.

Sample	Particle size (nm)	PDI	ζ-potential (mV)	pH	Transmittance (%)	Osmolality (mOsm/kg)
Final formulation	150 ± 1	0.13	-42 ± 1	6.6	7.2	186

FD, freeze-drying; NPs, nanoparticles; PDI, polydispersity index.

Overall, we consider that this work compiles in a great manner with the MIRIBEL recommendations for material characterization [31]. Here, we have provided a detailed description of the synthesis method of the formulation, together with an evaluation of the different parameters that may have an effect on the final NPs. Furthermore, the values of size, shape, zeta potential, density, concentration and drug loading were thoroughly studied and reported in this work, and in many cases confirmed by several complementary techniques. Besides, three different batches of the forming components have been employed to guarantee the reproducibility of the formulation, among other aspects. Overall, the results of this manuscript compile with the MIRIBEL recommendations, which we hope will help in the standardization and application of stablished methodologies for the characterization of nanosystems.

4. Conclusions

In this work, we have shown the feasibility of a potential HIV nanovaccine candidate to be manufactured in a pilot plant. By implementing a QbD approach, the most critical aspects of the process that have an impact on the formulation attributes were highlighted. This strategy helped to identify that the phase incorporation rate had the most significant effect over the final properties of the nanoformulation. In addition, we emphasized the importance of combining orthogonal techniques to guarantee a realistic and complete characterization of the formulation. The definition of all these critical process parameters led to the successful transfer of the HIV nanovaccine manufacturing procedure from the laboratory to the pilot plant production, and its scale-up by both the microfluidic

and the batch-mode methods. All these results validate that this nanomedicine would be ready to move towards an industrial manufacturing set up.

References

[1] Z. Niu, I. Conejos-Sánchez, B.T. Griffin, C.M. O'Driscoll, M.J. Alonso, Lipid-based nanocarriers for oral peptide delivery, Adv. Drug Deliv. Rev. 106 (2016) 337–354. doi:10.1016/j.addr.2016.04.001.

[2] M. Yu, J. Wu, J. Shi, O.C. Farokhzad, Nanotechnology for protein delivery: overview and perspectives, J. Control. Release. 240 (2016) 24–37. doi:10.1016/j.jconrel.2015.10.012.

[3] I. Santalices, A. Gonella, D. Torres, M.J. Alonso, Advances on the formulation of proteins using nanotechnologies, J. Drug Deliv. Sci. Technol. 42 (2017) 155–180. doi:10.1016/j.jddst.2017.06.018.

[4] E. Samaridou, M.J. Alonso, Nose-to-brain peptide delivery – the potential of nanotechnology, Bioorg. Med. Chem. 26 (2018) 2888–2905. doi:10.1016/j.bmc.2017.11.001.

[5] Z. Li, T.M. Rana, Therapeutic targeting of microRNAs: current status and future challenges, Nat. Rev. Drug Discov. 13 (2014) 622–638. doi:10.1038/nrd4359.

[6] Y. Liu, C.-F. Xu, S. Iqbal, X.-Z. Yang, J. Wang, Responsive nanocarriers as an emerging platform for cascaded delivery of nucleic acids to cancer, Adv. Drug Deliv. Rev. 115 (2017) 98–114. doi:10.1016/j.addr.2017.03.004.

[7] S.M. Saraiva, V. Castro-López, C. Pañeda, M.J. Alonso, Synthetic nanocarriers for the delivery of polynucleotides to the eye, Eur. J. Pharm. Sci. 103 (2017) 5–18. doi:10.1016/j.ejps.2017.03.001.

[8] J.C. Kaczmarek, P.S. Kowalski, D.G. Anderson, Advances in the delivery of RNA therapeutics: from concept to clinical reality, Genome Med. 9 (2017) 60. doi:10.1186/s13073-017-0450-0.

[9] D.J. Irvine, M.C. Hanson, K. Rakhra, T. Tokatlian, Synthetic nanoparticles for vaccines and immunotherapy, Chem. Rev. 115 (2015) 11109–11146. doi:10.1021/acs.chemrev.5b00109.

[10] A.S. Cordeiro, M.J. Alonso, Recent advances in vaccine delivery, Pharm. Pat. Anal. 5 (2015) 49–73. doi:10.4155/ppa.15.38.

[11] T.G. Dacoba, A. Olivera, D. Torres, J. Crecente-Campo, M.J. Alonso, Modulating the immune system through nanotechnology, Semin. Immunol. 34 (2017) 78–102. doi:10.1016/j.smim.2017.09.007.

[12] K.T. Gause, A.K. Wheatley, J. Cui, Y. Yan, S.J. Kent, F. Caruso, Immunological principles guiding the rational design of particles for vaccine delivery, ACS Nano. 11 (2017) 54–68. doi:10.1021/acsnano.6b07343.

[13] D. Bobo, K.J. Robinson, J. Islam, K.J. Thurecht, S.R. Corrie, Nanoparticle-based medicines: a review of FDA-approved materials and clinical trials to date, Pharm. Res. 33 (2016) 2373–2387. doi:10.1007/s11095-016-1958-5.

[14] A.C. Anselmo, S. Mitragotri, Nanoparticles in the clinic, Bioeng. Transl. Med. 1 (2016) 10–29. doi:10.1002/btm2.10003.

[15] C.L. Ventola, Progress in nanomedicine: approved and investigational nanodrugs, P T. 42 (2017) 742–755.

[16] N. Desai, Challenges in development of nanoparticle-based therapeutics, AAPS J. 14 (2012) 282–295. doi:10.1208/s12248-012-9339-4.

[17] H. Ragelle, F. Danhier, V. Préat, R. Langer, D.G. Anderson, Nanoparticle-based drug delivery systems: a commercial and regulatory outlook as the field matures, Expert Opin. Drug Deliv. 14 (2017) 851–864. doi:10.1080/17425247.2016.1244187.

[18] S. Hua, M.B.C. de Matos, J.M. Metselaar, G. Storm, Current trends and challenges in the clinical translation of nanoparticulate nanomedicines: pathways for translational development and commercialization, Front. Pharmacol. 9 (2018) 1–14. doi:10.3389/fphar.2018.00790.

[19] F. Dormont, M. Rouquette, C. Mahatsekake, F. Gobeaux, A. Peramo, R. Brusini, S. Calet, F. Testard, S. Lepetre-Mouelhi, D. Desmaële, M. Varna, P. Couvreur, Translation of nanomedicines from lab to industrial scale synthesis: the case of squalene-adenosine nanoparticles, J. Control. Release. 307 (2019) 302–314. doi:10.1016/j.jconrel.2019.06.040.

[20] A. Gabizon, M. Bradbury, U. Prabhakar, W. Zamboni, S. Libutti, P. Grodzinski, Cancer nanomedicines: closing the translational gap, Lancet. 384 (2014) 2175–2176. doi:10.1016/S0140-6736(14)61457-4.

[21] L.X. Yu, G. Amidon, M.A. Khan, S.W. Hoag, J. Polli, G.K. Raju, J. Woodcock, Understanding pharmaceutical quality by design, AAPS J. 16 (2014) 771–783. doi:10.1208/s12248-014-9598-3.

[22] A. Wicki, D. Witzigmann, V. Balasubramanian, J. Huwyler, Nanomedicine in cancer therapy: challenges, opportunities, and clinical applications, J. Control. Release. 200 (2015) 138–157. doi:10.1016/j.jconrel.2014.12.030.

[23] V. Agrahari, V. Agrahari, Facilitating the translation of nanomedicines to a clinical product: challenges and opportunities, Drug Discov. Today. 23 (2018) 974–991. doi:10.1016/j.drudis.2018.01.047.

[24] W.C. Zamboni, V. Torchilin, A.K. Patri, J. Hrkach, S. Stern, R. Lee, A. Nel, N.J. Panaro, P. Grodzinski, Best practices in cancer nanotechnology: perspective from NCI nanotechnology alliance, Clin. Cancer Res. 18 (2012) 3229–3241. doi:10.1158/1078-0432.CCR-11-2938.

[25] E. Pallagi, R. Ambrus, P. Szabó-Révész, I. Csóka, Adaptation of the quality by design concept in early pharmaceutical development of an intranasal nanosized formulation, Int. J. Pharm. 491 (2015) 384–392. doi:10.1016/j.ijpharm.2015.06.018.

[26] F. Rose, J.E. Wern, P.T. Ingvarsson, M. van de Weert, P. Andersen, F. Follmann, C. Foged, Engineering of a novel adjuvant based on lipid-polymer hybrid nanoparticles: a quality-by-design approach, J. Control. Release. 210 (2015) 48–57. doi:10.1016/j.jconrel.2015.05.004.

[27] B. Shah, D. Khunt, H. Bhatt, M. Misra, H. Padh, Intranasal delivery of venlafaxine loaded nanostructured lipid carrier: risk assessment and QbD based optimization, J. Drug Deliv. Sci. Technol. 33 (2016) 37–50. doi:10.1016/j.jddst.2016.03.008.

[28] H. Raina, S. Kaur, A.B. Jindal, Development of efavirenz loaded solid lipid nanoparticles: risk assessment, quality-by-design (QbD) based optimisation and physicochemical characterisation, J. Drug Deliv. Sci. Technol. 39 (2017) 180–191. doi:10.1016/j.jddst.2017.02.013.

[29] J. Marto, E. Ruivo, S.D. Lucas, L.M. Gonçalves, S. Simões, L.F. Gouveia, R. Felix, R. Moreira, H.M. Ribeiro, A.J. Almeida, Starch nanocapsules containing a novel neutrophil elastase inhibitor with improved pharmaceutical performance, Eur. J. Pharm. Biopharm. 127 (2018) 1–11. doi:10.1016/j.ejpb.2018.01.011.

[30] A. Simões, F. Veiga, A. Figueiras, C. Vitorino, A practical framework for implementing quality by design to the development of topical drug products: nanosystem-based dosage forms, Int. J. Pharm. 548 (2018) 385–399. doi:10.1016/j.ijpharm.2018.06.052.

[31] M. Faria, M. Björnmalm, K.J. Thurecht, S.J. Kent, R.G. Parton, M. Kavallaris, A.P.R. Johnston, J.J. Gooding, S.R. Corrie, B.J. Boyd, P. Thordarson, A.K. Whittaker, M.M. Stevens, C.A. Prestidge, C.J.H. Porter, W.J. Parak, T.P. Davis, E.J. Crampin, F. Caruso, Minimum information reporting in bio–nano experimental literature, Nat. Nanotechnol. 13 (2018) 777–785. doi:10.1038/s41565-018-0246-4.

[32] S. Vicente, M. Peleteiro, B. Díaz-Freitas, A. Sanchez, Á. González-Fernández, M.J. Alonso, Co-delivery of viral proteins and a TLR7 agonist from polysaccharide nanocapsules: a needle-free vaccination strategy, J. Control. Release. 172 (2013) 773–781. doi:10.1016/j.jconrel.2013.09.012.

[33] J.F. Correia-Pinto, N. Csaba, J. Schiller, M.J. Alonso, Chitosan-poly (I:C)-PADRE based nanoparticles as delivery vehicles for synthetic peptide vaccines, Vaccines. 3 (2015) 730–750. doi:10.3390/vaccines3030730.

[34] J.V. González-Aramundiz, E. Presas, I. Dalmau-Mena, S. Martínez-Pulgarín, C. Alonso, J.M. Escribano, M.J. Alonso, N.S. Csaba, Rational design of protamine nanocapsules as antigen delivery carriers, J. Control. Release. 245 (2017) 62–69. doi:10.1016/j.jconrel.2016.11.012.

[35] J. Crecente-Campo, S. Lorenzo-Abalde, A. Mora, J. Marzoa, N. Csaba, J. Blanco, Á. González-Fernández, M.J. Alonso, Bilayer polymeric nanocapsules: a formulation approach for a thermostable and adjuvanted E. coli antigen vaccine, J. Control. Release. 286 (2018) 20–32. doi:10.1016/j.jconrel.2018.07.018.

[36] H. Li, M. Nykoluk, L. Li, L.R. Liu, R.W. Omange, G. Soule, L.T. Schroeder, N. Toledo, M.A. Kashem, J.F. Correia-Pinto, B. Liang, N. Schultz-Darken, M.J. Alonso, J.B. Whitney, F.A. Plummer, M. Luo, Natural and

cross-inducible anti-SIV antibodies in Mauritian cynomolgus macaques, PLoS One. 12 (2017) e0186079.

[37] T.G. Dacoba, R.W. Omange, H. Li, J. Crecente-Campo, M. Luo, M.J. Alonso, Polysaccharide nanoparticles can efficiently modulate the immune response against an HIV peptide antigen, ACS Nano. 13 (2019) 4947–4959. doi:10.1021/acsnano.8b07662.

[38] H. Li, R.W. Omange, B. Liang, N. Toledo, Y. Hai, L.R. Liu, D. Schalk, J. Crecente-Campo, T.G. Dacoba, A.B. Lambe, S.-Y. Lim, L. Li, M.A. Kashem, Y. Wan, J.F. Correia-Pinto, X.Q. Liu, R.F. Balshaw, Q. Li, E. Rakasz, N. Schultz-Darken, M.J. Alonso, J.B. Whitney, F.A. Plummer, M. Luo, A novel vaccine targeting the viral protease cleavage sites protects Mauritian cynomolgus macaques against vaginal SIVmac251 infection, BioRxiv. (2019). doi:10.1101/842955.

[39] A.S. Rathore, H. Winkle, Quality by design for biopharmaceuticals, Nat. Biotechnol. 27 (2009) 26–34. doi:10.1038/nbt0109-26.

[40] European Medicines Agency, ICH guideline Q8 (R2) on pharmaceutical development, (2017). http://www.ema.europa.eu/docs/en_GB/document_library/Scientific_guideline/2009/09/WC500002872.pdf (accessed December 5, 2019).

[41] International Organization for Standardization, Particle size analysis — Dynamic light scattering (DLS) (ISO/DIS Standard No. 22412), (2017).

[42] S.M. Hartig, Basic image analysis and manipulation in ImageJ, Curr. Protoc. Mol. Biol. 102 (2013) 1–12. doi:10.1002/0471142727.mb1415s102.

[43] M. Klein, M. Menta, T.G. Dacoba, J. Crecente-Campo, M.J. Alonso, D. Dupin, I. Loinaz, B. Grassl, F. Séby, Advanced nanomedicine characterization by DLS and AF4-UV-MALS: application to a HIV nanovaccine, J. Pharm. Biomed. Anal. 179 (2020) 113017. doi:10.1016/j.jpba.2019.113017.

[44] V.K. Rapalli, A. Khosa, G. Singhvi, V. Girdhar, R. Jain, S.K. Dubey, Application of QbD principles in nanocarrier-based drug delivery systems, in: S. Beg, M.S. Hasnain (Eds.), Pharm. Qual. by Des., Elsevier, 2019: pp. 255–296. doi:10.1016/B978-0-12-815799-2.00014-9.

[45] H. Li, R.W. Omange, F.A. Plummer, M. Luo, A novel HIV vaccine targeting the protease cleavage sites, AIDS Res. Ther. 14 (2017) 51. doi:10.1186/s12981-017-0174-7.

[46] A.S. Cordeiro, M.J. Alonso, M. de la Fuente, Nanoengineering of vaccines using natural polysaccharides, Biotechnol. Adv. 33 (2015) 1279–1293. doi:10.1016/j.biotechadv.2015.05.010.

[47] C. Prego, P. Paolicelli, B. Díaz, S. Vicente, A. Sánchez, Á. González-Fernández, M.J. Alonso, Chitosan-based nanoparticles for improving immunization against hepatitis B infection, Vaccine. 28 (2010) 2607–2614. doi:10.1016/j.vaccine.2010.01.011.

[48] F. Rose, J.E. Wern, F. Gavins, P. Andersen, F. Follmann, C. Foged, A strong adjuvant based on glycol-chitosan-coated lipid-polymer hybrid nanoparticles potentiates mucosal immune responses against the recombinant Chlamydia trachomatis fusion antigen CTH522, J. Control. Release. 271 (2018) 88–97. doi:10.1016/j.jconrel.2017.12.003.

[49] S. Sharma, T.K. Mukkur, H.A. Benson, Y. Chen, Enhanced immune response against Pertussis toxoid by IgA-loaded chitosan–dextran sulfate nanoparticles, J. Pharm. Sci. 101 (2012) 233–244. doi:10.1002/jps.22763.

[50] J.F. Correia-Pinto, N. Csaba, M.J. Alonso, Vaccine delivery carriers: insights and future perspectives, Int. J. Pharm. 440 (2013) 27–38. doi:10.1016/j.ijpharm.2012.04.047.

[51] A. Stano, C. Nembrini, M.A. Swartz, J.A. Hubbell, E. Simeoni, Nanoparticle size influences the magnitude and quality of immune response after intranasal immunization, Vaccine. 30 (2012) 7541–7546. doi:10.1016/j.vaccine.2012.10.050.

[52] R.J.A. England, J.J. Homer, L.C. Knight, S.R. Ell, Nasal pH measurement: a reliable and repeatable parameter, Clin. Otolaryngol. 24 (1999) 67–68. doi:10.1046/j.1365-2273.1999.00223.x.

[53] U.S. Food and Drug Administration, Guidance for industry: nasal spray and inhalation solution, suspension, and spray drug products — chemistry, manufacturing, and controls documentation, (2002).

https://www.fda.gov/media/70857/download (accessed December 1, 2019).

[54] J.C. May, R.M. Wheeler, N. Etz, A. Del Grosso, Measurement of final container residual moisture in freeze-dried biological products., Dev. Biol. Stand. 74 (1992) 153–164.

[55] I.P. Kaur, V. Kakkar, P.K. Deol, M. Yadav, M. Singh, I. Sharma, Issues and concerns in nanotech product development and its commercialization, J. Control. Release. 193 (2014) 51–62. doi:10.1016/j.jconrel.2014.06.005.

[56] C.M. Maguire, M. Rösslein, P. Wick, A. Prina-Mello, Characterisation of particles in solution – a perspective on light scattering and comparative technologies, Sci. Technol. Adv. Mater. 19 (2018) 732–745. doi:10.1080/14686996.2018.1517587.

[57] F. Caputo, J. Clogston, L. Calzolai, M. Rösslein, A. Prina-Mello, Measuring particle size distribution of nanoparticle enabled medicinal products, the joint view of EUNCL and NCI-NCL. A step by step approach combining orthogonal measurements with increasing complexity, J. Control. Release. 299 (2019) 31–43. doi:10.1016/j.jconrel.2019.02.030.

[58] European Nanomedicine Characterisation Laboratory, Measuring batch mode DLS, (2016). http://www.euncl.eu/about-us/assay-cascade/PDFs/Prescreening/EUNCL-PCC-001.pdf?m=1468937875& (accessed December 5, 2019).

[59] J. Shang, X. Gao, Nanoparticle counting: towards accurate determination of the molar concentration, Chem. Soc. Rev. 43 (2014) 7267–7278. doi:10.1039/c4cs00128a.

[60] H.R. Lakkireddy, D. Bazile, Building the design, translation and development principles of polymeric nanomedicines using the case of clinically advanced poly(lactide(glycolide))–poly(ethylene glycol) nanotechnology as a model: an industrial viewpoint, Adv. Drug Deliv. Rev. 107 (2016) 289–332. doi:10.1016/j.addr.2016.08.012.

[61] European Medicines Agency, Questions and answers on the supply situation of Caelyx, (2013). http://www.ema.europa.eu/docs/en_GB/document_library/Medicine_QA/2013/04/WC500142510.pdf (accessed December 5, 2019).

[62] M.A. Vetten, C.S. Yah, T. Singh, M. Gulumian, Challenges facing sterilization and depyrogenation of nanoparticles: effects on structural stability and biomedical applications, Nanomedicine Nanotechnology, Biol. Med. 10 (2014) 1391–1399. doi:10.1016/j.nano.2014.03.017.

[63] Y. Tsukada, K. Hara, Y. Bando, C.C. Huang, Y. Kousaka, Y. Kawashima, R. Morishita, H. Tsujimoto, Particle size control of poly(DL-lactide-co-glycolide) nanospheres for sterile applications, Int. J. Pharm. 370 (2009) 196–201. doi:10.1016/j.ijpharm.2008.11.019.

[64] V. Masson, F. Maurin, H. Fessi, J.P. Devissaguet, Influence of sterilization processes on poly(ε-caprolactone) nanospheres, Biomaterials. 18 (1997) 327–335. doi:10.1016/S0142-9612(96)00144-5.

[65] U.S. Food and Drug Administration, Guidance for industry Q1A(R2) stability testing of new drug substances and products, ICH Guidel. (2003). https://www.fda.gov/media/71707/download (accessed December 5, 2019).

[66] E. Szymańska, K. Winnicka, Stability of chitosan – a challenge for pharmaceutical and biomedical applications, Mar. Drugs. 13 (2015) 1819–1846. doi:10.3390/md13041819.

[67] P.M. Valencia, O.C. Farokhzad, R. Karnik, R. Langer, Microfluidic technologies for accelerating the clinical translation of nanoparticles, Nat. Nanotechnol. 7 (2012) 623.

[68] A.D. Stroock, Chaotic mixer for microchannels, Science. 295 (2002) 647–651. doi:10.1126/science.1066238.

[69] E. Samaridou, H. Walgrave, E. Salta, D.M. Álvarez, V. Castro-López, M. Loza, M.J. Alonso, Nose-to-brain delivery of enveloped RNA - cell permeating peptide nanocomplexes for the treatment of neurodegenerative diseases, Biomaterials. 230 (2020) 119657. doi:10.1016/j.biomaterials.2019.119657.

[70] C.B. Roces, D. Christensen, Y. Perrie, Translating the fabrication of protein-loaded poly(lactic-co-glycolic acid) nanoparticles from bench to scale-independent production using microfluidics, Drug Deliv. Transl.

Res. (2020). doi:10.1007/s13346-019-00699-y.

[71] R. Paliwal, R.J. Babu, S. Palakurthi, Nanomedicine scale-up technologies: feasibilities and challenges, AAPS PharmSciTech. 15 (2014) 1527–1534. doi:10.1208/s12249-014-0177-9.

Supporting Information

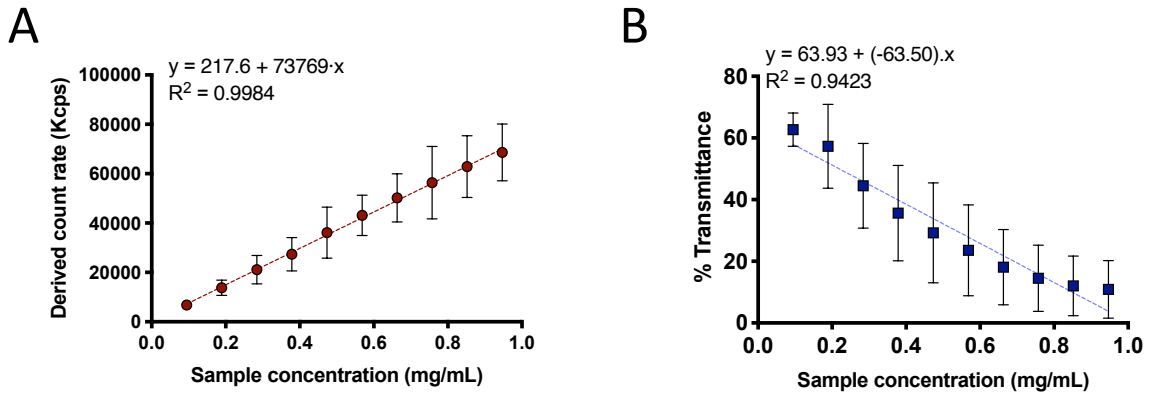

Supporting Figure S1. Calibration curves for the determination of nanoparticle content using (A) the values of the derived count rate and (B) the % of transmittance. Values represent mean ± SD (n ≥ 3).

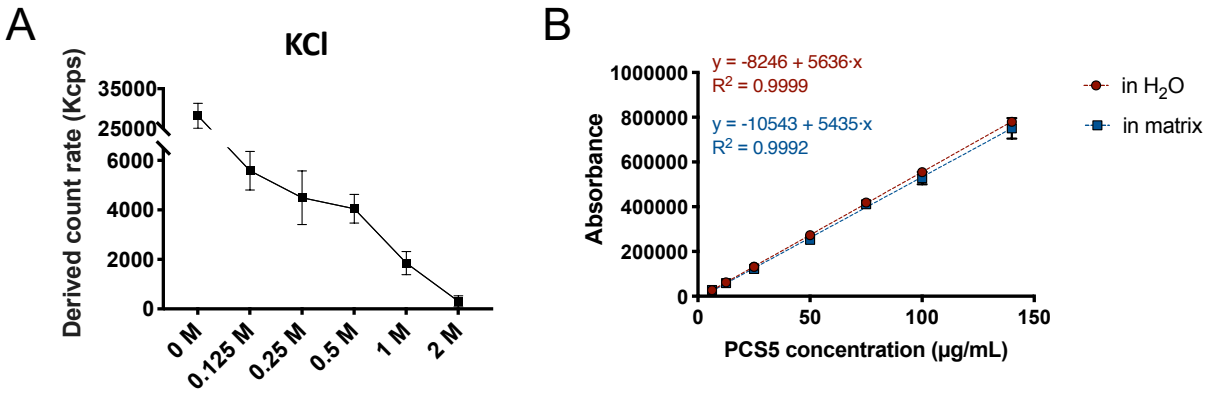

Supporting Figure S2. Nanoparticle disassembling in the presence of high ionic strength solutions. (A) Effect of the concentration of KCl on the derived count rate. (B) Calibration curves of the peptide PCS5 in water (red) and in NPs disrupted with KCl (matrix, in dark blue). Values represent mean ± SD (n = 3).

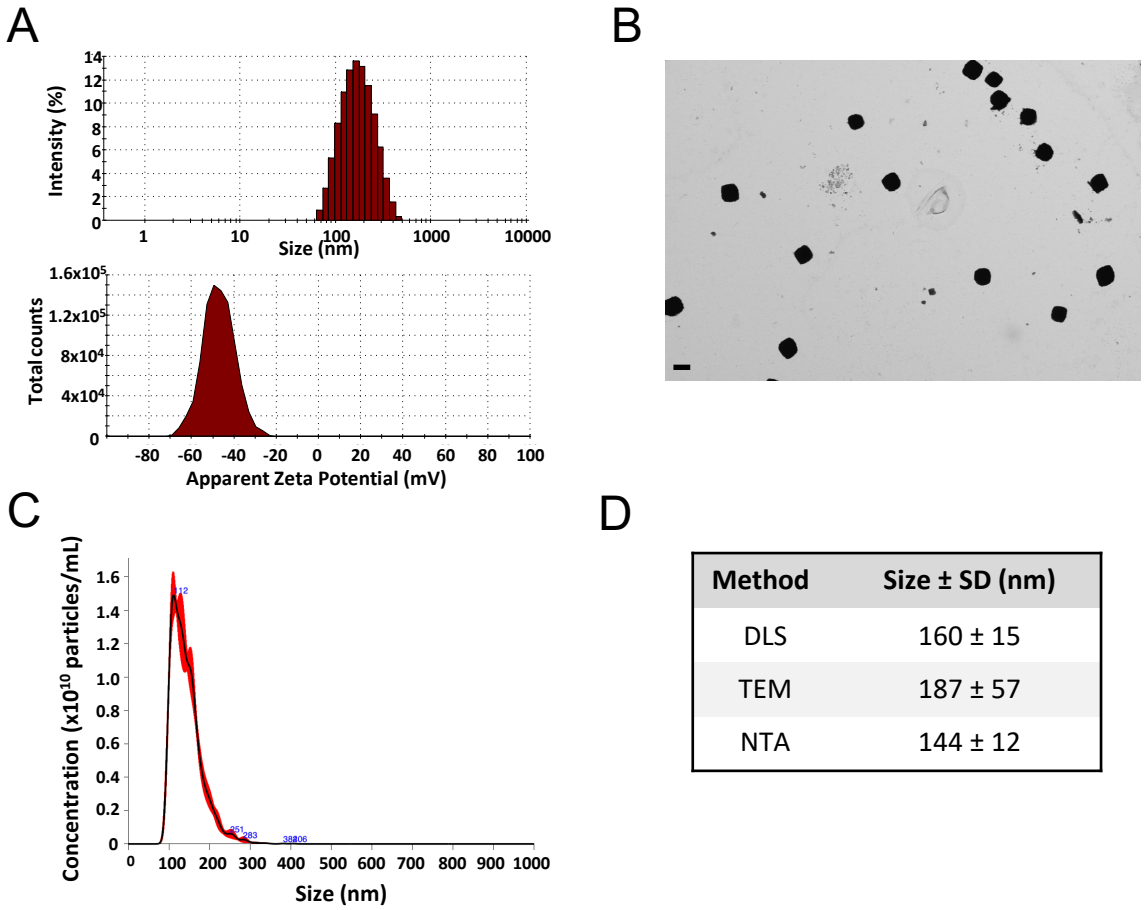

Method	Size ± SD (nm)
DLS	160 ± 15
TEM	187 ± 57
NTA	144 ± 12

Supporting Figure S3. Physicochemical characterization of the redispersed freeze-dried nanoparticles. (A) DLS intensity histograms (top) and surface charge vaules (bottom), (B) Micrographs of the NPs by FESEM with the STEM detector (size bar represents 200 nm), and (C) NTA size distribution. (D) Summary of the mean size values of the nanoparticles measured by the three complementary techniques evaluated. DLS, dynamic light scattering; FESEM, field emission scanning electron microscopy; NTA, nanoparticle tracking analysis.

Supporting Table S1. Comparison of the physicochemical properties of the nanoparticles prepared with non-filtered and filtered starting materials.

Starting materials	Particle size (nm)	PDI	ζ-potential (mV)	Derived count rate (kcps)
Non-filtered	138 ± 14	0.14	-53 ± 4	65300 ± 1900
Filtered	135 ± 12	0.15	-50 ± 3	51500 ± 1600

PDI, polydispersity index.

Supporting Table S2. Comparison of the physicochemical properties of the nanoparticles prepared with different batches of chitosan and dextran sulfate.

CS batch	DS batch	Particle size (nm)	PDI	Z-potential (mV)
batch 1	**batch 1**	118 ± 7	0.15	-45 ± 5
batch 2	**batch 1**	135 ± 4	0.14	-41 ± 1
batch 2	**batch 2**	113 ± 9	0.12	-46 ± 2
batch 3	**batch 2**	128 ± 4	0.14	-46 ± 2

CS, chitosan; DS, dextran sulfate; PDI, polydispersity index

Supporting Table S3. Comparison of the physicochemical properties of the resuspended nanoparticles prepared in three different laboratories with the established specifications (CQAs).

Lab	Particle size (nm)	PDI	ζ-potential (mV)	Content per vial (mg)	pH	Osmolality (mOsm/kg)	Transmittance	Dispersibility	Residual moisture	Peptide recovery
CQAs	100–300 D(10) 80–150 D(50) 150–250 D(90) 250–450 Span 0.4–3	<0.3	-30– -65	82.245 ± 10%	5 –7.5	100–200	< 10%	Yes	<5%	90–110%
USC	164 ± 24 D(10) 99 ± 10 D(50) 171 ± 17 D(90) 308 ± 44 Span 1.2 ± 0.2	0.16	-43 ± 7	75.6 ± 0.5%	7 ± 0.6	149 ± 4	4 ± 2%	Yes	n.d.	96 ± 13%
UT2A [42]	181 ± 6 D(10) 139 ± 6 D(50) 229 ± 12 D(90) 377 ± 34 Span 1.1 ± 0.1	0.17	n.d.	n.d.	n.d.	n.d.	n.d.	Yes	n.d.	110 ± 2%
CIDETEC	157 ± 17 D(10) 96 ± 11 D(50) 170 ± 8 D(90) 309 ± 4 Span 1.3 ± 0.2	0.17	-45 ± 7	**n.d.**	6 ± 1	154 ± 6	5 ± 2%	Yes	1 ± 0.4	100 ± 4%

n.d., not determined; PDI, polydispersity index.

Chapter 3

Arginine-based poly(I:C)-loaded nanocomplexes for the re-education of tumor-associated macrophages

Chapter 3

Arginine-based poly(I:C)-loaded nanocomplexes for the re-education of tumor-associated macrophages

This work has been done in collaboration with the Clinical and Research Hospital Humanitas (Italy).

Abstract

Tumor-associated macrophages (TAMs), with a M2 tolerogenic profile, are key players in the development and dissemination of tumors. Hence, their therapeutic re-education towards an M1 pro-inflammatory and anti-tumoral phenotype can be critical to fight against cancer cells. The activation of the endosomal toll-like receptor 3 by its agonist poly(I:C) has been shown to efficiently drive this polarization process. Unfortunately, poly(I:C) presents significant systemic toxicity, and its clinical use is restricted to a local administration. The objective of this work has been to improve the delivery of poly(I:C) to TAMs, through the use of nanotechnology. Namely, poly(I:C) nanocomplexes with different arginine-rich polymers were developed and, subsequently, enveloped with anionic polymers in order to improve their biodistribution. Poly(I:C) nanocomplexes presented sizes lower than 200 nm, with surface charges ranging from +40 to -20 mV, depending on the enveloping polymer. All the systems presented high poly(I:C) loading values, from 12 to 50% (w/w), and adequate stability in cell culture media. *In vitro*, poly(I:C) nanocomplexes were highly taken up by macrophages, compared to the free drug. The treatment of macrophages with these nanocomplexes stimulated the secretion of the T-cell recruiter chemokines CXCL10 and CCL5, which are of key importance for stablishing an effective anti-tumor immune response. More importantly, poly(I:C) nanocomplexes increased the ability of pre-treated macrophages to directly kill cancer cells. A preliminary study involving the intratumoral administration of the developed nanocomplexes to mice bearing lung tumors showed that the efficacy of poly(I:C) nanocomplexes in terms of reducing tumor growth was not translated *in vivo*. Further studies to assess the potential of this technology in a different *in vivo* setting are planned.

Graphical abstract

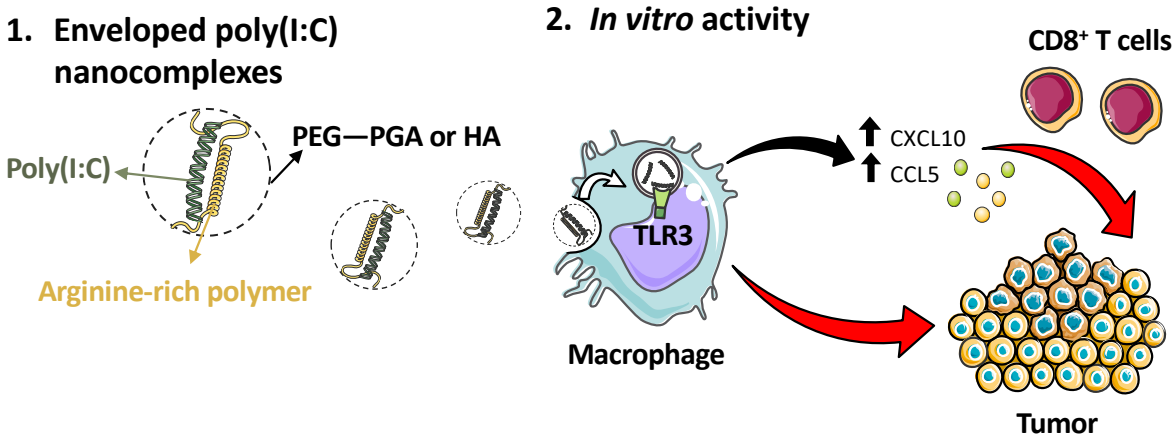

1. Introduction

The discovery of the capacity of the immune system to fight and eliminate tumors has represented a major paradigmatic change in the treatment of cancer, classically addressed with cytotoxic drugs [1,2]. Despite the inherent anti-tumoral capacity of immunocompetent cells, tumors produce immunosuppressive signals which lead to tumor immune tolerance, thus facilitating tumor progression [3–5]. Among the different cells involved in this process, tumor-associated macrophages (TAMs) are key players with the capacity to promote the proliferation of cancer cells, angiogenesis and metastasis [5–8]. TAMs present anti-inflammatory and tolerogenic features, characteristic of M2-like macrophages [9]. Importantly, recent investigations have proposed the possibility to reprogram TAMs towards pro-inflammatory and anti-tumoral M1 states as a promising approach to re-activate the immune response against the tumor [10–12].

An important strategy to re-educate TAMs towards an M1-like phenotype [13,14], has relied on the use of agents that activate the toll-like receptors (TLR) [12,15]. Upon interaction with their corresponding agonists, TLRs activate MyD88 and TRIF pathways, thereby triggering innate and adaptive immune responses [16,17]. Indeed, some of these agonists are already marketed, or under clinical trials, for vaccination and/or cancer applications [17]. Among the TLR agonists, poly(I:C), a double-stranded (ds)RNA that activates the TLR3, has shown the capacity to polarize TAMs towards a M1-like anti-tumoral phenotype [18]. Nevertheless, the clinical potential of poly(I:C) has been undermined by its indiscriminate biodistribution and subsequent systemic side effects [19]. In this sense, the association of poly(I:C) into a nano-delivery system could improve its accumulation into TAMs and, consequently, its safety profile [20–26].

Synthetic nanosystems for polynucleotide delivery are mainly based on their complexation with positively charged lipids or polymers [27–29]. For example, it has been reported that the complexation of poly(I:C) with cationic polymers, i.e. polyethyleneimine (PEI), leads to positive *in vivo* results in different cancer models [30], and is currently in a phase I clinical trial [31]. Unfortunately, PEI itself is not absent of systemic toxicity [32]. In our research group, we have explored alternative nanocarriers for the delivery of polynucleotides. Based on the known capacity of cell penetrating peptides (CPPs) to efficiently condense nucleic acids and facilitate their transport across biological barriers [33], we have developed polyarginine- (pArg) and protamine-based nanosystems, which have shown the capacity to efficiently deliver different polynucleotides [34–36]. Indeed, we have recently reported the formation of nanocomplexes of polynucleotides with cationic molecules, and their subsequent envelopment with an hydrophilic anionic polymer named as enveloped nanocomplexes (ENCPs), as a way to facilitate the delivery of miRNA to the brain [36].

Based on this background information, the main objective of this study has been to develop a delivery carrier for poly(I:C), that would enable its systemic administration and result in the re-education of TAMs. With this idea in mind, we selected different arginine-rich polymers and oligomers for the complexation of poly(I:C) and, subsequently, we enveloped these positively charged nanocomplexes with pegylated polyglutamic acid (PEG–PGA) or hyaluronic acid (HA) to produce ENCPs [36]. Following a rigorous characterization in terms of particle size, zeta potential and drug loading capacity, the ENCPs were evaluated *in vitro* for their toxicity, internalization and capacity to revert the polarization of macrophages towards an M1-like anti-tumoral phenotype. The capacity of the macrophages treated with nanoformulated poly(I:C) to secrete T-cell attracting chemokines and to kill cancer cells was also assessed. Finally, an *in vivo* efficacy study was conducted to evaluate the anti-tumor capacity of the developed ENCPs following intratumoral administration.

2. Materials and Methods

2.1. Materials

n-Butyl-poly(L-arginine) hydrochloride (pArg) (150 arginine residues, MW 24 kDa) and the different pegylated-poly(L-glutamic acid) (PEG–PGA) polymers were purchased from Polypeptide Therapeutic Solutions (PTS, Valencia, Spain). For the PEG–PGA, three types of branched conformations were acquired: PGA, either 10 or 30 units, with a molar substitution degree of 10 or 30% of PEG (5 kDa), referred as: PEG_{5k}10–PGA10, PEG_{5k}10–PGA30 and PEG_{5k}30–PGA10. Also, two conformation of the diblock PEG-PGA were purchased: 10 units of PGA and a 20 kDa PEG tail; and 30 units of PGA with a 5 kDa PEG tail, named as diblock PEG_{20k}–PGA10 and diblock PEG_{5k}–PGA30, respectively.

Octa-D-arginine (r8) and a laurate octa-D-arginine (C12r8) were obtained from ChinaPeptides (Shanghai, China). Sodium hyaluronate (HA) (MW 57 kDa) was purchased from Lifecore Biomedical (MN, USA). HMW poly(I:C) and poly(I:C)-rhodamine were acquired from InvivoGen (CA, USA). Endotoxin-free water was used for all the *in vitro* experiments.

2.2. Preparation of the nanocomplexes

2.2.1. Screening of arginine-rich polymers

To 400 µL of arginine-rich polymer solution (0.5, 1 or 2 mg/mL), 200 µL of poly(I:C) (at 1 or 0.5 mg/mL) were added under mild magnetic stirring. Weight ratios polymer to poly(I:C) 1:1, 2:1 and 4:1 were tested (**Table 1**). After 1–5 min of stirring, the resulting nanocomplexes were allowed to stabilize for at least 3 min before further characterization or envelopment.

Table 1. Summary of the weight ratio polymer to poly(I:C) tested, and the final concentration of each component.

(+) polymer	Ratio (+) polymer: poly(I:C) (w/w)	(+) polymer (mg/mL)	Poly(I:C) (mg/mL)
r8; C12r8; pArg	1:1	0.33	0.33
	2:1	0.33 / 0.67	0.17 / 0.33
	4:1	0.67 / 1.33	0.17 / 0.33

C12r8, laurate-octaarginine; pArg, poly-arginine; r8, octaarginine; w/w, weight/weight.

2.2.2. Envelopment with PEG–PGA polymers

A volume of 400 µL of a PEG–PGA aqueous solution at 1 mg/mL was added to a round bottom flask and the water evaporated in a rotavapor (Heidolph Hei−VAP Advantage, Schwabach, Germany) for 10 min, at 37 °C, under vacuum and mild rotary speed, until a thin film was formed. Then, the same volume of nanocomplexes (with a poly(I:C) concentration of 0.33 or 0.17 mg/mL) (**Table 2**), was added to the round bottom flask, in order to achieve their envelopment by PEG–PGA, under the same rotary speed, room temperature and at atmospheric pressure for 10 min.

Table 2. Final concentrations of poly(I:C), complexing polymers and polyglutamic pegylated acid in the enveloped nanocomplexes (ENCPs)

(+) polymer	Ratio (+) polymer:poly(I:C) :PEG–PGA (w/w)	(+) polymer (mg/mL)	Poly(I:C) (mg/mL)	PEG–PGA (mg/mL)
C12r8	2:1:6	0.33	0.17	1.00
	4:1:6	0.67	0.17	1.00
	4:1:3	1.33	0.33	1.00
pArg	1:1:3	0.33	0.33	1.00

C12r8, laurate-octaarginine; pArg, poly-arginine; PEG–PGA, pegylated polyglutamic acid; w/w, weight/weight.

2.2.3. Envelopment with HA

To 250 µL of the nanocomplexes with a poly(I:C) concentration of 0.33 or 0.17 mg/mL, the same volume of an HA solution of concentrations ranging from 0.25 to 2.00 mg/mL, was added under mild magnetic stirring, for a final poly(I:C) to HA weight ratio of 1:1.5, 1:3 or 1:6 (**Table 3**). The ENCPs were allowed to be formed for 5 min under stirring, and to be stabilized during other 5 min prior to their characterization.

Table 3. Final concentrations of poly(I:C), complexing polymers and hyaluronic acid in the enveloped nanocomplexes (ENCPs)

(+) polymer	Ratio (+) polymer: poly(I:C) : HA (w/w)	(+) polymer (mg/mL)	Poly(I:C) (mg/mL)	HA (mg/mL)
C12r8	2:1:1.5	0.17	0.08	0.13
	2:1:3	0.17	0.08	0.25
	2:1:6	0.17	0.08	0.50
	4:1:1.5	0.67	0.17	0.25
	4:1:3	0.67	0.17	0.50
	4:1:6	0.67	0.17	1.00
pArg	1:1:1.5	0.17	0.17	0.25
	1:1:3	0.17	0.17	0.50
	1:1:6	0.17	0.17	1.00

C12r8, laurate-octaarginine; HA, hyaluronic acid; pArg, poly-arginine; w/w, weight/weight.

2.3. Nanoparticle characterization by dynamic light scattering (DLS)

The mean particle size (Z-average) and polydispersity index (PDI) of the non-diluted samples were characterized by DLS. The zeta potential values were determined by Laser Doppler Anemometry (LDA), measuring the mean electrophoretic mobility after a 20-times dilution of the ENCPs in ultrapure water. These properties were measured using a Zetasizer® NanoZS, using the software Zetasizer v7.13 (Malvern Panalytical Ltd., Malvern, UK), and were performed at 25 °C with a detection angle of 173.

2.4. Electron microscopy

Field Emission Scanning Electron Microscopy (FESEM) (Zeiss Gemini Ultra Plus, Oberkochen, Germany) was used to evaluate the particle size and morphology. ENCPs were diluted between 1:100 to 1:1000 in water, and then 1:1 with phosphotungstic acid (2 % in water). A sample volume of 1 µL was placed on a copper grid with carbon films and, once dried, it was washed with 1 mL of ultrapure water. Dried samples were analyzed under the microscope using the InLens detector.

2.5. Nanocomplex stability in cell culture media

The colloidal stability of the different ENCPS in cell culture media (RPMI + 10% FBS + 2% penicillin/streptomycin) was assessed at 37 °C for up to 24 h. For this purpose, ENCPs were diluted 5 times in pre-warmed media, or water as the control, and particle size and PDI measured at 0, 4 and 24 h of incubation.

2.6. Agarose gel retardation assay

To qualitatively determine the amount of poly(I:C) complexed by the polymers, samples were loaded in an agarose gel at 1% w/v in Tris Acetate-EDTA buffer (Sigma-Aldrich, MO, USA) before and after the incubation with an excess of heparin for poly(I:C) displacement. Each lane was loaded with 2.5 μg of poly(I:C) and with 1x SYBR®Gold nucleic acid stain (Invitrogen, CA, USA). For the displacement with heparin, 20:1 and 500:1 weight ratios of heparin (Sigma-Aldrich, MO, USA) to poly(I:C) were added for the C12r8 or pArg ENCPs, respectively, and incubated for 30 min at 37 °C. Control lanes included a DNA 1kb ladder (Invitrogen, CA, USA), and free poly(I:C) in the same conditions as the ENCPs. Gels were run for 30 min at 90 V in a Sub-Cell GT cell 96/192 (Bio-Rad Laboratories, CA, USA), evaluated with an UV transilluminator (Molecular Imager® Gel Doc™ XR, Bio-Rad Laboratories, CA, USA) and analyzed with Image Lab™ Software (Bio-Rad Laboratories, CA, USA).

For the release of poly(I:C), ENCPs were incubated in cell culture media, in a 1:1 (v/v) ratio, for 4 or 24 h in prior to been processed as described above. Free poly(I:C) exposed to the same conditions was used as the control.

2.7. Human primary macrophage differentiation

Human primary monocytes from blood of healthy donors were purified through density gradients, as previously reported [37]. M0 macrophages were obtained by culturing 1 x 10^6 cells/mL human monocytes for 5 days in 5% FBS/RPMI supplemented with 25 ng/mL of recombinant human M-CSF (rhM-CSF; PeproTech, London, UK). M1 macrophages were polarized by stimulating M0 macrophages with LPS (100 ng/mL) (PeproTech, London, UK) and IFN-γ (50 ng/mL) (PeproTech, London, UK) for 24 h, and M2 macrophages were obtained by polarizing M0 macrophages with IL-4 (20 ng/mL) (PeproTech, London, UK) for 24 h. These cells were seeded in multiwell plates as indicated below for each experiment and incubated at 37 °C and 5% CO_2.

2.8. Cell viability studies

M0 and M2 human-derived macrophages were isolated and differentiated, as already described, and seeded in 96-well plates at a density of 1 x 10^5 cells/well. Cells were treated with poly(I:C), in solution or nanocomplexed, at poly(I:C) concentrations of 1, 5, 10 and 20 μg/mL. Macrophages were incubated with the nanosystems for 1, 24 or 48 h at 37 °C, and cell viability was determined by Alamar Blue assay (Invitrogen, CA, USA). This method is based on the capacity of living cells to reduce resazurin to resorufin, that is highly fluorescent. Fluorescence intensity was measured in a plate reader (Synergy H4, BioTek, VT, USA), setting the λ_{abs} at 560 nm and the λ_{em} at 590 nm. Macrophages treated only with

cell culture media were used as controls and considered as 100% cell viability. Cell viability was calculated according to **equation 1**.

$$\%\ Cell\ viability = \left(1 - \frac{Fluorescence}{Control\ fluorescence}\right) \times 100 \qquad \textbf{Eq. 1}$$

2.9. Uptake studies

Human monocytes were purified and polarized towards M0 macrophages as described in section 2.7. These cells were seeded at a density of 1 x 10^6 cells/well in low-attachment 24-well plates, and 0.5 mL of fresh RPMI media containing poly(I:C), either free or nanocomplexed, were added to them. The final poly(I:C) dose per well was of 5 µg/mL of poly(I:C), of which 0.25 µg/mL were poly(I:C)-rhodamine. After 24 h of incubation, cells were detached from the wells with trypsin-EDTA. Cells were then washed one time with FACS buffer (PBS 1% BSA) and fixed in FACS Fix for 20 min at 4 °C. Cell suspensions were centrifuged at 1750 rpm for 10 min and 4 °C. The supernatants were then discarded, and cells re-suspended in 300 µL of FACS buffer (PBS 1% BSA). Treated macrophages were analyzed by flow cytometry using a BD LSR Fortessa™ (BD Biosciences, CA, USA), and the resulting data analyzed by FACS Diva software (BD Biosciences, CA, USA), determining the mean fluorescence intensity (MFI) of rhodamine-positive cells. Results are expressed as fold change in comparison to the free poly(I:C)-rhodamine.

2.10. Co-localization studies

Purified human monocytes were seeded in 24-well plates with a round glass coverslip at the bottom, at a density of 1 x 10^6 cells/well in 1 mL complete RPMI supplemented with M-CSF (25 ng/ml) to differentiate them to M0 macrophages. At day 5, 10 µl/well of CellLight® lysosome-GFP, BacMam 2.0 (Molecular Probes, OR, USA) was added. At day 6, coverslips were washed and poly(I:C), free or in pArg:pIC ENCPs, was added in 500 µl of fresh complete RPMI for 2 or 8 h. The final poly(I:C) dose per well was 5 µg/mL, of which 0.25 µg/mL were poly(I:C)-rhodamine. After incubation, cells were washed one time with PBS and fixed in 4% PFA (in PBS) for 10 min at room temperature. The glass coverslip was then recovered, mounted and analyzed with a Leica TCS SP8 3X SMD confocal microscope (Leica Microsystems, Wetzla, Germany).

2.11. Macrophage surface marker expression

M0 or M2 human-derived macrophages were seeded in 24-well low-attachment plates at a density of 1 x 10^6 cells/well and incubated in 5% FBS supplemented RPMI for 48 h at 37 °C. Macrophages were then incubated with 5 µg/mL of poly(I:C), either in solution or nanocomplexed. M1 macrophages were

also used as control, and M2 macrophages were polarized towards M1 phenotypes upon incubation with LPS/IFN-γ. Prior to their staining, cells were washed, collected and resuspended in FACS buffer (PBS 1% BSA). They were then stained with APC-mouse anti-human HLA-DR (552764, BD Biosciences, CA, USA), FITC-mouse anti-human mannose receptor CD206 (551135), anti-human CD163-BV421 (562643), CD80 APC-H7-mouse anti-Human CD80 (Clone L307.4; 561134) and anti-human CD68-PE (556078) (all from BD Biosciences, CA, USA). Cells were analyzed by flow cytometry on FACS Canto II Instrument (BD Biosciences, CA, USA) and the generated data by FACS Diva software. The gated cells were plotted on APC (CD80), PerCP (MHC II), Pacific Blue (CD163) or FITC (CD206) and analyzed for mean fluorescent intensity (MFI). Results are expressed as fold change in comparison to untreated M0 macrophages.

2.12. Secretion of chemokines

The levels of the chemokines CXCL10 and CCL5 were measured by commercially available ELISA kits following the manufacturer's instructions (R&D Systems, MN, USA). The supernatants used were collected after 24 h of treatments.

2.13. Cytotoxicity of treated macrophages towards PANC-1 tumor cell line

The cytotoxicity of the treated macrophages towards cancer cells was performed as described in a recent publication [38]. Briefly, primary monocytes isolated from human healthy donors were stimulated with M-CSF in 5% FBS supplemented RMPI medium for 5 days. Then, macrophages were stimulated with the different ENCPs or free poly(I:C) in a dose of 5 µg/mL for 24 h. Alternatively, macrophages were treated with LPS/IFN-γ or IL-4 to polarize them towards M1 or M2 profiles. After, macrophages were washed and co-incubated for 2 days with 25,000 cells of a pancreatic cancer cell line (PANC-1), that were previously stained with Cell Trace Far Red (Invitrogen, CA, USA). The cells were trypsinized and fixed in FACS Fix for 20 min at 4 °C for flow cytometry analysis using FACS Canto II Instrument (BD Biosciences, CA, USA). For the flow cytometry analysis, acquisition was set to 45 seconds and the number of high fluorescence intensity events (corresponding only to proliferating PANC-1 cells) were counted for each sample and were normalized to the non-treated (M0) macrophages.

2.14. Animals

All animal experiments were done following national and international laws. Wild type C57BL/6 mice were purchased from Charles River Laboratories (Wilmington, MA, USA). Mice were kept in a

specific pathogen-free animal facility at Humanitas Research Institute (Milan, Italy). All efforts were made following the 3Rs principles to minimize the number of animals used and their suffering.

2.15. Anti-tumor efficacy *in vivo*

At day 0, mice were subcutaneously injected with 1 x 10^5 CMT167 cells (European Collection of Authenticated Cell Cultures, Salisbury, UK) in the right flank. Starting from day 9, mice received five intratumoral injections of 75 µL each (poly(I:C) dose = 25 µg/mouse/treatment) in alternative days, over a period of ten days. Mice were divided in groups of 8, and the following treatments were administered: physiological solution, pArg in solution (as negative control), pArg:pIC, pArg:pIC/PEG–PGA, pArg:pIC/HA ENCPs and free poly(I:C). Mice were euthanized at day 27. Tumor volume was monitored over the course of the experiment with a digital caliper. Tumor volume is presented in mm^3 calculated with **equation 2,** where d and D are the shortest and longest diameter in mm, respectively.

$$Tumor\ volume = \frac{d^2 \times D}{2} \qquad \textbf{Eq. 2}$$

2.16. Statistical analysis

Data analysis was performed with GraphPad Prism version 7.0 (GraphPad Inc). Statistical comparison was done using a two-way ANOVA followed by a Tukey's multiple comparison test, or alternatively an ordinary one-way ANOVA followed by a Tukey's multiple comparison test. Data are expressed as the mean ± standard deviation (SD). *p* values of 0.05 or less were considered statistically significant.

3. Results and Discussion

Despite the potential of poly(I:C) for polarizing macrophages towards an anti-tumoral M1-like phenotype with the capacity to fight tumors [38], the systemic administration of this TLR3 agonist presents significant side effects [20]. Therefore, in order to prevent its toxicity and to improve the transport of poly(I:C) to the tumor microenvironment, and more specifically, towards TAMs, we aimed at engineering a nanosystem to improve its delivery. Afterwards, the *in vitro* capacity of the nanocomplexed poly(I:C) to generate a polarization switch in the macrophages was evaluated in human-derived cells. Finally, the correlation of these results with an *in vivo* model was conducted.

3.1. Design and development of the nanocomplexes

3.1.1. Screening of different arginine-rich polymers

As the first step in the development of a poly(I:C)-loaded nanoformulation and, based on a nanotechnology recently reported by our group showing the capacity of modified octaarginine to complex polynucleotides [36], different positively-charged arginine-rich polymers were selected for its complexation. Oligo-arginines have been extensively employed for the delivery of different nucleic acids due to their CPP nature, which increases their uptake and, as a result, improves their therapeutic performance [33,36,39]. For this purpose, and taking as a reference our previous work [36] and additional reports [40], two oligopeptides were selected: octaarginine (r8) and a hydrophobically-modified r8, that contains a laurate chain (C12r8). As a comparison, a higher MW arginine polymer, polyarginine (pArg), was also selected. Weight ratios arginine-rich polymer/oligomer to poly(I:C) ranging from 1:1 to 4:1 were evaluated for their capacity to form nanocomplexes (**Fig. 1**). In the case of the unmodified r8, despite previous works making use of this biomaterial, no stable nanosystems were obtained at the different ratios and thus, its use was discarded. On the contrary, the hydrophobized r8 could form stable nanocomplexes at ratios 2:1 and 4:1, a fact that indicates that the hydrophobic tail of C12r8 is critical for improving the stability of the resulting complexes [41,42]. In the case of the pArg-based nanocomplexes, all ratios yielded particles with sizes increasing from 150 to 300 nm, as the amount of pArg increased (**Fig. 1A**). Positive surface charge values incremented following the same trend (**Fig. 1B**).

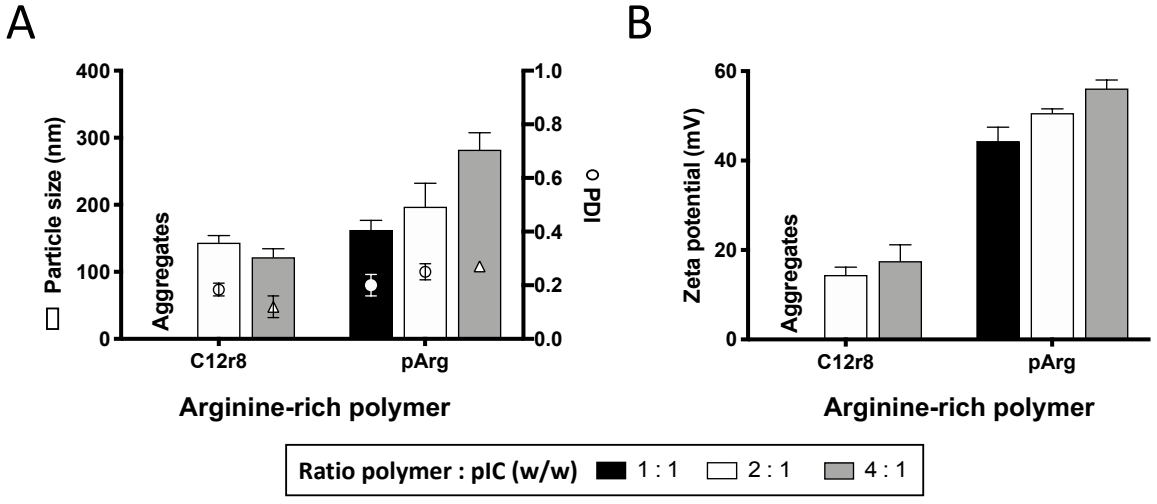

Figure 1. Screening of different arginine-rich polymers capable of complexing poly(I:C). Values of (A) particle size, PDI and (B) zeta potential of the nanocomplexes obtained for the different ratios tested. Values represent mean ± SD (n ≥ 3). C12r8, laurate-octaarginine; pArg, polyarginine; PDI, polydispersity index; pIC, poly(I:C); w/w, weight/weight.

In order to evaluate their suitability for *in vitro* testing, the nanocomplexes were incubated in cell culture media at 37 °C, to evaluate their stability. In the case of C12r8, the particle size of the nanocomplexes increased upon incubation in cell culture media (**Supporting Information, Fig. S1A**). On the contrary, pArg-based nanosystems (ratio 1:1) maintain their particle size under the same conditions (**Supporting Information, Fig. S1B**). We hypothesized that the different stability of the nanocomplexes could be due to their different MWs, since the long positive chains of the pArg would offer a higher number of positive sites for binding the dsRNA, in comparison to the smaller chains of the C12r8 [43].

3.1.2. Nanocomplexes enveloped with PEG–PGA

In order to improve the nanocomplexes stability, we applied the technology previously described from our group [36,44] and used different pegylated polyglutamic acid (PEG–PGA) copolymers for the envelopment of the nanocomplexes. The presence of PEG as the external layer of the system was intended to provide a steric protection and increase its colloidal stability [45]. Additionally, the combination of PEG and PGA as the external layer of polymeric nanocapsules has already been shown to facilitate their access to the tumor site in a passive manner [46], and to improve the stability of C12r8-based nanocomplexes in biologically relevant media [44,47].

It has been extensively reported that both, the PEG layer density and its conformation, are two key aspects in determining the fate and stability of the nanosystems [48,49]. In this work, we investigated different parameters of the copolymers with the idea to optimize the enveloping process, namely (*i*) a branched or diblock conformation, (*ii*) the length of the PGA chain, and (*iii*) the PEG density. For this purpose, branched copolymers with two PGA lengths (10 and 30 units) and different PEG substitution degrees (10 and 30%) were studied. At the same time, two diblock copolymer conformations with PGA lengths of 10 and 30 units, and a PEG tail of 20 and 5 kDa MW, were also evaluated (**Supporting Information, Fig. S2**).

For the enveloping process, we searched for the optimal amount of PEG–PGA for an efficient coating. First, the C12r8:pIC nanocomplexes were enveloped with PEG–PGA for a weight ratio C12r8:pIC:PEG–PGA 2:1:6. As illustrated in **Fig. 2A–B** (left panel), the resulting ENCPs presented highly dispersed sizes, and the surface charged decreased after the envelopment. On the other hand, the branched PEG10–PGA10 and the diblock PEG_{5k}–PGA30 were able to switch the zeta potential of these ENCPs towards negative values (**Fig. 2B**, left panel).

In parallel, we conducted the same envelopment for the C12r8:pIC nanocomplexes that have a higher amount of C12r8 (weight ratio C12r8:pIC:PEG–PGA 4:1:6). In this case, particle sizes were narrower and, although surface charge was decreased, only the diblock PEG_{5k}–PGA30 generated a zeta-potential inversion (**Fig. 2A–B,** mid panel).

Finally, taking into consideration that other works have employed a lower amount of PEG–PGA for the envelopment process [36,44], we evaluated the possibility of decreasing this value (weight ratio C12r8:pIC:PEG–PGA 4:1:3). Upon the envelopment, particle size slightly increased, while only a moderate decrease in the surface charge was observed, with no charge inversion for any of the conditions (**Fig. 2A–B,** right panel).

It is interesting to mention that the branched PEG30–PGA10 did not produce an important change in the surface charge of any of the ENCPs (**Fig. 2B**), behavior already reported for similar systems [44]. In this regard, we can speculate that the small size of the PGA chain, and the high number of PEG tails, might hinder the adequate interaction of the polymer with the systems, making this copolymer inadequate for an efficient coating of the nanocarriers.

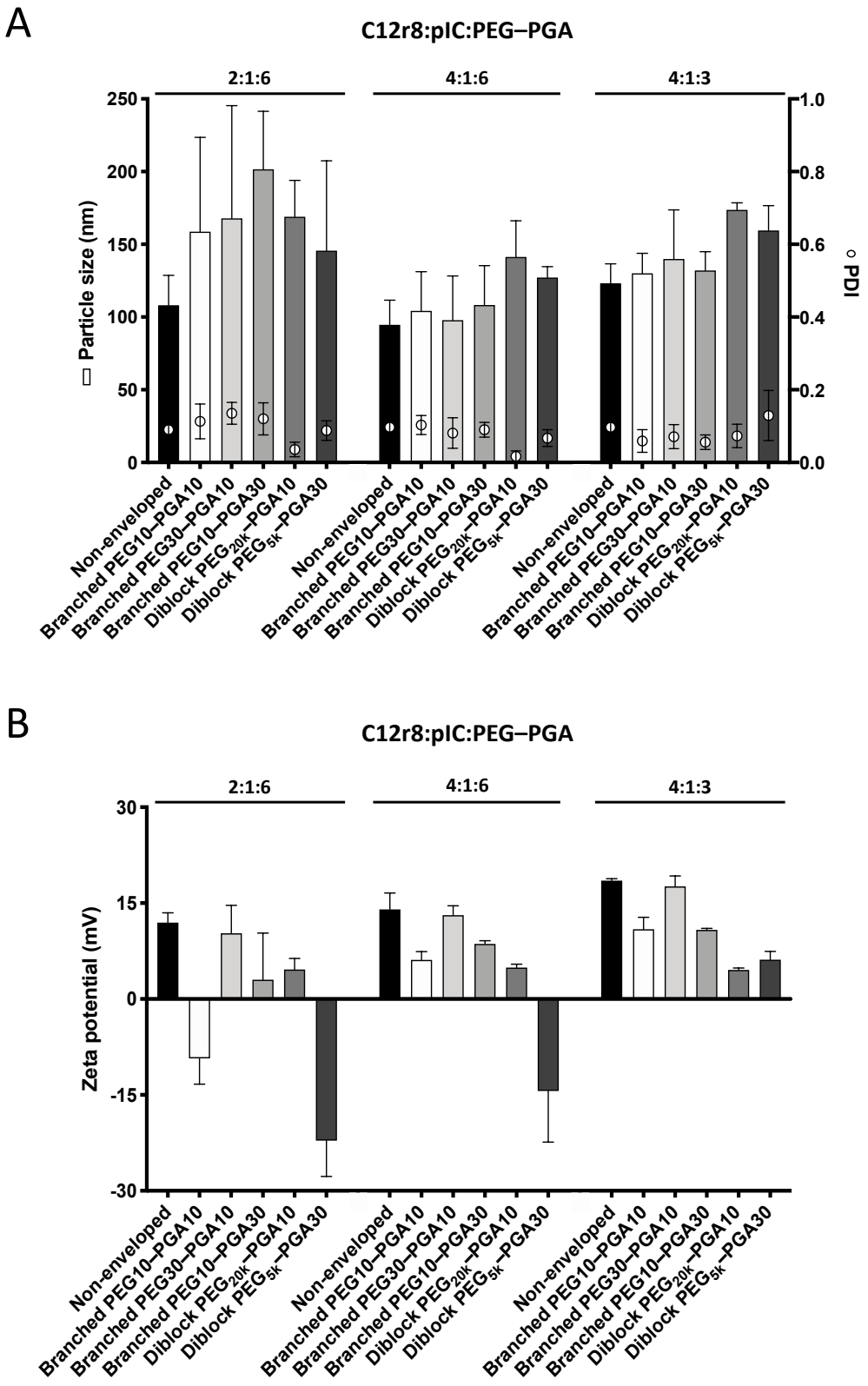

Figure 2. Envelopment of poly(I:C)-loaded nanocomplexes with PEG–PGA. (A) Particle size, PDI and (B) zeta potential of the C12r8 nanocomplexes yielded from the different ratios and types of PEG–PGA tested. Values represent mean ± SD (n ≥ 3). C12r8, laurate-octaarginine; PEG–PGA, pegylated polyglutamic acid; PDI, polydispersity index; pIC, poly(I:C).

To determine the efficiency of PEG–PGA envelopments in improving the ENCPs stability, the variation of their physicochemical properties in cell culture media were monitored (**Supporting Information, Fig. S3**). The results showed that only the diblock copolymer PEG_{20k}–PGA10 was able to stabilize the nanocomplexes in a weight ratio C12r8:pIC:PEG–PGA 4:1:3 (**Supporting Information, Fig. S3A–C**). As above-mentioned, this stability would probably be related to the steric protection provided by the PEG moieties, and, very likely, only this diblock polymer was able to generate an efficient PEG density surrounding the system. Similar C12r8 nanosystems enveloped with this PEG–PGA arrangement were also significantly stabilized [36,47], which confirms that this diblock combination of a low number of PGA units (10) with a long PEG tail (20 kDa) provides good steric protection to a nanosystem.

After the selection of the diblock PEG_{20k}–PGA10 polymer for enveloping the C12r8 nanocomplexes, we applied the same enveloping conditions to the pArg nanocomplexes (weight ratio pArg:pIC:PEG–PGA 1:1:3). These ENCPs presented a particle size of 190 ± 15 nm, low PDI values (0.18) and a lower positive surface charge (+26 ± 8 mV). Furthermore, the colloidal stability in cell culture media showed that all ENCPs properties were maintained after 24 h of incubation (**Supporting Information, Fig. S3D**), concluding that this diblock PEG_{20k}–PGA10 has highly interesting properties for increasing the stability of nanosystems.

3.1.3. Nanocomplexes enveloped with HA

Hyaluronic acid (HA) was also evaluated for the envelopment of the nanocomplexes, based on its anionic character and stealth properties [50–52]. Indeed, a recent report has claimed that HA coatings are able to decrease the adsorption of immunogenic proteins, in comparison to other anionic coatings [53]. All these characteristics were expected to confer stability to the ENCPs, together with longer circulation times.

In line with this, several weight ratios of HA were evaluated for enveloping the C12r8 and the pArg nanocomplexes. In the case of C12r8, the lowest amounts of HA (weight ratio C12r8:pIC:HA 2:1:1.5, 4:1:1.5 and 4:1:3) led to aggregation, probably because the surface charges of the ENCPs were close to neutrality. In the rest of the cases (weight ratios C12r8:pIC:HA 2:1:3, 2:1:6 and 4:1:6; and pArg:pIC:HA 1:1:1.5, 1:1:3 and 1:1:6), the ENCPs presented sizes of 150–200 nm and negative surface charges.

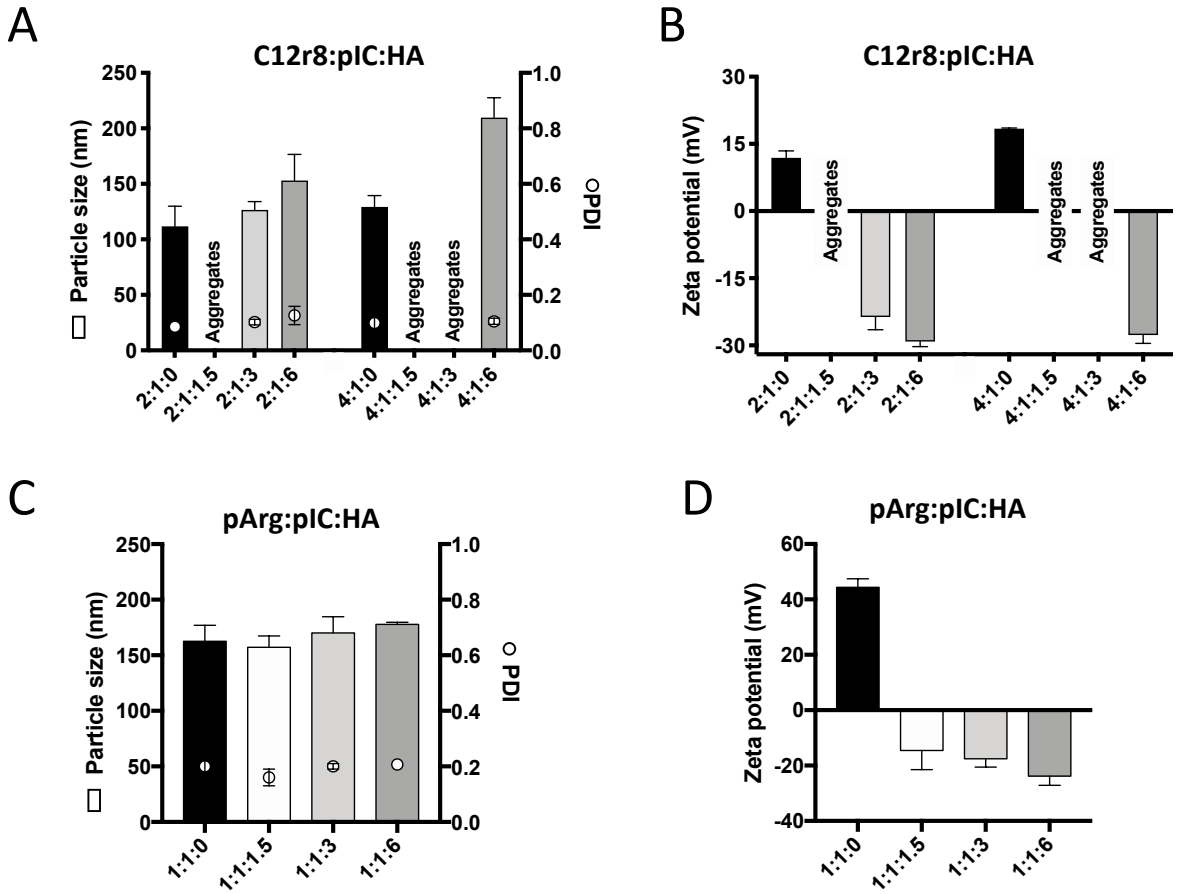

Figure 3. Envelopment of poly(I:C)-loaded nanocomplexes with hyaluronic acid. Influence of the ratio of arginine-rich polymer:pIC:HA for the different (A, B) C12r8 and (C, D) pArg nanocomplexes. Values of (A, C) particle size, PDI and (B, D) zeta potential of the nanocomplexes obtained after adding the different ratios of hyaluronic acid. Values represent mean ± SD (n ≥ 3). C12r8, laurate-octaarginine; HA, hyaluronic acid; pArg, poly-arginine; PDI, polydispersity index; pIC, poly(I:C).

When evaluating the stability in cell culture media, none of the C12r8 ENCPs were sufficiently stable after the envelopment with HA, reason why they were discontinued for the following experiments (**Supporting Information, Fig. S4A**). Oppositely, for HA-enveloped pArg nanosystems, all ENCPs were stable after incubation in cell culture media (**Supporting Information, Fig. S4B**). Among them, the weight ratio pArg:pIC:HA 1:1:1.5 showed the best properties in terms of its short-term stability (data not shown), and, therefore, was selected for further evaluation.

Regarding the different stability of the HA-enveloped nanosystems, it is known that the presence of salts and the high ionic strength of the cell culture media can potentially disturb the ionic interactions governing the stability of some colloidal systems [54]. Additionally, we hypothesized that the different MW of pArg and the C12r8 can cause a more tightly attachment of the HA coating in the case of the longer chains of the pArg, increasing their stability in cell culture media.

Overall, the conclusion from these envelopment tests is that the process needs to be optimized in a case-by-case basis, and that the envelopment is highly determined by the nanocomplexes composition and the nature of the enveloping polymer.

3.2. Association capacity of poly(I:C) to the enveloped nanocomplexes (ENCPs)

After the screenings described in the precedent sections, a total of four ENCPs were selected to investigate their capacity to polarize macrophages: non-enveloped, diblock PEG_{20k}–PGA10 enveloped and HA-enveloped pArg nanocomplexes (pArg:pIC ENCPs; pArg:pIC/PEG–PGA ENCPs and pArg:pIC/HA ENCPs, respectively) and diblock PEG_{20k}–PGA10 enveloped C12r8 nanocomplexes (C12r8:pIC/PEG–PGA ENCPs). Their main physicochemical properties are summarized in **Figure 4A**. All ENCPs presented particle sizes between 150 and 200 nm, with low PDIs and surface charges ranging from highly positive (pArg:pIC), through neutral (C12r8:pIC/PEG–PGA) to negatively charged (pArg:pIC/HA). Remarkably, high loading values of poly(I:C) were obtained for the different systems (**Fig. 4A**). Electron microscopy verified the size, homogeneity and spherical shape of the ENCPs (**Fig. 4B**).

Secondly, the efficacy of the ENCPs to associate poly(I:C) was qualitatively evaluated. An agarose gel retardation assay confirmed that all nanosystems efficiently interacted with poly(I:C), with no free poly(I:C) detected, and the incubation with the competitor polyanion heparin was able to partially displace the cargo (**Fig. 4C**). Moreover, the incubation of the nanocomplexed poly(I:C) in cell culture media during 4 or 24 h did not disrupt the interaction between poly(I:C) and pArg (**Fig. 4D** and **Supporting Information, Fig. S5A** lanes 2–7). Instead, free poly(I:C) suffered a degradation when exposed to the cell culture media, as noted by the decrease in the MW (**Fig. 4D** and **Supporting Information, Fig. S5A** lane 2). This degradation was probably caused by the RNases present in the media, since this degradation did not happen in water in the same conditions (**Supporting Information, Fig. S5B).**

In the case of the C12r8:pIC/PEG—PGA ENCPs, poly(I:C) was not released upon incubation in cell culture medium, but after the displacement with heparin some degradation could be observed at 4 and 24 h (**Fig. 4D** and **Supporting Information, Fig. S5A** lanes 9–10). Nevertheless, we cannot discard that this degradation in the C12r8:pIC/PEG—PGA ENCPs was due to the interaction of the displaced poly(I:C) with the media, since degradation occurs even after 15 min of incubation in media, but not in water (**Supporting Information, Fig. S5B).** Therefore, these results demonstrate the capacity of the ENCPs to protect and prevent the premature release of poly(I:C).

A

Formulation	Ratio (w/w)	Particle size (nm)	PDI	ζ-Potential (mV)	Poly(I:C) loading (%)
pArg:pIC	1:1	163 ± 14	0.20	+44 ± 3	50
pArg:pIC /PEG–PGA	1:1 :3	190 ± 14	0.18	+26 ± 8	20
pArg:pIC /HA	1:1 :1.5	157 ± 10	0.16	-15 ± 7	29
C12r8:pIC /PEG–PGA	4:1 :3	165 ± 14	0.07	+5 ± 1	12.5

Mean ± SD, n ≥ 12. C12r8, laurate octa-arginine; HA, hyaluronic acid; pArg, polyarginine; PDI, polydispersity index; PEG–PGA, pegylated polyglutamic acid; pIC, poly(I:C); w/w: weight/weight.

B

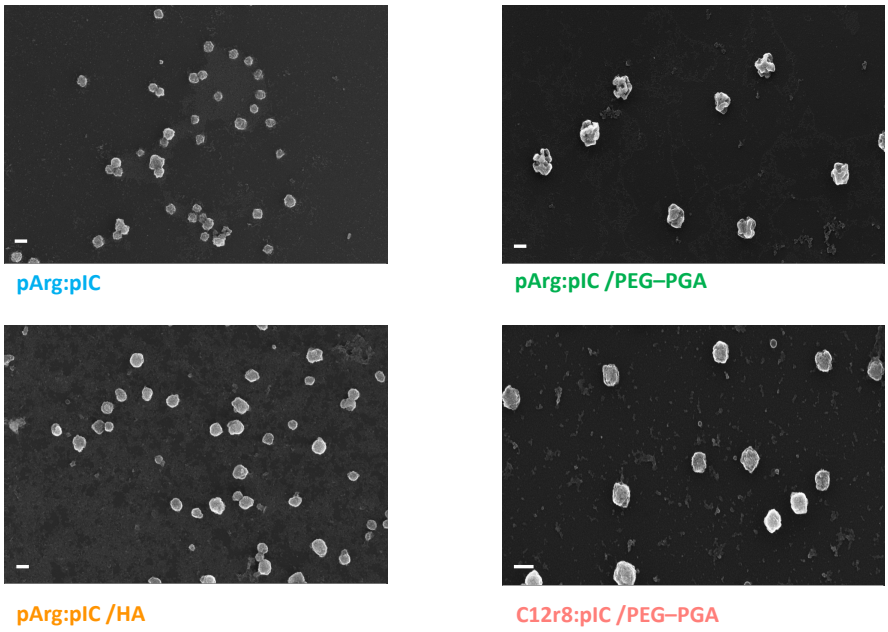

C

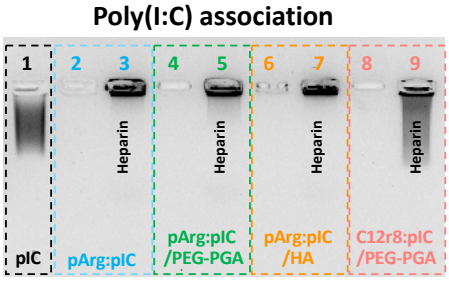

D

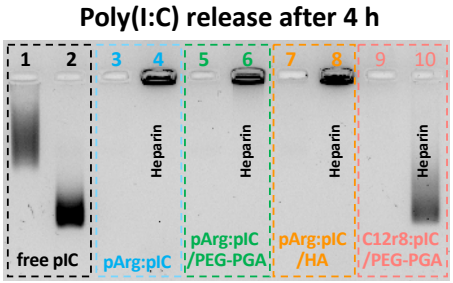

Figure 4. Physicochemical properties and poly(I:C) binding affinity of the selected nanocomplexes. (A) Summary of the main physicochemical properties of the four nanosystems, and (B) FESEM images of each prototype. Values represent mean ± SD (n ≥ 12). Size bars represent 200 nm. (C) Agarose gel retardation assay to evaluate the poly(I:C) binding capacity of the nanocomplexes. Lanes: (1) free poly(I:C), (2, 4, 6, 8) are pArg:pIC, pArg:pIC/PEG–PGA, pArg:pIC/HA and C12r8:pIC/PEG–PGA nanocomplexes, respectively; and (3, 5, 7, 9) are the corresponding nanocomplexes incubated with heparin. (D) Agarose gel retardation assay to evaluate the release and integrity of poly(I:C) after 4 h of incubation in cell culture media at 37 °C. Lanes: (1) free poly(I:C) in solution and (2) in cell culture media; (3, 5, 7, 9) are pArg:pIC, pArg:pIC/PEG–PGA, pArg:pIC/HA and C12r8:pIC/PEG–PGA nanocomplexes in cell culture media; and (4, 6, 8, 10) are the same conditions incubated with heparin. C12r8, laurate-octaarginine; FESEM, field emission scanning electron microscopy; HA, hyaluronic acid; pArg, poly-arginine; PEG–PGA, pegylated polyglutamic acid; PDI, polydispersity index; pIC, poly(I:C); w/w, weight/weight.

3.3. *In vitro* toxicity of the nanocomplexes

Considering that the target cells of the developed ENCPs are TAMs, primary human monocyte-derived macrophages were used to evaluate the *in vitro* toxicity of the nanosystems. M0 or M2 macrophages were incubated with the selected ENCPs for different times. When M0 macrophages were exposed to different concentrations of free or nanocomplexed poly(I:C) for 24 h, minor toxicity values were observed for the lowest doses (1 and 5 μg/mL), with no significant differences among ENCPs (**Fig. 5A**). At higher doses (10 and 20 μg/mL), the poly(I:C) nanocomplexed with C12r8 showed significantly higher toxicity than the free dsRNA (**Fig. 5A**). This increased toxicity could be caused by the higher amount of the polypeptide C12r8 in comparison to pArg for the same dose of poly(I:C) (weight ratio 4:1 and 1:1, respectively), and due to the intrinsic toxicity of CPPs [55]. Similarly, the pArg-based formulations at 20 μg/mL of poly(I:C) were also significantly more toxic than the free molecule in solution (**Fig. 5A**). It is expected that the better biodistribution in *in vivo* conditions will compensate this toxicity.

A similar tendency was observed for M2 macrophages, showing higher toxicities for all the ENCPs at 20 μg/mL of poly(I:C), while the lower doses were much better tolerated (**Fig. 5B**). As expected, shorter incubation times (**Supporting Information, Fig. S6A, C**) produced negligible toxicities, while longer incubation times decreased cell viability (**Supporting Information, Fig. S6B, D**).

As a whole, these experiments were also intended to find a compromise between biocompatible and effective doses of poly(I:C). In this sense, 5 μg/mL of poly(I:C) was selected as a suitable non-toxic concentration for the following experiments.

3.4. Uptake and cellular internalization of the nanocomplexes by macrophages

In order to bind to its intracellular receptor (TLR3), poly(I:C) must be internalized by the macrophages. Thus, we evaluated if the uptake of poly(I:C) was improved when included into the ENCPs. Using rhodamine-labeled poly(I:C), the ability of macrophages to internalize free and nanocomplexed poly(I:C), together with its localization inside the cells, were studied. When complexed only with pArg, the uptake of poly(I:C) was highly improved, which could be related to the high positive surface charge of these ENCPs (**Fig. 5C**). Similarly, a higher uptake versus the free poly(I:C) was also observed for the HA-ENCPs, probably associated to the CD44 affinity of HA [56]. In the case of the two PEG–PGA ENCPs, the uptake was only slightly better than the free dsRNA. These results could be caused by the effect of the PEG chains, which might decrease the interaction of the ENCPs with the cell membrane, thus preventing their uptake by macrophages, as reported before for other

nanoparticles [47,57]. However, in the *in vivo* scenario, the stealth properties of the polymer-enveloped nanosystems and their capacity to be accumulated in the tumor environment could compensate this drawback.

The ultimate target of the developed poly(I:C) ENCPs is the intracellular endosomal receptor TLR3. In order to confirm that the poly(I:C) associated to the ENCPs was able to reach this receptor, we studied the localization of the free and nanocomplexed poly(I:C) once inside the cells. For this, pArg:pIC ENCPs containing rhodamine-labeled poly(I:C), and CellLight® were used to track the cargo and the endosomes, respectively. Confocal microscopy studies confirmed the presence of high amounts of poly(I:C) (in red) inside the endosome (in green) after 2 and 8 h of incubation, confirming the co-localization of the drug and its target (**Fig. 5D** and **Supporting Information, Fig. S7**). A similar intracellular trafficking is expected for the C12r8 ENCPs, since other r8-based complexes have been shown to be taken up by endocytosis [58]. Therefore, the inclusion of poly(I:C) into ENCPs did not affect its internalization pathway, allowing the drug to reach its endosomal TLR3 target.

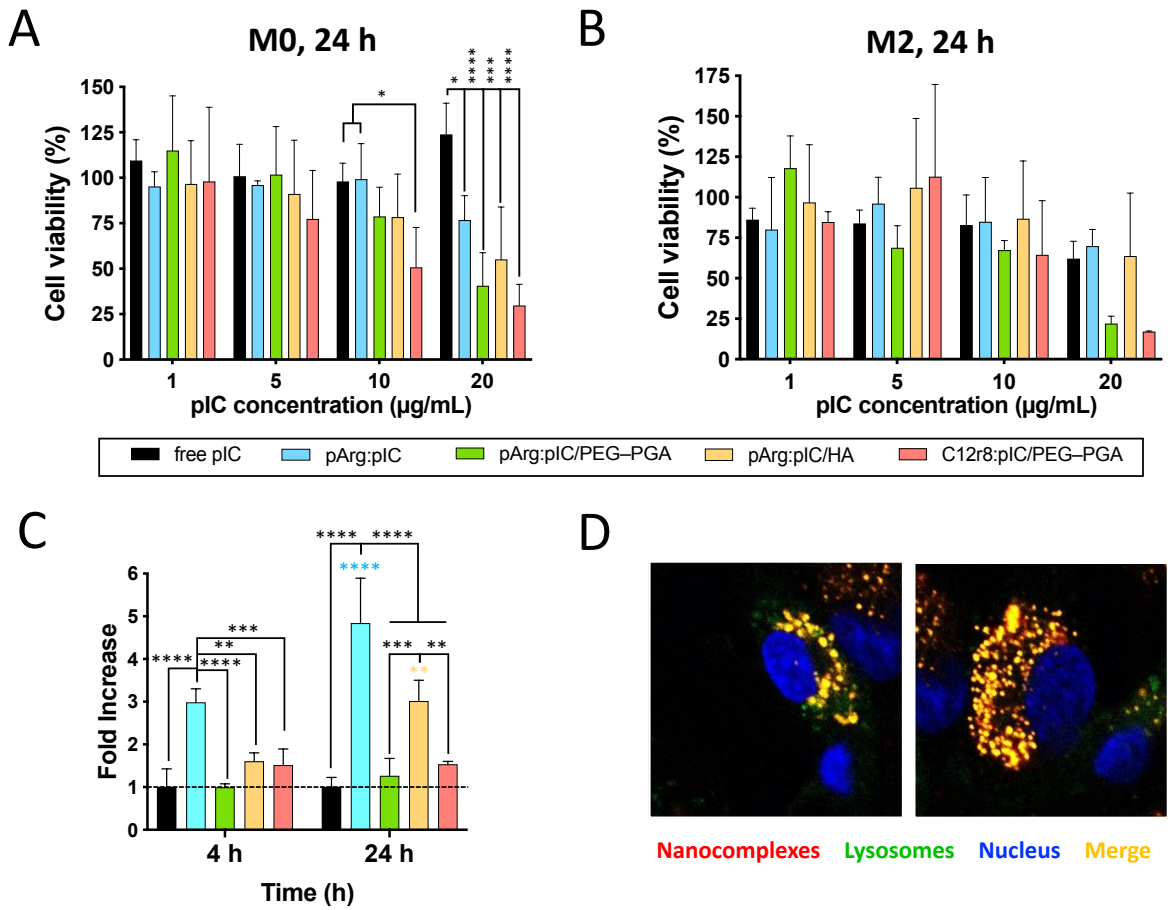

Figure 5. Toxicity, uptake and cellular localization of poly(I:C) and nanocomplexes. Toxicity towards (A) M0 and (B) M2 primary human monocyte-derived macrophages after 24 h of incubation. (C) Poly(I:C) uptake by primary human monocyte-derived macrophages when included in the different nanocomplexes after 4 and 24 h hours of incubation. (D) Co-localization with the endosome of rhodamine-labelled pArg:pIC nanocomplexes after 8 h of incubation (100x magnification). Values represent mean ± SD (n = 3). Statistical comparison was done using a two-way ANOVA followed by a Tukey's multiple comparison test. Statistically significant differences are represented as * ($p < 0.05$), *** ($p < 0.005$) and **** ($p < 0.001$). C12r8, laurate-octaarginine; HA, hyaluronic acid; pArg, poly-arginine; PEG–PGA, pegylated polyglutamic acid; pIC, poly(I:C).

3.5. Macrophage polarization towards a pro-inflammatory phenotype

The interaction of poly(I:C) with the endosomal TLR3 triggers an immune response through the TRIF pathway [59]. This pathway stimulates the expression of type I IFN genes, leading to increased expression of pro-inflammatory markers such as CD80 and MHC II; while the M2-like features (e.g., CD206 and CD163) are decreased (**Fig. 6**). Therefore, the change in the expression of both M1 and M2 markers was studied to determine if the treatment with nanocomplexed poly(I:C) was able to polarize macrophages [9,11]. Overall, no significant changes in the expression of surface CD80 and MHC II were observed in the ENCP-treated M0 or M2 macrophages at the time points of the study (**Fig. 6B,D,F,H**). Only a slight increase for the M1 markers CD80 and MHCII in macrophages exposed to

C12r8:pIC/PEG—PGA ENCPs was observed, but with no significant differences. A similar pattern was observed in the case of the mannose receptor CD206 (**Fig. 6J,L**). The presence of the scavenger receptor CD163 on the surface of macrophages was lower upon treatment with all ENCPs, with significant differences in M2 macrophages treated with C12r8:pIC/PEG—PGA ENCPs (**Fig. 6N,P**). The slight decrease of CD163 in macrophages exposed to ENCPS could be related to the polarization of macrophages towards an M1 phenotype, although we cannot discard that it might also be related with an involvement of this scavenger receptor in the uptake of the ENCPs. Further experiments would be required to fully understand the interaction of CD163 with the ENCPs. These results, which are in line with a recent publication on the evaluation of poly(I:C) *versus* imiquimod *in vitro*, show a very limited ability of free or nanocomplexed poly(I:C) to modulate the ratio of M1/M2 receptors on the surface of prototypical M0 or M2 macrophages [38]. Indeed, the dynamic turnover of these receptors could difficult their precise quantification to determine the M1/M2 phenotypes *in vitro*. On the basis of these data, and being conscious that the ability of poly(I:C) to polarize macrophages towards an M1-like anti-tumoral phenotype can be better evaluated by conducting functional assays, we tested the ability of macrophages to secrete chemokines involved in the recruitment of T cells and the cytotoxic potential of pre-treated macrophages towards cancer cells.

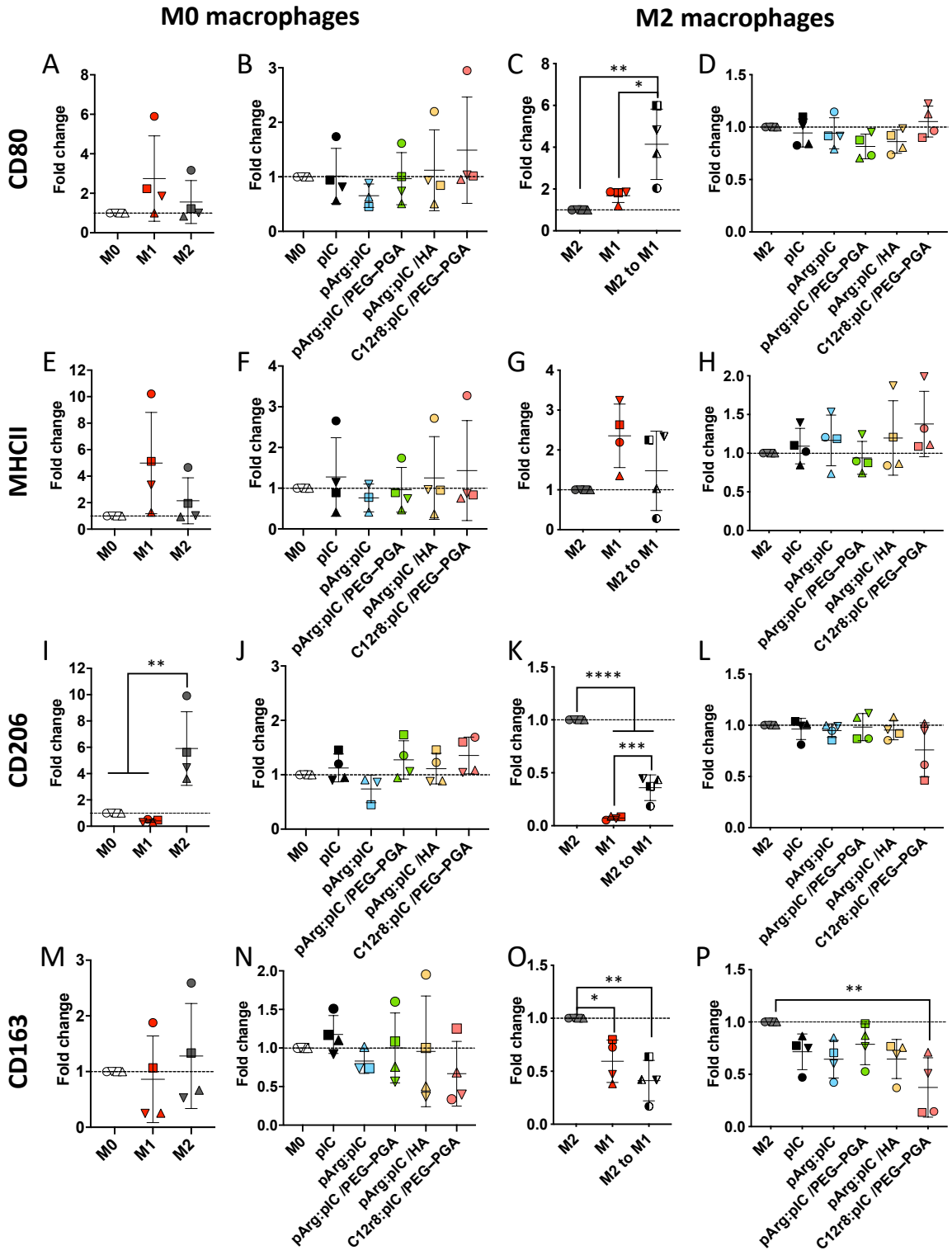

Figure 6. Polarization of M0 and M2 macrophages after treatment with free and nanocomplexed poly(I:C). Expression of the M1 markers (A–D) CD80, (E–H) MHCII, and the M2 markers (I–L) CD206 and (M–P) CD163 in treated M0 and M2 macrophages, in comparison to the prototypic phenotypes. Each symbol shape represents a different donor. Values represent mean ± SD (n ≥ 3). Statistical comparison was done using an ordinary one-way ANOVA followed by a Tukey's comparison test between groups. C12r8, laurate-octaarginine; HA, hyaluronic acid; pArg, poly-arginine; PEG–PGA, pegylated polyglutamic acid; pIC, poly(I:C).

Cytotoxic T cells (CTLs) are also important players in the anti-tumoral immune response [60,61]. CXCL10 and CCL5 are two key chemokines implicated in the recruitment of CTLs by macrophages towards the tumor to fight against the cancer cells. Thus, we have evaluated the secretion of these chemokines by macrophages exposed to ENCPs. We found a higher production of CXCL10 and CCL5 by macrophages treated with ENCPs *versus* free poly(I:C) and the control (non-treated M0 macrophages) (**Fig. 7** and **Supporting Information, Fig. S8**). Importantly, the levels of CXCL10 stimulated by the ENCPs were similar to the ones obtained with M1 macrophages at 24 h, or even higher, in the case of the pArg:pIC and C12r8:pIC/PEG–PGA ENCPs (**Fig. 7B**). Regarding CCL5, only the pArg:pIC/PEG–PGA ENCPs increased significantly the secretion of this chemokine (**Fig. 7D**).

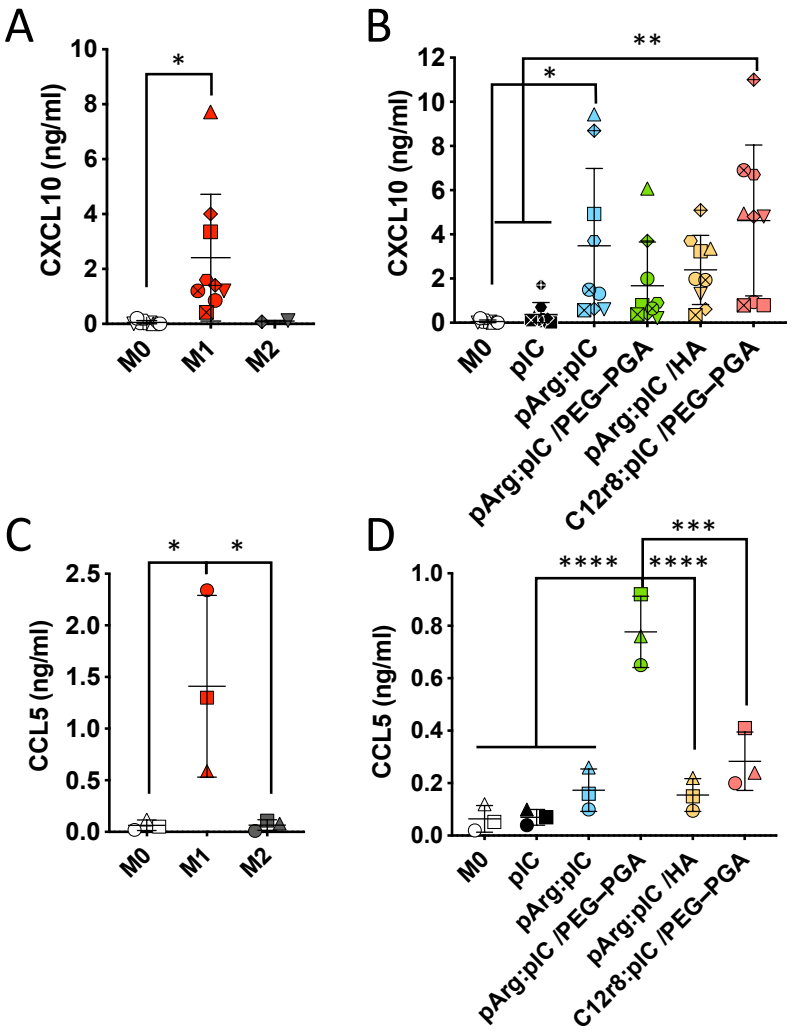

Figure 7. Secretion of the T cell attracting chemokines upon treatment with the poly(I:C) nanocomplexes. (A–B) CXCL10 secretion in (A) prototypic macrophages and in (B) M0 macrophages treated with the different nanocomplexes after 24 h of incubation. (C–D) CCL5 secretion in (C) prototypic macrophages and in (D) M0 macrophages treated with the different nanocomplexes after 24 h of incubation. Each symbol shape represents a different donor. Values represent mean ± SD (n ≥ 3). Statistical comparison was done using an ordinary one-way ANOVA followed by a Tukey's comparison test between groups. C12r8, laurate-octaarginine; HA, hyaluronic acid; pArg, poly-arginine; PEG–PGA, pegylated polyglutamic acid; pIC, poly(I:C).

These results indicate that, even though nanocomplexed poly(I:C) did not provoke an important change in the surface marker expression of macrophages, other anti-tumoral features such as the CTL recruitment capacity, were greatly improved. Therefore, it would be expected that within the tumor microenvironment, and upon treatment with the ENCPs, the secretion of these chemokines by TAMs would be increased, attracting CTLs towards the tumors.

3.6. Increased ability of pre-treated macrophages to kill tumor cells

Besides their role in activating the immune system to fight cancer, macrophages have also the capacity to directly kill tumor cells [62]. To assess the potential of the poly(I:C) ENCPs to re-educate macrophages towards an M1 anti-tumoral phenotype, we performed a functional assay to evaluate their ability to kill tumor cells (**Fig. 8A**). For this, M0 macrophages were treated with the different ENCPs during 24 h or differentiated to prototypical M1-like or M2-like phenotypes used as controls. These pre-treated macrophages were then co-cultured with stained pancreatic cancer cells (PANC-1) for 48 h. As expected, PANC-1 cells proliferated 15% more in co-culture with M2-like macrophages, compared to non-polarized M0 macrophages (**Fig. 8B**). On the other side, as a positive control, M1 macrophages presented a 60% increased ability to kill the cancer cells, when compared to M0 macrophages (**Fig. 8B**). In the case of macrophages pre-treated with free and nanocomplexed poly(I:C), a 30–40% increase in their cytotoxicity towards cancer cells was observed versus M0 macrophages (**Fig. 8C**). Of note, the cytotoxicity of ENCP-treated macrophages towards cancer cells was much higher than the one of M0 or M2 macrophages, achieving a similar activity than the prototypical M1-like macrophages exposed to LPS and IFN-γ. Also, nanocomplexed poly(I:C) performed as well as the free molecule, thus showing that the dsRNA remained active. These results corroborate the potential of nanocomplexed poly(I:C) to re-educate macrophages to fight cancer.

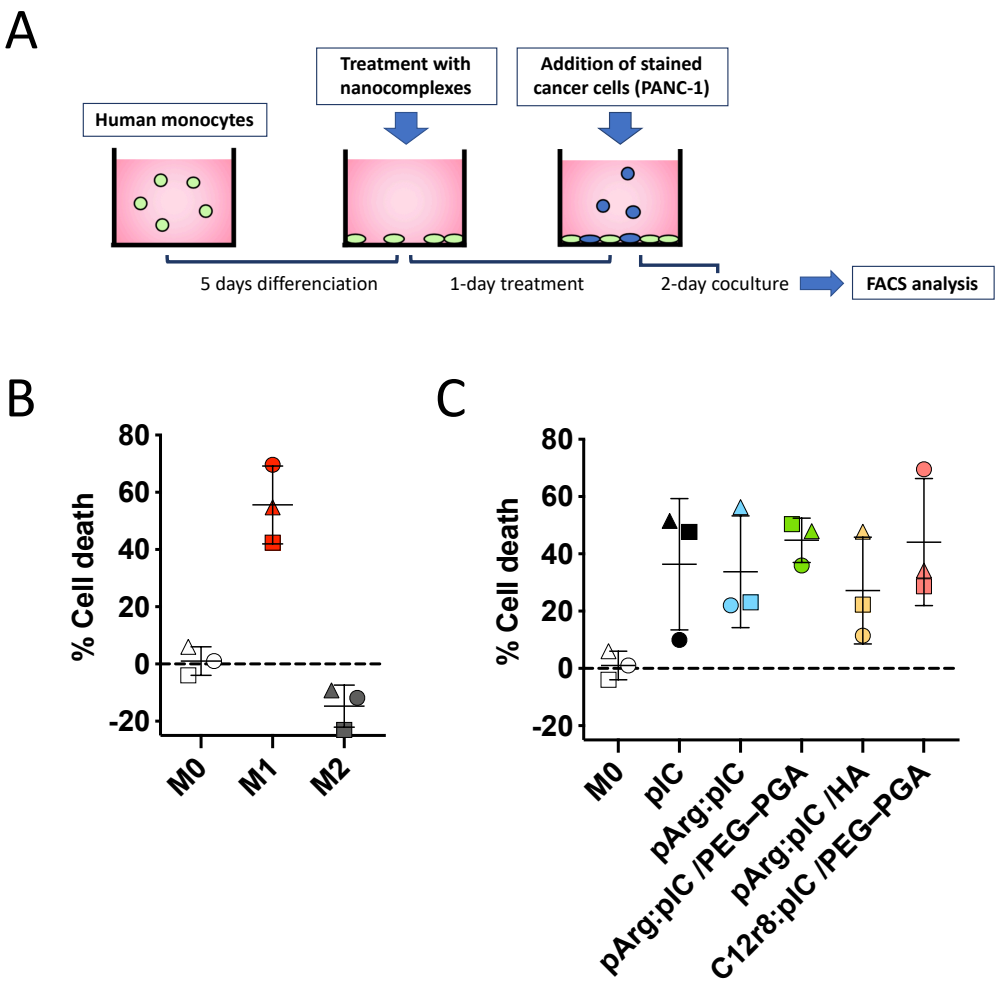

Figure 8. Macrophage cytotoxicity towards PANC-1 cancer cells after pre-treatment with the different nanocomplexes. (A) Schematic representation of the *in* vitro model for the determination of the killing capacity of pre-treated macrophages. (B–C) % of cancer cell death caused by (B) the prototypic macrophages or (C) M0 macrophages pre-treated with free or nanocomplexed poly(I:C). Each symbol shape represents a different donor. Values represent mean ± SD (n ≥ 3). Statistical comparison was done using an ordinary one-way ANOVA followed by a Tukey's multiple comparison test between groups. C12r8, laurate-octaarginine; HA, hyaluronic acid; pArg, poly-arginine; PANC-1, pancreatic cancer cells; PEG–PGA, pegylated polyglutamic acid; pIC, poly(I:C).

3.7. *In vivo* activity of poly(I:C)

The developed ENCPs showed the capacity to polarize macrophages towards a M1-like phenotype with anti-tumoral functions. An *in vivo* study in mice bearing CMT167 lung tumors was conducted to determine the efficacy of the treatment. Upon injection of a total of 125 µg of poly(I:C) in the tumor of each mouse (5 injections of 25 µg in alternative days) (**Fig. 9A**), we could observe a significant prevention of tumor growth in mice receiving the free poly(I:C) (**Fig. 9B,C**). For the groups treated with poly(I:C) ENCPs, both in the case of the C12r8- and the pArg-based ones, a continuous increase in the tumor volume was observed, with no differences in comparison to the control groups (equivalent amount of polymer alone or physiological solution) (**Fig. 9B,C**). These results are in disagreement with

the *in vitro* tests reported in the previous sections. Although an *in vitro/in vivo* correlation should not necessarily be expected, we have speculated about the potential reasons for the limited *in vivo* activity of the ENCPs. We have hypothesized about the potential higher difficulty for the ENCPs to diffuse across the tumor microenvironment. Although the presence of a hydrophilic polymer on the surface of nanocarriers was expected to facilitate their penetration across the tumor [46], the size of the ENCPs might have hampered their diffusion. Another hypothesis is the one that presumes that the high affinity of poly(I:C) towards the arginine polymers/oligomers, hinders its release and availability for interaction with the TLR3 targeted receptor. This slow release might have been sufficient to stimulate macrophages *in vitro* but not under *in vivo* conditions. Hence, additional dose-scaling studies are needed in order to understand the mechanistic behavior of ENCPs. Furthermore, as the main out-put expected from the delivery technology was a reduction of the systemic toxicity, a study making use of the intravenous administration and evaluating the systemic toxicity will be planned.

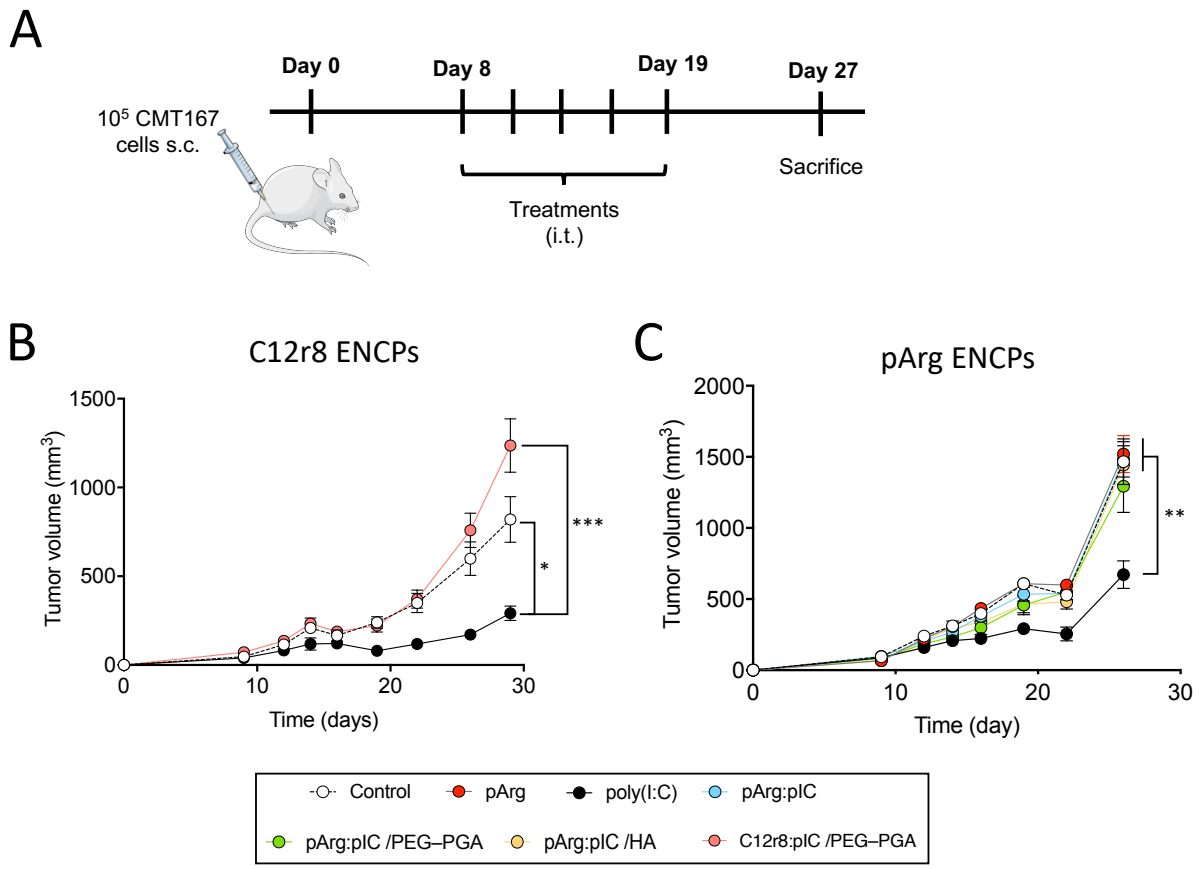

Figure 9. *In vivo* anti-tumor efficacy study of the developed nanocomplexes. (A) Schematic representation of the anti-tumor *in vivo* efficacy study. (B–C) Variation of tumor growth evaluated as tumor volume ($d^2xD/2$) of mice (B) physiological water (white), free poly(I:C) (black) and C12r8 nanocomplexes (pink); or (C) physiological solution (white), pArg solution (gray), free poly(I:C) (black), pArg:pIC ENCPs (blue), pArg:pIC/PEG–PGA ENCPs (red) and pArg:pIC/HA ENCPs (yellow). Values represent mean ± SD ($n > 8$). Statistical comparison was done using a two-way ANOVA followed by a Tukey's multiple comparison test. Statistically significant differences are represented as ** ($p < 0.01$) and **** ($p < 0.001$). C12r8, laurate-octaarginine; HA, hyaluronic acid; pArg, poly-arginine; PEG–PGA, pegylated polyglutamic acid; pIC, poly(I:C).

Overall, we have developed arginine-based ENCPs that are able to protect and stabilize poly(I:C). In addition, the delivery carrier facilitated the accumulation of poly(I:C) in the endosomal compartments, where the TLR3 is localized (**Fig. 10a–b**). Despite this accumulation, no significant changes in surface marker expression were detected, probably due to the limited time and/or dose selected in the study. However, in agreement with the targeted delivery, macrophages pre-treated with nanocomplexed poly(I:C) presented an enhanced secretion of T-cell attracting chemokines, which are critical for triggering effective anti-tumoral immune responses (**Fig. 10c–d**). Moreover, macrophages pre-treated with either free or nanocomplexed poly(I:C) presented an improved capacity to kill cancer cells (**Fig. 10e**). These positive *in vitro* results could not be translated into an enhanced anti-tumoral efficacy *in vivo* using an immunocompetent murine tumor model. This was probably due to the *in vivo*

experimental set-up, particularly the dose and the administration route, and/or to the different mechanistic behavior of the ENCPs under *in vitro* and *in vivo* conditions.

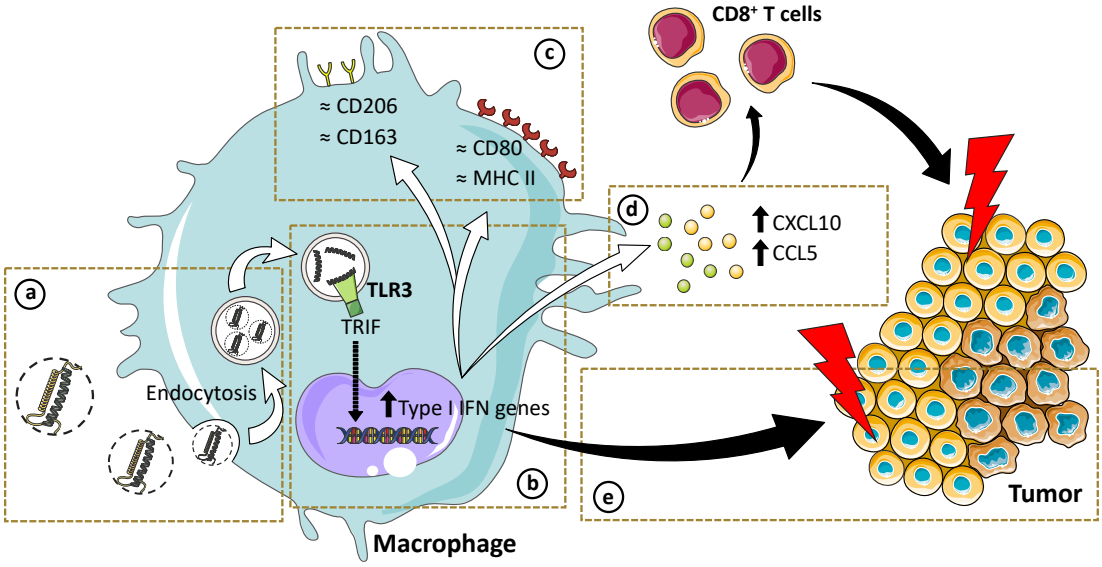

Figure 10. Schematic illustration of the *in vitro* effects of poly(I:C) nanocomplexes reported in this study. (a) Upon interaction with macrophages, poly(I:C) nanocomplexes are taken up. (b) This process allows poly(I:C) to reach its target receptor TLR3. It is expected that this interaction activates the TLR3 and the TRIF pathway, stimulating the upregulation of type I IFN genes. (c) The expression of M1 (CD80 and MHC II) and M2 (CD206 and CD163) surface markers is not substantially modified. Nevertheless, (d) CXCL10 and CCL5 chemokines, involved in the attraction of CD8 T cells to the tumor microenvironment, are secreted. (e) The direct cytotoxicity of macrophages towards cancer cells is also enhanced.

4. Conclusions

This work highlights the importance of a rational design in the development of poly(I:C) ENCPs. The complexation of poly(I:C) with arginine-rich polymers and their subsequent envelopment with either PEG–PGA or HA resulted in the formation of ENCPs with adequate physicochemical properties. This delivery strategy was found to increase the amount of poly(I:C) taken up by the macrophages and to activate macrophages. These results did not correlate well with those of a preliminary *in vivo* study intended to evaluate the capacity of the ENCPs to decrease tumor growth. These differences emphasize the need for a deeper understanding of the biodistribution and intracellular delivery of poly(I:C). Furthermore, *in vivo* toxicity studies following intravenous administration need to be performed in order to fully assessed the value of this delivery strategy. In this regard, ENCPs could present advantages for protecting the activity of their therapeutic cargo.

References

[1] R.D. Schreiber, L.J. Old, M.J. Smyth, Cancer immunoediting: integrating immunity's roles in cancer suppression and promotion, Science. 331 (2011) 1565–1570. doi:10.1126/science.1203486.

[2] J. Couzin-Frankel, Cancer immunotherapy, Science. 342 (2013) 1432–1433. doi:10.1126/science.342.6165.1432.

[3] W. Zou, Immunosuppressive networks in the tumour environment and their therapeutic relevance, Nat. Rev. Cancer. 5 (2005) 263–274. doi:10.1038/nrc1586.

[4] F. Balkwill, Cancer and the chemokine network, Nat. Rev. Cancer. 4 (2004) 540–550. doi:10.1038/nrc1388.

[5] A. Mantovani, A. Sica, Macrophages, innate immunity and cancer: balance, tolerance, and diversity, Curr. Opin. Immunol. 22 (2010) 231–237. doi:10.1016/j.coi.2010.01.009.

[6] P. Vlaicu, P. Mertins, T. Mayr, P. Widschwendter, B. Ataseven, B. Högel, W. Eiermann, P. Knyazev, A. Ullrich, Monocytes/macrophages support mammary tumor invasivity by co-secreting lineage-specific EGFR ligands and a STAT3 activator, BMC Cancer. 13 (2013) 197. doi:10.1186/1471-2407-13-197.

[7] R. Noy, J.W. Pollard, Tumor-associated macrophages: from mechanisms to therapy, Immunity. 41 (2014) 49–61. doi:10.1016/j.immuni.2014.06.010.

[8] A. Mantovani, F. Marchesi, A. Malesci, L. Laghi, P. Allavena, Tumour-associated macrophages as treatment targets in oncology, Nat. Rev. Clin. Oncol. 14 (2017) 399–416. doi:10.1038/nrclinonc.2016.217.

[9] A. Mantovani, S. Sozzani, M. Locati, P. Allavena, A. Sica, Macrophage polarization: tumor-associated macrophages as a paradigm for polarized M2 mononuclear phagocytes, Trends Immunol. 23 (2002) 549–555. doi:10.1016/S1471-4906(02)02302-5.

[10] M. Ovais, M. Guo, C. Chen, Tailoring nanomaterials for targeting tumor-associated macrophages, Adv. Mater. 31 (2019) 1808303. doi:10.1002/adma.201808303.

[11] S. Aras, M.R. Zaidi, TAMeless traitors: macrophages in cancer progression and metastasis, Br. J. Cancer. 117 (2017) 1583–1591. doi:10.1038/bjc.2017.356.

[12] C. Anfray, A. Ummarino, F.T. Andón, P. Allavena, Current strategies to target tumor-associated-macrophages to improve anti-tumor immune responses, Cells. 9 (2019) 46. doi:10.3390/cells9010046.

[13] W. Song, S.N. Musetti, L. Huang, Nanomaterials for cancer immunotherapy, Biomaterials. 148 (2017) 16–30. doi:10.1016/j.biomaterials.2017.09.017.

[14] F.T. Andón, E. Digifico, A. Maeda, M. Erreni, A. Mantovani, M.J. Alonso, P. Allavena, Targeting tumor associated macrophages: the new challenge for nanomedicine, Semin. Immunol. 34 (2017) 103–113. doi:10.1016/j.smim.2017.09.004.

[15] Q. Zeng, C.M. Jewell, Directing toll-like receptor signaling in macrophages to enhance tumor immunotherapy, Curr. Opin. Biotechnol. 60 (2019) 138–145. doi:10.1016/j.copbio.2019.01.010.

[16] X. Cen, S. Liu, K. Cheng, The role of Toll-like receptor in inflammation and tumor immunity, Front. Pharmacol. 9 (2018) 1–8. doi:10.3389/fphar.2018.00878.

[17] K. Iribarren, N. Bloy, A. Buqué, I. Cremer, A. Eggermont, W.H. Fridman, J. Fucikova, J. Galon, R. Špíšek, L. Zitvogel, G. Kroemer, L. Galluzzi, Trial watch: immunostimulation with Toll-like receptor agonists in cancer therapy, Oncoimmunology. 5 (2016) e1088631. doi:10.1080/2162402X.2015.1088631.

[18] H. Shime, M. Matsumoto, H. Oshiumi, S. Tanaka, A. Nakane, Y. Iwakura, H. Tahara, N. Inoue, T. Seya, Toll-like receptor 3 signaling converts tumor-supporting myeloid cells to tumoricidal effectors, Proc. Natl. Acad. Sci. 109 (2012) 2066–2071. doi:10.1073/pnas.1113099109.

[19] A.L. Engel, G.E. Holt, H. Lu, The pharmacokinetics of Toll-like receptor agonists and the impact on the immune system, Expert Rev. Clin. Pharmacol. 4 (2011) 275–289. doi:10.1586/ecp.11.5.

[20] A.M. Hafner, B. Corthésy, H.P. Merkle, Particulate formulations for the delivery of poly(I:C) as vaccine adjuvant, Adv. Drug Deliv. Rev. 65 (2013) 1386–1399. doi:10.1016/j.addr.2013.05.013.

[21] R.S. Riley, C.H. June, R. Langer, M.J. Mitchell, Delivery technologies for cancer immunotherapy, Nat. Rev. Drug Discov. 18 (2019) 175–196. doi:10.1038/s41573-018-0006-z.

[22] P. Nordly, F. Rose, D. Christensen, H.M. Nielsen, P. Andersen, E.M. Agger, C. Foged, Immunity by formulation design: induction of high CD8+ T-cell responses by poly(I:C) incorporated into the CAF01 adjuvant via a double emulsion method, J. Control. Release. 150 (2011) 307–317. doi:10.1016/j.jconrel.2010.11.021.

[23] J.F. Correia-Pinto, N. Csaba, J. Schiller, M.J. Alonso, Chitosan-poly (I:C)-PADRE based nanoparticles as delivery vehicles for synthetic peptide vaccines, Vaccines. 3 (2015) 730–750. doi:10.3390/vaccines3030730.

[24] H.D. Han, Y. Byeon, J.-H. Jang, H.N. Jeon, G.H. Kim, M.G. Kim, C.-G. Pack, T.H. Kang, I.D. Jung, Y.T. Lim, Y.J. Lee, J.-W. Lee, B.C. Shin, H.J. Ahn, A.K. Sood, Y.-M. Park, In vivo stepwise immunomodulation using chitosan nanoparticles as a platform nanotechnology for cancer immunotherapy, Sci. Rep. 6 (2016) 38348. doi:10.1038/srep38348.

[25] M. Cobaleda-Siles, M. Henriksen-Lacey, A.R. de Angulo, A. Bernecker, V.G. Vallejo, B. Szczupak, J. Llop, G. Pastor, S. Plaza-Garcia, M. Jauregui-Osoro, L.K. Meszaros, J.C. Mareque-Rivas, An iron oxide nanocarrier for dsRNA to target lymph nodes and strongly activate cells of the immune system, Small. 10 (2014) 5054–5067. doi:10.1002/smll.201401353.

[26] I. Schau, S. Michen, A. Hagstotz, A. Janke, G. Schackert, D. Appelhans, A. Temme, Targeted delivery of TLR3 agonist to tumor cells with single chain antibody fragment-conjugated nanoparticles induces type I-interferon response and apoptosis, Sci. Rep. 9 (2019) 1–15. doi:10.1038/s41598-019-40032-8.

[27] K.J. Kauffman, M.J. Webber, D.G. Anderson, Materials for non-viral intracellular delivery of messenger RNA therapeutics, J. Control. Release. 240 (2016) 227–234. doi:10.1016/j.jconrel.2015.12.032.

[28] J. Buck, P. Grossen, P.R. Cullis, J. Huwyler, D. Witzigmann, Lipid-based DNA therapeutics: hallmarks of non-viral gene delivery, ACS Nano. 13 (2019) 3754–3782. doi:10.1021/acsnano.8b07858.

[29] Q. Xiong, G.Y. Lee, J. Ding, W. Li, J. Shi, Biomedical applications of mRNA nanomedicine, Nano Res. 11 (2018) 5281–5309. doi:10.1007/s12274-018-2146-1.

[30] M.A. Aznar, L. Planelles, M. Perez-Olivares, C. Molina, S. Garasa, I. Etxeberría, G. Perez, I. Rodriguez, E. Bolaños, P. Lopez-Casas, M.E. Rodriguez-Ruiz, J.L. Perez-Gracia, I. Marquez-Rodas, A. Teijeira, M. Quintero, I. Melero, Immunotherapeutic effects of intratumoral nanoplexed poly I:C, J. Immunother. Cancer. 7 (2019) 116. doi:10.1186/s40425-019-0568-2.

[31] Exploratory study of BO-112 in adult patients with aggressive solid tumors, (2016). https://clinicaltrials.gov/ct2/show/NCT02828098 (accessed January 9, 2020).

[32] P. Chollet, M.C. Favrot, A. Hurbin, J.-L. Coll, Side-effects of a systemic injection of linear polyethylenimine-DNA complexes, J. Gene Med. 4 (2002) 84–91. doi:10.1002/jgm.237.

[33] V.P. Torchilin, Cell penetrating peptide-modified pharmaceutical nanocarriers for intracellular drug and gene delivery, Biopolymers. 90 (2008) 604–610. doi:10.1002/bip.20989.

[34] S. Reimondez-Troitiño, J. V. González-Aramundiz, J. Ruiz-Bañobre, R. López-López, M.J. Alonso, N. Csaba, M. de la Fuente, Versatile protamine nanocapsules to restore miR-145 levels and interfere tumor growth in colorectal cancer cells, Eur. J. Pharm. Biopharm. 142 (2019) 449–459. doi:10.1016/j.ejpb.2019.07.016.

[35] A.M. Ledo, M.S. Sasso, V. Bronte, I. Marigo, B.J. Boyd, M. Garcia-Fuentes, M.J. Alonso, Co-delivery of RNAi and chemokine by polyarginine nanocapsules enables the modulation of myeloid-derived suppressor cells, J. Control. Release. 295 (2019) 60–73. doi:10.1016/j.jconrel.2018.12.041.

[36] E. Samaridou, H. Walgrave, E. Salta, D.M. Álvarez, V. Castro-López, M. Loza, M.J. Alonso, Nose-to-brain delivery of enveloped RNA - cell permeating peptide nanocomplexes for the treatment of neurodegenerative diseases, Biomaterials. 230 (2020) 119657. doi:10.1016/j.biomaterials.2019.119657.

[37] T. Kawai, S. Akira, The role of pattern-recognition receptors in innate immunity: update on Toll-like receptors, Nat. Immunol. 11 (2010) 373–384. doi:10.1038/ni.1863.

[38] A. Maeda, E. Digifico, F.T. Andon, A. Mantovani, P. Allavena, Poly(I:C) stimulation is superior than imiquimod to induce the antitumoral functional profile of tumor-conditioned macrophages, Eur. J. Immunol. 49 (2019) 801–811. doi:10.1002/eji.201847888.

[39] T. Endoh, T. Ohtsuki, Cellular siRNA delivery using cell-penetrating peptides modified for endosomal escape, Adv. Drug Deliv. Rev. 61 (2009) 704–709. doi:10.1016/j.addr.2009.04.005.

[40] Y. Li, Y. Li, X. Wang, R.J. Lee, L. Teng, Fatty acid modified octa-arginine for delivery of siRNA, Int. J. Pharm. 495 (2015) 527–535. doi:10.1016/j.ijpharm.2015.09.006.

[41] C. Sun, T. Tang, H. Uludag, A molecular dynamics simulation study on the effect of lipid substitution on polyethylenimine mediated siRNA complexation, Biomaterials. 34 (2013) 2822–2833. doi:10.1016/j.biomaterials.2013.01.011.

[42] L. Pärnaste, P. Arukuusk, K. Langel, T. Tenson, Ü. Langel, The formation of nanoparticles between small interfering RNA and amphipathic cell-penetrating peptides, Mol. Ther. - Nucleic Acids. 7 (2017) 1–10. doi:10.1016/j.omtn.2017.02.003.

[43] D.J. Gary, N. Puri, Y.-Y. Won, Polymer-based siRNA delivery: perspectives on the fundamental and phenomenological distinctions from polymer-based DNA delivery, J. Control. Release. 121 (2007) 64–73. doi:10.1016/j.jconrel.2007.05.021.

[44] E. Samaridou, N. Kalamidas, I. Santalices, J. Crecente-Campo, M.J. Alonso, Tuning the PEG surface density of the PEG-PGA enveloped octaarginine-peptide nanocomplexes, Drug Deliv. Transl. Res. (2019). doi:10.1007/s13346-019-00678-3.

[45] M.J. Santander-Ortega, A.B. Jódar-Reyes, N. Csaba, D. Bastos-González, J.L. Ortega-Vinuesa, Colloidal stability of pluronic F68-coated PLGA nanoparticles: a variety of stabilisation mechanisms, J. Colloid Interface Sci. 302 (2006) 522–529. doi:10.1016/j.jcis.2006.07.031.

[46] R. Abellan-Pose, M. Rodríguez-Évora, S. Vicente, N. Csaba, C. Évora, M.J. Alonso, A. Delgado, Biodistribution of radiolabeled polyglutamic acid and PEG-polyglutamic acid nanocapsules, Eur. J. Pharm. Biopharm. 112 (2017) 155–163. doi:10.1016/j.ejpb.2016.11.015.

[47] Z. Niu, E. Samaridou, E. Jaumain, J. Coëne, G. Ullio, N. Shrestha, J. Garcia, M. Durán-Lobato, S. Tovar, M.J. Santander-Ortega, M.V. Lozano, M.M. Arroyo-Jimenez, R. Ramos-Membrive, I. Peñuelas, A. Mabondzo, V. Préat, M. Teixidó, E. Giralt, M.J. Alonso, PEG-PGA enveloped octaarginine-peptide nanocomplexes: an oral peptide delivery strategy, J. Control. Release. 276 (2018) 125–139. doi:10.1016/j.jconrel.2018.03.004.

[48] J.L. Perry, K.G. Reuter, M.P. Kai, K.P. Herlihy, S.W. Jones, J.C. Luft, M. Napier, J.E. Bear, J.M. DeSimone, PEGylated PRINT nanoparticles: the impact of PEG density on protein binding, macrophage association, biodistribution, and pharmacokinetics, Nano Lett. 12 (2012) 5304–5310. doi:10.1021/nl302638g.

[49] N. Bertrand, P. Grenier, M. Mahmoudi, E.M. Lima, E.A. Appel, F. Dormont, J.-M. Lim, R. Karnik, R. Langer, O.C. Farokhzad, Mechanistic understanding of in vivo protein corona formation on polymeric nanoparticles and impact on pharmacokinetics, Nat. Commun. 8 (2017) 777. doi:10.1038/s41467-017-00600-w.

[50] D. Peer, R. Margalit, Loading mitomycin C inside long circulating hyaluronan targeted nano-liposomes increases its antitumor activity in three mice tumor models, Int. J. Cancer. 108 (2004) 780–789. doi:10.1002/ijc.11615.

[51] K.Y. Choi, K.H. Min, J.H. Na, K. Choi, K. Kim, J.H. Park, I.C. Kwon, S.Y. Jeong, Self-assembled hyaluronic acid nanoparticles as a potential drug carrier for cancer therapy: synthesis, characterization, and in vivo biodistribution, J. Mater. Chem. 19 (2009) 4102. doi:10.1039/b900456d.

[52] X. Yang, Y. Li, M. Li, L. Zhang, L. Feng, N. Zhang, Hyaluronic acid-coated nanostructured lipid carriers for targeting paclitaxel to cancer, Cancer Lett. 334 (2013) 338–345. doi:10.1016/j.canlet.2012.07.002.

[53] A. Almalik, H. Benabdelkamel, A. Masood, I.O. Alanazi, I. Alradwan, M.A. Majrashi, A.A. Alfadda, W.M. Alghamdi, H. Alrabiah, N. Tirelli, A.H. Alhasan, Hyaluronic acid coated chitosan nanoparticles reduced the

immunogenicity of the formed protein corona, Sci. Rep. 7 (2017) 1–9. doi:10.1038/s41598-017-10836-7.

[54] S. Correa, N. Boehnke, E. Deiss-Yehiely, P.T. Hammond, Solution conditions tune and optimize Loading of therapeutic polyelectrolytes into layer-by-layer functionalized liposomes, ACS Nano. 13 (2019) 5623–5634. doi:10.1021/acsnano.9b00792.

[55] V. Lafarga, O. Sirozh, M. Hisaoka, E. Zarzuela, J. Boskovic, Generalized displacement of DNA- and RNA-binding factors mediates the toxicity of arginine-rich cell-penetrating peptides, BioRxiv. (2019). doi:10.1101/441808.

[56] T.G. Dacoba, A. Olivera, D. Torres, J. Crecente-Campo, M.J. Alonso, Modulating the immune system through nanotechnology, Semin. Immunol. 34 (2017) 78–102. doi:10.1016/j.smim.2017.09.007.

[57] Y. Qie, H. Yuan, C.A. von Roemeling, Y. Chen, X. Liu, K.D. Shih, J.A. Knight, H.W. Tun, R.E. Wharen, W. Jiang, B.Y.S. Kim, Surface modification of nanoparticles enables selective evasion of phagocytic clearance by distinct macrophage phenotypes, Sci. Rep. 6 (2016) 26269. doi:10.1038/srep26269.

[58] I. Khalil, S. Futaki, M. Niwa, Y. Baba, N. Kaji, H. Kamiya, H. Harashima, Mechanism of improved gene transfer by the N-terminal stearylation of octaarginine: enhanced cellular association by hydrophobic core formation, Gene Ther. 11 (2004) 636–644. doi:10.1038/sj.gt.3302128.

[59] B. Liu, Q. Liu, L. Yang, S.K. Palaniappan, I. Bahar, P.S. Thiagarajan, J.L. Ding, Innate immune memory and homeostasis may be conferred through crosstalk between the TLR3 and TLR7 pathways, Sci. Signal. 9 (2016) ra70–ra70. doi:10.1126/scisignal.aac9340.

[60] K. Franciszkiewicz, A. Boissonnas, M. Boutet, C. Combadiere, F. Mami-Chouaib, Role of chemokines and chemokine receptors in shaping the effector phase of the antitumor immune response, Cancer Res. 72 (2012) 6325–6332. doi:10.1158/0008-5472.CAN-12-2027.

[61] G. Arango Duque, A. Descoteaux, Macrophage cytokines: involvement in immunity and infectious diseases, Front. Immunol. 5 (2014) 1–12. doi:10.3389/fimmu.2014.00491.

[62] M. Singh, H. Khong, Z. Dai, X.-F. Huang, J.A. Wargo, Z.A. Cooper, J.P. Vasilakos, P. Hwu, W.W. Overwijk, Effective innate and adaptive antimelanoma immunity through localized TLR7/8 activation, J. Immunol. 193 (2014) 4722–4731. doi:10.4049/jimmunol.1401160.

Supporting Information

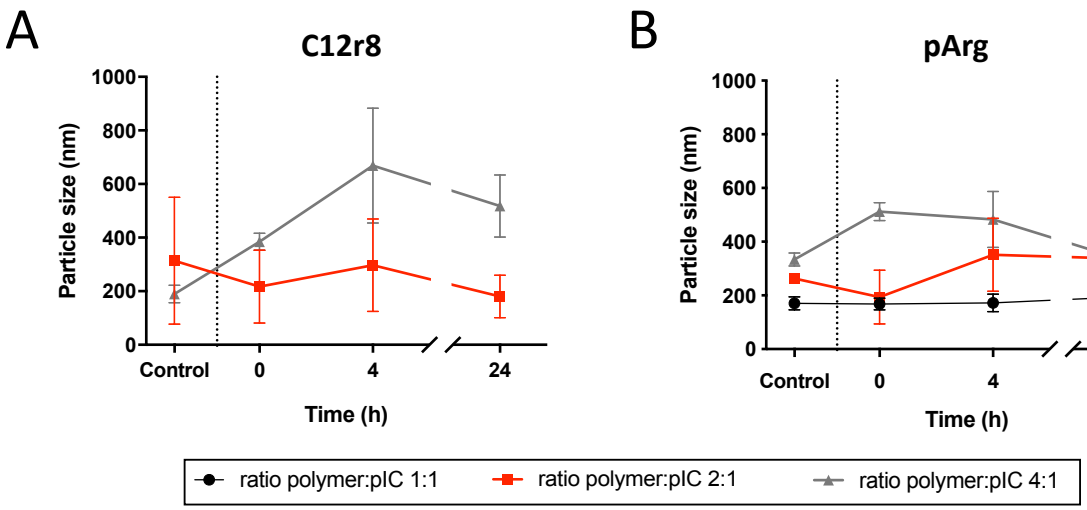

Supporting Figure S1. Stability of the non-enveloped nanocomplexes in cell culture media. Evolution of particle size of (A) C12r8-based nanocomplexes and (B) pArg-based nanocomplexes up to 24 h of incubation in cell culture media at 37 °C, in comparison with the nanocomplexes in water (control). Values represent mean ± SD (n ≥ 3). C12r8, laurate-octaarginine; pArg, poly-arginine; pIC, poly(I:C).

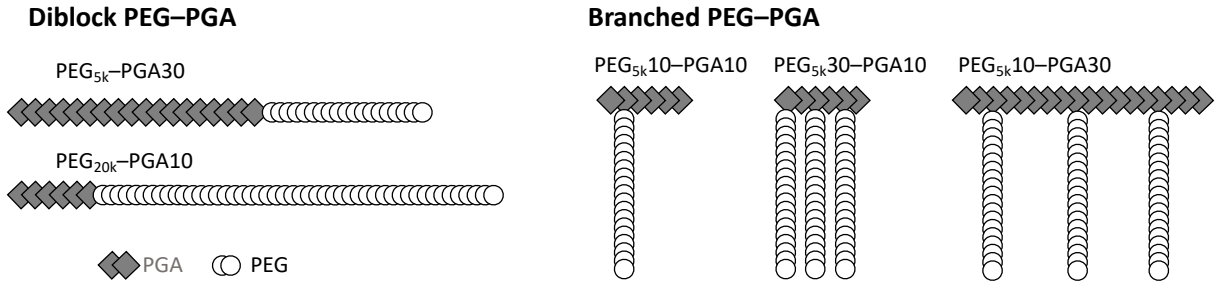

Supporting Figure S2. Schematic representation of the PEG–PGA structures tested in these studies.

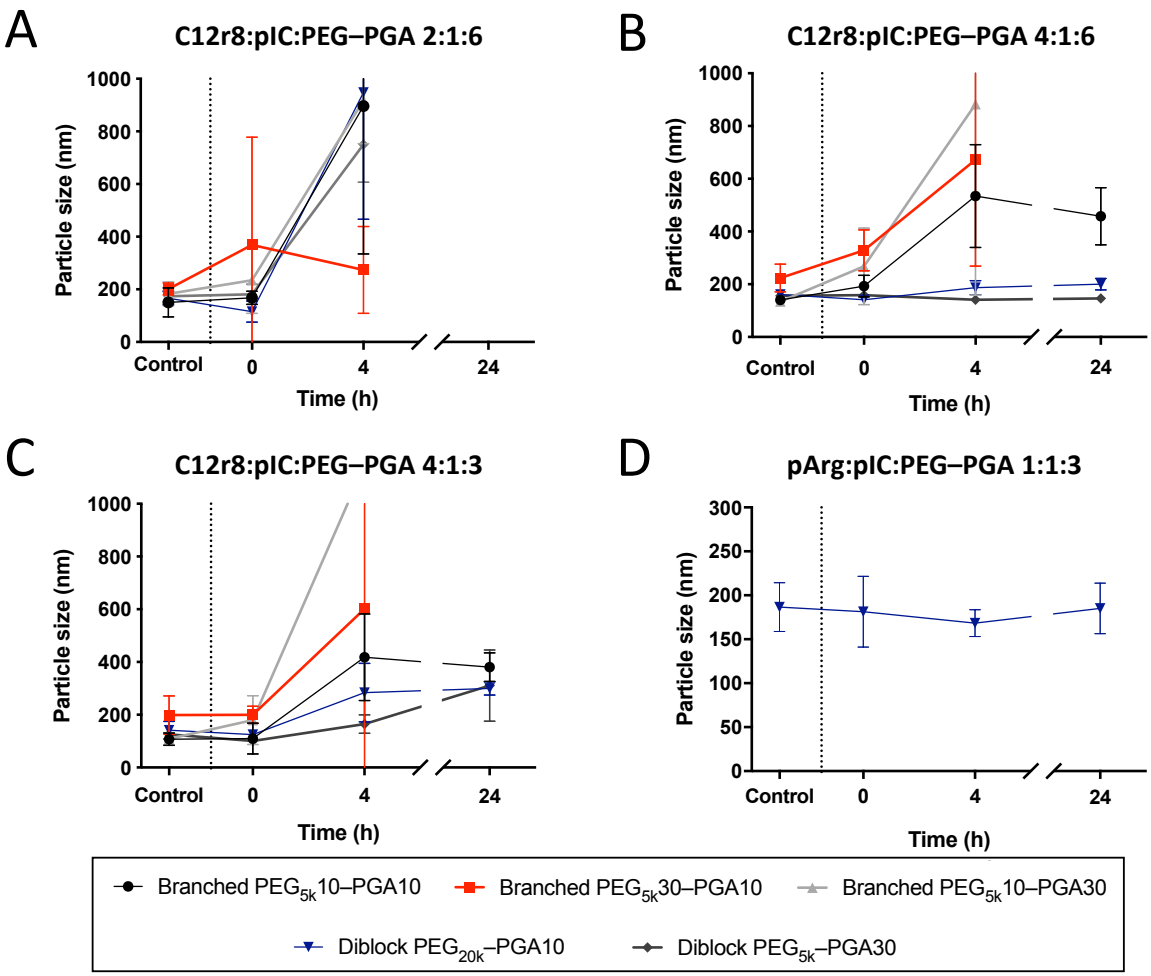

Supporting Figure S3. Stability of the PEG–PGA enveloped nanocomplexes in cell culture media. Evolution of particle size of PEG–PGA enveloped C12r8 nanocomplexes in a weight ratio (A) 2:1:6, (B) 4:1:6 and (C) 4:1:3 C12r8:pIC:PEG–PGA. (D) Evolution of particle size of diblock PEG_{20k}–PGA10 enveloped pArg nanocomplexes in a weight ratio 1:1:3 pArg:pIC:PEG–PGA. Nanocomplexes were incubated up to 24 h in cell culture media at 37 °C, and sizes were compared with those obtained in water (control). Values represent mean ± SD (n ≥ 3). C12r8, laurate-octaarginine; pArg, poly-arginine; PEG–PGA, pegylated polyglutamic acid; PDI, polydispersity index; pIC, poly(I:C).

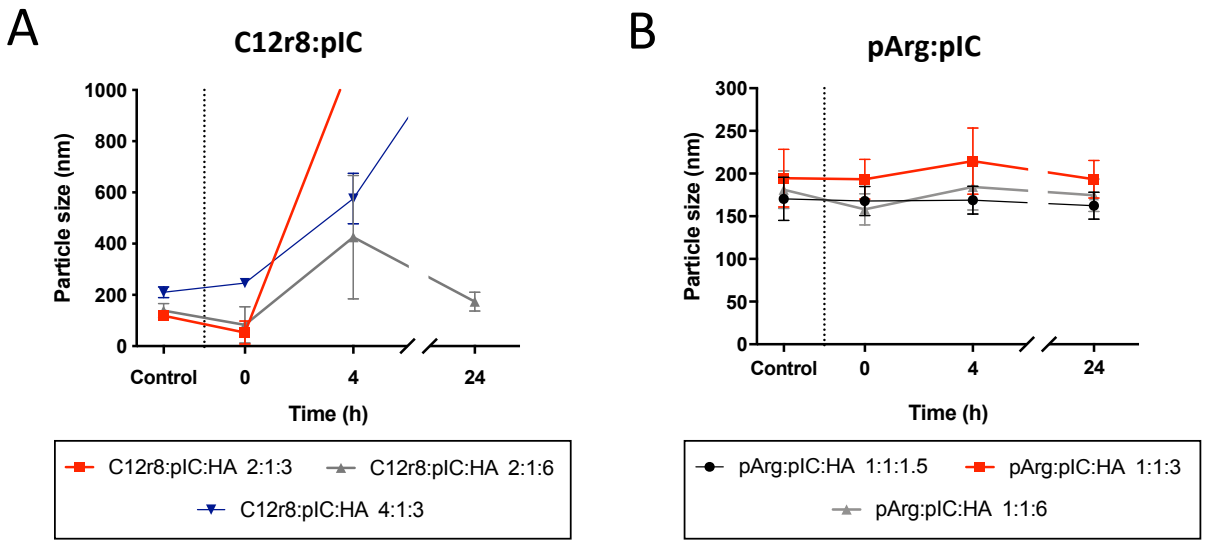

Supporting Figure S4. Stability of the HA-enveloped nanocomplexes in cell culture media. Evolution of particle size of (A) C12r8-based nanocomplexes and (B) pArg-based nanocomplexes enveloped with different weight ratios of HA up to 24 h of incubation in cell culture media at 37 °C, in comparison with the nanocomplexes in water (control). Values represent mean ± SD (n ≥ 3). C12r8, laurate-octaarginine; HA, hyaluronic acid; pArg, poly-arginine; pIC, poly(I:C).

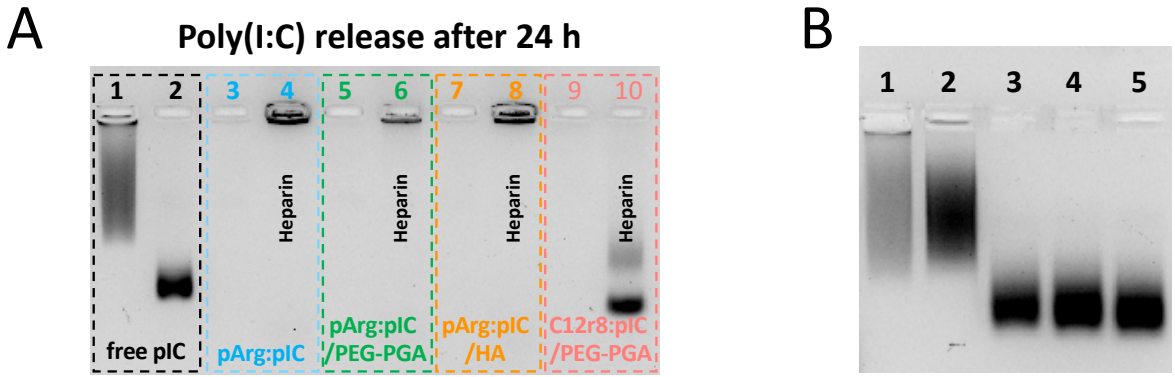

Supporting Figure S5. Poly(I:C) release from nanocomplexes and stability in cell culture media. (A) Agarose gel retardation assay to evaluate the release and integrity of poly(I:C) after 24 h of incubation in cell culture media at 37 °C. Lanes: (1) free poly(I:C) in solution and (2) in cell culture media; (3, 5, 7, 9) are pArg:pIC, pArg:pIC/PEG–PGA, pArg:pIC/HA and C12r8:pIC/PEG–PGA nanocomplexes in cell culture media; and (4, 6, 8, 10) are the same conditions incubated with heparin. (B) Agarose gel retardation assay to evaluate the degradation of poly(I:C) in different conditions. Lanes: (1) free poly(I:C); (2) free poly(I:C) incubated with heparin in water for 30 min at 37 °C; (3–5) free poly(I:C) incubated in cell culture media at 37 °C for 15, 30 and 60 min, respectively. C12r8, laurate-octaarginine; HA, hyaluronic acid; pArg, poly-arginine; PEG–PGA, pegylated polyglutamic acid; PDI, polydispersity index; pIC, poly(I:C).

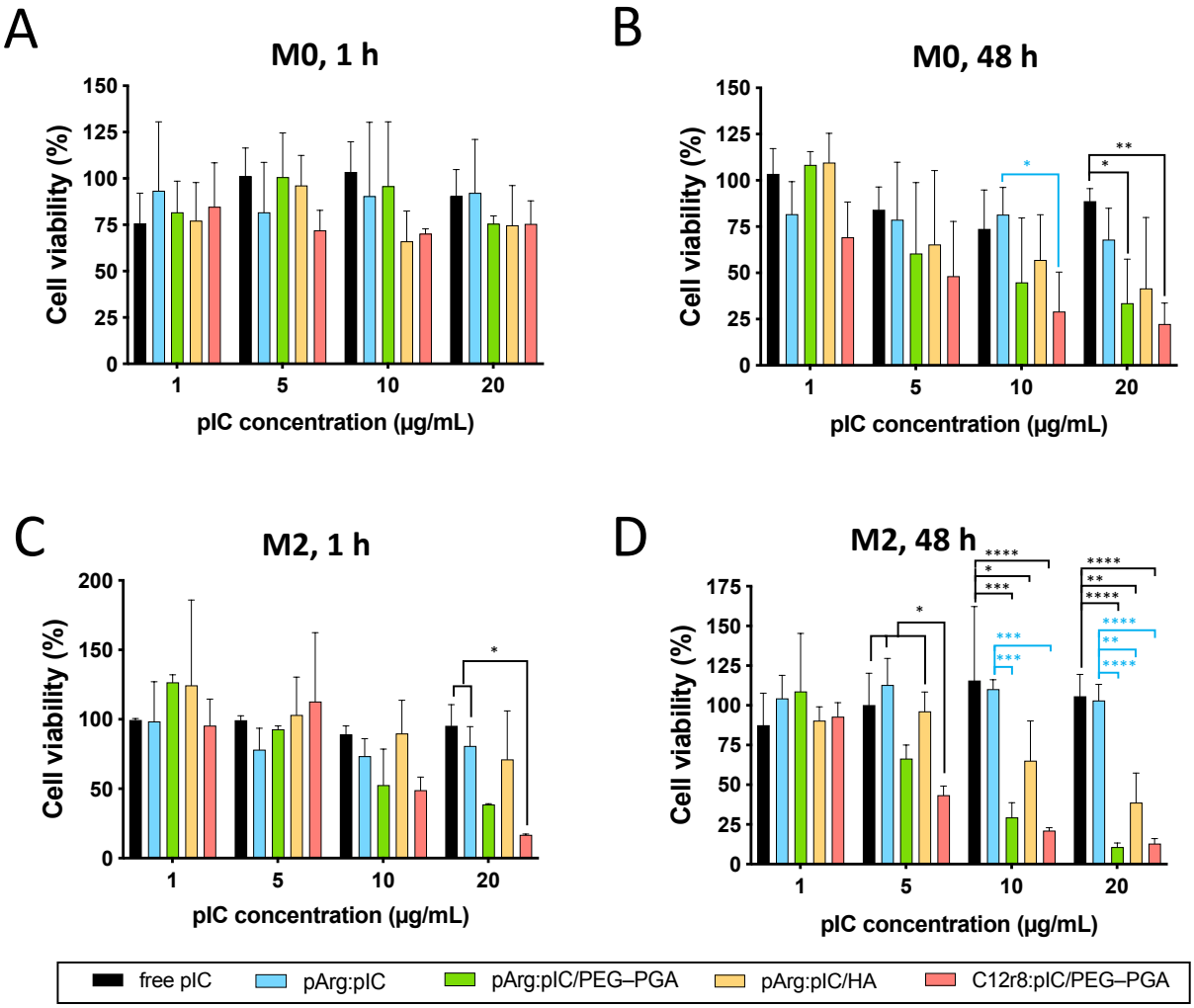

Supporting Figure S6. Toxicity of poly(I:C)-loaded nanocomplexes towards primary human monocyte-derived macrophages. Toxicity in (A–B) M0 and (C–D) M2 macrophages after 1 and 48 h of incubation with free and nanocomplexed poly(I:C). Values represent mean ± SD (n ≥ 3). Statistical comparison was done using a two-way ANOVA followed by a Tukey's multiple comparison test. Statistically significant differences are represented as * ($p < 0.05$), ** ($p < 0.01$), *** ($p < 0.005$) and **** ($p < 0.001$). C12r8, laurate-octaarginine; HA, hyaluronic acid; pArg, poly-arginine; PEG–PGA, pegylated polyglutamic acid; pIC, poly(I:C).

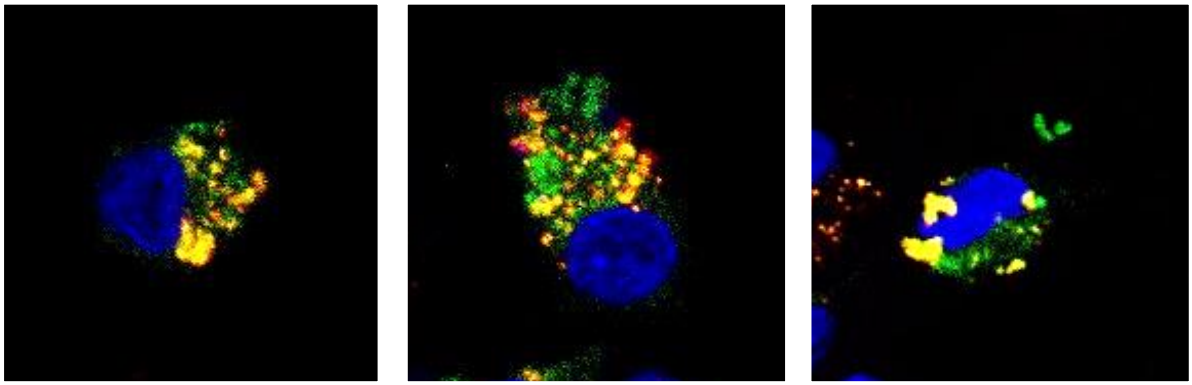

Nanocomplexes Lysosomes Nucleus Merge

Supporting Figure S7. Cellular localization of nanoformulated poly(I:C) in primary human monocyte-derived macrophages. Co-localization of rhodamine-labelled pArg:pIC nanocomplexes and the endosome after 2 h of incubation (100x magnification).

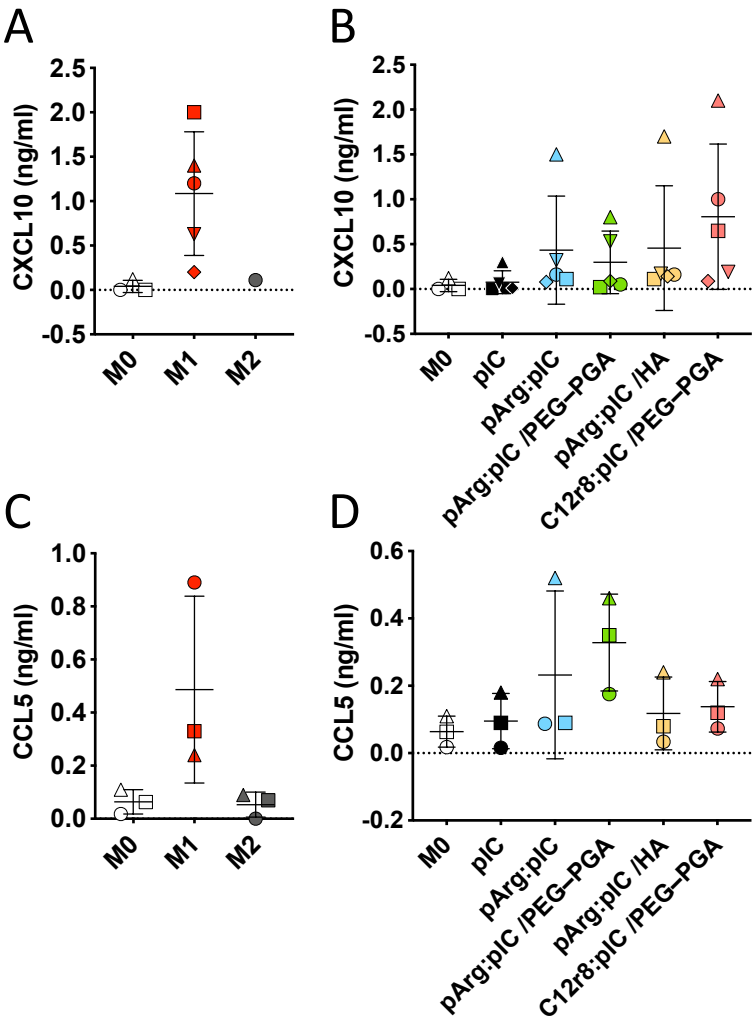

Supporting Figure S8. Secretion of the T cell attracting chemokines upon treatment with the poly(I:C) nanocomplexes. (A–B) CXCL10 secretion in (A) prototypic macrophages and in (B) M0 macrophages treated with the different nanocomplexes after 8 h of incubation. (C–D) CCL5 secretion in (C) prototypic macrophages and in (D) M0 macrophages treated with the different nanocomplexes after 8 h of incubation. Each symbol shape represents a different donor. Values represent mean ± SD (n ≥ 3). Statistical comparison was done using an ordinary one-way ANOVA followed by a Tukey's comparison test between groups. C12r8, laurate-octaarginine; HA, hyaluronic acid; pArg, poly-arginine; PEG–PGA, pegylated polyglutamic acid; pIC, poly(I:C).

General discussion

The immune system is formed by a complex network of organs, tissues, and innate and adaptive cells that crosstalk to trigger different responses. Furthermore, it can be involved in both, the development and the eradication of many diseases, such as infections, inflammatory, and autoimmune diseases, or even cancer. Hence, from a therapeutic perspective, targeting and modulating the immune system can prevent or treat a great number of the most important illnesses of our time.

Nanoparticles (NPs) are tunable systems that can be employed to modulate the responses of the immune system, for example, by diminishing inflammation, eliciting more prominent humoral or cellular responses, or by re-activating the immune system to fight cancer [1,2]. NPs can present sizes ranging from a few to several hundred nm, different surface properties, variable shapes and stiffness, parameters that will influence the interaction with these cells. At the same time, NPs can be functionalized with targeting moieties to specifically direct them towards a desired organ, tissue or cell population [1,2]. By bringing together all the growing knowledge about the role of the immune system in the physiopathology of diseases, and the capacity to rationally design nanosystems with tailored properties, the potential of nanomedicine is beyond any other therapies.

Our group has a three decades of experience using nanotechnology for the modulation of the immune system. More specifically, in the field of vaccines, the activity of our group has been focused on the design of different nanocarriers adapted specifically to the antigen nature. Our group started in the early 90's engineering NPs of poly-lactic acid (PLA) and derivatives in the context of single-dose vaccines for tetanus toxoid [3,4]. Later, the group developed a variety of polysaccharide- and polypeptide-based NPs and nanocapsules (NCs) for the delivery of tetanus toxoid, Hepatitis B antigens and uropathogenic *E. coli* antigen [5–14]. At the same time, regarding the development of immunotherapies for cancer, our group has employed NCs carrying cytokines and polynucleotides to diminish the presence of myeloid-derived suppressor cells in the tumor microenvironment [15].

Based on our background experience on antigen formulation we had the opportunity to collaborate with the University of Manitoba (Canada) in the development of a more challenging vaccine, the one intended to fight against HIV. The need of such a vaccine is clear if we take into account that HIV is still one of the most threatening infectious disease that remains elusive to vaccination [16]. Therefore, the first goal of this thesis was to design and develop polysaccharide-based NPs associating an SIV (the simian equivalent to HIV) peptide antigen, with the aim of improving the elicited immune response against SIV.

1. Engineering polysaccharide NPs for the modulation of the immune response against an SIV peptide antigen

Developing an effective HIV vaccine has proven to be particularly challenging due to the special characteristics of the HIV virus. HIV infects CD4 T cells, which have an important role in the development of the adaptive immune response. On the other hand, HIV mutates rapidly, leading to a deleterious activation of the immune system, which results in the generation of ineffective humoral and cellular responses. In addition, the different virus strains are highly variable, a fact that complicates the generation of broad and protective immune responses [17].

Our approach for the design of an HIV vaccine has been to use the peptide sequences that overlap the twelve HIV protease cleavage sites (PCSs) as antigens (**Fig. 1**). The protease is an essential enzyme for HIV because its function is to cleave specific proteins, such as Gag, Gag-Pol and Nef, that are key for the maturation of HIV virions, and thus, crucial to its infectivity [18–20]. The proteolysis of these proteins must take place on the twelve cleavage sites in a controlled and sequential way, and the interruption of this process, even in one single site, may interrupt virus maturation and, therefore, stop virus infection [18,19,21]. An additional advantage of the PCS peptide antigens relies on the fact that these PCSs are highly conserved regions among HIV-1 viruses and, therefore, the mutation of the virus will not diminish the activity of the vaccine [18–21]. In a prior approach, the twelve peptide antigens for the SIV (simian equivalent of HIV) were entrapped into CS/dextran sulfate (DS) NPs by simple ionic complexation. The NPs were administered intranasally to non-human primates (NHPs), that were previously primed with the twelve PCS-encoding plasmids cloned into viral vectors. The results showed a significant increase in the IgG responses against the PCSs after nasal boosting with the NPs [22,23].

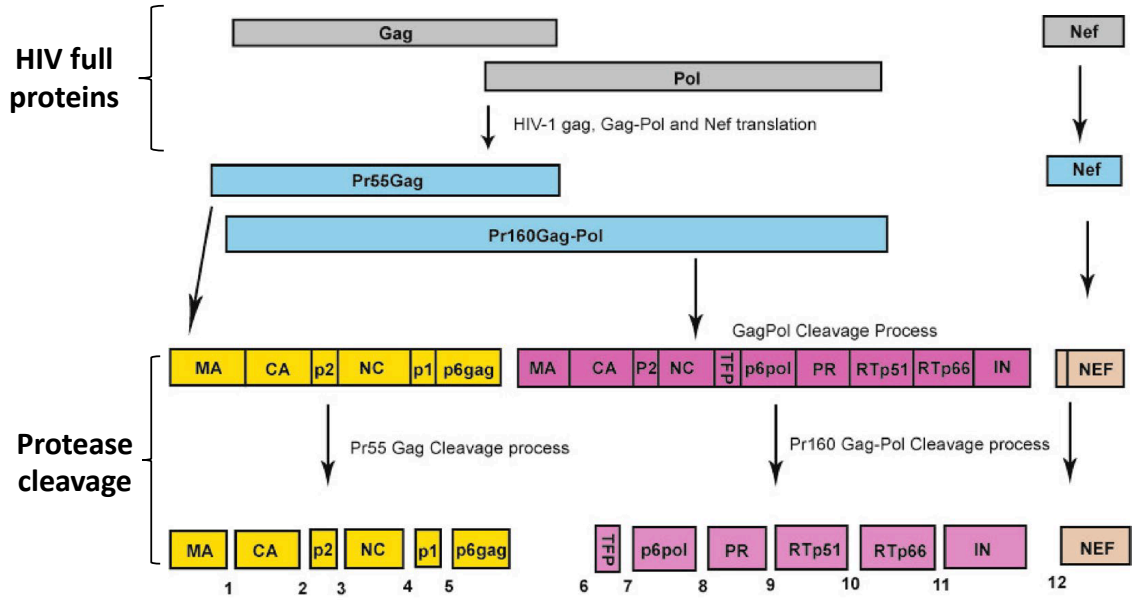

Figure 1. **HIV protease cleavage sites location** in the Gag, Pol and Nef proteins, and fragments generated after the cleavage. The twelve peptide antigens are twenty amino acid sequences that flank each of these twelve sequences (ten amino acids before and after each cleavage site). Image adapted from [19], and reproduced under a Creative Commons Attribution 4.0 International License. http://creativecommons.org/licenses/by/4.0/.

Based on this background information, the primary objective of this work was to evaluate if the chemical linkage of an SIV PCS peptide antigen (PCS5) to polysaccharide NPs, and the inclusion of the adjuvant poly(I:C), could improve its immunogenicity over the association to NPs by ionic forces. We hypothesized that the conjugation of the antigen to the polysaccharides might prevent its premature release until the particles are captured and processed by antigen presenting cells (APCs), thereby dually improving and prolonging the induced immune responses. CS and hyaluronic acid (HA) were the polysaccharides of choice to conjugate the selected peptide antigen, PCS5. Also, the TLR3 agonist poly(I:C) was included in these two nanosystems to stimulate a cellular response against the antigen [7,24–26]. As a control formulation, PCS5 was entrapped by ionic forces in CS/DS NPs, which were previously reported as good antigen carriers for the PCS peptide antigens through mucosal routes [22,23]. Polymer–PCS5 conjugates and the resulting NPs were characterized in terms of their chemical composition and structural organization. Then, their capacity to activate the immune system, regarding antibody production, T cell and APCs activation, was studied in mice. Finally, the most promising prototypes were optimized to associate three PCSs and were then administered to NHPs to assess the vaccine candidate efficacy.

1.1. Development of SIV peptide antigen-loaded polysaccharide NPs

Polysaccharides, and particularly CS, have attracted significant attention as biomaterials for the design of antigen delivery carriers [27–29]. Our group has originally reported the development of CS-based nanocarriers for the delivery of a variety of antigens [6,7,30–32]. Other authors have also disclosed the utility of nanosystems made of DS [27,33–35] or HA [36–41], both negatively charged polysaccharides, to enhance immune responses. In most of these reports, the association of the antigen to the polymeric nanocarrier was based on a simple entrapment process, normally driven mainly by ionic interactions between the polymers and the antigen. However, our objective in this work was to covalently conjugate the PCS5 peptide antigen to the NPs in order to achieve a more sustained and improved presentation of the antigen to the immune cells.

Using the preparation method for CS/DS NPs previously described by our laboratory [22], PCS5 was easily entrapped within the NPs by simply adjusting the ionic interaction of the cationic peptide (PCS5) and the cationic polysaccharide (CS), with the negatively charged polysaccharide (DS) (**Fig. 2A**).

For the covalent attachment of PCS5 to the polymers, the peptide was first conjugated to CS by an oxime bond. The resulting CS–PCS5 conjugate was then used to prepare NPs through ionic interactions with DS, together with poly(I:C) (**Fig. 2B**). Finally, for the third prototype, the conjugation of PCS5 to HA was achieved through the formation of a thioether bond, which has been reported to be cleaved in glutathione-rich environments, such as the cytosol [42]. A mass ratio CS/HA 1:1 was selected to form these NPs, since their positive surface charge was expected to allow the association of the negatively charged poly(I:C) to the system (**Fig. 2C**). In both cases, the covalent attachment was expected to help to display PCS5 on the surface, which, presumably, would facilitate the presentation of the antigen to B cells, and increase the humoral response against it, as already reported for similar antigen presentations [43,44]. In fact, for CS/HA–PCS5/pIC NPs, the analysis by X-ray photoelectron spectroscopy (XPS) confirmed the presence of PCS5 on the external layer of the particles.

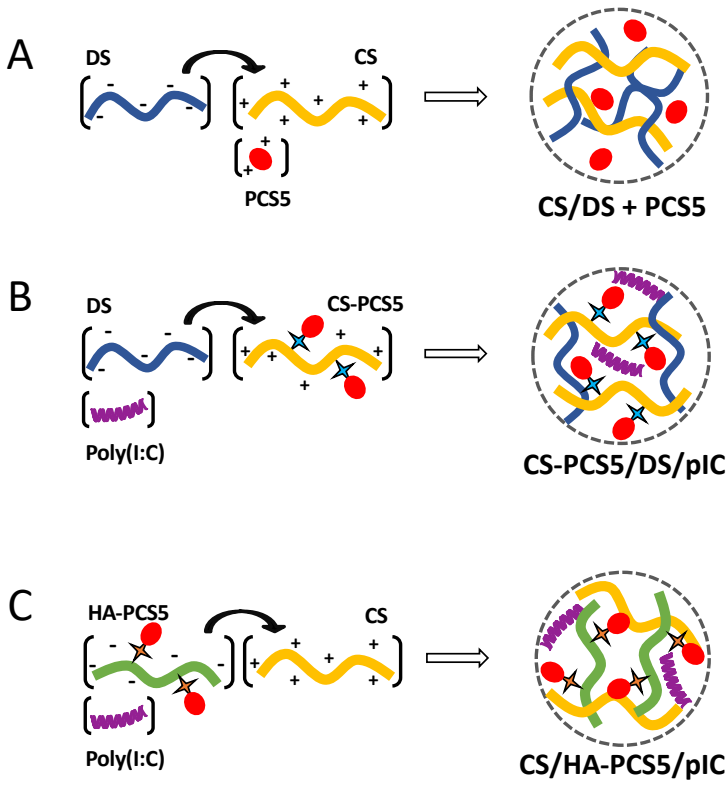

Particle size (nm)	119 ± 7
PDI	0.15
ζ-potential (mV)	-50 ± 3
Antigen loading (%)	7.9
Antigen attachment	Ionic interactions

Particle size (nm)	141 ± 6
PDI	0.17
ζ-potential (mV)	+29 ± 3
Antigen loading (%)	4.9
pIC loading (%)	0.3
Antigen attachment	Oxime bond

Particle size (nm)	211 ± 15
PDI	0.07
ζ-potential (mV)	+30 ± 1
Antigen loading (%)	4.6
pIC loading (%)	0.05
Antigen attachment	Thioether bond

Figure 2. **Composition of the different prototypes developed in this work**. Schematic representation of the preparation process for the three developed nanosystems: (A) CS/DS + PCS5 NPs, (B) CS–PCS5/DS/pIC NPs, and (C) CS/HA–PCS5/pIC NPs, and the corresponding physicochemical properties. CS, chitosan; DS, dextran sulfate; HA, hyaluronic acid; PCS5, protease cleavage site 5; pIC, poly(I:C); NPs, nanoparticles.

In order to improve the long-term stability of the antigen-loaded NPs, the different formulations were freeze-dried using trehalose as the cryoprotectant. The best results in terms of redispersion of the freeze-dried powder and preservation of the original properties of the nanosystems were obtained with a 7% of trehalose for both CS/DS + PCS5 and CS/HA–PCS5/pIC NPs, and 4% of trehalose for the CS–PCS5/DS/pIC NP formulation.

1.2. Release of the covalently attached PCS5 from the NPs

Taking into consideration that we aimed at comparing the influence of different covalent attachments in the generation of the immune response, we evaluated the release of PCS5 from the conjugates. The CS–PCS5 conjugation involved the formation of an oxime bond, which is known to be highly-stable at physiological pHs [45–47]. Therefore, our hypothesis was that the antigen would only be released after being processed by APCs.

In the case of the HA–PCS5 conjugate, a thioether bond was formed between HA and PCS5, which is known to undergo retro-Michael reactions in the presence of free thiols [42,48,49]. This bound was

expected to be broken in the presence of free thiols, present in great amounts in the cytosol of cells as part of glutathione (GSH) molecules. This hypothesis could be verified *in vitro*, where PCS5 was found to be released from the NPs in the presence of GSH, but not in regular PBS medium. Thus, we speculated that the peptide will not be released in the extracellular medium, but only in the intracellular compartments where high concentrations of GSH are present [50,51].

1.3. *In vivo* evaluation of the immune responses elicited in different animal models

1.3.1. Immune responses elicited in mice

Regarding the humoral responses in mice, overall, the IgG responses elicited by the three different NP formulations increased significantly over time, reaching their maximum values at the latest time point of the experiment (week 16) (**Fig. 3A**). At this time point, the amount of anti-PCS5 antibodies detected in all NPs was 3 times higher than the levels detected in unvaccinated mice. This increasing and prolonged immunogenic response is of particular interest in the design of an HIV vaccine, because persistent levels of antibodies seem to be important for an effective vaccination [52]. This response is also in agreement with previous data reported by our group that showed the capacity of the antigen-loaded NPs to induce significant IgG levels up to 28 or 37 weeks after immunization [12,13]. Considering these previous results, it is possible that the antigen-loaded NPs could still induce important levels of antibodies beyond the 16 weeks considered in our study.

In addition to eliciting a strong and maintained immune response, the results of this study also indicated that the covalent linkage between the peptide and the NPs did not have an effect on the humoral responses. This is in contrast with previous findings where the antigen conjugation to the polymeric constituents of the nanocarrier led to an improved humoral response [43,53].

To evaluate the activation of APCs, the expression of the co-stimulatory signals CD40 and CD86, both involved in the T-cell activation process [54–56], was measured. Regarding the levels of CD40 in macrophages, the prototype containing HA elicited the higher values, in comparison both to the control animals and the other two prototypes (**Fig. 3B**). In the case of CD86, both formulations with the covalent attachment and poly(I:C) were able to increase the expression of these surface marker (**Fig. 3C**). These results could support our hypothesis that covalent conjugation can indeed boost the immune response. At the same time, we cannot discard the potential role of poly(I:C) in the stimulation process [57].

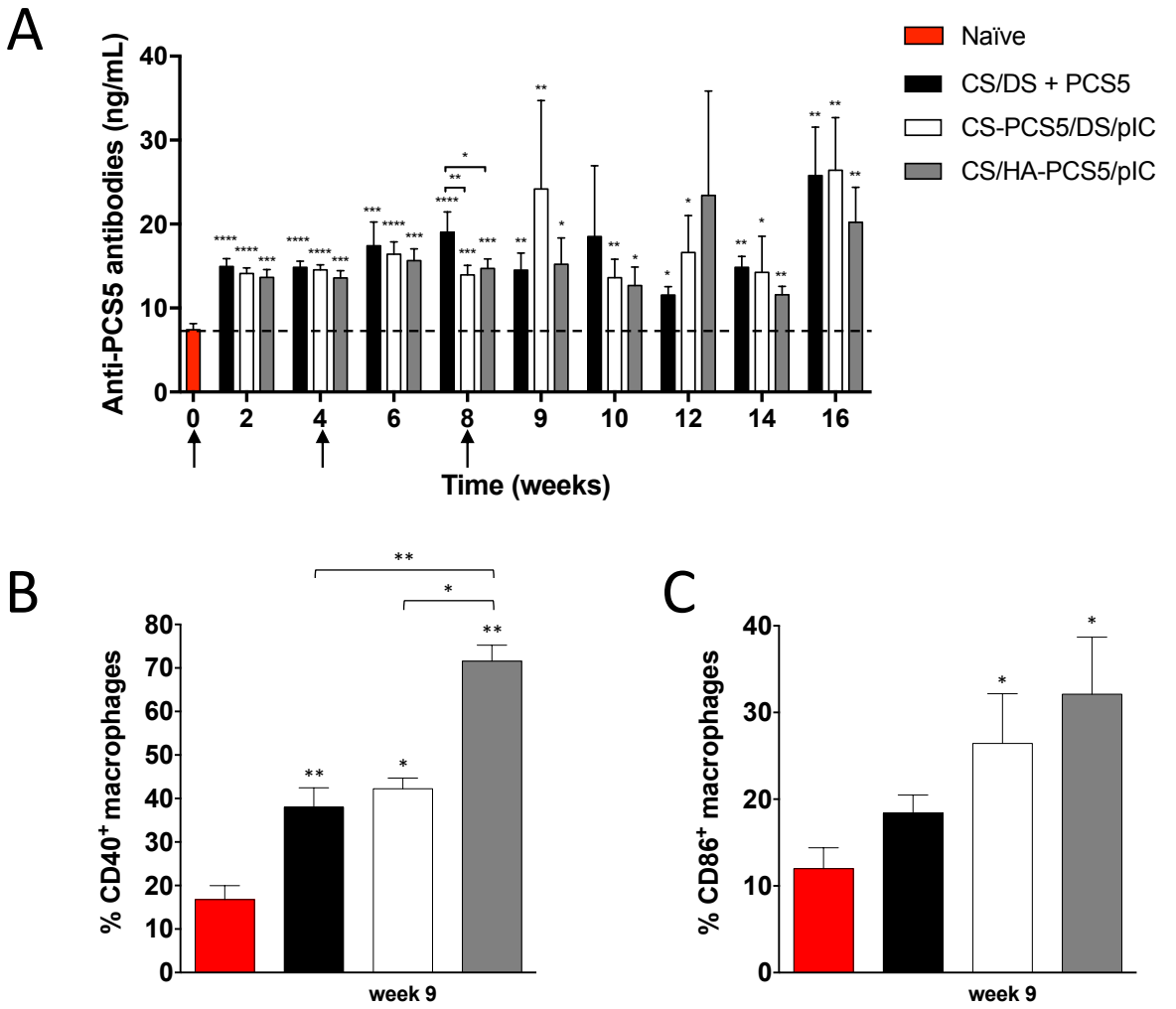

Figure 3. *In vivo* studies in mice. (A) Anti-PCS5 antibody levels after the intramuscular administration of the three nanoformulations. (B, C) Macrophage expression of the co-stimulatory factors CD40 and CD86 at 9 weeks post prime quantified by multicolor flow cytometry of mice splenocytes. Non-treated naïve mice (red bars), and mice vaccinated with CS/DS + PCS5 (black bars), CS–PCS5/DS/pIC (white bars), and CS/HA–PCS5/pIC (gray bars). Values represent mean ± SEM (n ≥ 5). Statistical comparison between groups was done using a Mann-Whitney test. Significant statistical differences are represented as * ($p < 0.05$), ** ($p < 0.01$), *** ($p < 0.001$) and **** ($p < 0.0001$) for comparison between groups and to naïve mice. CS, chitosan; DS, dextran sulfate; HA, hyaluronic acid; PCS5, protease cleavage site 5; pIC, poly(I:C); NPs, nanoparticles.

Finally, when assessing the activation of T cells by measuring the secretion of IL-2 and TNFα, the three prototypes were able to activate both CD4 and CD8 T cells, but with different cytokine secretion kinetics. The NPs based on ionic interactions (CS/DS + PCS5 NPs) stimulated the highest secretion of cytokines at a short time point (10 weeks). In the case of the formulation with the cleavable conjugate (CS/HA–PCS5/pIC NPs), a sustained secretion of IL-2 and TNFα was detected from weeks 12 to 16. Finally, the most stable attachment (in CS–PCS5/DS/pIC NPs), induced a stronger T cell activation at weeks 9, and specially at week 16 (**Fig. 4**). This pattern could indeed be caused by the different release

profiles of the antigen from the NPs, as previously discussed, although further studies will be needed to confirm this hypothesis. It is also worth mentioning that delayed T cell activation observed here has also been described for an mRNA-based vaccine [58], a result that raises questions regarding which is the ideal T cell activation profile to generate a preventive vaccination.

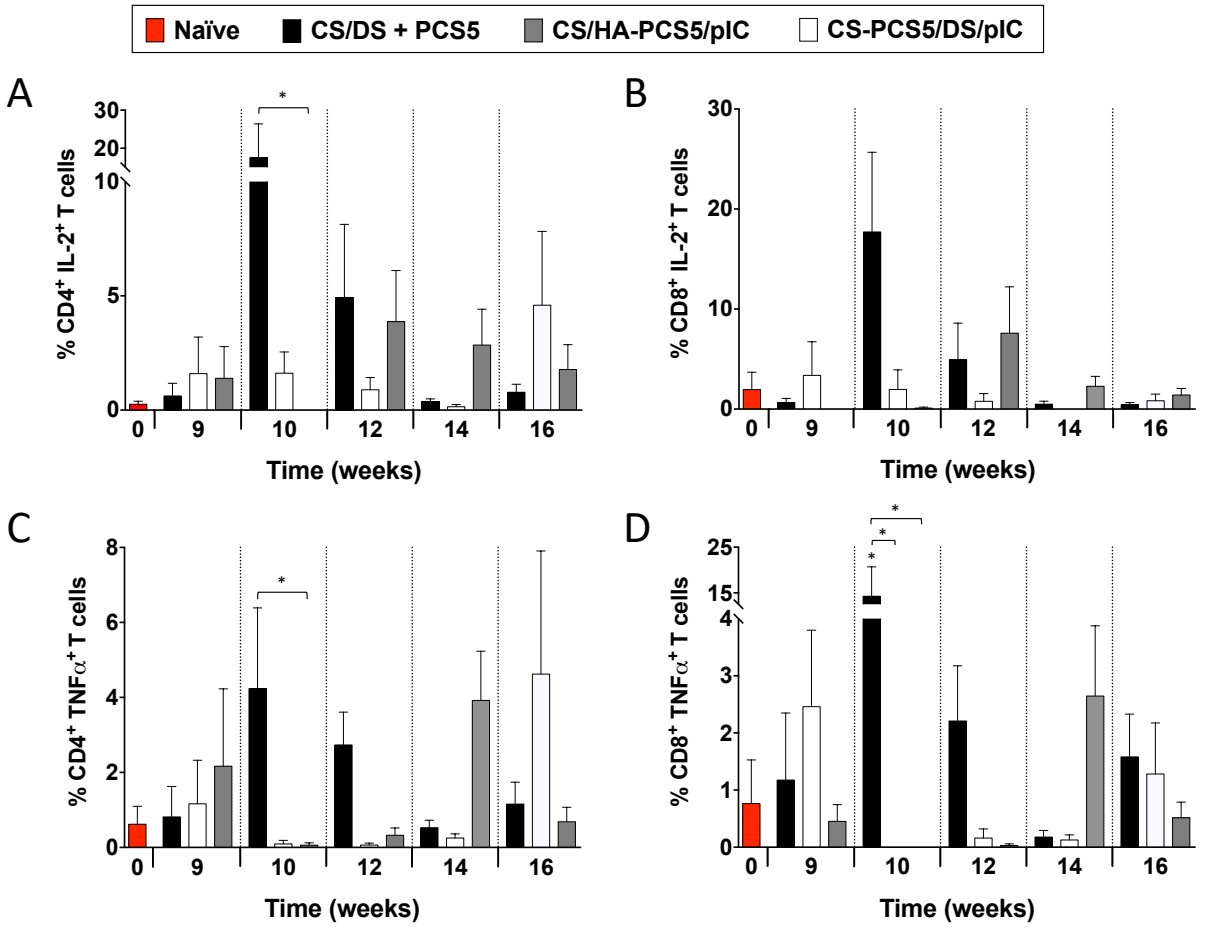

Figure 4. CD4 and CD8 T cell activation. IL-2 and TNFα secretion in (A, C) CD4 and (B, D) CD8 T cells were quantified by multicolor flow cytometry of T-cells derived from splenocytes from non-treated naïve mice (red bars) and NP-vaccinated mice: CS/DS + PCS5 (black bars), CS–PCS5/DS/pIC (white bars) or CS/HA–PCS5/pIC (gray bars). Values represent mean ± SEM (n ≥ 3). Statistical comparison between groups was done using a Mann-Whitney test. Significant statistical differences are represented as *($p < 0.05$) for comparison between groups and to naïve mice. CS, chitosan; DS, dextran sulfate; HA, hyaluronic acid; PCS5, protease cleavage site 5; pIC, poly(I:C); NPs, nanoparticles.

In brief, in this part of the thesis, we engineered different polysaccharide-based NPs loaded with an HIV peptide antigen candidate, PCS5. The results showed that different factors, such as the attachment of the antigen (ionic interactions, cleavable and non-cleavable conjugations), the presence of immunomodulatory molecules such as poly(I:C), or the nature of the polysaccharides (CS, DS or HA) could importantly influence the type of the elicited immune response in mice. Nevertheless, *in vivo*

studies in larger animal models will help to determine whether these humoral and cellular responses would translate into efficient protection in relevant models.

1.3.2. Immune responses elicited in non-human primates (NHP)

We selected two different prototypes of NPs containing PCS peptides in order to assess their performance in NHP, this being the preferred model for vaccination studies [59]. We chose CS/DS NPs due to their capacity to elicit cellular responses at short times after vaccination in mice [60]. Besides, this was the same composition as in the NPs employed in the reference twelve PCS-based vaccine, which had offered good *in vivo* responses in NHPs [22,23]. Since these NPs had been administered intranasally (i.n.) targeting mucosal immunity, with important IgG levels detected at mucosal sites [23], the same route of administration was maintained in this new study. On the other hand, we also selected a prototype consisting of CS/HA/pIC NPs, based on their capacity to elicit a modest but sustained T cell activation in mice [60]. These NPs were administered intramuscularly (i.m.) in order to generate a broad systemic immune response. With regard to the selection of the antigens, our goal was to evaluate the potential of a vaccine with a minimum amount of PCS antigens. Thus, rather than using the twelve peptides previously investigated, we selected the PCS5 peptide that was used for the initial evaluation in mice, as well as the PCS2 and PCS12 peptides. The concept behind this selection was based on the fact that single mutations surrounding these particular sites were reported to significantly impair viral fitness, thus hampering the capacity of the virus to replicate (data not shown).

After the formulation of the NPs with the three PCSs, and the adaptation of the freeze-drying process, the efficacy of these formulations in terms of SIV prevention was assessed in NHPs. Additionally, their efficacy was compared to that of the reference formulation, composed of CS/DS NPs associating the twelve PCSs, combined with the rVSV vectors coding for these sequences (rVSV + Nano, 12 PCSs) [61].

The combination of the CS/DS and CS/HA/pIC NPs containing the three peptides (Nano, 3 PCSs) were administered to eight female macaques. Each animal received both, at the same time, an i.n. instillation of the CS/DS + PCS NPs, and an i.m. injection of the CS/HA–PCS/pIC NPs, every four weeks, for a total of four doses each (**Fig. 5A**). In parallel, the reference formulation containing the twelve PCSs delivered in viral vectors and in NPs (rVSV + Nano, 12 PCSs) was also administered to eight female macaques. In this group, each animal was first primed with the rVSVs i.m., and then boosted with a combination of the NPs i.n. and the rVSVs i.m. (in the 1st and 3rd boosts), only the NPs i.n. (in the 2nd boost) or the rVSVs i.m. alone (in the 4th boost) (**Fig. 5B**) [61]. In both cases, animals were challenged every two weeks, and viral loads monitored.

Figure 5 shows the number of non-infected animals after each challenge, in comparison to the control group. In the case of the reference formulation containing the twelve PCSs (rVSV + Nano, 12 PCSs), after seven intravaginal challenges, 75% of the NHPs remained uninfected, in comparison to the 25% uninfected in the control group. On the other hand, in the case of the NP-based formulation containing three PCSs (Nano, 3 PCSs), after these seven challenges, 50% of the vaccinated animals remained uninfected.

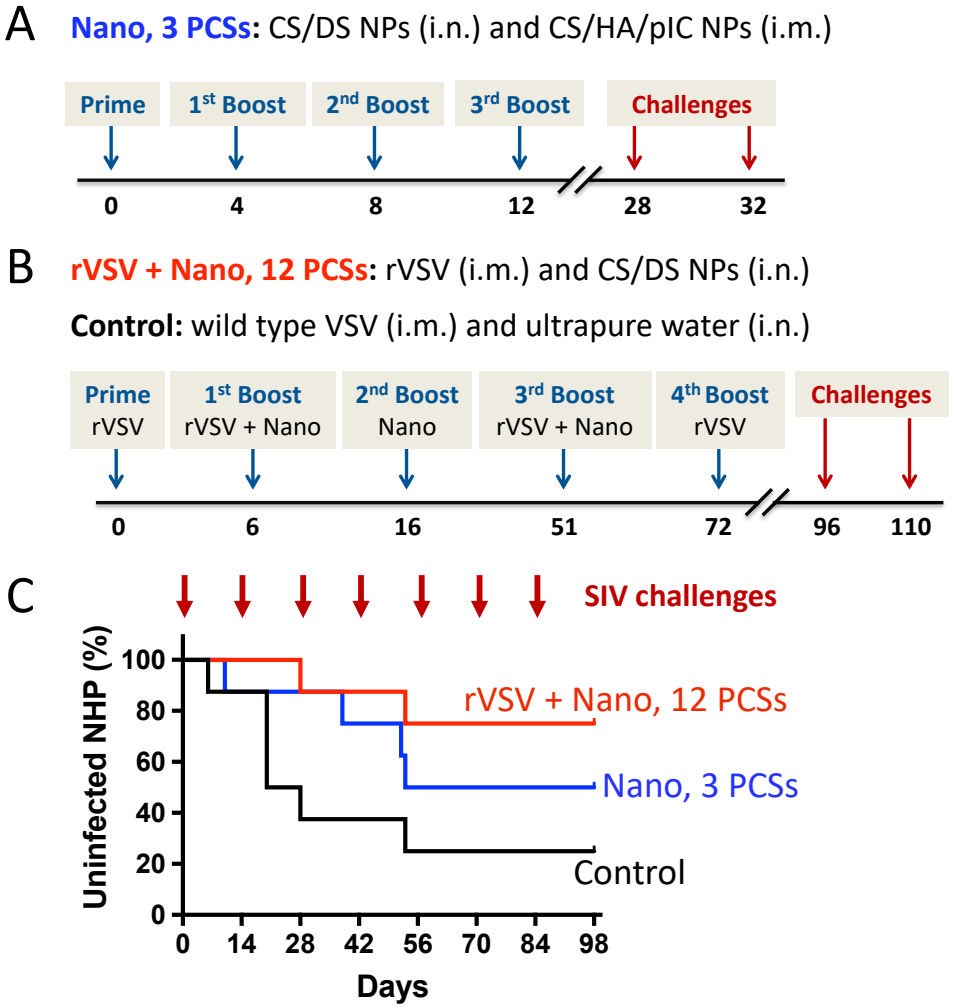

Figure 5. **Efficacy of the studied vaccines in terms of protection against SIV intravaginal challenges**. (A–B) Vaccination groups, administration and challenges scheme for (A) the combination of the CS/DS and CS/HA/pIC nanoparticles with the three PCSs, administered intranasally and intramuscularly, respectively; and (B) the reference formulation based on the viral vectors and CS/DS nanoparticles containing the twelve peptide antigens, administered intramuscularly and intranasally, respectively [15]. (C) Non-human primates were vaccinated either with the CS/DS and CS/HA/pIC nanoparticles containing the three PCSs (Nano, 3 PCSs; in blue); the reference formulation based the twelve peptide antigens delivered in viral vectors and in CS/DS nanoparticles (rVSV + Nano, 12 PCSs; in red) [15]; or with the control VSVs without the peptides and ultrapure water (Control; in black). Percentage of uninfected animals after every intravaginal challenge with SIV, up to seven challenges. CS, chitosan; DS, dextran sulfate; HA, hyaluronic acid; i.m., intramuscular; i.n.; intranasal; NPs, nanoparticles; PCS, protease cleavage site; rVSV, recombinant vesicular stomatitis virus.

These preliminary studies in NHPs indicate that a vaccine targeting three of the twelve PCSs is a strategy that can delay and prevent SIV infection in a moderate extent. It is important to highlight that this formulation contains only three of the twelve that have been described to difficult virus maturation [18,19]. Indeed, the formulation with the twelve peptides and a highly immunogenic carrier (rVSV + Nano, 12 PCSs) showed very promising results in terms of SIV prevention [61]. Therefore, it is possible that a better selection of peptides or an increase of this number might improve the potency of the NP-based vaccine. Besides, the incorporation of additional adjuvants might help to increase the levels of protection. Altogether, we believe that there is still space to optimize the NP-based vaccine in order to generate a more potent SIV vaccine candidate based on NPs with a low number of antigens.

Considering the prominent levels of protection achieved in NHP using the PCSs associated to CS/DS NPs by ionic interactions, our next objective was to adapt the manufacturing process of these polysaccharide-based NPs to be implemented in a pilot plant.

2. Technological challenges in the preclinical development of an HIV nanovaccine candidate

Our objective in this part of the work was to optimize and adapt the nanoformulation for its production in a pilot plant for preclinical and, potentially, future clinical trials. Although the vaccine assessed in NHP was composed of twelve different antigens [22,23,61], bearing in mind that the formulation process for each of the peptides is essentially the same, the nanoformulation containing one peptide antigen (PCS5) was selected for its technological transfer.

The complexity of some nanoformulations and the lack of well-defined standard analytical methodologies for their complete characterization are some of the main hurdles that have hampered the arrival of more nanomedicines to the market [62]. Indeed, important differences between NPs prepared in a lab or in an industrial scale have already been reported [63]. Therefore, ensuring a good reproducibility and choosing the adequate characterization methods are important steps that have to be more addressed in the literature. Here, our aim was to transfer the development of a nanovaccine from the bench to an industrial environment, highlighting the critical requirements that all nanovaccines should fulfill in order to progress towards commercialization.

First, we applied the quality-by-design (QbD) approach to stablish both the quality target product profile and the critical quality attributes of our formulation. Also, an Ishikawa diagram allowed us to

identify the potential variables with the highest impact on the formulation attributes. NPs were prepared by ionic complexation of the positively charged components (CS and the peptide PCS5) and the negatively charged DS (**Fig. 6A**). By analyzing the formulation parameters, we observed that low incorporation rates of DS caused the aggregation of the NPs, with significant changes in particle size and PDI.

Regarding the analytical tools for its physicochemical characterization, dynamic light scattering (DLS) techniques are fast and easy methods to determine particle size and polydispersity, however, they present several drawbacks [64,65]. Nevertheless, this method has several drawbacks, such as a bias towards detecting the larger particles of the sample, limited resolution between subpopulations with similar particle size, or the assumption that the particles are spherical [64]. Therefore, the combination of DLS results with other complementary orthogonal techniques, such as electron microscopy or nanoparticle tracking analysis (NTA), is highly recommended by competent organizations, such as the EUNCL [65]. Here, by applying all these techniques, we could determine the physicochemical properties of the nanoformulation, offering comparable results between them (**Fig. 6B–E**). Interestingly, after freeze-drying the NPs, the different techniques also showed similar results. In addition, the freeze-dried formulation was able to extend the long-term stability of the NPs to up to 15 months, and up to 6 in an accelerated study, following ICH recommendations.

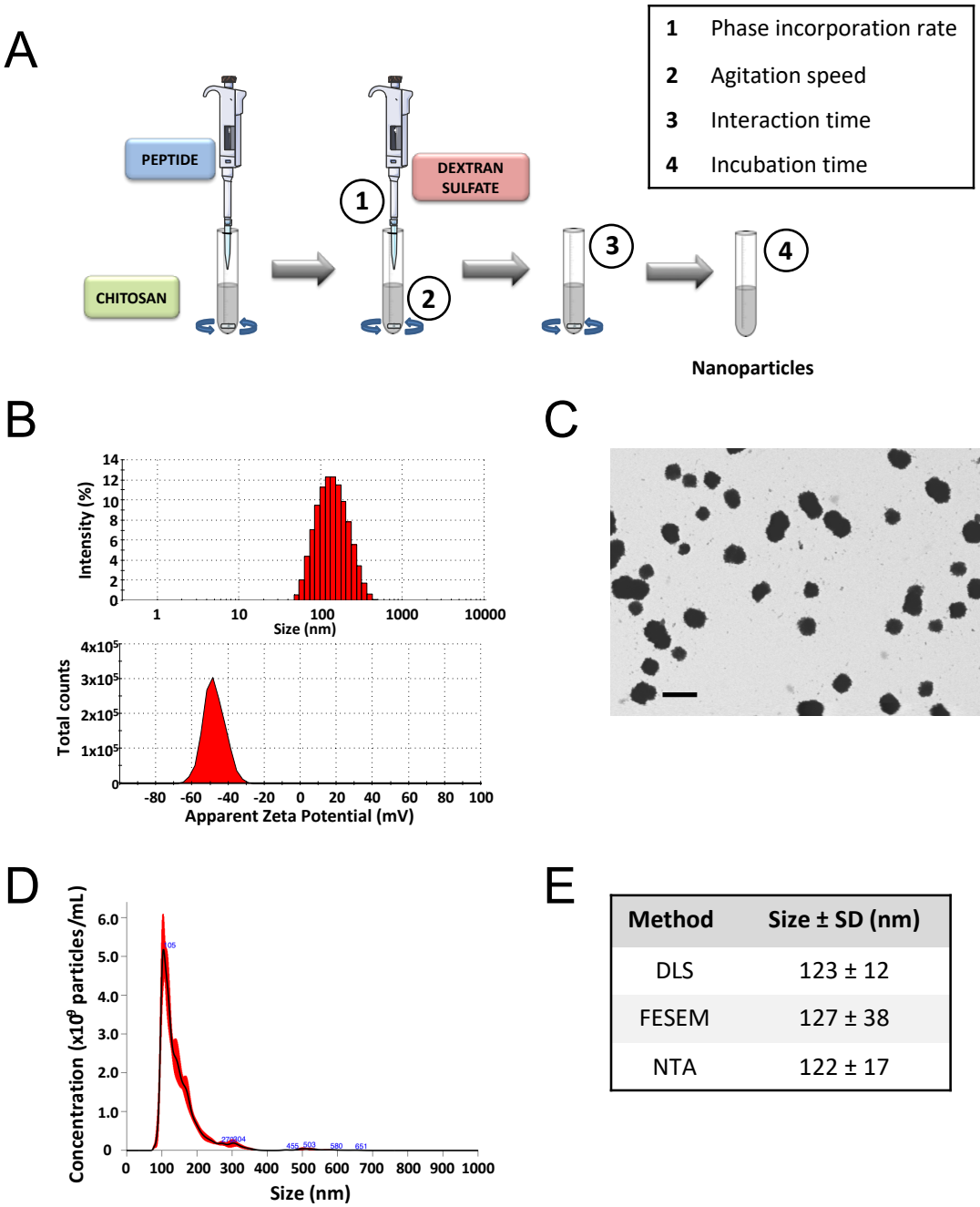

Method	Size ± SD (nm)
DLS	123 ± 12
FESEM	127 ± 38
NTA	122 ± 17

Figure 6. Nanoparticle manufacturing process and characterization. (A) Fabrication of the nanoparticles. The peptide antigen is added to the chitosan solution. Then, (1; phase incorporation rate) the solution of dextran sulfate is incorporated into the chitosan/peptide solution, (2; agitation speed) under magnetic stirring. (3; interaction time) Components are kept under agitation to allow their interaction, and then (4; incubation time) they are kept for 10 additional min in the absence of agitation. (B–E) Physicochemical characterization of the nanoparticles through orthogonal techniques: (B) DLS intensity histograms (top) and surface charge values (bottom), (C) Micrographs of the nanoparticles by FESEM with the STEM detector (size bar represents 200 nm), (D) NTA size distribution. (E) Summary of the mean size values of the nanoparticles by the three complementary techniques evaluated. DLS, dynamic light scattering; FESEM, field emission scanning electron microscopy; NTA, nanoparticle tracking analysis.

As previously stated, another important requirement for the good manufacturing of a nanoformulation is to ensure that the production procedure is reproducible across different people and laboratories. Hence, the formulation process was transferred to three different laboratories with different personnel, and the resulting batches of loaded NPs (from 1.65 to 200 mL) were thoroughly characterized and compared. In the different centers, the physicochemical properties of the batches were found to be within the specification values previously established. Besides, the scaling-up by microfluidics and a batch-mode preparation yielded particles within the critical quality attributes. Finally, the preparation of a large batch (200 mL) was conducted in the pilot plant under good manufacturing practices (GMP)-like conditions. In this regard, production processes, materials and personal flow were designed in qualified facilities according to GMP guidelines. The physicochemical properties of the final formulation were found within the previously described attributes (**Table 1**). Therefore, the translation of the nanovaccine from the bench to an industrial environment was successfully achieved.

Table 1. Physicochemical properties of the nanovaccine fabricated in the pilot plant.

Sample	Particle size (nm)	PDI	ζ-potential (mV)	pH	Transmittance (%)	Osmolality (mosm/kg)
Final formulation	150 ± 1	0.13	-42 ± 1	6.6	7.2	186

PDI, polydispersity index.

Overall, we have demonstrated the feasibility of an HIV nanovaccine to be manufactured in a pilot plant. By implementing a QbD approach, the most critical aspects with an impact on the formulation attributes were highlighted. In addition, we have emphasized the importance of combining orthogonal techniques to guarantee an accurate and complete characterization of the formulation. Finally, the interlaboratory reproducibility and scalability of the nanoformulation confirmed that this nanomedicine would be ready to move towards an industrial manufacturing set up.

A different objective of this thesis, but still in line with our interest on the potential of nanotechnology for the modulation of the immune system, was the re-activation of the immune system in the context of cancer. For this purpose, we used an already known molecule, the TLR3 agonist poly(I:C). This is a dsRNA that upon interaction with this receptor, upregulates the expression of type I IFN genes, ultimately generating pro-inflammatory features [66]. Within the tumor microenvironment, tumor-associated macrophages (TAMs) present anti-inflammatory and tolerogenic features and promote cancer cell migration. Their treatment with poly(I:C) has shown to polarize them to anti-tumoral states in which they are re-activated to fight cancer [67]. Therefore, the final objective

of this thesis was to design and develop poly(I:C) nanocomplexes with tunable properties to target and polarize TAMs.

3. Arginine-based poly(I:C)-loaded nanocomplexes for the re-education of TAMs

Despite the known potential of poly(I:C) for polarizing macrophages towards an anti-tumoral M1-like phenotype with ability to fight tumors [68], the systemic administration of this TLR3 agonist presents significant side effects [25]. Currently, it has been reported that the complexation of poly(I:C) with cationic polymers, i.e. polyethyleneimine (PEI), leads to positive *in vivo* results in different cancer models [69], and it is currently in a phase I clinical trial [70]. Unfortunately, PEI itself is not absent of systemic toxicity [71]. Therefore, the main objective of this study has been to develop a carrier for poly(I:C), alternative to PEI, endowed with the capacity to re-educate TAMs, and that would be adequate for systemic administration.

3.1. Design and development of the nanocomplexes

As the first step in the development of a poly(I:C)-loaded nanoformulation and, based on a nanotechnology recently reported by our group showing the capacity of modified octaarginine to complex polynucleotides [72], different positively-charged arginine-rich polymers were selected for poly(I:C) complexation. Oligo-arginines have been extensively employed for the delivery of different nucleic acids due to their cell-penetrating peptide (CPP) nature, which increases their uptake and, as a result, improves their therapeutic performance [72–74]. Although, initially, octaarginine (r8), laurate-octaarginine (C12r8) and polyarginine (pArg) were the polypeptides selected, only the last two were able to form nanocomplexes with the dsRNA. In the case of C12r8, the hydrophobic tail was probably critical to improve the stability of the resulting complexes, in comparison to the unmodified r8 [75,76]. For pArg, its long chains would offer a higher number of positive sites for the binding of the dsRNA, in comparison to the smaller chains of the r8 [77].

In order to improve the nanocomplexes stability, we applied the technology previously described by our group to envelop the nanocomplexes with either pegylated polyglutamic acid (PEG–PGA) copolymers or with HA, thereby generating enveloped nanocomplexes (ENCPs) [72,78]. For the PEG–PGA, the presence of PEG as the external layer of the system was expected to provide a steric protection and increase the colloidal stability of the system [79]. Additionally, the combination of PEG and PGA has already been shown to facilitate the passive access of enveloped nanocapsules to the tumor site [80]. Out of the screening of the different PEG–PGA copolymers varying (*i*) their

conformation (branched or diblock), (*ii*) the length of the PGA chain, and (*iii*) the PEG density, only the diblock copolymer PEG_{20k}–PGA10 was able to stabilize the nanocomplexes for at least 24 h of incubation in cell culture media. Indeed, other C12r8 ENCPs enveloped with this PEG–PGA arrangement were also significantly stabilized [72,81], which confirms that this diblock combination of a low number of PGA units (10) with a long PEG tail (20 kDa) provides good steric protection to a nanosystem.

Regarding HA, this negatively charged polymer was selected based on its anionic character and stealth properties [82–84]. Indeed, a recent report has claimed that HA coatings are able to decrease the adsorption of immunogenic proteins, in comparison to other anionic coatings [85]. All these characteristics were expected to confer stability and to increase the ENCPs circulation time.

Based on these data, a total of four ENCPs were selected to investigate their capacity to polarize macrophages: non-enveloped, diblock PEG_{20k}–PGA10 enveloped and HA-enveloped pArg nanocomplexes (pArg:pIC ENCPs; pArg:pIC/PEG–PGA ENCPs and pArg:pIC/HA ENCPs, respectively) and diblock PEG_{20k}–PGA10 enveloped C12r8 nanocomplexes (C12r8:pIC/PEG–PGA ENCPs). All ENCPs presented particle sizes between 150 and 200 nm, with low PDIs and surface charges ranging from highly positive (pArg:pIC), through neutral (C12r8:pIC/PEG–PGA) to negatively charged (pArg:pIC/HA). Remarkably, high loading values of poly(I:C) were obtained for the different systems (**Fig. 7A,B**). Finally, all the systems efficiently associated poly(I:C), while protecting it from the degradation in cell culture media (**Fig. 7C,D**).

A

Formulation	Ratio (w/w)	Particle size (nm)	PDI	ζ-Potential (mV)	Poly(I:C) loading (%)
pArg:pIC	1:1	163 ± 14	0.20	+44 ± 3	50
pArg:pIC /PEG–PGA	1:1 :3	190 ± 14	0.18	+26 ± 8	20
pArg:pIC /HA	1:1 :1.5	157 ± 10	0.16	-15 ± 7	29
C12r8:pIC /PEG–PGA	4:1 :3	165 ± 14	0.07	+5 ± 1	12.5

Mean ± SD, n ≥ 12. C12r8, laurate octa-arginine; HA, hyaluronic acid; pArg, polyarginine; PDI, polydispersity index; PEG–PGA, pegylated polyglutamic acid; pIC, poly(I:C); w/w: weight/weight.

B

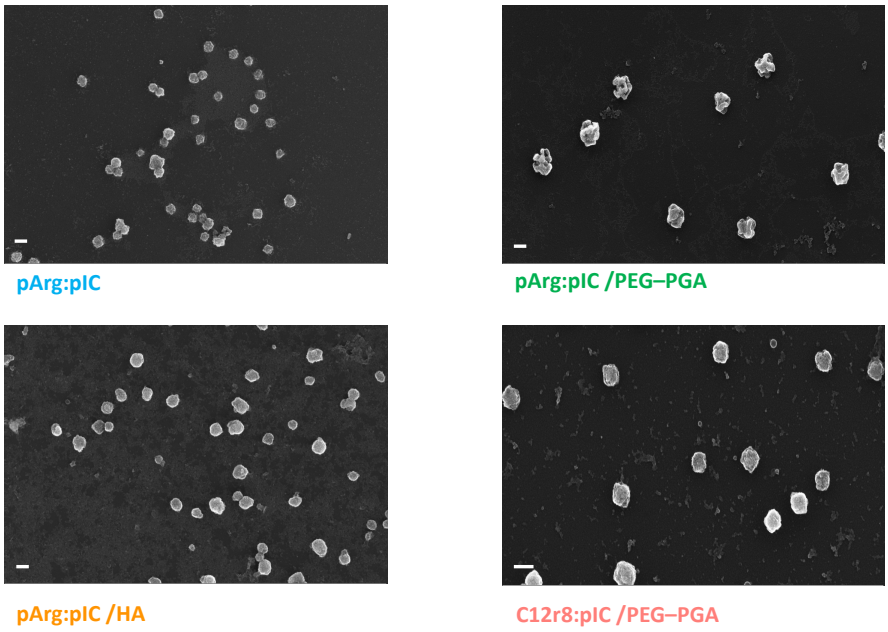

C

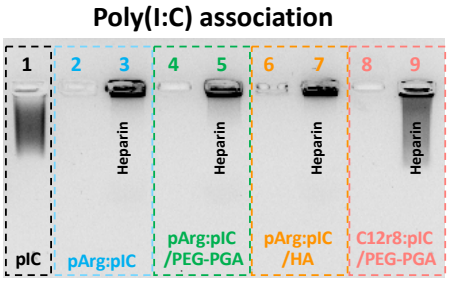

D

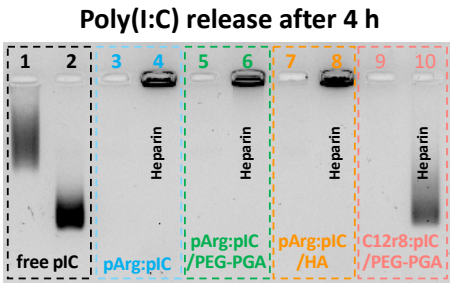

Figure 7. Physicochemical properties and poly(I:C) binding affinity of the selected nanocomplexes. (A) Summary of the main physicochemical properties of the four nanosystems, and (B) FESEM images of each prototype. Values represent mean ± SD (n ≥ 12). Size bars represent 200 nm. (C) An agarose gel retardation assay was performed to evaluate the poly(I:C) binding capacity of the nanocomplexes. Lanes: (1) free poly(I:C), (2, 4, 6, 8) are pArg:pIC, pArg:pIC/PEG–PGA, pArg:pIC/HA and C12r8:pIC/PEG–PGA nanocomplexes, respectively; and (3, 5, 7, 9) are the corresponding nanocomplexes incubated with heparin. (D) An agarose gel retardation assay was performed to evaluate the release and integrity of poly(I:C) after 4 h of incubation in cell culture media at 37 °C. Lanes: (1) free poly(I:C) in solution and (2) in cell culture media; (3, 5, 7, 9) are pArg:pIC, pArg:pIC/PEG–PGA, pArg:pIC/HA and C12r8:pIC/PEG–PGA nanocomplexes in cell culture media; and (4, 6, 8, 10) are the same conditions incubated with heparin. C12r8, laurate-octaarginine; FESEM, field emission scanning electron microscopy; HA, hyaluronic acid; pArg, poly-arginine; PEG–PGA, pegylated polyglutamic acid; PDI, polydispersity index; pIC, poly(I:C); w/w, weight/weight.

3.2. Macrophage polarization towards a pro-inflammatory phenotype

The target of the developed poly(I:C) ENCPs is the intracellular endosomal receptor TLR3. In order to confirm that the poly(I:C) associated to the ENCPs was able to reach this receptor, we studied the localization of the free and nanocomplexed poly(I:C) once inside the cells. By using poly(I:C)-rhodamine and CellLight® to track the cargo and the endosomes, respectively, confocal microscopy studies confirmed the presence of high amounts of nanocomplexed poly(I:C) (in red) inside the endosome (in green), after 8 h of incubation (**Fig. 8A**).

Once we confirmed that the target was reached, the following step was to determine if poly(I:C) was able to activate TLR3 and, therefore, to polarize macrophages. First, the expression of surface markers related to M1 pro-inflammatory (CD80 and MHC II) and M2 pro-tumoral (CD206 and CD163) phenotypes was studied. Overall, low changes in the expression of these markers were observed for the free and nanocomplexed poly(I:C). These results, which are in line with a recent publication on the evaluation of poly(I:C) *versus* imiquimod *in vitro*, show a very limited ability of free poly(I:C) to modulate the ratio of M1/M2 receptors on the surface of prototypical M0 or M2 macrophages [68].

On the basis of these data, the ability of poly(I:C) to polarize macrophages towards an M1-like anti-tumoral phenotype was evaluated by conducting functional assays. Therefore, we tested the ability of pre-treated macrophages to secrete chemokines involved in the recruitment of cytotoxic T cells (CTLs) to fight cancer cells [86,87]. In this regard, we found a higher production of the chemokines CXCL10 and CCL5 by macrophages treated with ENCPs in comparison to the free poly(I:C) and the control non-treated M0 macrophages (**Fig. 8B**) These results demonstrate that, even though nanocomplexed poly(I:C) did not provoke an important change in the surface marker expression of macrophages, other anti-tumoral features such as the CTL recruitment capacity, were greatly improved. Therefore, it would be expected that within the tumor microenvironment, and upon treatment with the nanocomplexes, the secretion of these chemokines by TAMs would be increased, attracting CTLs towards the tumors.

Besides their role in activating the immune system to fight cancer, macrophages have also the capacity to directly kill tumor cells [88]. To assess the potential of the poly(I:C) ENCPs to re-educate macrophages towards killing tumor cells, we performed another functional assay. For this, pre-treated macrophages were co-cultured with stained pancreatic cancer cells (PANC-1) for 48 h. After this time, the cytotoxicity of nanocomplex-treated macrophages towards cancer cells (30–40%) was much higher than the one of M0 or M2 macrophages (0 and -15%, respectively), and only slightly lower than the targeted M1-like macrophages (60%) (**Fig. 8C**). These results corroborate the high potential of nanocomplexed poly(I:C) to re-educate macrophages to fight cancer.

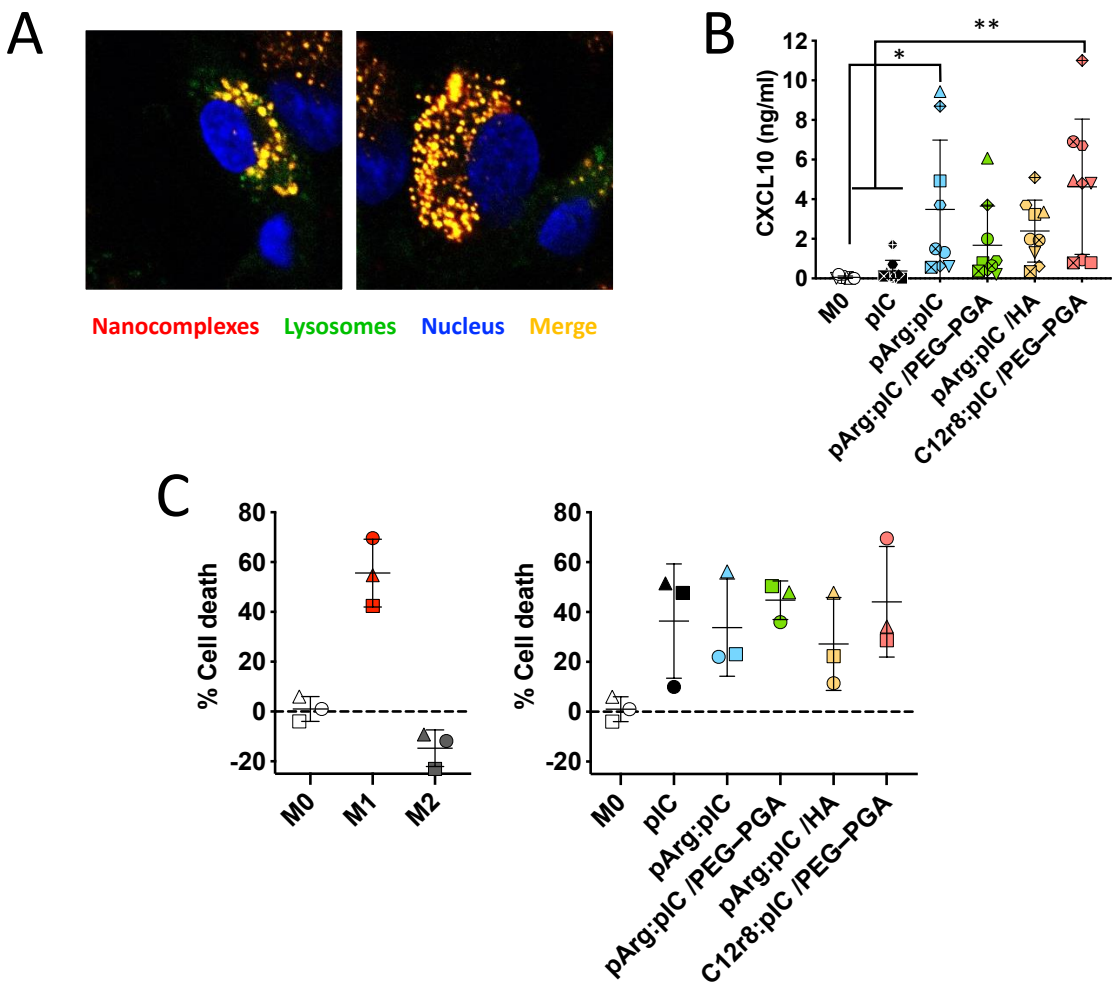

Figure 8. Nanocomplexed poly(I:C) cellular distribution, and capacity to polarize macrophage towards M1 phenotypes. (A) Co-localization with the endosome of rhodamine-labeled pArg:pIC nanocomplexes after 8 h of incubation (100x magnification). (B) Secretion of the chemoattractant molecules CXCL10 by (M0 macrophages pre-treated with free or nanocomplexed poly(I:C). (C) % of cancer cell death caused by (left) the prototypic macrophages or (right) M0 macrophages pre-treated with free or nanocomplexed poly(I:C). Each symbol shape represents a different donor. Values represent mean ± SD (n ≥ 3). Statistical comparison was done using an ordinary one-way ANOVA followed by a Tukey's multiple comparison test between groups. C12r8, laurate-octaarginine; HA, hyaluronic acid; pArg, poly-arginine; PANC-1, pancreatic cancer cells; PEG–PGA, pegylated polyglutamic acid; pIC, poly(I:C).

Unexpectedly, these positive *in vitro* results could not be translated into an enhanced anti-tumoral efficacy *in vivo* using an immunocompetent murine tumor model. Although an *in vitro/in vivo* correlation should not necessarily be expected, we have speculated about the potential reasons for the limited *in vivo* activity of the ENCPs. One of our hypotheses is the potential difficulty for the ENCPs to diffuse across the tumor microenvironment. Although the presence of a hydrophilic polymer on the surface of nanocarriers was expected to facilitate the diffusion [80], it could be accepted that the size of the ENCPs might have hampered this process. Another hypothesis is the one that presumes that the

high affinity of poly(I:C) towards the arginine polymers/oligomers, hinders its release and availability for interaction with the TLR3 targeted receptor. This slow release might have been sufficient to stimulate macrophages *in vitro* but not under *in vivo* conditions. Hence, additional dose-scaling studies are needed in order to understand the mechanistic behavior of ENCPs.

To sum up, the arginine-based nanocomplexes developed during this thesis were able to protect and stabilize poly(I:C). Nanocomplexed poly(I:C) was able to reach the endosome, where its target TLR3 is found, and to polarize macrophages towards the secretion of T cell recruiter chemokines, together with cytotoxic properties. These results did not correlate well with those of a preliminary exploratory *in vivo* study intended to evaluate the capacity of the ENCPs to prevent tumor growth. These differences emphasize the need for a deeper understanding of the biodistribution and intracellular delivery of poly(I:C). Furthermore, *in vivo* toxicity studies following intravenous administration need to be performed in order to fully determine the value of the delivery strategy. In this regard, ENCPs could present advantages for protecting the activity of their therapeutic cargo.

Overall, in this thesis we have shown that by tuning the properties of NPs, the immune system can be modulated both in the context of a preventive HIV vaccine and of cancer treatment. The tunability of NPs, that allows to attach the cargos by different approaches, and to tailor the surface of the nanosystem, together with the capacity to co-encapsulate several molecules, is a potential tool for the development of more effective medicines. Finally, we have also shown that NP fabrication can be successfully transferred towards a pilot plant working under GMP-like conditions, by carefully monitoring and analyzing the critical attributes of the formulation.

References

[1] D.J. Irvine, M.C. Hanson, K. Rakhra, T. Tokatlian, Synthetic nanoparticles for vaccines and immunotherapy, Chem. Rev. 115 (2015) 11109–11146. doi:10.1021/acs.chemrev.5b00109.

[2] T.G. Dacoba, A. Olivera, D. Torres, J. Crecente-Campo, M.J. Alonso, Modulating the immune system through nanotechnology, Semin. Immunol. 34 (2017) 78–102. doi:10.1016/j.smim.2017.09.007.

[3] M. Tobío, R. Gref, A. Sánchez, R. Langer, M.J. Alonso, Stealth PLA-PEG nanoparticles as protein carriers for nasal administration, Pharm. Res. 15 (1998) 270–275. doi:10.1023/A:1011922819926.

[4] A. Vila, A. Sánchez, C. Évora, I. Soriano, J.L. Vila Jato, M.J. Alonso, PEG-PLA nanoparticles as carriers for nasal vaccine delivery, J. Aerosol Med. 17 (2004) 174–185. doi:10.1089/0894268041457183.

[5] P. Calvo, C. Remuñán-López, J.L. Vila-Jato, M.J. Alonso, Novel hydrophilic chitosan-polyethylene oxide nanoparticles as protein carriers, J. Appl. Polym. Sci. 63 (1997) 125–132.

[6] C. Prego, P. Paolicelli, B. Díaz, S. Vicente, A. Sánchez, Á. González-Fernández, M.J. Alonso, Chitosan-based nanoparticles for improving immunization against hepatitis B infection, Vaccine. 28 (2010) 2607–2614. doi:10.1016/j.vaccine.2010.01.011.

[7] J.F. Correia-Pinto, N. Csaba, J. Schiller, M.J. Alonso, Chitosan-poly (I:C)-PADRE based nanoparticles as delivery vehicles for synthetic peptide vaccines, Vaccines. 3 (2015) 730–750. doi:10.3390/vaccines3030730.

[8] M. Peleteiro, E. Presas, J.V. González-Aramundiz, B. Sánchez-Correa, R. Simón-Vázquez, N. Csaba, M.J. Alonso, Á. González-Fernández, Polymeric nanocapsules for vaccine delivery: influence of the polymeric shell on the interaction with the immune system, Front. Immunol. 9 (2018). doi:10.3389/fimmu.2018.00791.

[9] A.S. Cordeiro, J. Crecente-Campo, B.L. Bouzo, S.F. González, M. de la Fuente, M.J. Alonso, Engineering polymeric nanocapsules for an efficient drainage and biodistribution in the lymphatic system, J. Drug Target. 27 (2019) 646–658. doi:10.1080/1061186X.2018.1561886.

[10] J. Crecente-Campo, J. Guerra-Varela, M. Peleteiro, C. Gutiérrez-Lovera, I. Fernández-Mariño, A. Diéguez-Docampo, Á. González-Fernández, L. Sánchez, M.J. Alonso, The size and composition of polymeric nanocapsules dictate their interaction with macrophages and biodistribution in zebrafish, J. Control. Release. 308 (2019) 98–108. doi:10.1016/j.jconrel.2019.07.011.

[11] J. Crecente-Campo, M.J. Alonso, Engineering, on-demand manufacturing, and scaling-up of polymeric nanocapsules, Bioeng. Transl. Med. 4 (2019) 38–50. doi:10.1002/btm2.10118.

[12] S. Vicente, M. Peleteiro, B. Díaz-Freitas, A. Sanchez, Á. González-Fernández, M.J. Alonso, Co-delivery of viral proteins and a TLR7 agonist from polysaccharide nanocapsules: a needle-free vaccination strategy, J. Control. Release. 172 (2013) 773–781. doi:10.1016/j.jconrel.2013.09.012.

[13] J.V. González-Aramundiz, E. Presas, I. Dalmau-Mena, S. Martínez-Pulgarín, C. Alonso, J.M. Escribano, M.J. Alonso, N.S. Csaba, Rational design of protamine nanocapsules as antigen delivery carriers, J. Control. Release. 245 (2017) 62–69. doi:10.1016/j.jconrel.2016.11.012.

[14] J. Crecente-Campo, S. Lorenzo-Abalde, A. Mora, J. Marzoa, N. Csaba, J. Blanco, Á. González-Fernández, M.J. Alonso, Bilayer polymeric nanocapsules: a formulation approach for a thermostable and adjuvanted E. coli antigen vaccine, J. Control. Release. 286 (2018) 20–32. doi:10.1016/j.jconrel.2018.07.018.

[15] A.M. Ledo, M.S. Sasso, V. Bronte, I. Marigo, B.J. Boyd, M. Garcia-Fuentes, M.J. Alonso, Co-delivery of RNAi and chemokine by polyarginine nanocapsules enables the modulation of myeloid-derived suppressor cells, J. Control. Release. 295 (2019) 60–73. doi:10.1016/j.jconrel.2018.12.041.

[16] HIV vaccines go to trial, Nat. Med. 25 (2019) 703. doi:10.1038/s41591-019-0460-0.

[17] Y. Liu, C. Chen, Role of nanotechnology in HIV/AIDS vaccine development, Adv. Drug Deliv. Rev. 103 (2016) 76–89. doi:10.1016/j.addr.2016.02.010.

[18] M. Luo, R. Capina, C. Daniuk, J. Tuff, H. Peters, M. Kimani, C. Wachihi, J. Kimani, T.B. Ball, F.A. Plummer, Immunogenicity of sequences around HIV-1 protease cleavage sites: potential targets and population

coverage analysis for a HIV vaccine targeting protease cleavage sites, Vaccine. 31 (2013) 3000–3008. doi:10.1016/j.vaccine.2013.04.057.

[19] H. Li, R.W. Omange, F.A. Plummer, M. Luo, A novel HIV vaccine targeting the protease cleavage sites, AIDS Res. Ther. 14 (2017) 51. doi:10.1186/s12981-017-0174-7.

[20] H. Li, R.W. Omange, C. Czarnecki, J.F. Correia-Pinto, J. Crecente-Campo, M. Richmond, L. Li, N. Schultz-Darken, M.J. Alonso, J.B. Whitney, F.A. Plummer, M. Luo, Mauritian cynomolgus macaques with M3M4 MHC genotype control SIVmac251 infection, J. Med. Primatol. 46 (2017) 137–143. doi:10.1111/jmp.12300.

[21] A.H. Kaplan, J.A. Zack, M. Knigge, D.A. Paul, D.J. Kempf, D.W. Norbeck, R. Swanstrom, Partial inhibition of the human immunodeficiency virus type 1 protease results in aberrant virus assembly and the formation of noninfectious particles, J. Virol. 67 (1993) 4050–4055.

[22] H. Li, M. Nykoluk, L. Li, L.R. Liu, R.W. Omange, G. Soule, L.T. Schroeder, N. Toledo, M.A. Kashem, J.F. Correia-Pinto, B. Liang, N. Schultz-Darken, M.J. Alonso, J.B. Whitney, F.A. Plummer, M. Luo, Natural and cross-inducible anti-SIV antibodies in Mauritian cynomolgus macaques, PLoS One. 12 (2017) 1–20. doi:10.1371/journal.pone.0186079.

[23] H. Li, Y. Hai, S.-Y. Lim, N. Toledo, J. Crecente-Campo, D. Schalk, L. Li, R.W. Omange, T.G. Dacoba, L.R.L.R. Liu, M.A. Kashem, Y. Wan, B. Liang, Q. Li, E. Rakasz, N. Schultz-Darken, M.J. Alonso, F.A. Plummer, J.B. Whitney, M. Luo, Mucosal antibody responses to vaccines targeting SIV protease cleavage sites or full-length Gag and Env proteins in Mauritian cynomolgus macaques, PLoS One. 13 (2018) e0202997. doi:10.1371/journal.pone.0202997.

[24] J.F. Correia-Pinto, M. Peleteiro, N. Csaba, Á. González-Fernández, M.J. Alonso, Multi-enveloping of particulated antigens with biopolymers and immunostimulant polynucleotides, J. Drug Deliv. Sci. Technol. 30 (2015) 424–434. doi:10.1016/j.jddst.2015.08.010.

[25] A.M. Hafner, B. Corthésy, H.P. Merkle, Particulate formulations for the delivery of poly(I:C) as vaccine adjuvant, Adv. Drug Deliv. Rev. 65 (2013) 1386–1399. doi:10.1016/j.addr.2013.05.013.

[26] H. Park, L. Adamson, T. Ha, K. Mullen, S.I. Hagen, A. Nogueron, A.W. Sylwester, M.K. Axthelm, A. Legasse, M. Piatak, J.D. Lifson, J.M. McElrath, L.J. Picker, R.A. Seder, Polyinosinic-polycytidylic acid is the most effective TLR adjuvant for SIV Gag protein-induced T cell responses in nonhuman primates, J. Immunol. 190 (2013) 4103–4115. doi:10.4049/jimmunol.1202958.

[27] A.S. Cordeiro, M.J. Alonso, M. de la Fuente, Nanoengineering of vaccines using natural polysaccharides, Biotechnol. Adv. 33 (2015) 1279–1293. doi:10.1016/j.biotechadv.2015.05.010.

[28] J. Shi, P.W. Kantoff, R. Wooster, O.C. Farokhzad, Cancer nanomedicine: progress, challenges and opportunities, Nat. Rev. Cancer. 17 (2017) 20–37. doi:10.1038/nrc.2016.108.

[29] F. Rose, J.E. Wern, F. Gavins, P. Andersen, F. Follmann, C. Foged, A strong adjuvant based on glycol-chitosan-coated lipid-polymer hybrid nanoparticles potentiates mucosal immune responses against the recombinant Chlamydia trachomatis fusion antigen CTH522, J. Control. Release. 271 (2018) 88–97. doi:10.1016/j.jconrel.2017.12.003.

[30] A. Vila, A. Sánchez, M. Tobío, P. Calvo, M.J. Alonso, Design of biodegradable particles for protein delivery, J. Control. Release. 78 (2002) 15–24. doi:10.1016/S0168-3659(01)00486-2.

[31] A. Vila, A. Sánchez, K. Janes, I. Behrens, T. Kissel, J.L. Vila-Jato, M.J. Alonso, Low molecular weight chitosan nanoparticles as new carriers for nasal vaccine delivery in mice, Eur. J. Pharm. Biopharm. 57 (2004) 123–131. doi:10.1016/j.ejpb.2003.09.006.

[32] S. Vicente, B. Diaz-Freitas, M. Peleteiro, A. Sanchez, D.W. Pascual, A. Gonzalez-Fernandez, M.J. Alonso, A polymer/oil based nanovaccine as a single-dose immunization approach, PLoS One. 8 (2013) 2–9. doi:10.1371/journal.pone.0062500.

[33] L. Cui, J.A. Cohen, K.E. Broaders, T.T. Beaudette, J.M.J. Fréchet, Mannosylated dextran nanoparticles: a pH-sensitive system engineered for immunomodulation through mannose targeting, Bioconjug. Chem.

22 (2011) 949–957. doi:10.1021/bc100596w.

[34] S. Sharma, T.K. Mukkur, H.A. Benson, Y. Chen, Enhanced immune response against Pertussis toxoid by IgA-loaded chitosan–dextran sulfate nanoparticles, J. Pharm. Sci. 101 (2012) 233–244. doi:10.1002/jps.22763.

[35] K. Perica, A. Tu, A. Richter, J.G. Bieler, M. Edidin, J.P. Schneck, Magnetic field-induced T cell receptor clustering by nanoparticles enhances T cell activation and stimulates antitumor activity, ACS Nano. 8 (2014) 2252–2260. doi:10.1021/nn405520d.

[36] B.J.G. Baaten, R. Tinoco, A.T. Chen, L.M. Bradley, Regulation of antigen-experienced T cells: lessons from the quintessential memory marker CD44, Front. Immunol. 3 (2012) 1–12. doi:10.3389/fimmu.2012.00023.

[37] C.C. Termeer, J. Hennies, U. Voith, T. Ahrens, J. M. Weiss, P. Prehm, J.C. Simon, Oligosaccharides of hyaluronan are potent activators of dendritic cells, J. Immunol. 165 (2000) 1863–1870. doi:10.4049/jimmunol.165.4.1863.

[38] C. Ke, D. Wang, Y. Sun, D. Qiao, H. Ye, X. Zeng, Immunostimulatory and antiangiogenic activities of low molecular weight hyaluronic acid, Food Chem. Toxicol. 58 (2013) 401–407. doi:10.1016/j.fct.2013.05.032.

[39] Y. Fan, P. Sahdev, L.J. Ochyl, J. J. Akerberg, J.J. Moon, Cationic liposome–hyaluronic acid hybrid nanoparticles for intranasal vaccination with subunit antigens, J. Control. Release. 208 (2015) 121–129. doi:10.1016/j.jconrel.2015.04.010.

[40] L. Liu, F. Cao, X. Liu, H. Wang, C. Zhang, H. Sun, C. Wang, X. Leng, C. Song, D. Kong, G. Ma, Hyaluronic acid-modified cationic lipid–PLGA hybrid nanoparticles as a nanovaccine induce robust humoral and cellular immune responses, ACS Appl. Mater. Interfaces. 8 (2016) 11969–11979. doi:10.1021/acsami.6b01135.

[41] J.V. González-Aramundiz, M. Peleteiro Olmedo, Á. González-Fernández, M.J. Alonso, N.S. Csaba, Protamine-based nanoparticles as new antigen delivery systems, Eur. J. Pharm. Biopharm. 97 (2015) 51–59. doi:10.1016/j.ejpb.2015.09.019.

[42] A.D. Baldwin, K.L. Kiick, Tunable degradation of maleimide-thiol adducts in reducing environments, Bioconjug. Chem. 22 (2011) 1946–1953. doi:10.1021/bc200148v.

[43] J.J. Moon, H. Suh, V. Li, C.F. Ockenhouse, A. Yadava, D.J. Irvine, Enhancing humoral responses to a malaria antigen with nanoparticle vaccines that expand Tfh cells and promote germinal center induction, Proc. Natl. Acad. Sci. 109 (2012) 1080–1085. doi:10.1073/pnas.1112648109.

[44] V. V. Temchura, D. Kozlova, V. Sokolova, K. Überla, M. Epple, Targeting and activation of antigen-specific B-cells by calcium phosphate nanoparticles loaded with protein antigen, Biomaterials. 35 (2014) 6098–6105. doi:10.1016/j.biomaterials.2014.04.010.

[45] J. Shao, J.P. Tam, Unprotected peptides as building blocks for the synthesis of peptide dendrimers with oxime, hydrazone, and thiazolidine linkages, J. Am. Chem. Soc. 117 (1995) 3893–3899. doi:10.1021/ja00119a001.

[46] H. Cho, T. Daniel, Y.J. Buechler, D.C. Litzinger, Z. Maio, A.-M.H. Putnam, V.S. Kraynov, B.-C. Sim, S. Bussell, T. Javahishvili, S. Kaphle, G. Viramontes, M. Ong, S. Chu, B. GC, R. Lieu, N. Knudsen, P. Castiglioni, T.C. Norman, D.W. Axelrod, A.R. Hoffman, P.G. Schultz, R.D. DiMarchi, B.E. Kimmel, Optimized clinical performance of growth hormone with an expanded genetic code, Proc. Natl. Acad. Sci. 108 (2011) 9060–9065. doi:10.1073/pnas.1100387108.

[47] C. Pifferi, N. Berthet, O. Renaudet, Cyclopeptide scaffolds in carbohydrate-based synthetic vaccines, Biomater. Sci. 5 (2017) 953–965. doi:10.1039/C7BM00072C.

[48] N.M. Molino, A.K.L. Anderson, E.L. Nelson, S.W. Wang, Biomimetic protein nanoparticles facilitate enhanced dendritic cell activation and cross-presentation, ACS Nano. 7 (2013) 9743–9752. doi:10.1021/nn403085w.

[49] J. Yang, J. Li, X. Li, X. Wang, Y. Yang, N. Kawazoe, G. Chen, Nanoencapsulation of individual mammalian cells with cytoprotective polymer shell, Biomaterials. 133 (2017) 253–262. doi:10.1016/j.biomaterials.2017.04.020.

[50] F. Meng, W.E. Hennink, Z. Zhong, Reduction-sensitive polymers and bioconjugates for biomedical applications, Biomaterials. 30 (2009) 2180–2198. doi:10.1016/j.biomaterials.2009.01.026.

[51] R. Cheng, F. Feng, F. Meng, C. Deng, J. Feijen, Z. Zhong, Glutathione-responsive nano-vehicles as a promising platform for targeted intracellular drug and gene delivery, J. Control. Release. 152 (2011) 2–12. doi:10.1016/j.jconrel.2011.01.030.

[52] G.K. Lewis, A.L. DeVico, R.C. Gallo, Antibody persistence and T-cell balance: two key factors confronting HIV vaccine development, Proc. Natl. Acad. Sci. 111 (2014) 15614–15621. doi:10.1073/pnas.1413550111.

[53] D.S. Watson, V.M. Platt, L. Cao, V.J. Venditto, F.C. Szoka, Antibody response to polyhistidine-tagged peptide and protein antigens attached to liposomes via lipid-linked nitrilotriacetic acid in mice, Clin. Vaccine Immunol. 18 (2011) 289–297. doi:10.1128/CVI.00425-10.

[54] R.D. Stout, J. Suttles, The many roles of CD40 in cell-mediated inflammatory responses, Immunol. Today. 17 (1996) 487–492. doi:10.1016/0167-5699(96)10060-I.

[55] I.S. Grewal, R.A. Flavell, CD40 and CD154 in cell-mediated immunity, Annu. Rev. Immunol. 16 (1998) 111–135. doi:10.1146/annurev.immunol.16.1.111.

[56] C.B. Thompson, Distinct roles for the costimulatory ligands B7-1 and B7-2 in T helper cell differentiation?, Cell. 81 (1995) 979–982. doi:10.1016/S0092-8674(05)80001-7.

[57] H. Song, P. Huang, J. Niu, G. Shi, C. Zhang, D. Kong, W. Wang, Injectable polypeptide hydrogel for dual-delivery of antigen and TLR3 agonist to modulate dendritic cells in vivo and enhance potent cytotoxic T-lymphocyte response against melanoma, Biomaterials. 159 (2018) 119–129. doi:10.1016/j.biomaterials.2018.01.004.

[58] N. Moyo, A.B. Vogel, S. Buus, S. Erbar, E.G. Wee, U. Sahin, T. Hanke, Efficient Induction of T cells against conserved HIV-1 regions by mosaic vaccines delivered as self-amplifying mRNA, Mol. Ther. - Methods Clin. Dev. 12 (2019) 32–46. doi:10.1016/j.omtm.2018.10.010.

[59] T. Hatziioannou, D.T. Evans, Animal models for HIV/AIDS research, Nat. Rev. Microbiol. 10 (2012) 852–867. doi:10.1038/nrmicro2911.

[60] T.G. Dacoba, R.W. Omange, H. Li, J. Crecente-Campo, M. Luo, M.J. Alonso, Polysaccharide nanoparticles can efficiently modulate the immune response against an HIV peptide antigen, ACS Nano. 13 (2019) 4947–4959. doi:10.1021/acsnano.8b07662.

[61] H. Li, R.W. Omange, B. Liang, N. Toledo, Y. Hai, L.R. Liu, D. Schalk, J. Crecente-Campo, T.G. Dacoba, A.B. Lambe, S.-Y. Lim, L. Li, M.A. Kashem, Y. Wan, J.F. Correia-Pinto, X.Q. Liu, R.F. Balshaw, Q. Li, E. Rakasz, N. Schultz-Darken, M.J. Alonso, J.B. Whitney, F.A. Plummer, M. Luo, A novel vaccine targeting the viral protease cleavage sites protects Mauritian cynomolgus macaques against vaginal SIVmac251 infection, BioRxiv. (2019). doi:10.1101/842955.

[62] H. Ragelle, F. Danhier, V. Préat, R. Langer, D.G. Anderson, Nanoparticle-based drug delivery systems: a commercial and regulatory outlook as the field matures, Expert Opin. Drug Deliv. 14 (2017) 851–864. doi:10.1080/17425247.2016.1244187.

[63] F. Dormont, M. Rouquette, C. Mahatsekake, F. Gobeaux, A. Peramo, R. Brusini, S. Calet, F. Testard, S. Lepetre-Mouelhi, D. Desmaële, M. Varna, P. Couvreur, Translation of nanomedicines from lab to industrial scale synthesis: the case of squalene-adenosine nanoparticles, J. Control. Release. 307 (2019) 302–314. doi:10.1016/j.jconrel.2019.06.040.

[64] C.M. Maguire, M. Rösslein, P. Wick, A. Prina-Mello, Characterisation of particles in solution – a perspective on light scattering and comparative technologies, Sci. Technol. Adv. Mater. 19 (2018) 732–745. doi:10.1080/14686996.2018.1517587.

[65] F. Caputo, J. Clogston, L. Calzolai, M. Rösslein, A. Prina-Mello, Measuring particle size distribution of nanoparticle enabled medicinal products, the joint view of EUNCL and NCI-NCL. A step by step approach combining orthogonal measurements with increasing complexity, J. Control. Release. 299 (2019) 31–43. doi:10.1016/j.jconrel.2019.02.030.

[66] B. Liu, Q. Liu, L. Yang, S.K. Palaniappan, I. Bahar, P.S. Thiagarajan, J.L. Ding, Innate immune memory and homeostasis may be conferred through crosstalk between the TLR3 and TLR7 pathways, Sci. Signal. 9 (2016) ra70–ra70. doi:10.1126/scisignal.aac9340.

[67] H. Shime, M. Matsumoto, H. Oshiumi, S. Tanaka, A. Nakane, Y. Iwakura, H. Tahara, N. Inoue, T. Seya, Toll-like receptor 3 signaling converts tumor-supporting myeloid cells to tumoricidal effectors, Proc. Natl. Acad. Sci. 109 (2012) 2066–2071. doi:10.1073/pnas.1113099109.

[68] A. Maeda, E. Digifico, F.T. Andon, A. Mantovani, P. Allavena, Poly(I:C) stimulation is superior than imiquimod to induce the antitumoral functional profile of tumor-conditioned macrophages, Eur. J. Immunol. 49 (2019) 801–811. doi:10.1002/eji.201847888.

[69] M.A. Aznar, L. Planelles, M. Perez-Olivares, C. Molina, S. Garasa, I. Etxeberría, G. Perez, I. Rodriguez, E. Bolaños, P. Lopez-Casas, M.E. Rodriguez-Ruiz, J.L. Perez-Gracia, I. Marquez-Rodas, A. Teijeira, M. Quintero, I. Melero, Immunotherapeutic effects of intratumoral nanoplexed poly I:C, J. Immunother. Cancer. 7 (2019) 116. doi:10.1186/s40425-019-0568-2.

[70] Exploratory study of BO-112 in adult patients with aggressive solid tumors, (2016). https://clinicaltrials.gov/ct2/show/NCT02828098 (accessed January 9, 2020).

[71] P. Chollet, M.C. Favrot, A. Hurbin, J.-L. Coll, Side-effects of a systemic injection of linear polyethylenimine-DNA complexes, J. Gene Med. 4 (2002) 84–91. doi:10.1002/jgm.237.

[72] E. Samaridou, H. Walgrave, E. Salta, D.M. Álvarez, V. Castro-López, M. Loza, M.J. Alonso, Nose-to-brain delivery of enveloped RNA - cell permeating peptide nanocomplexes for the treatment of neurodegenerative diseases, Biomaterials. 230 (2020) 119657. doi:10.1016/j.biomaterials.2019.119657.

[73] T. Endoh, T. Ohtsuki, Cellular siRNA delivery using cell-penetrating peptides modified for endosomal escape, Adv. Drug Deliv. Rev. 61 (2009) 704–709. doi:10.1016/j.addr.2009.04.005.

[74] V.P. Torchilin, Cell penetrating peptide-modified pharmaceutical nanocarriers for intracellular drug and gene delivery, Biopolymers. 90 (2008) 604–610. doi:10.1002/bip.20989.

[75] C. Sun, T. Tang, H. Uludag, A molecular dynamics simulation study on the effect of lipid substitution on polyethylenimine mediated siRNA complexation, Biomaterials. 34 (2013) 2822–2833. doi:10.1016/j.biomaterials.2013.01.011.

[76] L. Pärnaste, P. Arukuusk, K. Langel, T. Tenson, Ü. Langel, The formation of nanoparticles between small interfering RNA and amphipathic cell-penetrating peptides, Mol. Ther. - Nucleic Acids. 7 (2017) 1–10. doi:10.1016/j.omtn.2017.02.003.

[77] D.J. Gary, N. Puri, Y.-Y. Won, Polymer-based siRNA delivery: perspectives on the fundamental and phenomenological distinctions from polymer-based DNA delivery, J. Control. Release. 121 (2007) 64–73. doi:10.1016/j.jconrel.2007.05.021.

[78] E. Samaridou, N. Kalamidas, I. Santalices, J. Crecente-Campo, M.J. Alonso, Tuning the PEG surface density of the PEG-PGA enveloped octaarginine-peptide nanocomplexes, Drug Deliv. Transl. Res. (2019). doi:10.1007/s13346-019-00678-3.

[79] M.J. Santander-Ortega, A.B. Jódar-Reyes, N. Csaba, D. Bastos-González, J.L. Ortega-Vinuesa, Colloidal stability of pluronic F68-coated PLGA nanoparticles: a variety of stabilisation mechanisms, J. Colloid Interface Sci. 302 (2006) 522–529. doi:10.1016/j.jcis.2006.07.031.

[80] R. Abellan-Pose, M. Rodríguez-Évora, S. Vicente, N. Csaba, C. Évora, M.J. Alonso, A. Delgado, Biodistribution of radiolabeled polyglutamic acid and PEG-polyglutamic acid nanocapsules, Eur. J. Pharm. Biopharm. 112 (2017) 155–163. doi:10.1016/j.ejpb.2016.11.015.

[81] Z. Niu, E. Samaridou, E. Jaumain, J. Coëne, G. Ullio, N. Shrestha, J. Garcia, M. Durán-Lobato, S. Tovar, M.J.

Santander-Ortega, M.V. Lozano, M.M. Arroyo-Jimenez, R. Ramos-Membrive, I. Peñuelas, A. Mabondzo, V. Préat, M. Teixidó, E. Giralt, M.J. Alonso, PEG-PGA enveloped octaarginine-peptide nanocomplexes: an oral peptide delivery strategy, J. Control. Release. 276 (2018) 125–139. doi:10.1016/j.jconrel.2018.03.004.

[82] D. Peer, R. Margalit, Loading mitomycin C inside long circulating hyaluronan targeted nano-liposomes increases its antitumor activity in three mice tumor models, Int. J. Cancer. 108 (2004) 780–789. doi:10.1002/ijc.11615.

[83] K.Y. Choi, K.H. Min, J.H. Na, K. Choi, K. Kim, J.H. Park, I.C. Kwon, S.Y. Jeong, Self-assembled hyaluronic acid nanoparticles as a potential drug carrier for cancer therapy: synthesis, characterization, and in vivo biodistribution, J. Mater. Chem. 19 (2009) 4102. doi:10.1039/b900456d.

[84] X. Yang, Y. Li, M. Li, L. Zhang, L. Feng, N. Zhang, Hyaluronic acid-coated nanostructured lipid carriers for targeting paclitaxel to cancer, Cancer Lett. 334 (2013) 338–345. doi:10.1016/j.canlet.2012.07.002.

[85] A. Almalik, H. Benabdelkamel, A. Masood, I.O. Alanazi, I. Alradwan, M.A. Majrashi, A.A. Alfadda, W.M. Alghamdi, H. Alrabiah, N. Tirelli, A.H. Alhasan, Hyaluronic acid coated chitosan nanoparticles reduced the immunogenicity of the formed protein corona, Sci. Rep. 7 (2017) 1–9. doi:10.1038/s41598-017-10836-7.

[86] K. Franciszkiewicz, A. Boissonnas, M. Boutet, C. Combadiere, F. Mami-Chouaib, Role of chemokines and chemokine receptors in shaping the effector phase of the antitumor immune response, Cancer Res. 72 (2012) 6325–6332. doi:10.1158/0008-5472.CAN-12-2027.

[87] G. Arango Duque, A. Descoteaux, Macrophage cytokines: involvement in immunity and infectious diseases, Front. Immunol. 5 (2014) 1–12. doi:10.3389/fimmu.2014.00491.

[88] M. Singh, H. Khong, Z. Dai, X.-F. Huang, J.A. Wargo, Z.A. Cooper, J.P. Vasilakos, P. Hwu, W.W. Overwijk, Effective innate and adaptive antimelanoma immunity through localized TLR7/8 activation, J. Immunol. 193 (2014) 4722–4731. doi:10.4049/jimmunol.1401160.

Conclusions

The scope of this thesis was to evaluate the potential of nanotechnology to target the immune system in two different disease contexts: HIV and cancer. Within the frame of HIV vaccination, the objective was to design and develop polysaccharide-based nanoparticles with the capacity to carry HIV peptide antigens. On the other hand, in the context of cancer, the objective was to design and develop a new formulation of the immunomodulator poly(I:C), intended to facilitate its transport to tumor-associated macrophages and their subsequent polarization towards anti-tumoral phenotypes. The experimental work conducted in this thesis allowed us to conclude:

1. Nanoparticles consisting of a combination of polysaccharides, with or without the adjuvant poly(I:C), were designed to load an HIV peptide antigen. The peptide antigen could be linked to the particles following different approaches, such as ionic interactions and covalent, cleavable or non-cleavable, bonds. In all cases, the resulting nanoparticles presented adequate particle sizes and high antigen loading capacities. The administration of these nanoparticles to mice demonstrated that the different formulations were able to elicit robust humoral responses. Moreover, T cell activation patterns varied depending on the type of antigen linkage, with more labile linkages activating T cells at earlier time points and more stable linkages showing a delayed effect. The two most promising formulations were successfully optimized to associate a total of three peptide antigens. The vaccination of non-human primates with these nanoparticles was able to modestly delay SIV infection, and protect 50% of the animals, compared to the 25% protection achieved for the control group. Nevertheless, a vaccine based on twelve peptide antigens in nanoparticles and viral vectors was the most successful strategy to prevent SIV acquisition, reaching a 75% of protection.

2. The fabrication of chitosan/dextran sulfate nanoparticles containing an HIV peptide antigen was successfully translated to a pilot plant, under GMP-like conditions. The definition of the quality attributes of the formulation, the implementation of risk analysis tools, the combination of orthogonal techniques, and the optimization of several analytical techniques resulted in the production of reproducible 200-mL batches of the nanoparticles. Additionally, we proved that both, the continuous and the discontinuous scale-up methods, were suitable for the fabrication of these particles.

3. New formulations of the immunomodulator poly(I:C), consisting on nanocomplexes with different types of arginine-rich peptides, were developed. They were subsequently enveloped with anionic hydrophilic polymers intended to provide them with adequate stability. The *in vitro* studies performed in human-derived macrophages indicated that the nanoformulation of poly(I:C) could be internalized by these cells and could reach the endosomal compartment where its target is found. Additionally, the macrophages pre-treated with the nanocomplexed poly(I:C) showed certain pro-inflammatory phenotypes, measured as their capacity to secret T cell attracting chemokines and as their ability to directly kill tumor cells. Despite these positive results, preliminary *in vivo* studies did not show a robust enough anti-tumor response. Hence, further studies are needed in order to assess the value of the developed formulation.

Overall, we have shown that by understanding the role of the immune system in the development of different diseases, it is possible to rationally design nanomedicines that might represent new promising therapies. Indeed, we have demonstrated that nanotechnology can be used (*i*) to boost the humoral and cellular responses against HIV peptide antigens, that conferred protection against infection to *Mauritian cynomolgus* macaques; and (*ii*) to re-activate macrophages *in vitro* to fight tumor cells.

List of abbreviations

°C, degree Celsius

aAPC, artificial antigen presenting cell

Ab, antibody

AE, association efficiency

ANOVA, analysis of variance

APC, antigen presenting cell

ASEM, N-(2-aminoethyl)maleimide trifluoroacetate salt

BE, binding energy

bNAb, broadly-neutralizing antibody

BSA, bovine serum albumin

C12r8, laurate octa-arginine

CAR, chimeric antigen receptor

CCL5, C-C motif ligand 5

CD, cluster of differentiation

Chol, cholesterol

CpG, cytosine-phosphorothioester-guanine

CPP, cell penetrating peptides

CS, chitosan

CTL: cytotoxic T lymhocyte

CTLA4, cytotoxic T lymphocyte antigen 4

CXCL10, C-X-C motif ligand 10

DC, dendritic cell

DLS, dynamic light scattering

DMSO, dimethylsulfoxide

DNA, deoxyribonucleic acid

DOSY, diffusion-ordered spectroscopy

DS, dextran sulfate

dsRNA, double-stranded ribonucleic acid

EDC, N-(3-Dimethylaminopropyl)-N´-ethylcarbodiimide hydrochloride

EDTA, ethylenediaminetetraacetic acid

EMA, European medicines agency

Env, envelope

FACS, fluorescence-activated cell sorting (flow cytometry)

FBS, fetal bovine serum

FD, freeze-dry

FDA, US Food and Drug Administration

FESEM, field emission scanning electron microscopy

Fig, figure

FITC, 2-(6-hydroxy-3-oxo-(3H)-xanthen-9-yl)-5-isothiocyanatobenzoic acid

Gag, group antigens

GFP, green fluorescent protein

GMMA, generalized modules of membrane antigen

GRAS, generally recognized as safe

GSH, glutathione

h, hour

HA, sodium hyaluronate

HIV, human immunodeficiency virus

HLA, human leukocyte antigens

HPV, human papilloma virus

ICH, International Council for Harmonisation of Technical Requirements for Pharmaceuticals for Human Use

ICS, intracellular cytokine staining

IFNγ, Interferon gamma

Ig, immunoglobulin

IL, interleukin

i.m., intramuscular

IMV, ImmunoVaccine

i.n., intranasal

InLens, immersion lens

kDa, kilodalton

LDA, laser doppler anemometry

LNPs, lipid nanoparticles

LPS, lipopolysaccharide

M-CSF, macrophage colony-stimulating factor

MAAs, melanoma-associated antigens

mAb, monoclonal antibody

MALS, multi-angle light scattering

MDSC, myeloid-derived suppressor cell

MFI, mean fluorescence intensity

mg, milligram

MHC, major histocompatibility complex

min, minute

mL, milliliter

MP, microparticle

MPLA, monophosphoryl lipid A

mRNA, messenger ribonucleic acid

MW, molecular weight

MyD88, myeloid differentiation primary response 88

NC, nanocapsules

NHP, non-human primate

NHS, N-hydroxysuccinimide

NIAID, National Institute of Allergy and Infectious Diseases

NK, natural killer

NKT, natural killer T

nm, nanometer

NMR, nuclear magnetic resonance

NP, nanoparticle

NTA, nanoparticle tracking analysis

ODN, oligodeoxynucleotide

OVA, ovalbumin

PAMPs, pathogen-associated molecular patterns

PANC-1, pancreatic cancer cell

pArg, polyarginine

PBS, phosphate buffered saline

PCS, protease cleavage site

PD-1, programmed cell death 1

PD-L1, programmed cell death ligand 1

PDI, polydispersity index

PE, phycoerythrin

PEG–PGA, pegylated polyglutamic acid

PEG, polyethylene glycol

PerCP, peridinin chlorophyll protein

PFA, paraformaldehyde

PGA, poly-glutamic acid

pI: isoelectric point

PLA, poly-lactide

PLGA, poly(lactic-co-glycolic acid)

poly(I:C), polyinosinic:polycytidylic acid

Pro, protease

PRRs, pattern recognition receptors

r8, octa-arginine

recMAGE-A3: recombinant melanoma-associated antigen 3

rHBsAg, recombinant hepatitis B surface antigen

RNA, ribonucleic acid

RPMI, Roswell Park Memorial Institute

RSV, respiratory syncytial virus

rVSV, recombinant vesicular stomatitis virus

s, second

S4FB, N-succinimidyl 4-formylbenzoate

SD, standard deviation

SEC, size exclusion chromatography

SEM, standard error of the mean

SIV, simian immunodeficiency virus

ssRNA, single-stranded ribonucleic acid

STEM, scanning transmission electron microscopy

TAA, tumor-associated antigen

TAM, tumor-associated macrophage

TEM, transmission electron microscopy

TLR, toll-like receptor

TNFα, tumor necrosis factor-alfa

Transm, transmittance

TRIF, TIR-domain-containing adapter-inducing interferon-β

UPLC, ultra-performance liquid chromatography

UV, ultraviolet

v/v, volume/volume

w/v, weight/volume

w/w, weight/weight

XPS, X-ray photoelectron spectroscopy

µL, microliter

Ethical considerations and Permission

Animal studies

The studies in mice described in Chapter 1.A were done at the University of Manitoba (Canada). All animals were treated in a humane manner in accordance with the Principles of the Canadian Council on Animal Care contained in the "Guide to the Care and Use of Experimental Animals". The experiments were authorized by the Animal Care Committee of the Canadian Science Centre for Human & Animal Health, and are summarized in the animal use document with number H-14-004.Rev.1.

The efficacy studies in non-human primates described in Chapter 1.B were conducted at Wisconsin National Primate Research Center (USA). The experiments were approved by the University of Wisconsin (Institutional Animal Care and Use Committees protocol number G005765), in accordance with the US Animal Welfare Act and following the recommendations of the National Research Council Guide for the Care and Use of Laboratory Animals, 8th Edition, and the Weatherall report, The Use of Nonhuman Primates in Research. The Wisconsin National Primate Research Center is fully accredited by Association for Assessment and Accreditation of Laboratory Animal Care International (AAALAC) under the University of Wisconsin, Division of Vice-Chancellor for Research and Graduate Education.

The anti-tumor efficacy studies in mice reported in Chapter 3 were conducted at Istituto Clinico Humanitas (Milan, Italy) and were approved by *Ministerio della Salute,* according to the article 31 of the legislative decree 4 March 2014, n. 26, and with authorization number 166/2016-PR. They were also in accordance with governing Italian law and European Directives and Guidelines for the use of animals in animal studies, in compliance with the Directive 2010/63/EU of the European Parliament and Council of 22nd September 2010 on the protection of animals used for scientific purposes

Human-derived samples

Evaluation of nanoparticles in human-derived monocytes described in Chapter 3 was conducted at Istituto Clinico Humanitas (Milan, Italy), in accordance with Italian and European law. Primary human immune cells from healthy donors for the preparation of monocytes and macrophages are recovered from the buffy coats of blood donations. Buffy coats are obtained from anonymous healthy blood donors at an authorized organization (in this case the San Matteo Hospital in Pavia, Italy), after the donors have signed an informed consent.

Authorization of Animal Experiments (Chapter 1.A)

Notice of CSCHAH - ACC Approval of Animal Use Document

Document I.D. No.	H-14-004 Rev. 1
Project Title	A Novel HIV Vaccine Targeting the 12 Protease Cleavage Sites
Date Submitted	April 2014
Principal Investigator	Dr. Ma Luo
Associate Investigator(s)	Dr. Gary Kobinger
Project Period Approved	July 2014 - July 2015
Animal No. & Type	Mice, BALB/c, 6 to 8 weeks, Total = 185

Date: April 11, 2014

To: Dr. Ma Luo

Following review of the application, the Canadian Science Centre for Human & Animal Health - Animal Care Committee (CSCHAH - ACC) has approved the animal use described in the above referenced Animal Use Document Application, a signed copy of which is attached to this notice. In accordance with the Canadian Council on Animal Care (CCAC), AUDs will now be approved on a yearly basis with the possibility of two annual renewals, for a total of three years. An annual review must be submitted each year from the start of this project (i.e. when the first animals are ordered).

Please ensure that all persons identified in the application as participating in any way in manipulations on the live animals are fully informed of the approved experimental design and procedures, and that significant deviations in procedures are not permissible without prior approval of the CSCHAH - ACC.

Please be advised that animals may be ordered only after Safety & Environmental Services (SES) approval has been granted.

Dr. Carissa Embury-Hyatt
Chair, CSCHAH - ACC

cc: ACC files
Animal Care Veterinarian
Animal Care Supervisor

Authorization of Animal Experiments (Chapter 1.B)

New Protocol Approved by College of Letters and Science and Vice Chancellor for Research and Graduate Education Centers Institutional Animal Care and Use Committee

Protocol PI: NANCY SCHULTZ-DARKEN
Protocol Title: A novel HIV-1 vaccine targeting the 12 protease cleavage sites
Protocol ID: G005765
Protocol Approval Date: 2/13/2017
Protocol Expiration Date: 2/12/2020
Amendment Approval Date:

Only those procedures described in this New Protocol are approved by the Institutional Animal Care and Use Committee (IACUC). Performing activities not approved by the IACUC is a protocol violation and will be dealt with in accordance with All Campus Policy 1999-008 (http://rarc.wisc.edu/policy/1999-008.html).

NOTE: IACUC approval of an animal care and use protocol, or modifications of a protocol, is not a guarantee of research space, equipment, or other resources.

If you have any questions or concerns regarding this action, please contact your RARC veterinarian or the IACUC Administrator.

_
Holly McEntee
IACUC Administrator
608-265-9241
mcentee@rarc.wisc.edu

Authorization of Animal Experiments (Chapter 3)

Ministero della Salute
DGSAF
0004495-P-23/02/2016
175751317

Ministero della Salute

Direzione Generale della Sanità Animale e dei Farmaci Veterinari
Ufficio VI (ex DGSA – Benessere Animale)

Istituto Clinico Humanitas
Rozzano (Milano)
pec: direzione.sanitaria.humanitas@pec.it
c.a. Dr.ssa Cecilia GARLANDA
e-mail: cecilia.garlanda@humanitasresearch.it
e, per conoscenza
ASL Milano 2
Dipartimento Prevenzione Veterinaria
dipartimento.prevenzioneveterinaria@pec.aslmi2.it

OGGETTO: D.lgs. 26/2014 sulla protezione degli animali utilizzati a fini scientifici.
Trasmissione autorizzazione ai sensi dell'art. 31.
Autorizzazione n° 166/2016-PR (Risp. a **prot. 6B2B3.2 del 13/11/2015**)

Si trasmette l'autorizzazione **n° 166/2016-PR** rilasciata in data **19/02/2016**, ai sensi dell'art. 31 del D.lgs. 26/2014.

IL DIRETTORE DELL'UFFICIO VI
Dr. Vincenzo Ugo SANTUCCI

Referenti: G. Botta e-mail: g.botta@sanita.it; g. Aleandri e-mail: g.aleandri-esterno@sanita.it
HUMANITAS Allavena 02MMXVI

Ministero della Salute

DIREZIONE GENERALE DELLA SANITÀ ANIMALE E DEI FARMACI VETERINARI
UFFICIO VI ex DGSA

Autorizzazione n. 166 /2016-PR

IL DIRETTORE GENERALE

Vista la domanda di autorizzazione del progetto di ricerca **"Sviluppo e valutazione di nanomedicine per il targeting terapeutico di macrofagi associati a tumori"**, ex articolo 31 del decreto legislativo 4 marzo 2014, n. 26, acquisita con prot. 6B2B3.2 del 13/11/2015, inoltrata dall'**Istituto Clinico Humanitas - IRCCS, sede legale in Rozzano (MI), Via Manzoni, 56**, per il tramite dell'Organismo preposto al benessere degli animali di cui all'articolo 25 del menzionato d.lgs. n. 26/2014, e finalizzata all'esecuzione di un progetto di ricerca come descritto nella documentazione allegata alla domanda;

Visto l'articolo 31, comma 1, del d.lgs. n. 26/2014, nel quale il Ministero della salute è individuato quale autorità competente al rilascio dell'autorizzazione all'esecuzione di progetti di ricerca che prevedono l'utilizzo di animali a fini scientifici secondo le finalità di cui all'articolo 5, comma 1, in continuità con la precedente normativa di cui al decreto legislativo 27 gennaio 1992, n. 116;

Visti gli articoli 12, 13, 14, 15, 16 e 17 del succitato d.lgs. n. 26/2014, che stabiliscono le modalità di utilizzazione degli animali nelle procedure condotte a fini scientifici;

Visti gli articoli 31, 32, 34 e 35, nonché gli Allegati IV, VI, VII e IX del d.lgs. n. 26/2014, che fissano i requisiti generali per il rilascio di autorizzazione per progetti di ricerca;

Visto la nota n. 3802 del 10/02/2016, con cui l'Istituto Superiore di Sanità ha comunicato l'esito positivo della valutazione tecnico-scientifica sul progetto di ricerca;

Considerato che ricorrono i requisiti stabiliti dal d.lgs. n. 26/2014 per il progetto da autorizzare;

Preso atto che il responsabile del progetto di ricerca, ai sensi dell'articolo 3, comma 1, lettera g) del d.lgs. n. 26/2014, è la **Dr.ssa Paola ALLAVENA**;

Considerato che lo **stabilimento utilizzatore dell'Istituto Clinico HUMANITAS, sito in Pieve Emanuele (MI), Via Sardegna, 7, è regolarmente autorizzato con decreto n. 158/2011-A, del 14/09/2011, ai sensi del D.lgs. 116/92**;

Visto l'articolo 4, comma 2 e l'articolo 16 del decreto legislativo 30 marzo 2001, n. 165 e successive modifiche, recanti le funzioni dei dirigenti di uffici dirigenziali;

Responsabile del procedimento: Dr. Vincenzo Ugo SANTUCCI
Referenti: Botta g.botta@sanita.it; Aleandri: g.aleandri-esterno@sanita.it

AUTORIZZA

1. L'**Istituto Clinico Humanitas - IRCCS, sede legale in Rozzano (MI), Via Manzoni, 56**, all'esecuzione del progetto di ricerca ex articolo 31 del decreto legislativo 4 marzo 2014, n. 26, in conformità a quanto indicato nella richiesta di autorizzazione citata in premessa ed, in particolare, con riferimento a:

"Sviluppo e valutazione di nanomedicine per il targeting terapeutico di macrofagi associati a tumori"

2. La **Dr.ssa Paola ALLAVENA** quale responsabile del progetto di ricerca, ai sensi dell'articolo 3, comma 1, lettera g) del d.lgs. n. 26/2014.

3. L'**Istituto Clinico Humanitas - IRCCS, sede legale in Rozzano (MI), Via Manzoni, 56**, all'esecuzione del progetto di ricerca di cui al punto 1 nello **stabilimento utilizzatore dell'Istituto Clinico HUMANITAS, sito in Pieve Emanuele (MI), Via Sardegna, 7, regolarmente autorizzato con decreto n. 158/2011-A, del 14/09/2011, ai sensi del D.lgs. 116/92**.

Alla conclusione del progetto di ricerca il responsabile di cui all'articolo 3, comma 1, lettera g) del d.lgs. n. 26/2014 dovrà inviare la documentazione necessaria ai fini della valutazione retrospettiva come previsto dall'articolo 32 del citato decreto.

La presente autorizzazione ha una durata di trentasei mesi e può essere revocata secondo quanto previsto dall'articolo 31, comma 15 del d.lgs. n. 26/2014.

19 FEB. 2016

IL DIRETTORE GENERALE
(Dott. Silvio BORRELLO)

Responsabile del procedimento: Dr. Vincenzo Ugo SANTUCCI
Referenti: Botta: g.botta@sanita.it; Aleandri: g.aleandri-esterno@sanita.it

Permission to re-use graphical material as Figure 3 of the Introduction

Thank you for your order!

Dear Tamara Gomez Dacoba,

Thank you for placing your order through Copyright Clearance Center's RightsLink® service.

Order Summary

Licensee:	Tamara Gómez Dacoba
Order Date:	Jan 13, 2020
Order Number:	4747011486414
Publication:	Immunity
Title:	Oncology Meets Immunology: The Cancer-Immunity Cycle
Type of Use:	reuse in a thesis/dissertation
Order Total:	0.00 EUR

View or print complete details of your order and the publisher's terms and conditions.

Sincerely,

Copyright Clearance Center

Tel: +1-855-239-3415 / +1-978-646-2777
customercare@copyright.com
https://myaccount.copyright.com

Copyright Clearance Center RightsLink®

Attributions to the icons employed in the graphical abstract of Chapter 2

All the icons used in Chapter 2 for the construction of the graphical abstract were designed by Freepick at www.flaticon.com.

Permission to use an extract from a published review in the Introduction

Origin review: T.G. Dacoba, A. Olivera, D. Torres, J. Crecente-Campo, M.J. Alonso, Modulating the immune system through nanotechnology, Semin. Immunol. 34 (2017) 78–102. doi:10.1016/j.smim.2017.09.007.

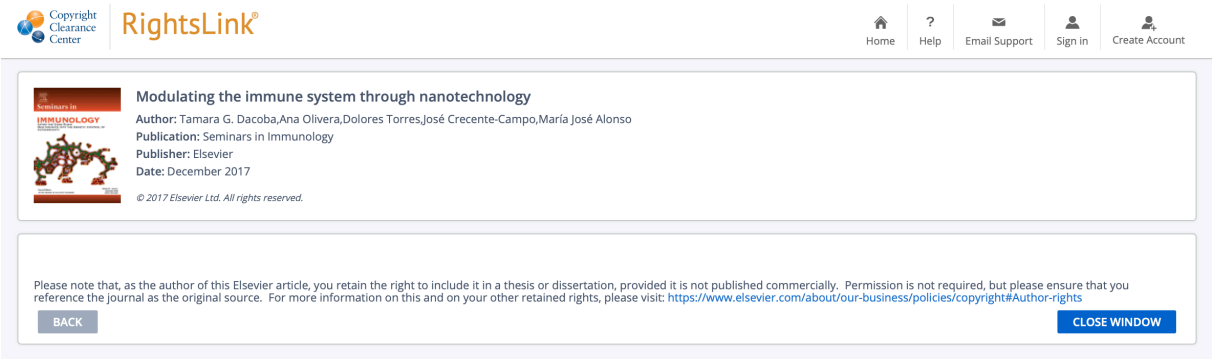

Permission to re-use a published paper as Chapter 1.A

Original paper: T.G. Dacoba, R.W. Omange, H. Li, J. Crecente-Campo, M. Luo, M.J. Alonso, Polysaccharide nanoparticles can efficiently modulate the immune response against an HIV peptide antigen, ACS Nano. 13 (2019) 4947–4959. doi:10.1021/acsnano.8b07662.
Source: https://pubs.acs.org/doi/10.1021/acsnano.8b07662
Further permission to the re-use of this material has to be directed to ACS.

ACS Chemistry for Life®

Dear Tamara,

Your permission requested is granted and there is no fee for this reuse.

In your planned reuse, you must cite the ACS article as the source, add this direct link: <https://pubs.acs.org/doi/10.1021/acsnano.8b07662>, and include a notice to readers that further permissions related to the material excerpted should be directed to the ACS.

Please do not hesitate to contact me if you need any further assistance.

Regards,
Jawwad Saeed
ACS Customer Services & Information
https://help.acs.org

Incident Information:

Incident #: 3278610
Date Created: 2020-01-24T09:59:14
Priority: 3
Customer: tamara.gomez.dacoba@usc.es
Title: Re-use material
Description: Hello,
I am one of the first authors of the article with doi: 10.1021/acsnano.8b07662
I am writing my thesis, and I want to include it as a chapter of the thesis.
As I understand from the ACS Journal Publishing Agreement, I am allowed to do so, specially considering that it is ACS Author choice.
But in any case, I would like to get a written confirmation of this.

Thanks you so much,
Have a good day,
Best,
Tamara